

Investigation of the regulation of exocytosis and endocytosis pathways in *Saccharomyces cerevisiae*

Inauguraldissertation
zur
Erlangung der Würde eines Doktors der Philosophie
vorgelegt der
Philosophisch-Naturwissenschaftlichen Fakultät
der Universität Basel
von

Alicja Maria Ritz

aus Danzig, Polen



Basel, 2014

Genehmigt von der Philosophisch-Naturwissenschaftlichen Fakultät
auf Antrag von

Prof. Dr. Anne Spang

Prof. Dr. Martin Spiess

Basel, den. 12. November 2013

Prof. Dr. Jörg Schibler

Dekan der Philosophisch-
Naturwissenschaftlichen Fakultät

For clarification purposes, the figure numbering of Chapter 6 has been adapted to suit this document.

This work has been funded by Boehringer Ingelheim Fonds and the Swiss National Science Foundation

Cover image: Artistic representation of transport vesicles inspired by Polish folk art by Alicja Ritz.

*I dedicate this thesis to my grandfathers:
to Bronisław Drozdowski, a chemistry professor
and the most youthful, perseverant person I know
and to Stefan Śliwiński, who taught me how to read,
garden and distinguish butterfly breeds.*

1. Table of Contents

2. Summary	11
3. Introduction	13
3.1 The early secretory pathway.....	14
3.2 Organization of the late secretory and endosomal pathway in yeast	15
3.3 Trafficking between membrane compartments	16
3.4 Small GTPases – Sar1, Arfs and Rabs	18
3.5 Cargo sorting at the trans-Golgi network	19
3.5.1 Clathrin-mediated sorting at the TGN	21
3.5.2 The exomer complex	23
3.6 Endocytosis	26
3.7 Plasma membrane remodeling during polarized growth.....	27
3.8 Cell polarity machinery	28
3.9 Plasma membrane remodeling upon stress	29
3.10 Pin2 is a prion domain containing protein.....	31
4. Aim of the study	33
5. Chs5, ChAP, and Chs3 cargo interaction	35
5.1 Supplementary figures	51
6. Regulated trafficking of the exomer-dependent cargo, Pin2	55
6.1 Abstract.....	57
6.2 Introduction	58
6.3 Results	60
6.3.1 The prion domain protein Pin2p is a novel exomer-dependent cargo	60
6.3.3 Pin2p and Skg6p interact with exomer components <i>in vitro</i>	62
6.3.4 Either Bch1p or Bch2p is sufficient to support Pin2p-GFP plasma membrane localization.....	63
6.3.5 Exomer binds to the Pin2p C- terminus <i>in vitro</i>	66
6.3.6 Pin2p recycles between endosomes and TGN.....	67
6.3.7 Ubiquitin-mediated endocytosis of Pin2p is required for its proper plasma membrane localization	70
6.3.8 Pin2p contains a prion domain and is a prion-inducing protein	72
6.3.9 Pin2p forms aggregates upon environmental stress and localizes to internal structures	74
6.3.10 Pin2p aggregation in internal structures is reversible.....	77
6.4 Discussion	78
6.5 Materials and Methods	80
6.5.1 Identification of novel exomer-dependent cargo	80
6.5.2 Strains, yeast genetic methods and growth conditions	81
6.5.3 Plasmids.....	81
6.5.4 Western Blot detection.....	82
6.5.5 Microscopy	82
6.5.6 Trypsin protection assay.....	82
6.5.7 Protein agarose gel electrophoresis of Pin2p SDS-resistant aggregates.....	82
6.5.8 Blue native agarose gel electrophoresis	83
6.5.9 GST tagged protein purification	83
6.5.10 GST pull downs.....	83

6.5.11 Denaturing immunoprecipitations.....	84
6.5.12 [PSI+] induction assay.....	84
6.6 Acknowledgements	85
7. Chs5, ChAP and Pin2 cytosolic domain interaction	87
8. Regulation of Pin2 transport by reactive cysteines.....	91
8.1 Abstract.....	93
8.2 Introduction	94
8.3 Results	95
8.3.1 A four-cysteine cluster in Pin2 chelates metal ions <i>in vitro</i>	95
8.3.2 Palmitoylation of Pin2 is required for its efficient plasma membrane localization..	97
8.3.3 A luminal pin structure is required for Pin2 export.	99
8.4 Discussion and outlook	102
8.4.1 The cytosolic four-cysteine cluster is most likely palmitoylated <i>in vivo</i> and seems to coordinate metal ions <i>in vitro</i>	102
8.4.2 The luminal cysteines engage in the formation of a disulfide-linked pin structure for Pin2 export	103
8.5 Materials and methods	105
8.5.1 Strains, yeast genetic methods, growth conditions and plasmids.....	105
8.5.2 GST-Pin2(72-282)p purification and atomic absorptions spectroscopy	105
8.5.3 Western Blot detection.....	106
8.5.4 Microscopy.....	106
8.5.5 Non-reducing SDS-PAGE	106
9. Further Discussion	107
9.1 Direct TGN to plasma membrane export of selected cargo mediated by exomer	108
9.2 The concerted binding of Chs5 and ChAPs to cargo	110
9.3 Restriction of cargo to the exomer pathway not only requires a cytosolic AP-1 binding motif, but also depends on the luminal domain.	112
9.4 Cycling within the late secretory pathway as a means to regulate steady state localization of cargos.....	112
9.5 Role of the prion domain in Pin2 trafficking.....	114
9.6 Pin2 could function as a stress sensor	116
10. Appendix.....	117
10.1 Materials.....	119
10.1.1 Instruments	119
10.1.2 Kits	119
10.1.3 Chemicals and consumables	120
10.1.4 Media	121
10.1.5 Common solutions and buffers.....	122
10.2 Plasmids.....	125
10.3 Strains.....	127
10.11 Oligonucleotides	129
10.5 Biochemical Methods	137
10.5.1 GST-tagged Pin2 protein purification	137
10.5.2 GST-Skg6 lysate preparation	137
10.5.3 Spheroplasting of yeast cells.....	138
10.5.4 Yeast extract pull-down with GST-tagged proteins.....	138
10.5.5 Denaturing immunoprecipitations.....	139
10.5.6 Crosslinker immunoprecipitations	140
10.5.7 Subcellular fractionation	141

10.5.8 Trypsin protection assay	141
10.5.9 Preparation of lysates under non-reducing and reducing conditions	141
10.5.10 Preparation of samples for blue native agarose gel electrophoresis and agarose gel electrophoresis of Pin2 SDS-resistant aggregates	142
10.5.11 Blue native vertical agarose gel electrophoresis	142
10.5.12 Protein agarose vertical gel electrophoresis of Pin2 SDS-resistant aggregates	143
10.5.13 Standard immunoblotting	143
10.5.14 Non-standard immunoblot detection	144
10.6 Molecular biology techniques.....	145
10.6.1 Plasmids	145
10.6.2 Site-directed Mutagenesis.....	146
10.6.3 Chromosomal manipulation of yeast DNA.....	147
10.6.4 Yeast transformation.....	147
10.6.5 Analytical PCR of yeast colonies.....	148
10.6.6 Drop assays.....	148
10.6.7 Live fluorescence microscopy	148
10.6.8 [PSI ⁺] induction assay.....	149
10.7 Formulas and web resources.....	150
10.7.1 Determination of protein secondary structure and transmembrane domains.....	150
10.7.2 Retrieval of annotated data on genes and proteins.....	150
10.7.3 Determination of yeast generation times.....	150
10.8 Abbreviations.....	151
10.9 References	154
10.10 Curriculum Vitae.....	175
10.11 Acknowledgements	178

2. Summary

Polarized growth and remodeling of the plasma membrane proteome in response to environmental changes in yeast depends on regulated exocytosis and endocytosis. The yeast chitin synthase III, Chs3, shuttles between internal compartments and the plasma membrane to allow its cell cycle-dependent expression at the bud neck and uniform discharge at the cell surface upon heat stress. The exomer complex, comprised of Chs5 and the ChAP family of cargo recognition subunits, mediates the direct, controlled export of Chs3 from the trans-Golgi network (TGN) to the plasma membrane. To further establish the role of exomer in regulated trafficking, we characterized a novel exomer-dependent cargo, the prion-domain containing protein, Pin2.

The Pin2 cytosolic domain encompasses an exomer-binding site, located within the C-terminal prion domain, and most likely another interaction site towards the N-terminal region. In parallel, we found that a vast portion of the ChAP Chs6, required for Chs3 export, confers Chs3 specificity, suggesting a proportionally large binding surface on the cargo.

Pin2, like Chs3, localizes to the plasma membrane in a polarized, cell cycle-dependent manner. Moreover Pin2 and Chs3 share several trafficking requirements. Apart from exomer-mediated export, Pin2 and Chs3 undergo active recycling through endocytosis and clathrin adaptor complex 1 (AP-1)-mediated retrograde transport from early endosomes to the TGN. Recognition of AP-1 and most likely of the AP-2 endocytic adaptor could occur through a tyrosine rich YGENYYY sequence in Pin2. The active shuttling of Pin2 between the TGN, early endosomes and the plasma membrane is required for the polarized localization of Pin2 and seems to allow its immediate, stress-responsive redistribution. Upon lithium treatment Pin2 is rapidly endocytosed and maintained in internal compartments. Stress relief results in fast re-export of Pin2 to the plasma membrane.

The Pin2 prion domain contains the exomer and potential AP-1/AP-2 binding motifs. Therefore aggregation of this region may modify the interaction of Pin2 with sorting machineries. Indeed, we found that polarized localization and maintenance of Pin2 in internal compartments is compromised in a Pin2(QNtoED), prion domain mutant. Mutation of QN residues to charged amino acids in Pin2(QNtoED) inhibits the formation of SDS-resistant prion aggregates upon overexpression.

Reversible posttranslational modifications contribute an additional level of Pin2 trafficking regulation. Ubiquitylation of Pin2 is required for its endocytosis under physiological conditions and seems to play a crucial role in Pin2 internalization upon lithium stress. Modification within a cluster of four cytosolic cysteines by palmitoylation seems to support

Summary

Pin2 cell surface expression. Interestingly, the presence of two luminal cysteines, which engage in the formation of disulfide-linked pin structure, is crucial for Pin2 export. Together this data demonstrates that several cytosolic motifs and the Pin2 prion domain, as well as a defined luminal structure, determine the regulated trafficking of Pin2.

3. Introduction

Regulated exocytosis and endocytosis play a significant role in polarity maintenance and reshape the cell surface proteome in response to environmental signals. The budding yeast *Saccharomyces cerevisiae* is a single cell organism that undergoes polarized growth and asymmetric division and has evolved to survive in changing environments. Yeast cells, which display a high turgor pressure, are encapsulated by a cell wall that expands with the growing yeast bud and provides mechanical protection. The integral membrane protein, Chs3 is one of the three enzymes that synthesize chitin in the cell wall. It is exported in a spatially and temporally regulated fashion to the yeast bud neck early and late in the cell cycle to allow timely deposition of chitin between mother and daughter cell. Upon heat stress it is discharged over the entire plasma membrane for cell wall reinforcement. Therefore the budding yeast, and in particular, Chs3, provide an excellent system for the study of regulated trafficking that shapes the plasma membrane according to cell cycle signals or stress.

3.1 The early secretory pathway

To allow organization of the multiplicity of processes with their specific enzymatic and environmental requirements, the eukaryotic cell is subdivided into membrane-enclosed compartments. A transmembrane domain-containing protein destined for the plasma membrane will travel and mature through the secretory pathway starting with the recognition of its signal sequence by the signal recognition particle, synthesis at and translocation into the endoplasmic reticulum (ER) (Sabatini *et al.*, 1971; Milstein *et al.*, 1972; Rapoport, 2007). In the ER, proteins assemble into oligomers and undergo additional post-translational modifications such as disulfide bridge formation or N-glycosylation. The ER also constitutes the environment and quality control system for protein folding for proteins destined for delivery along the secretory pathway (Ellgaard and Helenius, 2003; Braakman and Bulleid, 2011)

Chs3 is a large, multi-spanning membrane protein and shows a propensity to aggregate. Chs3 folding to a native state for subsequent ER export is aided through its palmitoylation by the DHHC protein Pfa4 and by Chs7, an integral membrane protein that seems to act as a Chs3-specific chaperone (Trilla *et al.*, 1999; Kota, 2004; Lam *et al.*, 2006). Chs7 is a limiting factor for Chs3 activity and its transcription is upregulated under conditions promoting elevated chitin synthesis such as mating or calcofluor-induced cell wall stress (Trilla *et al.*, 1999). From the ER proteins are transported directly or, in mammalian cells, through the intermediate ERGIC compartment (Appenzeller-Herzog, 2006) to the Golgi apparatus. An oligomerization step is required for Chs3 progression to the late secretory

pathway. Inhibition of Chs3 oligomer formation mediated by its cytosolic, N-terminus results in Chs3 retrieval from the Golgi to the ER (Sacristan *et al.*, 2013).

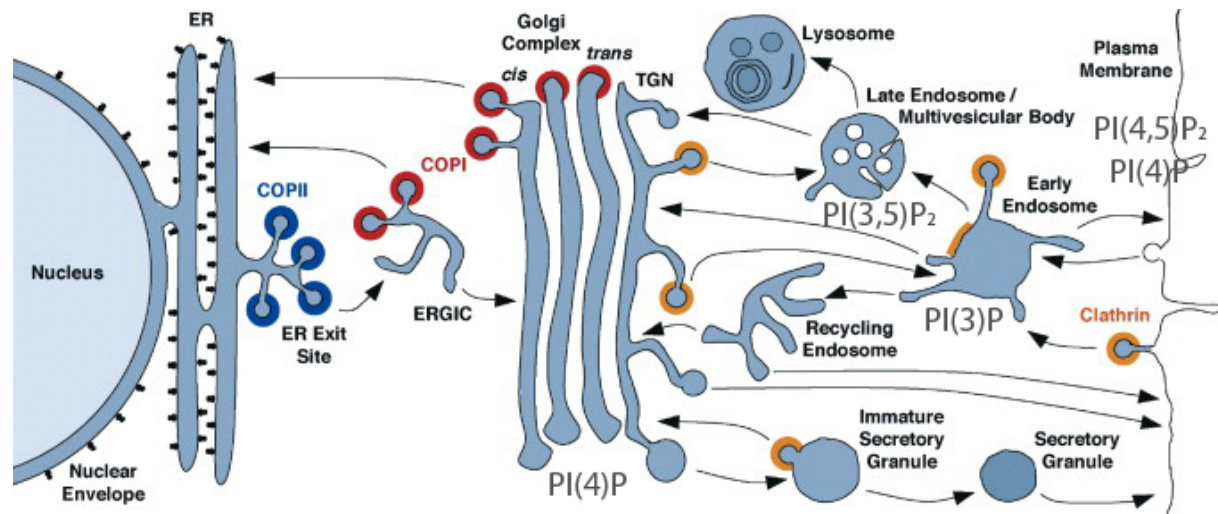


Figure 3.1 The secretory and endosomal pathway in higher eukaryotes with indicated coat complexes for vesicular transport and compartment-specific phosphatidylinositides. From Bonifacino and Glick, 2004, modified with information from (Di Paolo and De Camilli, 2006) Di Paolo and De Camilli, 2006.

Proteins enter the cis-Golgi network and travel consecutively through the cis, medial and trans cisternae. This transport is accompanied by protein sulfation (Huttner, 1988) and by the addition and remodelling of sugar moieties on glycoproteins and glycolipids (Stanley, 2011). The organization of the Golgi apparatus differs among eukaryotes. In plants, *Drosophila melanogaster* and the yeast *Pichia pastoris* the Golgi appears as a stack of flattened cisternae (Boevink *et al.*, 1998; Nebenführ *et al.*, 1999; Rossanese *et al.*, 1999; Bard *et al.*, 2006). In mammals a so-called Golgi ribbon is formed by cisternae stacks interconnected by tubules (Ward and Brandizzi, 2004). In *Saccharomyces cerevisiae*, the Golgi is generally unstacked (Rossanese *et al.*, 1999). Sorting of secretory and membrane proteins occurs at the most distal Golgi subcompartment – the trans Golgi network (TGN) (Sossin *et al.*, 1990; De Matteis and Luini, 2008; Anitei and Hoflack, 2011). From here the cargo can be targeted to the plasma membrane, endosomal compartments or lysosomes (Figure 3.1). At the TGN Chs3 is sorted into carriers that travel directly to the plasma membrane. Export of Chs3 at this stage is dependent on a specialized complex, called exomer (Santos *et al.*, 1997; Ziman *et al.*, 1998; Trautwein *et al.*, 2006).

3.2 Organization of the late secretory and endosomal pathway in yeast

The secretory and endosomal pathways converge at early endosomes. From early endosomes membrane proteins can recycle back to the plasma membrane (Maxfield and

McGraw, 2004; Grant and Donaldson, 2009), undergo retrograde transport to the TGN (Bonifacino and Rojas, 2006) or get sorted into intraluminal vesicles, at endosomes which then will fuse with lysosomes (Spang, 2009; Huotari and Helenius, 2011) (Figure 3.1). The yeast vacuole, which serves as protein degradation compartment, storage organelle and pH- and osmoregulator has been proposed to be analogous to the animal lysosome (Matile and Wiemken, 1967; Li and Kane, 2009). Both early endosomal and late endosomal compartments have been identified in yeast (Singer and Riezman, 1990; Singer-Krüger *et al.*, 1993). As in plants, it is also still debatable whether early endosomes and the TGN are independent compartments. Clear separation of both organelles, either based on detection of typical organelle markers, or by separation of endocytosed α -factor (yeast mating pheromone) from late Golgi markers by density gradient centrifugation, has so far been problematic (Singer-Krüger *et al.*, 1993; Valdivia *et al.*, 2002).

3.3 Trafficking between membrane compartments

Visualization of small protein-containing vesicles (approx. 40 – 100 nm in diameter) (Jamieson and Palade, 1967), that accumulate upon trafficking block (Novick *et al.*, 1980), their isolation from cells (Pearse, 1975), or generation in *in vitro* systems (Orci *et al.*, 1986; Barlowe *et al.*, 1994; Spang and Schekman, 1998; Bremser *et al.*, 1999) became the basis of the vesicular transport hypothesis. This hypothesis proposes that cargo is selectively incorporated and travels from one to another membrane organelle in vesicular carriers that bud from donor compartments and fuse with the acceptor organelle (Bonifacino and Glick, 2004). To ensure transport specificity, compartments carry identity tags allowing their recognition by distinct transport machineries. These localization signals are constituted by short-lived molecules such as phosphoinositides (Figure 3.1) or activated forms of GTPases. In the dynamic environment of the secretory and endocytic pathways this allows precision on one hand and plasticity – enabling new vesicles to cast aside the identity of the donor organelle, on the other (Behnia and Munro, 2005).

The small GTPases Sar1 and Arf1 recruit coat complexes to the donor membrane in the first step of vesicular transport (Lee *et al.*, 2004; Traub, 2005). In case of clathrin-mediated endocytosis, the clathrin coat is recruited to the plasma membrane by the phosphatidylinositide, PI(4,5)P₂, although the GTPase Arf6 has also been demonstrated to be involved in the process (Krauss *et al.*, 2003; Paleotti *et al.*, 2005; Traub, 2005). The coats recognize and sequester cargo proteins, interacting with sorting motifs present within the amino acid sequence of the cargoes. The polymerizing coat induces membrane curvature and vesicle budding (Spang, 2008). Upon scission the vesicle is released and can be

transported to the target compartment on actin cables, microtubules (Hehny and Stamnes, 2007), or through diffusion in case of closely opposing membrane compartments (Witte *et al.*, 2011; Okamoto *et al.*, 2012). A tether on the acceptor compartment catches the incoming vesicle. Certain tethers, such as the TRAPPI complex at the Golgi, or Dsl1 at the ER, interact with coat subunits (Barlowe, 1997; Andag *et al.*, 2001; Vanrheenen *et al.*, 2001; Cai *et al.*, 2007; Lord *et al.*, 2011). In case of the multisubunit exocyst complex at the plasma membrane, a part of the subunits seem to travel with the vesicle and meet the remaining tether components at the target membrane (Boyd, 2004). The final transport step – fusion with the acceptor compartment requires SNARE protein pairing (Brown and Pfeffer, 2010) and must be preceded by vesicle uncoating. Most SNAREs are transmembrane domain proteins that carry a 60-70 amino acid long “SNARE” motif, which participates in the formation of a coiled-coil structure with other SNAREs (Bock *et al.*, 2001). SNAREs are present on both vesicles – v-SNAREs and on the target compartment – t-SNAREs. The zipping up of one v-SNARE α -helix and three t-SNARE α -helices into a four helical bundle (Fasshauer *et al.*, 1997; Sutton *et al.*, 1998) is proposed to produce free energy required to bring together two opposing membranes for their subsequent fusion (Hanson *et al.*, 1997; Weber *et al.*, 1998; Chen and Scheller, 2001) (Figure 3.2). Recognition of vesicles by appropriate tethers and preferential cognate SNARE-pairing contribute to transport fidelity (Parlati *et al.*, 2002; Kamena and Spang, 2004; Bethani *et al.*, 2007).

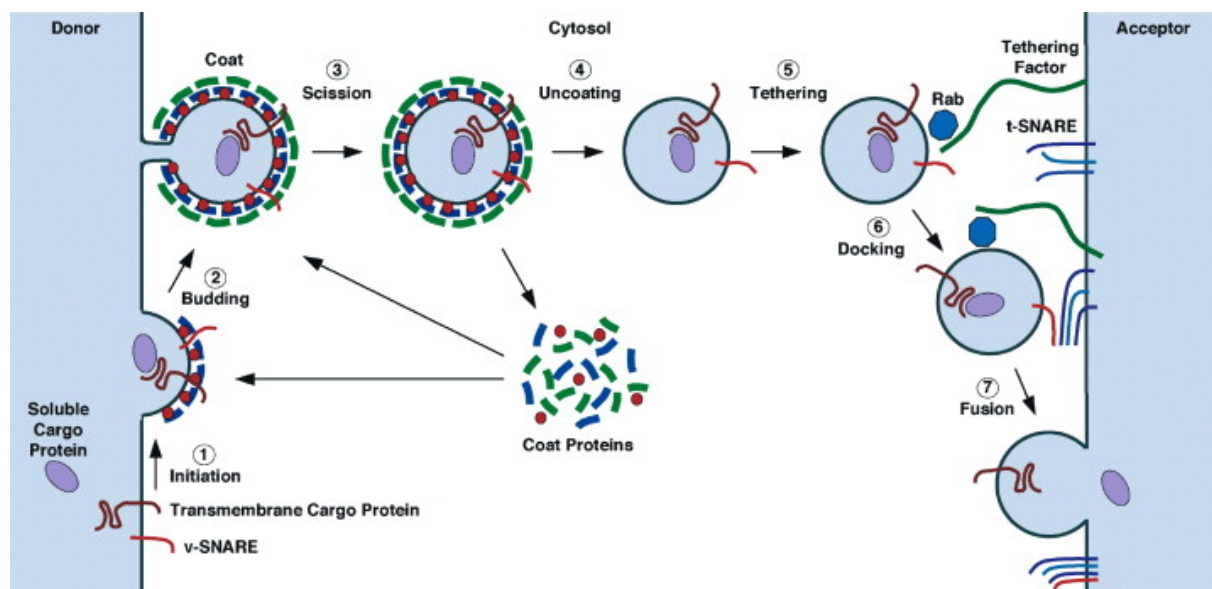


Figure 3.2. Life cycle of a transport vesicle carrying integral membrane cargo and soluble cargo, bound by a receptor. From Bonifacino and Glick, 2004.

3.4 Small GTPases – Sar1, Arfs and Rabs

Small GTPases play major regulatory roles in vesicular transport. Rab GTPases can serve as compartment identity signals (Behnia and Munro, 2005; Segev, 2011; Pfeffer, 2013). There are 11 Rab-related Ypt proteins in yeast and 66 Rab proteins identified in humans (Diekmann *et al.*, 2011; Elias *et al.*, 2012). Most Rabs associate with distinct membrane compartments (Chavrier *et al.*, 1990), where they recruit effector proteins such as tethers or molecular motors (Hutagalung and Novick, 2011). The small GTPase Sar1 recruits the COPII coat to the ER, for anterograde trafficking to the Golgi. At the Golgi, Arf1 engages the COPI coat for ER and intra-Golgi transport and the clathrin/adaptor coats for late secretory transport. Arf1 has also been shown to associate with a putative vesicle tether and lipid modifying enzymes (Brown *et al.*, 1993; Panaretou and Tooze, 2002; Gillingham, 2004; Faini *et al.*, 2013). Finally, Arf1 binds to and recruits the exomer complex at the TGN, for transport of Chs3 to the plasma membrane (Trautwein *et al.*, 2006; Wang *et al.*, 2006; Barfield *et al.*, 2009)

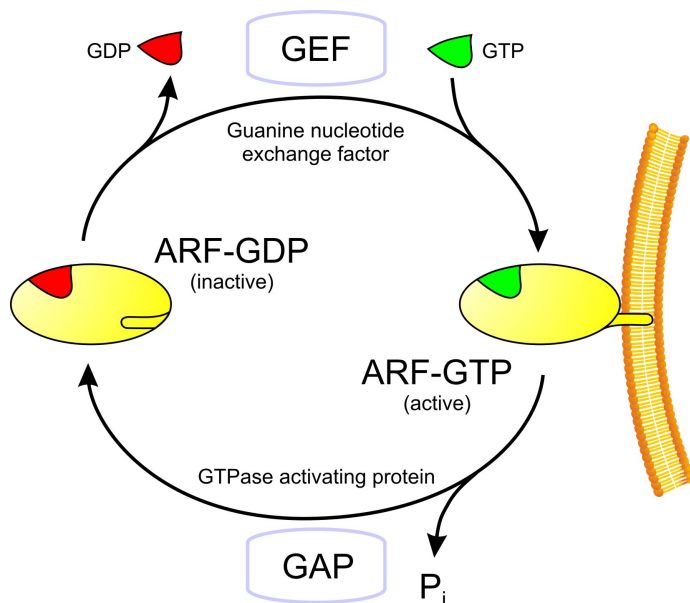


Figure 3.3. GTPase cycle of Arf proteins. From Rockenbauch 2012

The dynamic association with membranes and coat/effector molecule binding of small GTPases is regulated by their nucleotide-binding state. GTP-bound forms are active and membrane-associated, whereas GDP-bound molecules are cytosolic and inactive. Nucleotide exchange from GDP to GTP is promoted by guanine nucleotide exchange factors (GEFs) (Itzen and Goody, 2011), which are thought to be the main determinants of Arf/Sar protein localization. The N-terminus of Arf GTPases is myristoylated and forms an amphipathic helix with positively charged residues on one side and hydrophobic amino acids

on the opposite surface. The myristoylated N-terminus is buried within the Arf1-GDP molecule. The GDP to GTP switch pushes out the myristoylated N-terminal helix allowing interaction and stable association with the membrane (Amor *et al.*, 1994; Goldberg, 1998; Pasqualato *et al.*, 2002). The conformational change induced upon Arf activation also exposes the switch I and switch II regions for effector interaction (Amor *et al.*, 1994; Pasqualato *et al.*, 2002). Inactivation and dissociation from membranes is mediated by GTP hydrolysis, stimulated by GTPase activating proteins (GAPs) (Spang *et al.*, 2010) (Figure 3.3).

3.5 Cargo sorting at the trans-Golgi network

The TGN is considered the exit site and central sorting station for cargoes destined for the plasma membrane and endo-lysosomal compartments (Griffiths and Simons, 1986). It also receives input from the endosomal system (Sandvig and van Deurs, 2002). In mammalian cells the TGN appears as a network of interconnected tubular and reticular membrane structures emanating from the trans side of the Golgi (Farquhar and Palade, 1981). Sorting at the TGN in animals is one of the foundations for polarity maintenance in neuronal and epithelial cells, mediating dendritic/axonal and apical/basolateral sorting, respectively (Lasiecka and Winckler, 2011; Ang and Fölsch, 2012). Interestingly, typical apical and basolateral cargoes exit the TGN also in separate carriers in non-polarized cells. In endocrine cells, hormones are sorted from the TGN into secretory granules to allow their regulated discharge (Traub and Kornfeld, 1997; Tooze, 1998).

In mammalian cells, many post-Golgi carriers appear as large, pleomorphic tubular structures, often interconnected or with fenestrated membranes (Hirschberg *et al.*, 1998; Polishchuk *et al.*, 2003; Puertollano *et al.*, 2003; Polishchuk *et al.*, 2006). They extend from the TGN and actually seem to be fragments of TGN membranes into which cargo has been sorted. The formation of tubular carriers seems to depend on the actin and, in animals, microtubule cytoskeleton, together with the pulling force provided by the action of motor proteins (Egea *et al.*, 2006; De Matteis and Luini, 2008; Anitei and Hoflack, 2011). A role of lipids such as diacylglycerol (DAG) at the cytosolic lipid bilayer leaflet, which would induce lipid phase separation and membrane invagination towards the lumen, has been suggested to mediate the final scission step (Bard and Malhotra, 2006). Arf1 is a major player in TGN sorting and carrier formation. It recruits the clathrin coat through AP-1 and GGA (Golgi-localized, γ -ear-containing, ARF-binding proteins) adaptors and also binds AP-3 and AP-4 adaptor complexes for lysosomal and endosomal transport, respectively (Robinson and Bonifacino, 2001; Hirst *et al.*, 2011). Also long coiled-coiled GRIP-Golgins and several BAR

domain proteins, that may sense and stabilize tubular curvature have been implicated in formation of TGN-derived vesicles (Egea *et al.*, 2006; De Matteis and Luini, 2008; Anitei and Hoflack, 2011). Recently, a novel carrier involved in direct trafficking from the TGN to the plasma membrane has been described in HeLa cells: Rab6 and Rab8 positive CARTS (Carriers of the TGN to the cell Surface) carry specific cargoes such as PAUF (pancreatic adenocarcinoma upregulated factor), synaptotagmin II and TGN46, but not VSV-G or the bulky cargo procollagen (Wakana *et al.*, 2012).

Sorting machineries and coats are cytosolic and interact with signal motifs on cytosolic domains of integral membrane proteins. However glycosylation on luminal domains, and membrane-transmembrane domain interactions may influence cargo transport at this step. A comparison of transmembrane domain (TMD) sequences shows that TMDs have organelle-specific features. Integral membrane proteins with TMDs longer than 20 amino acids with a lower amino acid residue volume at the outer leaflet can be sorted to the plasma membrane, whereas those with a high residue volume are rather retained at the Golgi (Sharpe *et al.*, 2010). Aggregation of the secretory protein, chromogranin B, has also been shown to mediate its sorting into secretory vesicles and prevents its mis-sorting into the constitutive secretory pathway (Tooze, 1998).

Two, independent post-Golgi secretory pathways to the plasma membrane have been identified in yeast. Secretory vesicles, accumulated in a temperature-sensitive exocyst subunit mutant, *sec6-4*, can be separated into two fractions by equilibrium isodensity centrifugation. The denser vesicles contain acid phosphatase and the periplasmic enzyme, invertase (Harsay and Bretscher, 1995; Kruckeberg *et al.*, 1999). The high-density vesicles represent carriers that traffic through endosomes to the plasma membrane and require the clathrin coat and the aminophospholipid transferase, Dsp2, for their formation (Harsay and Bretscher, 1995; Gall *et al.*, 2002). These carriers accumulate in cells carrying the *act1-1*, actin gene allele and in a Δ *sla2* actin cytoskeleton assembly mutant (Harsay and Bretscher, 1995; Mulholland *et al.*, 1997; Gall *et al.*, 2002). The vesicles in the lighter density fractions contain the plasma membrane proton pump, Pma1, the hexose transporter Hxt2, the cell wall protein, Bgl2, and Chs3. The light density vesicles seem to constitute a direct secretory pathway to the plasma membrane (Harsay, 2002). Plasma membrane fusion of low-density vesicles is predominantly blocked in Exo70 exocyst component, *exo70-35* and *exo70-38* mutants, which however do not affect the assembly or localization of the tethering complex (He *et al.*, 2007). The yeast-specific exomer complex is the single machinery identified to date to act in the sorting into light secretory vesicles for direct TGN export to the plasma membrane. No such machinery has been identified in the formation of the direct plasma

membrane carrier, the mammalian CARTS (Wakana *et al.*, 2012). Exomer is required for the export of Chs3 and Fus1, a protein involved in cell fusion during mating (Santos *et al.*, 1997; Santos and Snyder, 1997; Ziman *et al.*, 1998; Santos and Snyder, 2003; Valdivia and Schekman, 2003; Trautwein *et al.*, 2006; Barfield *et al.*, 2009), but not for the cell surface targeting of Pma1 or Hxt2 also found in the light density vesicle fraction (Zanolari *et al.*, 2011). Therefore other sorting complexes or coats must be involved in this transport pathway.

3.5.1 Clathrin-mediated sorting at the TGN

High-density vesicle formation is dependent on clathrin (Harsay, 2002). Adaptor proteins constitute the inner layer of clathrin coats. Among these are the large heterotetrameric adaptor complexes: AP-1 and AP-2 (Boehm and Bonifacino, 2001) as well as the GGA proteins (Puertollano *et al.*, 2003). Three additional adaptors AP-3, AP-4 and AP-5 (in *Saccharomyces cerevisiae*, only AP-3) have been identified, however they function independently of clathrin (Robinson and Bonifacino, 2001; Hirst *et al.*, 2011). The clathrin cage consisting of clathrin heavy and light chains forms the outer layer of the coat (Faini *et al.*, 2013).

AP-1, GGAs, AP-4 and to a smaller extent AP-3 localize to the TGN (Robinson and Bonifacino, 2001). I will focus on the function of AP-1 and GGAs in TGN – endosomal trafficking. AP-1 (and similarly all AP complexes) contains two large subunits γ and $\beta 1$, a medium subunit $\mu 1$ and a small subunit $\sigma 1$ (Robinson and Bonifacino, 2001). The $\mu 1$ subunit recognizes tyrosine based YXX Φ (where Φ represents a residue with a bulky hydrophobic side chain) sorting motifs on cargo (Traub, 2003; Owen *et al.*, 2004). The D/EXXXLL/I dileucine motif is thought to bind to the $\gamma/\sigma 1$ hemicomplex (Traub, 2005). In the cytosolic state, the YXX Φ contact site is occluded and inaccessible to cargo (Heldwein *et al.*, 2004). A recent structural and biochemical study has demonstrated that AP-1 interaction with Arf1-GTP drives the open state of the adaptor (Ren *et al.*, 2013). Two molecules of Arf1 bind to two different sites on the AP-1 molecule pivoting the trunk domains and causing their opening (Ren *et al.*, 2013). The recruitment of AP-1 to the TGN requires Arf1-GTP, the Golgi phosphatidylinositol, PI(4)P, and the anchored YXX Φ sorting signal (Zhu *et al.*, 1998) (Figure 3.4)

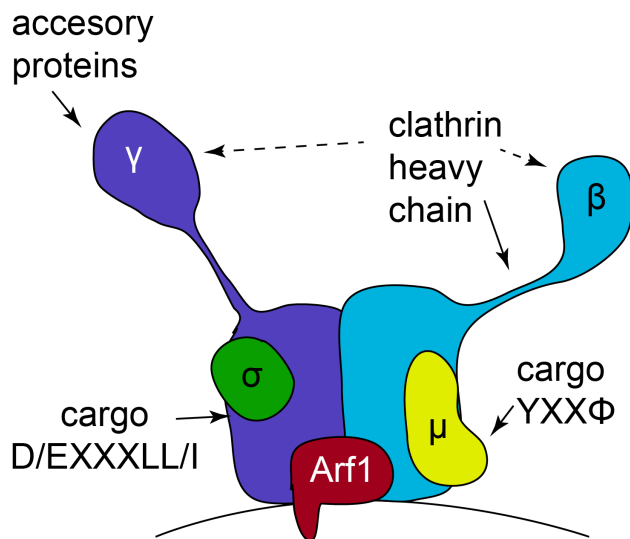


Figure 3.4 AP-1 adaptor complex recruited to the membrane by Arf1-GTP. Interaction sites for sorting motifs on cargoes, accessory proteins and the clathrin-box motif are indicated by arrows. Dashed arrows point to additional sites that display clathrin-binding activity. Modified from Faini *et al.*, 2013 with information from Robinson and Bonifacino, 2001; (Gallusser and Kirchhausen, 1993; Morgan *et al.*, 2000; Owen *et al.*, 2000) Owen *et al.*, 2004, Traub *et al.*, 2003, Traub 2005

GGAs are largely unstructured proteins that carry a VHS domain for cargo recognition (Nakayama and Wakatsuki, 2003). GGAs bind to dileucine motifs preceded by a cluster of acidic residues, but have also been shown to mediate the sorting of the SNARE, Pep12, through a FSDSPEF motif (Robinson and Bonifacino, 2001). GGAs also contain ubiquitin-binding domains (Bilodeau *et al.*, 2004). In fact, yeast GGAs only recognize ubiquitylated cargoes (Misra *et al.*, 2002; Scott *et al.*, 2004). Newly synthesized Gap1, a yeast amino acid transporter, is degraded under rich nitrogen source conditions. Lysosomal targeting of ubiquitylated Gap1 relies on GGA-dependent recognition and sorting (Scott *et al.*, 2004).

AP-1 and GGA clathrin adaptors mediate TGN – endosome trafficking. There is much debate about the directionality of AP-1 and GGA mediated transport and the contribution of the two in the process (Hanners, 2003). A popular view in the field is that AP-1 mediates anterograde transport from TGN to endosomes (Hille-Rehfeld, 1995; Höning *et al.*, 1996; Touz *et al.*, 2004), or even directly to the plasma membrane (Gravotta *et al.*, 2012). However, several lines of evidence suggest a role for AP-1 in retrograde trafficking from early endosomes to the TGN. First, the mannose-6-phosphate receptor (MPR), a receptor required for lysosomal hydrolase sorting, rather than being blocked in the TGN compartment in μ 1a knockout mice seems to be mis-sorted to an alternative pathway to the plasma membrane. Endocytosis causes its accumulation in early endosomal compartments (Meyer *et al.*, 2000). Similarly, deletion of AP-1 subunits in yeast rescues the export of Chs3 to the plasma membrane in strains deleted for exomer components, normally essential for Chs3 plasma membrane localization (Figure 3.5) (Valdivia *et al.*, 2002). It also causes missorting of the SNARE Tlg1, involved in fusion of endosome-derived vesicles with the late Golgi (Holthuis *et al.*, 1998). Tlg1, which is a TGN and early endosomal resident protein, is incorporated into

secretory vesicles in *AP-1* mutants (Valdivia *et al.*, 2002). Both studies support the role of AP-1 in retrieval of cargoes from endosomes for the maintenance of their localization at the TGN or for promoting their sorting into correct anterograde transport pathways.

A recent study has confirmed the role of AP-1 in retrograde transport from endosomes using a novel knock-sideways system in HeLa cells (Hirst *et al.*, 2012). This method allowed rapid depletion of AP-1 and GGA2 from their cognate compartments and was followed by proteomic analysis of clathrin-coated vesicles (CCVs). Using this approach, Hirst and colleagues (Hirst *et al.*, 2012) were able to propose the existence of two classes of CCVs. One population labeled by both AP-1 and GGAs would be required for anterograde transport of lysosomal hydrolases and their receptors. Vesicles only positive for AP-1, would be involved in retrieval to the TGN of ligand free receptors, SNAREs, and proteins such as ATP7A and ATP7B – copper-transporting ATPases, maintained in intracellular compartments in the absence of copper (Hirst *et al.*, 2012). Which adaptors are involved in sorting cargoes to the plasma membrane and whether it is AP-1 is not yet resolved.

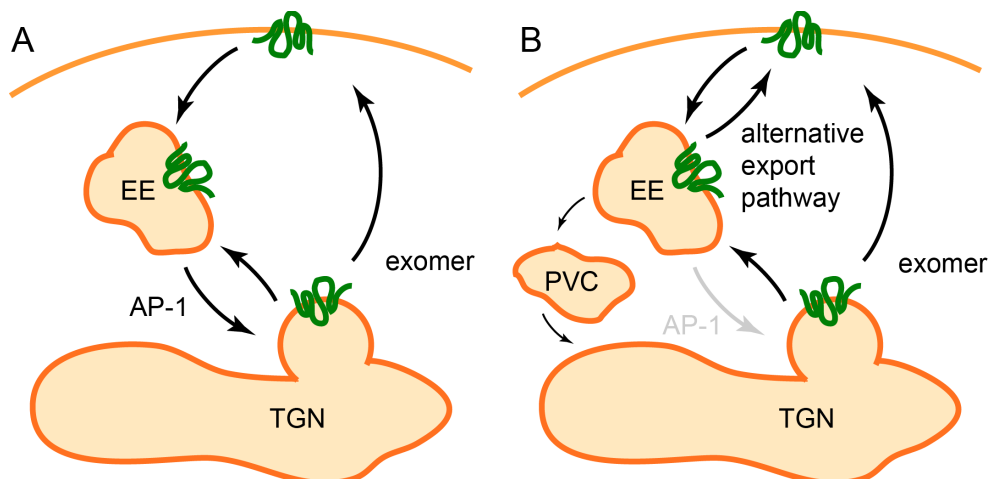


Figure 3.5 Chs3 shuttles between the plasma membrane, TGN and early endosomes (EE) (A). Deletion of *AP-1* allows Chs3 to exit to the plasma membrane through an alternative export route through early endosomes (B). This circumvents the requirement of Chs3 for exomer-dependent export. In *AP-1* deletion strains, Chs3 seems to be retrieved to the TGN through the prevacuolar compartment (PVC). Modified from Valdivia *et al.*, 2002.

3.5.2 The exomer complex

The timely export of Chs3 from the TGN to the bud neck during the cell cycle and uniform discharge over the plasma membrane under heat stress conditions is exomer dependent (Santos *et al.*, 1997; Ziman *et al.*, 1998; Valdivia and Schekman, 2003; Trautwein *et al.*, 2006). As previously mentioned, deletion of AP-1 components, which mediate retrograde transport from early endosomes to the TGN, allows re-routing of Chs3 to the plasma

membrane through the alternative secretory pathway via endosomes (Valdivia *et al.*, 2002) (Figure 3.5). However, this export pathway does not guarantee a fully polarized localization of Chs3 at the bud neck (Zanolari, unpublished data). It also does not permit enhanced Chs3 export and uniform distribution over the plasma membrane upon heat stress (Valdivia and Schekman, 2003). This suggests that exomer could act as a specialized machinery for cell-cycle and stress regulated TGN export.

The TGN-localized peripheral membrane protein, Chs5 and four paralogous proteins: Bch1, Bch2, Bud7 and Chs6, called collectively the ChAPs (Chs5p-Arf1p-binding Proteins) form exomer. A complex of these five proteins can be co-purified from yeast or when heterologously expressed in a baculovirus system (Sanchatjate and Schekman, 2006; Trautwein *et al.*, 2006) (Figure 3.6 A).

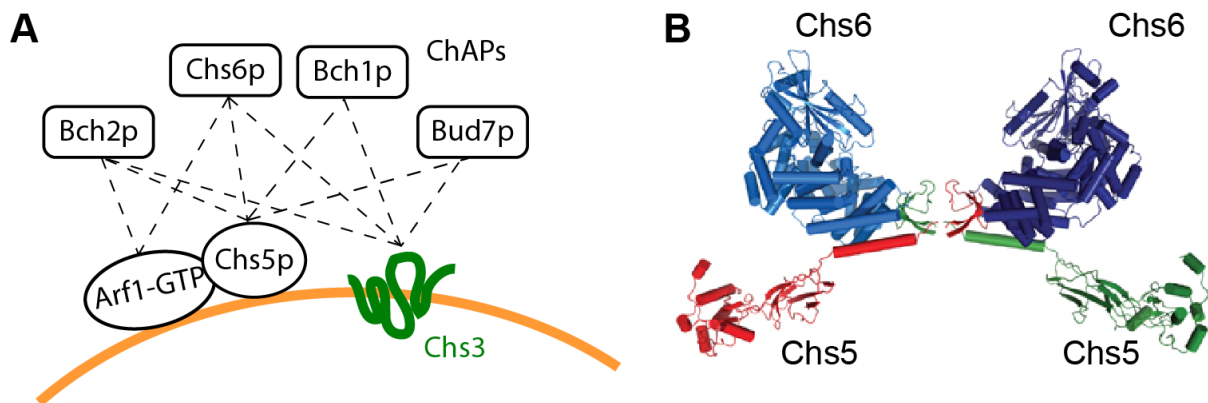


Figure 3.6 The exomer complex. (A) Schematic representation of exomer components and their interactions. Direct interactions are either indicated by proximity or dashed lines, apart from the ChAP-membrane interaction. (B) Structure of Chs5-Chs6 heterotetramer (Paczkowski *et al.*, 2012)

The ChAPs seem to act as cargo recognition subunits and interact with Chs3. Interestingly Chs3 requires specific ChAPs for its export: Chs6 or the ChAP pair Bch1/Bud7 (Trautwein *et al.*, 2006). A strong export defect of Fus1, the second identified exomer cargo, can also be observed in a double $\Delta bch1\Delta bud7$ ChAP deletion, but not in a $\Delta chs6$, or any other single ChAP deletion strain (Barfield *et al.*, 2009). Different ChAP deletions also display distinct phenotypes. $\Delta chs6$ cells are calcofluor-resistant, reminiscent of chitin reduction due to a Chs3 export defect, $\Delta bud7$ cells display a random budding pattern in diploids, whereas $\Delta bch1$ strains are sensitive to high ammonium levels. The recognition of various, also unidentified cargoes, by distinct exomer-complexes with different ChAP composition, could account for the different ChAP phenotypes. In support of this notion, the ChAPs form complexes of different stoichiometries (Trautwein *et al.*, 2006).

The $\Delta chs5$ strain displays all ChAP deletion phenotypes (Trautwein *et al.*, 2006). This puts Chs5 upstream, as the core exomer subunit. Chs5 binding to the ChAPs is required for their TGN association (Trautwein *et al.*, 2006) and also enhances or stabilizes their binding with the cargo, for example Chs3 (Sanchatjate and Schekman, 2006). The ChAPs bind Chs5 independently of each other and require the last 13 C-terminal amino acids for this interaction (Trautwein *et al.*, 2006). However, the interaction between ChAPs themselves is dependent on Chs5 (Sanchatjate and Schekman, 2006). This is supported by a recent structural study, which shows that two Chs6 and two Chs5 (aa 1-274 – minimal functional domain; full length aa 1-671) molecules form a heterotetramer, through a Chs5 dimer. This interaction is mediated by a N-terminal antiparallel β -sheet in Chs5 on each of the two molecules, which extends and contacts the neighboring Chs6 molecule *in trans*. The Chs6-Chs5 contact interface is formed by two helices on each of the proteins. These helices form an intermolecular tetratricopeptide (TPR)-like motif. The heterotetramer model implies that mixed (containing two different ChAPs) and homogenous (containing two ChAPs of the same kind) exomer complexes may form in cells to recognize and sort cargoes (Paczkowski *et al.*, 2012) (Figure 3.6 B).

The initial recruitment of the exomer complex to membranes is most likely mediated by activated Arf1-GTP. Both Chs5 and the ChAPs (this has been demonstrated for Bch2 and Chs6) can bind Arf1-GTP (Trautwein *et al.*, 2006; Wang *et al.*, 2006; Paczkowski *et al.*, 2012). Chs5 and Chs6 have also been shown to interact directly with lipids (Wang *et al.*, 2006; Paczkowski *et al.*, 2012). Paczkowski and colleagues (Paczkowski *et al.*, 2012) proposed that efficient recruitment of exomer to the TGN most likely depends on a combination of interactions: exomer subunits with Arf1, membranes and each other in the heterotetramer.

The interactions within the exomer complex and with Arf1 are reminiscent of a coat. Indeed purified exomer formed a spiky structure on liposomes preincubated with Arf1-GTP γ S. However, unlike COPI and COPII coats, exomer was not able to deform membrane structures to form buds or vesicles (Wang *et al.*, 2006). It is also conceivable that exomer acts as a sorting complex. No consensus motif in Chs3 and Fus1 has been found for exomer recognition. Fus1 requires an IXTPK motif for export and exomer binding. This motif is absent from Chs3 and could not render an unrelated cargo exomer-dependent (Barfield *et al.*, 2009).

3.6 Endocytosis

Internalization of membrane proteins such as receptors, transporters and uptake of particles from the environment occurs through the inward invagination and budding off of the plasma membrane in the process of endocytosis (Mayor and Pagano, 2007). One form of these invaginations are clathrin-coated pits (CCPs). In yeast, the first proteins to arrive at the incipient pit are clathrin and the endocytic adaptors Ede1 and Syp1 (homologues of the mammalian Eps15 and FCHo1/2 proteins, respectively) (Stimpson *et al.*, 2009). AP-2 is the major adaptor involved in clathrin-mediated endocytosis (CME). It recruits the clathrin coat through interaction with the plasma membrane phosphatidylinositide PI(4,5)P₂ and recognizes YXXΦ sorting signals on cargoes (Traub, 2005). The next to arrive are components that link the initial endocytic machinery with the actin cytoskeleton: Sla2/End4 (the homologue of the mammalian Hip1R), followed by a complex of End3, Pan1 and Sla1 (Tang *et al.*, 1997; 2000). At this time also clathrin adaptors such as the epsins Ent1/2 are recruited to endocytic sites (Kaksonen *et al.*, 2005; Newpher *et al.*, 2005; Toshima *et al.*, 2006; Stimpson *et al.*, 2009). Endocytosis in yeast occurs at actin patches and nucleation of the actin cytoskeleton drives membrane invagination to form an endocytic vesicle (Moreau *et al.*, 1997; Young, 2004; Rodal *et al.*, 2005; Moseley and Goode, 2006)

Polyubiquitylation by K-63 linked linear ubiquitin chains, mono- and multiubiquitylation can serve as a signal for the internalization of plasma membrane proteins (Acconcia *et al.*, 2009; Haglund and Dikic, 2012). Several endocytic adaptors possess ubiquitin-binding domains. The yeast epsin homologues Ent1/2 bear tandem ubiquitin-interaction motifs (UIMs) and Ede1 contains a single ubiquitin-associated (UBA) domain (Traub and Lukacs, 2007). Ubiquitin moieties are transferred to plasma membrane proteins by the E3 ligase Rsp5 (Hein *et al.*, 1995; Galan *et al.*, 1996). Arrestin-Related Trafficking adaptors (ARTs) have been shown to act as the cargo recognition modules of Rsp5 for several transporters (Lin *et al.*, 2008; Nikko *et al.*, 2008; Nikko and Pelham, 2009). There are nine yeast proteins bearing an arrestin motif, out of which only Art9 cannot bind to Rsp5 (Lin *et al.*, 2008). Recognition by ARTs can be preceded by cargo phosphorylation (Nikko *et al.*, 2008) or protein misfolding under stress conditions (Zhao *et al.*, 2013). This suggests that the Rsp5-ART network could regulate the cell surface proteome, in response to signaling events e.g. triggered by excess substrate and represent a novel quality control mechanism at the plasma membrane.

Ubiquitylation is a reversible modification. The balance between ubiquitylation and deubiquitylation is proposed to act as a determinant of cargo fate – recycling to the plasma membrane or ESCRT-mediated multivesicular body (MVB) sorting followed by lysosomal

degradation (Clague *et al.*, 2012). The *Drosophila* and mammalian Frizzled (Fz) receptor undergoes constant endocytosis and re-export. This is accompanied by cycles of ubiquitylation and deubiquitylation, mediated by the endosomal DUB USP8/UBPY. Loss of the DUB activity causes Fz receptor mis-sorting to MVBs (Mukai *et al.*, 2010). Similarly the AMSH1 and Cezanne DUBs promote the recycling of the EGFR receptor (Bowers *et al.*, 2006; Pareja *et al.*, 2012).

Plasma membrane expression of Chs3 is regulated by its shuttling between the cell surface and internal compartments, which share characteristics of the TGN and early endosomes (Chuang and Schekman, 1996; Valdivia *et al.*, 2002). Maintenance of Chs3 polarized localization is highly dependent on endocytosis (Chuang and Schekman, 1996; Ziman *et al.*, 1996; Reyes *et al.*, 2007; Zanolari *et al.*, 2011). Chs3 is ubiquitylated and this seems to promote its internalization (Peng *et al.*, 2003; Sacristan *et al.*, 2013). Since Chs3 is a metabolically stable protein and its plasma membrane expression is rather regulated by shuttling between internal compartments and the cell surface than by protein level regulation (Chuang and Schekman, 1996), it is very likely that it undergoes deubiquitylation for its re-export.

3.7 Plasma membrane remodeling during polarized growth

Saccharomyces cerevisiae grows in a highly polarized fashion (Pruyne and Bretscher, 2000; Park and Bi, 2007; Bi and Park, 2012). Vegetative growth in yeast occurs through budding. In this process a daughter cell forms out from a mother cell separated by a constriction termed the bud neck (Knop, 2011). Polarized growth of the yeast cell is mirrored by the expansion of its cell wall at the bud and formation of a corresponding constriction at the bud neck – the chitin ring, synthesized by Chs3 (Shaw *et al.*, 1991; Chuang and Schekman, 1996; Schmidt, 2003).

Bud formation and growth requires targeted delivery of lipid and protein cargo to the bud by secretory vesicles. This is achieved by polarization of actin cables, which act as tracks for secretory vesicles (Adams and Pringle, 1984; Pruyne *et al.*, 1998) and polarization of final exocytosis sites (Finger *et al.*, 1998). Polarized sites of growth are first localized to the bud tip from late G1 to end of S-phase. This results in so-called “apical growth”, which lengthens the daughter cell. In G2 “apical growth” switches to “isotropic growth” (Farkas *et al.*, 1974) in a Cdk1(Cdc28)-dependent manner (Richardson *et al.*, 1992; Lew and Reed, 1993; Ahn *et al.*, 2001) resulting in uniform bud growth. Finally to allow mother and daughter separation polarized growth is directed to the bud neck towards late anaphase/ telophase (Figure 3.7).

The cell wall expands in a coordinated manner with the maturing bud. This requires targeting of cell wall biosynthetic proteins to specific plasma membrane domains. For example, Rho1 and Fks1, components of the $\beta(1\rightarrow3)$ glucan synthase complex, colocalize with sites of polarized growth to allow concomitant extension of the cell wall (Yamochi *et al.*, 1994; Drgonová *et al.*, 1996; Qadota *et al.*, 1996). Chs3 localizes to the bud neck in G1/S phase to synthesize the chitin ring and in M phase to allow lateral cell wall synthesis before final mother-daughter separation (Figure 3.7). (Shaw *et al.*, 1991; Chuang and Schekman, 1996; Schmidt, 2003).

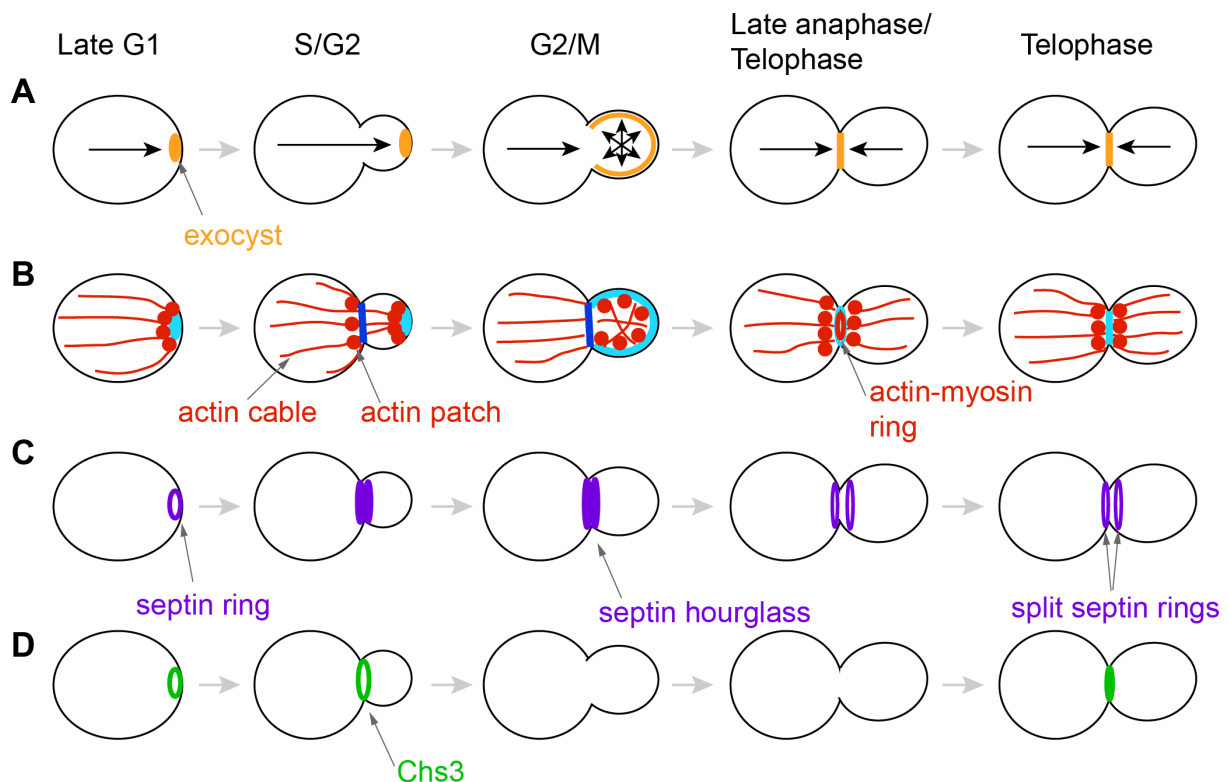


Figure 3.7 Localization of the polarity machinery and the yeast chitin synthase III, an integral membrane protein displaying polarized localization during the cell cycle. (A) Localization of the exocyst, vesicle tethering, complex and direction of polarized growth, indicated by arrows. (B) Organization of the actin cytoskeleton, depicting two arrays of actin cables and actin patches localized to sites of polarized growth. Formins that nucleate the actin arrays are depicted in blue (C) Septin ring localization and organization during the cell cycle. The septin ring is recruited to the incipient bud site, by Cdc42, expands into an hourglass structure upon bud emergence and splits into two rings at cytokinesis onset. (D) Localization of the yeast chitin III, Chs3. Modified from Bi and Park 2012; Chuang and Schekman 1996; Guo *et al.* 2001 (Guo *et al.*, 2001)

3.8 Cell polarity machinery

As previously mentioned, secretory vesicles in yeast are transported along polarized actin cables. The actin cables are organized into two sets, one running towards the bud cortex and the second one towards the bud neck (Pruyne *et al.*, 2004) (Figure 3.7). Secretory vesicles

are transported along actin cables by a specialized myosin motor – Myo2p (Schott *et al.*, 2002). The exocyst complex finally tethers the vesicles to sites of polarized growth at the plasma membrane, prior to their fusion (TerBush *et al.*, 1996). Apart from actin cables, actin patches localize to sites of polarized growth (Doyle and Botstein, 1996; Waddle *et al.*, 1996) (Figure 3.6). Actin patches are formed by short, branched actin cables nucleated by the Arp2/3 complex (Young, 2004; Rodal *et al.*, 2005; Moseley and Goode, 2006) and are, in yeast, sites of endocytosis (Engqvist-Goldstein and Drubin, 2003). Interestingly, a recent study has shown that endocytosis constricts sites of exocytosis to maintain cellular polarity (Jose *et al.*, 2013). Finally asymmetric division and polarity maintenance in yeast depends on the septin ring. Septins are soluble GTP-binding proteins that assemble into heterooligomeric high-order structures (Figure 3.7). The septin ring has a scaffolding function. The septins recruit landmark proteins for bud site selection at the beginning of the cell cycle and the formin Bnr1 for nucleation of actin cables. At the end of mitosis the septin split ring sandwiches the contractile actin-myosin ring for cytokinesis (Oh and Bi, 2011; Buttery *et al.*, 2012). The septins can also act as a diffusion barrier for polarity factors and exocyst components (Barral *et al.*, 2000). At the plasma membrane Chs3 is tethered to the septin ring via Chs4 and, early in the cell cycle, also through Bni4 (DeMarini *et al.*, 1997; Kozubowski *et al.*, 2003).

3.9 Plasma membrane remodeling upon stress

Under non-stress conditions chitin makes up about 2% of the cell wall mass. In mutants that induce cell wall stress chitin content can rise up to 20% (Popolo *et al.*, 1997; García-Rodríguez *et al.*, 2000; Valdivieso *et al.*, 2000). Heat stress induces a mobilization of Chs3 from internal stores to the cell surface, where it is distributed over the plasma membrane in a depolarized fashion for cell wall reinforcement (Valdivia and Schekman, 2003). The $\beta(1\rightarrow3)$ glucan synthase, Fks1, displays a similar redistribution upon heat treatment (Delley and Hall, 1999). The depolarization of Chs3 and Fks1 upon cell wall stress coincides with depolarization of the actin cytoskeleton and Myo2p motor (Chowdhury *et al.*, 1992; Lillie and Brown, 1994; Delley and Hall, 1999). The depolarization reaches maximum after approximately 30 minutes heat treatment and is reversed after 120 minutes (Delley and Hall, 1999). This suggests that the redistribution of both cell wall biosynthetic enzymes can be accounted to the regulation of their trafficking and relocalization of the exocytic machinery rather than to dissipation of a diffusion barrier. Depolarization of the actin cytoskeleton and uniform delivery of Chs3 and Fks1 to the plasma membrane under heat stress is dependent on Rho1 and Pkc1 (Delley and Hall, 1999; Valdivia and Schekman, 2003).

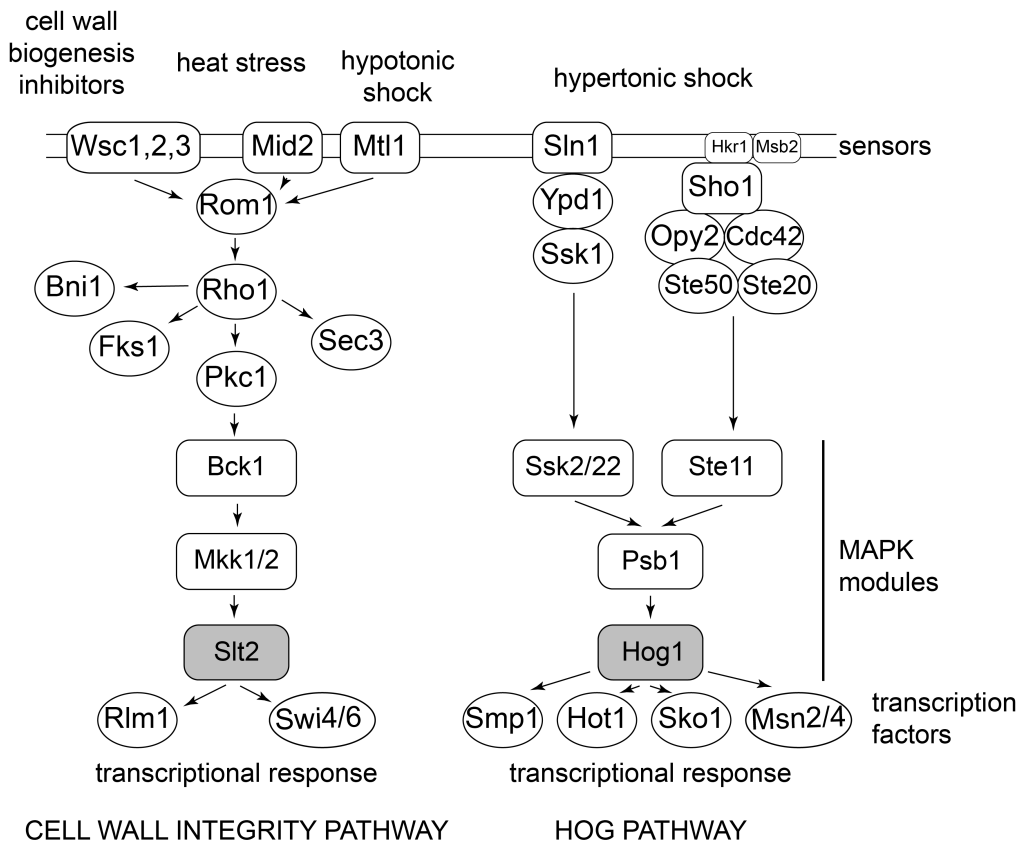


Figure 3.7. The CWI and HOG MAP kinase signaling pathways. Adapted from Rodriguez and Pena, 2010. Modified with information from Ketela *et al.*, 1999; de Nobel *et al.*, 2001; Martin *et al.*, 2000; Kamada *et al.*, 1995; Levin *et al.*, 2011.

Two mitogen-activated protein kinase (MAPK) signaling pathways: the Cell Wall Integrity (CWI) and the high-osmolarity glycerol (HOG) pathway are responsible for stress response in yeast. The CWI pathway is activated upon treatment with factors that interfere with cell wall biogenesis such as: Calcofluor white (Ketela *et al.*, 1999), Congo red, caffeine and zymolyase (de Nobel *et al.*, 2000; Martin, 2000). It is also stimulated by heat stress or hypotonic shock – conditions that weaken the cell wall (Kamada *et al.*, 1995). Five cell surface sensors Wsc1, -2, -3, Mid2 and Mtl1 initiate CWI signalling. The signal is relayed to Rho1, which activates several effectors: the formin Bni1; the $\beta(1\rightarrow3)$ glucan synthase, Fks1; a member of the exocyst tethering complex, Sec3 and the kinase Pkc1, a component of the CWI MAPK cascade that will activate the transcription of genes encoding cell wall glycoproteins and cell wall biosynthetic proteins. For a recent review see (Levin, 2011). The HOG pathway is in general activated by hyperosmotic stress. The stress signal is transmitted to the MAPK Hog1 through two branches: the first initiated by the sensor Sln1, the second by Hkr1 and Msb2. The majority of phosphorylated Hog1 is transported to the nucleus by Nmd5, a beta importin homologue, where it regulates cell cycle and transcription (Ferrigno *et al.*, 1998; Posas *et al.*, 2000; Rep *et al.*, 2000) (Figure 3.7).

3.10 Pin2 is a prion domain containing protein

We wanted to test whether exomer in general would mediate temporally and spatially controlled discharge of cargoes to the plasma membrane in response to cell cycle and stress signals. To achieve this Mark Trautwein used a mass spectrometry-based approach to detect interactors in exomer subunit pull-downs from cross-linked yeast extracts. He identified Pin2 as a novel cargo. The function of Pin2 is unknown, however it has been described as – and its name stands for – *[PSI⁺]* Inducibility factor. *[PSI⁺]* is the prion of the translational terminator Sup35 in yeast (Ter-Avanesyan *et al.*, 1994; Derkatch *et al.*, 1996). For *[PSI⁺]* to appear, either spontaneously or through Sup35 overexpression, the cells must possess an epigenetic *[PIN⁺]* element (Derkatch *et al.*, 1997). Derkatch and colleagues discovered that overexpression of several prion domain containing proteins can give rise to *[PIN⁺]* (Derkatch *et al.*, 2001). Among these proteins are the known prion proteins Rnq1 and Ure2, but also Pin2. The presence of other prions could either cross-seed the Sup35 prion or titrate away aggregation inhibitors (Derkatch *et al.*, 2001).

Most prions form stable aggregates of amyloid fibers. Amyloids consist of layers of β -sheets that run perpendicular to the long axis of the fiber, are resistant to protease treatment or denaturing conditions such as presence of sodium dodecyl sulphate (SDS) and bind to dyes like Congo Red or Thioflavin T (Prusiner *et al.*, 1983; Taylor, 1999; Salnikova, 2004). Amyloid structures arise through a conformational switch that can be propagated and inherited – in yeast to daughters and through mating (Wickner *et al.*, 2013). In humans this is the basis for infectivity in case of spongiform encephalopathies and possibly for progression of other neurodegenerative diseases (Costanzo and Zurzolo, 2013). The prion domain of the yeast proteins Ure2 and Sup35 are rich in glutamine and asparagine residues (Q/N-rich) (Ter-Avanesyan *et al.*, 1994; Masison and Wickner, 1995). New prion domains have been identified and even engineered based on this property (Michelitsch and Weissman, 2000; Harrison and Gerstein, 2003; Alberti *et al.*, 2009; Toombs *et al.*, 2012). Several “amyloid-like” mechanisms, that are not heritable and “prion-like mechanisms”, that involve self-propagation of a conformational change but do not strictly require amyloid formation, have also been reported (Gilks *et al.*, 2004; Adda *et al.*, 2009; Hou *et al.*, 2011; Kato *et al.*, 2012; Majumdar *et al.*, 2012).

It is becoming apparent that the propensity to propagate ordered structures by prions and prion-like domains plays a role in several biological processes (Newby and Lindquist, 2013). A large fraction of prion-domain containing proteins are transcriptional factors and mRNA binding proteins (Michelitsch and Weissman, 2000). Several stress granule and P-body components, which sequester mRNAs for their storage and decay, contain Q/N and Q-

rich domains. Aggregation through these sequences is required for granule assembly (Gilks *et al.*, 2004; Vessey, 2006; Decker *et al.*, 2007). In a recent study, the aggregation of the Whi3 mRNP through its Q-rich domain was demonstrated to regulate cyclin transcript localization (Lee *et al.*, 2013). Amyloid transformation can also act as an activation switch. The kinase domains of RIP1 and RIP3 aggregate into amyloid fibers for phosphorylation of downstream substrates inducing necrosis upon *Vaccinia* infection (Li *et al.*, 2012). Finally, in microbial communities, prion switching and propagation may serve as an efficient bet-hedging mechanism, compared to genetic mutations. Prion formation in a fraction of the cells may create heritable, phenotypic diversity, allowing survival of some cells under harsh environmental conditions (Newby and Lindquist, 2013). 1.69% of ORFs in *S. cerevisiae* and approximately 0.3% in humans encode proteins with potential prion domains (Michelitsch and Weissman, 2000; Osherovich and Weissman, 2002). Several of these proteins are annotated as integral or plasma membrane (Harrison and Gerstein, 2003). Whether prion domains could regulate their membrane transport remains an exciting possibility.

4. Aim of the study

The discharge of the yeast chitin synthase III, Chs3, at the plasma membrane is regulated in response to cell cycle and stress cues. Under physiological conditions Chs3 has a polarized localization. Rather than being controlled at the protein level, Chs3 is shuttled between the plasma membrane and internal compartments to allow its spatially and temporally restricted plasma membrane expression. The exomer complex mediates the timely export of Chs3 from the TGN. To date, there are only two confirmed exomer cargoes, Fus1, which is only expressed during mating and the chitin synthase Chs3. To further elucidate the role of the exomer complex in regulated protein trafficking, we employed the novel exomer cargo, Pin2, identified by Mark Trautwein in the lab to:

1. Define a general transport pattern for exomer cargoes. Chs3 has specific trafficking requirements. Apart from exomer mediated TGN export, it depends on endocytosis to maintain its polarized localization, it is retrieved from early endosomes to the TGN in an AP-1 dependent manner and also undergoes reversible posttranslational modifications such as palmitoylation and ubiquitylation, which regulate its trafficking. We wanted to test, whether Pin2 would have the same trafficking requirements.
2. Identify sorting signals for exomer-binding and interaction with other transport machineries. Chs3 is a large protein with six predicted transmembrane domains. Pin2 is only 282 residues long and has a single TMD, making it a much more tractable candidate for such studies.
3. Study exomer-cargo interaction based on binding studies with the Pin2 cytosolic domain.
4. Gain further insight into the significance of the exomer complex in yeast physiology by defining Pin2 function.
5. Investigate the role of the Pin2 prion domain in its transport.

5. Chs5, ChAP, and Chs3 cargo interaction

5. The complex interaction of Chs5p, the ChAPs and the cargo Chs3p.

The following manuscript was submitted to *Molecular Biology of the Cell* and was accepted on September 18, 2012. The following authors have contributed to the manuscript.

Uli Rockenbauch performed the experiments represented in figures: 1; 2; 3 B-D; 4; 6; 7 A-C; 8 A-D; Suppl. Figs. S1-S3. He wrote parts of the manuscript and provided critical comments on the rest.

Alicja Ritz performed the experiments represented in figures: 3A; 5; 7 D and E; 8 E; 9; 10 Suppl. Figs. S3 D and S4. She wrote parts of the manuscript and provided critical comments on the rest.

Carlos Sacristan performed the initial experiments on the C-terminal truncations of Chs3 (Fig. 6.8, A and B).

Cesar Roncero provided critical comments on the manuscript.

Anne Spang supervised the experiments and wrote the manuscript.

The complex interactions of Chs5p, the ChAPs, and the cargo Chs3p

Uli Rockenbauch^a, Alicja M. Ritz^a, Carlos Sacristan^b, Cesar Roncero^b, and Anne Spang^a

^aBiozentrum, Universität Basel, 4056 Basel, Switzerland; ^bInstituto de Biología Funcional and Departamento de Microbiología y Genética, Consejo Superior de Investigaciones Científicas/Universidad de Salamanca, 37008 Salamanca, Spain

ABSTRACT The exomer complex is a putative vesicle coat required for the direct transport of a subset of cargoes from the *trans*-Golgi network (TGN) to the plasma membrane. Exomer comprises Chs5p and the ChAPs family of proteins (Chs6p, Bud7p, Bch1p, and Bch2p), which are believed to act as cargo receptors. In particular, Chs6p is required for the transport of the chitin synthase Chs3p to the bud neck. However, how the ChAPs associate with Chs5p and recognize cargo is not well understood. Using domain-switch chimeras of Chs6p and Bch2p, we show that four tetratricopeptide repeats (TPRs) are involved in interaction with Chs5p. Because these roles are conserved among the ChAPs, the TPRs are interchangeable among different ChAP proteins. In contrast, the N-terminal and the central parts of the ChAPs contribute to cargo specificity. Although the entire N-terminal domain of Chs6p is required for Chs3p export at all cell cycle stages, the central part seems to predominantly favor Chs3p export in small-budded cells. The cargo Chs3p probably also uses a complex motif for the interaction with Chs6, as the C-terminus of Chs3p interacts with Chs6p and is necessary, but not sufficient, for TGN export.

Monitoring Editor

Benjamin S. Glick
University of Chicago

Received: Dec 15, 2011

Revised: Sep 17, 2012

Accepted: Sep 18, 2012

INTRODUCTION

The *trans*-Golgi network (TGN) is the central sorting station for exocytic and endocytic cargoes. In the yeast *Saccharomyces cerevisiae*, several sorting machineries and vesicular carriers operate along at least two routes to the cell surface, marked by high-density or low-density secretory vesicles (Harsay and Bretscher, 1995; Harsay and Schekman, 2002; Bard and Malhotra, 2006). In addition,

a subset of cargoes travels directly to the plasma membrane in low-density carriers, a subset of which require the exomer complex. This complex is a potential coat complex formed by the peripheral Golgi protein Chs5p and a protein family termed ChAPs, for Chs5p- and Arf1p-binding proteins. In budding yeast, this family includes the paralogues Chs6p, Bud7p, Bch1p, and Bch2p (Ziman *et al.*, 1998; Sancharjate and Schekman, 2006; Trautwein *et al.*, 2006; Wang *et al.*, 2006). Chs5p and the ChAPs are recruited from the cytosol to the TGN membrane by the small GTPase Arf1p. Together, they facilitate the incorporation of specific transmembrane cargoes into secretory vesicles (Trautwein *et al.*, 2006; Wang *et al.*, 2006).

Some specialized cargoes, such as chitin synthase III (Chs3p) or Fus1p, depend on exomer for their transport to the cell surface (Santos and Snyder, 1997; Ziman *et al.*, 1998; Barfield *et al.*, 2009). However, Chs3p and Fus1p do not share a common sorting motif (Barfield *et al.*, 2009), suggesting that the exomer complex recognizes cargoes individually, perhaps in order to allow differential sorting. This provides an attractive model system for a protein trafficking pathway that is distinct from the major transport routes, allowing the cell to fine tune the surface expression of cargoes depending on

This article was published online ahead of print in MBoC in Press (<http://www.molbiolcell.org/cgi/doi/10.1091/mbc.E11-12-1015>) on September 26, 2012.

A.S. and U.R. conceived the study, U.R. and A.D. performed the experiments (U.R.: Figures 1, 2; 3, B–D; 4; 6; 7, A–C; and 8, A–D; and Supplemental Figures S1–S3; A.D.: Figures 3A; 5; 7, D and E; 8E; 9; and 10; and Supplemental Figures S3D and S4), C.S. and R.C. contributed the Chs3 truncations and the information that this was an interaction site, A.S., U.R., and A.D. wrote the manuscript, and all authors commented on the manuscript.

Address correspondence to: Anne Spang (anne.spang@unibas.ch).

Abbreviations used: TGN, *trans*-Golgi network; TPR, tetratricopeptide repeat; TM, transmembrane.

© 2012 Rockenbauch *et al.* This article is distributed by The American Society for Cell Biology under license from the author(s). Two months after publication it is available to the public under an Attribution–Noncommercial–Share Alike 3.0 Unported Creative Commons License (<http://creativecommons.org/licenses/by-nc-sa/3.0>).

“ASCB®,” “The American Society for Cell Biology®,” and “Molecular Biology of the Cell®” are registered trademarks of The American Society of Cell Biology.

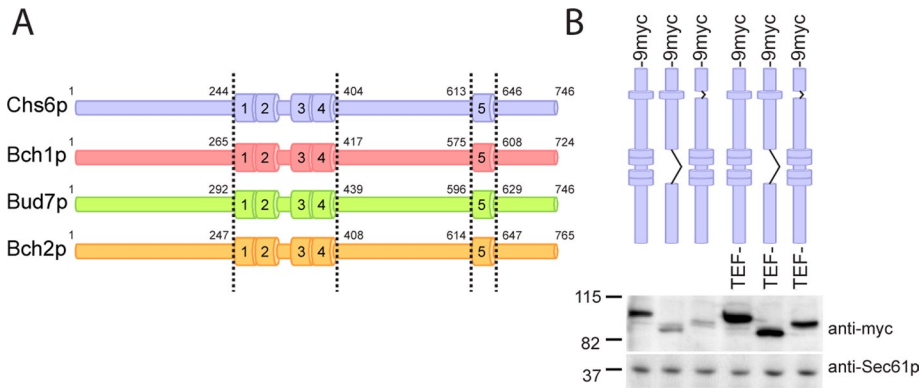


FIGURE 1: Deletion of TPRs in ChAPs only mildly affects protein expression levels. (A) Domain structure of the ChAP family members. Numbers indicate the first and last amino acid of the TPR domains. The same coloring scheme is used in all subsequent figures. (B) Expression of yeast lysates; Sec61p serves as loading control. Note that all mutants were generated chromosomally.

the cell cycle stage or potentially also in response to the nutrient status and/or stress conditions.

The exomer components display a functional hierarchy. Whereas individual ChAP deletions—or combinations thereof—lead to certain cellular defects, a deletion of *CHS5* collectively causes all ChAPs-associated defects (Trautwein *et al.*, 2006). Given that these phenotypes are most likely due to the inability of specific cargoes to leave the TGN, this places Chs5p functionally upstream of the ChAPs. For example, $\Delta chs6$ cells cannot export Chs3p and thus have chitin synthesis defects, whereas $\Delta bch1$ cells are sensitive to ammonium (Trautwein *et al.*, 2006). Accordingly, cells lacking *CHS5* are both chitin deficient and ammonium sensitive. Interestingly, Chs3p export is also blocked when *BCH1* and *BUD7* are simultaneously deleted, suggesting that the ChAPs have partially overlapping functions. Alternatively, the ChAPs may also play a structural role in exomer complex assembly.

Chs5p requires activated Arf1p for TGN recruitment, whereas the ChAPs require both Chs5p and Arf1p, reflecting the functional hierarchy. The ChAPs do not coprecipitate in the absence of Chs5p, suggesting that they do not directly bind to each other (Sanchatjate and Schekman, 2006; Trautwein *et al.*, 2006). How Chs5p and the ChAPs associate into a complex has not been investigated in detail. Because of their association with distinct cargoes, it is believed that the ChAPs act as soluble receptors for transmembrane cargoes. However, their mode of cargo recognition has not been characterized.

In this study, we performed a functional analysis of the ChAP Chs6p and found that the ChAP family members contain five essential tetratricopeptide repeats (TPRs), four of which are required for binding to Chs5p and other ChAPs. Export from the TGN and bud-neck localization of the Chs6p-dependent cargo Chs3p were dependent on extended Chs6p-specific sequences outside of the TPRs, suggesting an extensive interaction between Chs3p and Chs6p. The N-terminal 244 amino acids (aa) were required for Chs3p export early and late in the cell cycle, whereas the central part (aa 405–612) was specifically engaged in Chs3p transport early in the cell cycle. Similarly, we found that the C-terminal part of Chs3p bound to Chs6p. Although this interaction was necessary for Chs3p export from the TGN, it was not sufficient, as transplanting the signal onto another protein did not make this protein an exomer-dependent cargo.

RESULTS

The ChAPs contain tetratricopeptide repeats

The ChAPs appear to interact directly with exomer-dependent cargoes. To gain a better understanding of how cargo recognition and the interaction with other exomer components are achieved, we decided to examine the domain structure of the ChAPs. To this end, we performed a BLASTP search of the *S. cerevisiae* ChAP *CHS6* against other fungal genomes. The resulting alignment showed that particular stretches of the protein were highly conserved across species, whereas other sequences were more variable (Supplemental Figure S1A). We expected the more conserved stretches to correspond to domains essential for function, whereas the sequences with a higher degree of variation might represent parts of the protein that are not involved in functions

specific to the ChAPs family. Alternatively, those variable domains could be engaged in cargo recognition, because the cargoes studied thus far, Fus1p and Chs3p, do not share obvious motifs that are commonly recognized by all ChAPs (Barfield *et al.*, 2009).

To analyze the conserved regions in more detail, we used a number of different algorithms of the Bioinformatics Toolkit (<http://toolkit.tuebingen.mpg.de>; Biegert *et al.*, 2006). Interestingly, the conserved regions contained tetratricopeptide repeats (TPRs; Figure 1A), four of which were clustered in the central region of Chs6p, with a fifth one located toward the C-terminus. The TPRs were conserved among the different *S. cerevisiae* ChAPs, indicating that they may represent a common feature of this protein family (Figure 1A and Supplemental Figure S1B). This hypothesis is supported by the finding that automatic sequence annotation detected TPRs in ChAPs from *Kluyveromyces lactis*, *Ashbya gossypii*, and others (see, e.g., National Center for Biotechnology Information, www.ncbi.nlm.nih.gov/protein/CAG98421.1).

TPRs are highly versatile protein–protein interaction domains. Each repeat consists of a degenerate 34–amino acid motif, which exhibits a conserved helix–turn–helix fold and the ability to form clusters of multiple repeats (Blatch and Lassle, 1999; Zhang *et al.*, 2010). Interestingly, several cases of cargo recognition by TPRs have been described: peroxin 5, which harbors a six-TPR tunnel recognizing the C-terminal SKL motif for peroxisomal import (Gatto *et al.*, 2000); Tom20, which facilitates mitochondrial import (Abe *et al.*, 2000); and kinesin light chain, which binds multiple cargoes via its TPR domain (Kamal *et al.*, 2000; Hammond *et al.*, 2008). Alternatively, TPRs can also have more-structural roles, for example, in the assembly of multiprotein complexes such as the COPI vesicle coat (Hsia and Hoelz, 2010) or the anaphase-promoting complex (Zhang *et al.*, 2010). Thus finding TPRs in the ChAPs family members raised the possibility that these repeats would be of functional importance for the exomer complex and could potentially provide protein–protein interaction surfaces.

The TPRs are essential for Chs6p function

The TPRs in the ChAPs might serve either as interaction modules for other exomer components or as cargo recognition sites. To distinguish between these possibilities, we created two internal truncations in Chs6p. The first truncation, Chs6(Δ TPR1-4), lacked the entire central cluster of TPRs. In the second construct, Chs6(Δ TPR5), the last and most conserved repeat in the protein was deleted

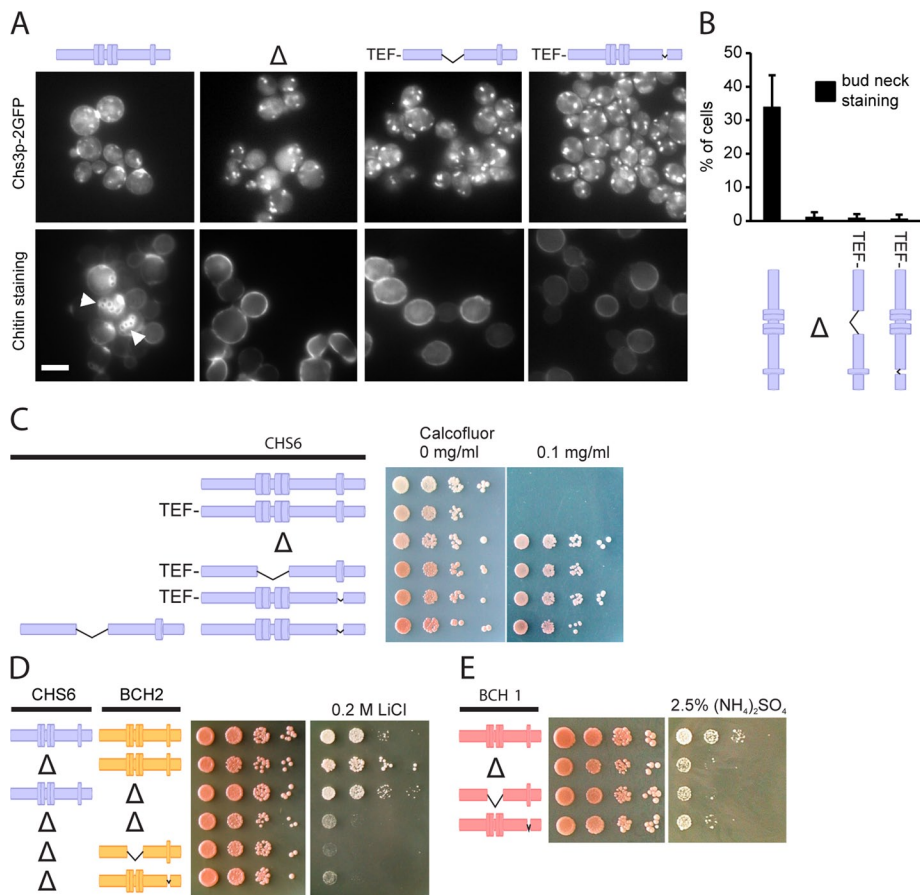


FIGURE 2: The TPRs are essential for the function of the ChAPs. (A) Chs3p-2GFP localized exclusively to internal structures in $\Delta chs6$, Chs6($\Delta TPR1-4$), and Chs6($\Delta TPR5$) strains. Accordingly, whereas calcofluor-stained wild-type cells showed bud scar chitin staining (arrowheads), this was absent in the mutants. Scale bar, 5 μ m (B) Quantification of results in A. Graph shows an average of three experiments. Bud-neck staining was scored for the entire cell population in at least 100 cells per experiment. Bars, SD. (C) Chs6($\Delta TPR1-4$) and Chs6($\Delta TPR5$) strains were resistant to calcofluor. This defect was as pronounced as for a $\Delta chs6$ strain. The two mutant alleles showed no cross-complementation. Drop tests: plates were incubated at 30°C for 2–3 d. Blue, Chs6p alleles. Δ refers to $\Delta chs6$. (D) Bch2p requires TPRs for functionality. A CHS6 deletion in combination with a $\Delta bch2$, Bch2($\Delta TPR1-4$), or Bch2($\Delta TPR5$) allele led to lithium sensitivity. Drop tests were performed as described. Yellow, Bch2p alleles. Δ refers to $\Delta chs6$ and $\Delta bch2$, respectively. (E) Bch1p requires TPRs for functionality. Bch1($\Delta TPR1-4$) and Bch1($\Delta TPR5$) cells, like $\Delta bch1$, were sensitive to ammonium. Red, Bch1p alleles. Δ refers to $\Delta bch1$.

(Figure 1A). The mutant proteins showed only a mild reduction in expression compared with wild type, indicating that removing one or more TPRs did not cause the protein to be largely unfolded and hence degraded (Figure 1B). The truncations did not massively shorten the proteins. Removing TPR1–4 reduced the molecular weight by ~15 kDa, and eliminating TPR5 caused a 5-kDa reduction. To have consistently comparable expression levels, we decided to replace the endogenous promoter in all cases by the somewhat stronger TEF promoter (Figure 1B).

To assess the functionality of Chs6($\Delta TPR1-4$) and Chs6($\Delta TPR5$), we monitored the localization and activity of Chs3p, whose TGN export depends on functional Chs6p. Both truncation mutants were unable to export Chs3p-2 GFP from the TGN, as GFP staining was absent from the bud neck and Chs3p accumulated in intracellular structures, mimicking a CHS6 deletion (Figure 2, A and B). Chs3p synthesizes a chitin ring around the yeast bud neck, which can be visualized by calcofluor staining (Lord et al., 2002). The chitin ring was absent in $\Delta chs6$, Chs6($\Delta TPR1-4$), and Chs6($\Delta TPR5$) (Figure 2A and Table 1). All three

mutants were calcofluor resistant, a hallmark of chitin synthesis-defective cells (Ziman et al., 1998), demonstrating a lack of chitin synthase III activity at the plasma membrane (Figure 2C).

The ChAPs form complexes with Chs5p in varying stoichiometries (Trautwein et al., 2006). We therefore wondered whether the truncations, when expressed together, could cross-complement and rescue the calcofluor sensitivity. However, this was not the case, indicating that each Chs6p molecule must contain the full set of TPR motifs (Figure 2C). In summary, these findings demonstrate that the TPRs of Chs6p are required for export of Chs3p from the TGN.

TPR function is conserved in the ChAPs

ChAPs share some degree of redundancy, indicated by the fact that some cellular phenotypes only arise upon deletion of multiple ChAPs (Trautwein et al., 2006; Barfield et al., 2009). For example, double deletion of CHS6 and BCH2 renders cells lithium sensitive, a phenotype that could not be observed for either single deletion (Figure 2D). This finding implicates Chs6p in the export of another, yet-unidentified, cargo involved in lithium homeostasis.

We used this paradigm to test whether the TPRs in other ChAPs might be of equal importance for function. Indeed, Bch2($\Delta TPR1-4$ or $\Delta TPR5$), combined with a CHS6 deletion, also displayed the lithium-sensitivity phenotype (Figure 2D). Moreover, we constructed analogous truncation mutants in Bch1p and tested these for ammonium sensitivity, which is a characteristic phenotype of $\Delta bch1$ cells (Trautwein et al., 2006). Both TPR mutants behaved like the BCH1 deletion (Figure 2D), indicating that at least three (Chs6p, Bch2p, Bch1p) of the four ChAPs require their TPRs for functionality.

Chs6p requires its TPRs for efficient Golgi recruitment

The strong defect of the TPR mutants in cargo export could be explained by impaired recruitment of the mutant proteins to the Golgi, failure to form a productive exomer–cargo complex, or a combination of both. We therefore tested first whether the TPRs were required for Golgi association and determined the subcellular localization of the TPR mutants using differential centrifugation. Chs6($\Delta TPR1-4$)-9myc and Chs6($\Delta TPR5$)-9myc were depleted from the fractions containing Golgi membranes and were found almost exclusively in the cytosol (Figure 3A).

To corroborate our findings, we also monitored the localization of the truncations by live imaging. A 3xGFP-tagged version of wild-type Chs6p mostly localized to punctate structures, which overlapped with the TGN marker Sec7p-dsRed (Figure 3B). As previously observed, some Chs6p-3GFP was also found in the cytoplasm (Ziman et al., 1998; Trautwein et al., 2006). Consistent with the in vitro fractionation, in vivo, both Chs6($\Delta TPR1-4$)-3GFP and Chs6($\Delta TPR5$)-3GFP were not efficiently recruited to the TGN, as

Chs6p mutant	Name	Calcofluor sensitivity	Chs3p export	TGN localization	Cargo binding	Complex assembly
	WT	+	+	+	+	+
	Chs6(ΔTPR1-4)	-	-	-	+	-
	Chs6(ΔTPR5)	-	-	+/-	+	+
	Chs6(LG-WD)	-	-	N.D.	+	N.D.
	Chs6(ΔC13)	-	N.D.	-	+	-

Chimeras	Transplanted domain(s)	Calcofluor sensitivity	Chs3p export
Chs6p with transplanted domains from Bch2p			
	TPR1-4	+	+
	TPR5	+	+
	CD	-	-
	NT1 (aa 1-77)	-	-
	NT2 (aa 78-164)	-	-
	NT3 (aa 165-246)	-	-
	CD1 (aa 409-464)	-	+/-
	CD2 (aa 465-563)	-	+/-
	CD3 (aa 564-613)	+	+
Bch2p with transplanted domains from Chs6p			
	TPR5	-	-
	CD	-	-
	NT + TPR1-4 + CD	-	-
	CD + TPR5 + CT	-	-
	NT + CD + CT	+/-	+

Shaded boxes: data added from previous work (Trautwein et al., 2006).

TABLE 1: Summary of results for Chs6p mutants used in the study.

Chs6(ΔTPR1-4)-3GFP was found entirely in the cytoplasm, whereas a minor fraction of Chs6(ΔTPR5)-3GFP was present at the TGN (Figure 3, B and C). Thus all five TPRs contribute to efficient Golgi recruitment, whereby TPRs 1-4 seem to play a more predominant role.

TPR1-4 are required for interaction with Chs5p and other ChAPs

We showed previously that the ChAPs require Chs5p for steady-state Golgi localization (Trautwein et al., 2006). Therefore, we asked next whether Chs5p interaction was also impaired in the TPR mutants and whether this was the cause of the cytoplasmic localization of the mutants. Chs6(ΔTPR1-4) could not be coprecipitated with Chs5p (Figure 4A), indicating that the lack of this interaction might

be the cause of the cytoplasmic localization of Chs6(ΔTPR1-4). In contrast, Chs5p and Chs6(ΔTPR5) coprecipitated, suggesting that TPR5 is not involved in Chs5p binding.

Chs6p copurifies with Bch1p in a Chs5p-dependent manner (Sancharjate and Schekman, 2006). Thus we expected that Chs6(ΔTPR5) would still bind to other ChAPs, whereas Chs6(ΔTPR1-4) would not. Alternatively, TPR5 of Chs6p could interact with the TPR5 of other ChAPs. Chs6(ΔTPR1-4), but not Chs6(ΔTPR5), specifically failed to interact with Bch1p (Figure 4B). Similarly, Bud7p bound to Chs6(ΔTPR5) but not Chs6(ΔTPR1-4) (Supplemental Figure S2). These results suggest that the ChAPs require their first four TPRs for the association with Chs5p and thus for assembly into a complex with other exomer components.

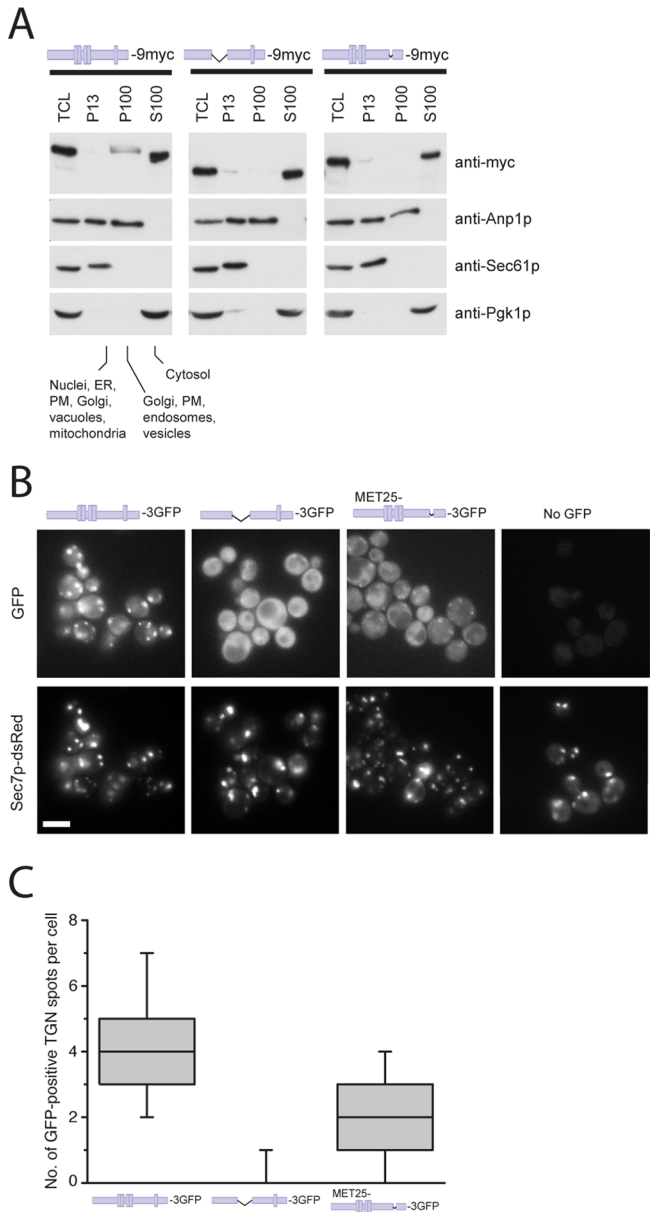


FIGURE 3: Chs6(ΔTPR1-4) and Chs6(ΔTPR5) cannot be efficiently recruited to the Golgi. (A) Chs6(ΔTPR1-4)-9myc and Chs6(ΔTPR5)-9myc display a reduced membrane association in cell lysates. Ten OD₆₀₀ of cells were spheroplasted, regenerated, and subsequently lysed in hypotonic buffer. Lysates were cleared of unbroken cells and subjected to differential centrifugation at 4°C. TCL, total cell lysate; P13, 13,000 × g pellet; S100, 100,000 × g supernatant; P100, 100,000 × g pellet; PM, plasma membrane. All constructs were chromosomally expressed under the native *CHS6* promoter. (B) TPR mutants show inefficient Golgi localization in vivo. Chs6p-3GFP and Chs6(ΔTPR1-4)-3GFP were chromosomally expressed under the native *CHS6* promoter. Chs6(ΔTPR1-4)-3GFP was almost entirely cytoplasmic and showed no association with Golgi membranes. Chs6(ΔTPR5)-3GFP, expressed at a level similar to wild-type Chs6p using an inducible methionine promoter, was partially Golgi localized (arrowheads). Scale bar, 5 μm. (C) Quantification of results in B. Graph shows a total of three experiments. At least 95 cells were scored per experiment; only budded cells were used for scoring; only GFP dots overlapping with Sec7-dsRed were considered as TGN. Drawn with Origin software (OriginLab, Northampton, MA). Lower whisker represents 5th percentile; box represents 25th, 50th, and 75th percentiles; upper whisker represents 95th percentile.

The TPRs are dispensable for cargo recognition

Chs6p interacts with both Chs5p and the cargo Chs3p, and Chs5p is required for Chs6p binding to Chs3p (Trautwein *et al.*, 2006; Figure 5A). Because the cargo interaction site in the ChAPs is not known and TPRs mediate protein–protein interactions, we tested whether the TPRs would be involved in this process. The binding between a cargo and its cargo receptor is usually rather transient (Appenzeller *et al.*, 1999; Muniz *et al.*, 2000; Zhang *et al.*, 2005). To “freeze” the interaction, we performed immunoprecipitations after chemical cross-link from yeast lysates. This approach has been used previously to detect exomer–cargo interactions (Sanchatjate and Schekman, 2006; Trautwein *et al.*, 2006; Barfield *et al.*, 2009). Interestingly, both TPR mutants were efficiently cross-linked to Chs3p (Figure 5, C and D), indicating that the potential to recognize cargo in vitro was not strongly impaired in Chs6(ΔTPR1-4) or Chs6(ΔTPR5). This result was somewhat unexpected because in the wild-type situation Chs6p requires the presence of Chs5p to interact efficiently with Chs3p in vitro (Trautwein *et al.*, 2006; Figure 5D). Yet, Chs6(ΔTPR1-4) did not bind Chs5p and interacted with cargo independent of the presence of Chs5p. These findings would indicate that cargo binding and Chs5p interaction are separable in Chs6p but that Chs5p may negatively influence cargo binding by weakening the receptor–cargo interaction. To test this hypothesis, we used another truncation of Chs6p, one in which the C-terminal 13 amino acids were deleted (Chs6(ΔC13)). This truncation fails to bind Chs5p and cannot be recruited to the Golgi apparatus (Trautwein *et al.*, 2006). Again, like the TPR mutants, Chs6(ΔC13) still bound Chs3p (Supplemental Figure S3D). Taken together, our data suggest that Chs5p binding to Chs6p decreases the stability of Chs6p–cargo interaction.

So far we used deletions of the different TPRs. Despite the small size of the deletions, they still may change the structure of the protein and hence influence the binding. To less disturb the overall structure, we constructed a point mutant, Chs6p-L619W/G620D (LG-WD), in which two critical residues of the TPR5 backbone were mutated (Magliery and Regan, 2004) but the protein was otherwise left intact. As expected, this mutant also caused Chs3p-2GFP to accumulate in the TGN and was calcofluor resistant (Supplemental Figure S3, A–C). Again, this protein also interacted with Chs3p in vitro (Figure 5C). Therefore, the results presented so far indicate no major role of the TPRs in cargo recognition and specificity.

The TPRs are interchangeable among the ChAPs

We have shown thus far that TPRs 1–4 are required for interaction with Chs5p and other ChAPs and that neither TPR1–4 nor TPR5 appeared to play a major role in cargo recognition. To corroborate our results, we aimed to least disturb the structure of the protein and constructed chromosomally chimeric mutants of the ChAPs. If the TPRs perform functions that are conserved among the ChAPs, such as Chs5p binding, they should be interchangeable between two different ChAPs. If the TPRs perform a specific function, such as cargo recognition, the TPR chimera should be nonfunctional. We chose *CHS6* and *BCH2* for these experiments because the functionality of Chs6p could be monitored easily by both Chs3p localization and chitin synthesis. Bch2p, on the other hand, is entirely dispensable for Chs3p traffic. As expected, transplantation of TPR1–4 or TPR5 from *BCH2* to *CHS6* had no effect on calcofluor sensitivity or Chs3p localization (Figure 6), demonstrating that Chs6p chimera carrying the alien TPR1–4 or TPR5 were indeed functional. Thus the TPRs in Chs6p are most likely not required for cargo recognition.

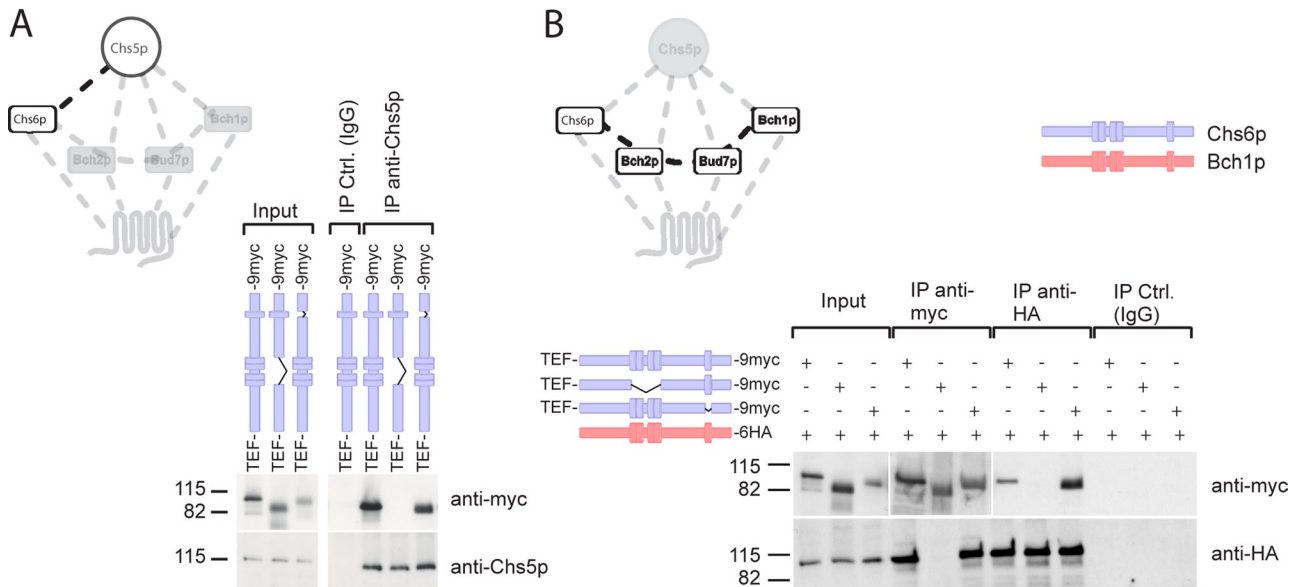


FIGURE 4: Chs6(Δ TPR1-4) fails to interact with other exomer components. (A) Chs6(Δ TPR1-4) failed to bind to Chs5p, whereas Chs6(Δ TPR5) still interacted. Coimmunoprecipitation experiments were performed using an anti-Chs5p antibody and lysates generated from cells expressing chromosomally tagged Chs6(Δ TPR1-4)-9myc or Chs6(Δ TPR5)-9myc. (B) Chs6(Δ TPR1-4) also failed to coprecipitate with other ChAPs, such as Bch1p. Blue, Chs6p alleles; red, Bch1p alleles. Two different exposures were cropped together because of the strong signal of the precipitated myc-tagged constructs.

Cargo specificity of the ChAPs is not conveyed by a simple linear sequence

Because the TPRs were not involved in cargo specificity, we asked next where the cargo recognition site was located in Chs6p and how cargo specificity was achieved. We again used our chimera approach to address these questions and concentrated on the regions outside the TPRs (Figure 7A and Supplemental Figure S4). First, we exchanged the central domain (CD, located between TPR4 and TPR5) of Chs6p for the CD of Bch2p. This strain did not export Chs3p from the TGN and was calcofluor resistant, suggesting that this chimeric Chs6p was unable to recognize Chs3p as a cargo (Figure 7B). However, the inverse experiment—transplantation of the corresponding region from *CHS6* to *BCH2*—did not change the cargo specificity of Bch2p and failed to rescue Δ *chs6* defects, indicating that the central domain of the ChAPs is necessary but not sufficient to convey cargo specificity (Figure 7C). Strikingly, similar results were obtained when we individually exchanged longer sequences, like the C-terminal half (aa 409–765) of Bch2p or even the N-terminus, TPR1–4, and the central domain together (aa 1–613) for the homologous sequences in Chs6p. These results were not due to a positioning effect in the genome, because insertion of the full-length *CHS6* ORF into the *BCH2* locus restored Chs3p export and calcofluor sensitivity (Figure 7C). Moreover, the chimeric constructs were expressed and stable (unpublished data). In summary, these results suggest that the N-terminal, central, and C-terminal domains were necessary for cargo specificity, but none was sufficient by itself. In fact, only transplanting all corresponding sequences except for TPR1–4 and TPR5 restored Chs3p bud-neck localization and reduced calcofluor resistance to close to wild-type levels (Figure 7C). These data suggest a model in which the TPRs provide the interaction surface for Chs5p, whereas the sequences outside of these repeats may be involved in cargo recognition.

To test this hypothesis, we divided each of the N-terminus and the central domain again into three smaller regions and replaced

them individually by the corresponding sequences from Bch2p (Figure 7A). All substitutions in the N-terminal region caused Chs3p to be in internal structures and conferred resistance to calcofluor (Figure 7, D and E), indicating that indeed large parts of the N-terminal region of Chs6p are involved in Chs3p export. In contrast, we could narrow down the region in the central domain necessary for Chs3p export. The truncation in which aa 557–612 (closest to TPR5) had been swapped showed Chs3p localization similar to the wild-type control, and the strain was sensitive to calcofluor (Figure 7, D and E). Of importance, the other two chimera of the central domain mislocalized Chs3p only early in the cell cycle (Figure 7, D and E). The bud-neck localization of Chs3p in large-budded cells (late in the cell cycle) was mostly achieved in these strains. Consistently, the calcofluor resistance was reduced. These data imply a general role for the Chs6p N-terminus in cargo transport, whereas parts of the central domain would be required only early in the cell cycle and dispensable for transport late in the cell cycle.

Chs6p interacts with the C-terminus of Chs3p

Although we could assign parts in Chs6 that were involved in cargo recognition, the size of the area—especially the N-terminal region—seemed to make it unlikely to identify a small motif that would provide the interaction site with Chs3p. On the other hand, we might be able to identify individual parts of Chs3p required for the interaction with Chs6p, similar to the short, linear motif in Fus1p that binds to exomer (Barfield *et al.*, 2009). Because the topology of Chs3p is still disputed (Cos *et al.*, 1998; Meissner *et al.*, 2010), and even the number of transmembrane (TM) domains is debated—varying between four and eight—we decided to focus on the C-terminal part of Chs3p. Cos *et al.* (1998) generated two C-terminal truncations that rendered the cells calcofluor resistant (Figure 8A), suggesting a defect in either Chs3p function or localization. Interestingly, we found that GFP-tagged versions of these mutant proteins failed to reach the cell surface and were retained at the TGN,

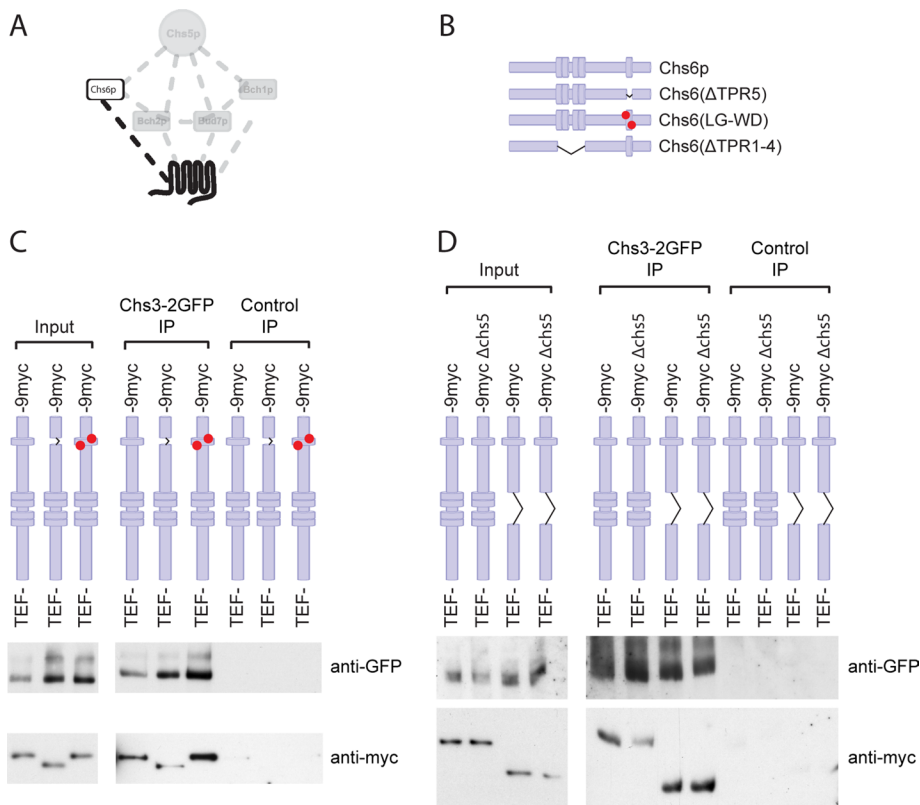


FIGURE 5: TPRs are not required for stable association with cargo. (A) Schematic representation of the interaction between the cargo, Chs3p, and the exomer–cargo recognition subunit, Chs6p. (B) Chromosomally generated Chs6p TPR mutants. (C) Chs6(Δ TPR5) and Chs6(LG-WD) interact with cargo. To assess cargo interaction, Chs3p-2GFP was precipitated from DSP cross-linked lysates with anti-GFP monoclonal antibodies, and the precipitates were probed for different Chs6p constructs. Control immunoprecipitations were performed using monoclonal HA antibody. Chs6(Δ TPR5) and a double TPR5 point mutant Chs6(LG-WD) retained association with Chs3p. (D) Chs6(Δ TPR1-4) interacts with Chs3p and does so independently of Chs5p, the core exomer subunit. The cross-linker immunoprecipitation was performed as described in B.

indicated by colocalization with Sec7p-dsRed (Figure 8B). These results suggest that the C-terminal 21 amino acids of Chs3p might be important for binding of the exomer complex and thus for incorporation into secretory vesicles.

We therefore performed GST pull-down experiments using the C-terminal cytoplasmic tail of Chs3p, which has a total length of 55 amino acids following the last predicted TM domain. The corresponding truncation constructs lacked the final 21 and 37 amino acids, respectively. Immobilized GST fusion proteins were then incubated with whole-cell lysate and analyzed for binding of Chs6p. Chs6p-9myc bound to full-length glutathione S-transferase (GST)-Chs3CT but not to GST alone, GST-Chs3CT(Δ 21), or GST-Chs3CT(Δ 37) (Figure 8, C and D). Consistently, the Chs3p tail truncations did also not bind to Chs6(TPR1-4) and Chs6(TPR5) (Figure 8E). This result suggests that the Chs3p C-terminus contains an exomer recognition site, which is necessary for Chs6p binding *in vitro* and for Chs3p export *in vivo*. This site is likely to be located within the last 21 amino acids, as the Δ 21 mutation was sufficient to abolish Chs3p transport to the cell surface and abrogate Chs6 binding.

We next tested whether the C-terminal tail would be sufficient to drive TGN export and bud-neck localization of another, unrelated protein. For this, we replaced the C-terminus of the TGN/endosome-localized Kex2p protease with the one of Chs3p (Figure 9A), similar to the approach used for Fus1p (Barfield *et al.*, 2009). The

Chs3p C-terminal tail was not sufficient to cause export of Kex2 Δ C-Chs3CT-GFP to the plasma membrane in either the presence or absence of Chs5p (Figure 9). Yet Kex2p localization was partially altered, as some of it accumulated in the vacuolar lumen, an effect that was not entirely due to the removal of the Kex2p endogenous C-terminus, as Kex2 Δ C-GFP was most predominantly found on the vacuolar rim. One possible explanation of the difference in localization of both constructs is that Kex2 Δ C-Chs3CT-GFP could be exported to the plasma membrane and was then rapidly endocytosed. However, inhibiting endocytosis by the Δ end3 mutation did not alter the localization of Kex2 Δ C-Chs3CT-GFP (Figure 9B), indicating that this construct does not reach the plasma membrane; it might still become a substrate for the ESCRT complex and be included into the intraluminal vesicles of the late endosome.

Taken together, these results suggest that although the C-terminus of Chs3p is necessary and sufficient to interact, albeit weakly, with Chs6p, it is not sufficient to drive the plasma membrane localization of another protein. Therefore, it is likely that other motifs in Chs3p exist that contact Chs6p and that these combined interactions temporally control the export of Chs3p from the TGN.

DISCUSSION

The late secretory pathway controls the trafficking of proteins to the cell surface and the endosomal system, but how the multitude of cargoes is correctly sorted to control their spatial and temporal localization is not well understood. In recent years, the exomer complex, comprising Chs5p and the ChAPs family, has emerged as a crucial sorting determinant for a subset of cargoes (Santos and Snyder, 1997, 2003; Trautwein *et al.*, 2006). However, little is known about how exomer assembles at the TGN and recognizes specific cargo proteins. To gain insight into the exomer function and cargo interaction, we performed a structure–function analysis of the ChAP Chs6p. We chose Chs6p because it has one well-established cargo, the chitin synthase Chs3p, and is required for proper Chs3p localization at the bud neck early and late in the cell cycle (Zanolari *et al.*, 2011).

The search for conserved structural motifs yielded a cluster of four TPRs in the center and one TPR toward the C-terminus of all ChAPs. TPR1–4 were required for interaction with Chs5p and other ChAPs, as well as for localization to the Golgi, probably through the interaction with Chs5p. In contrast, the fifth TPR, which is the most conserved one by sequence among the ChAPs, probably does not interact with Chs5p or other ChAPs directly and is not actively involved in cargo recognition. However, this TPR is still necessary for efficient Golgi recruitment. Because at least three TPRs appear to be necessary for biological relevant functions, that is, to serve as protein–protein interaction scaffolds (D’Andrea and Regan, 2003; Zeytuni and Zarivach, 2012), it is conceivable that the single TPR5 would contact TPR1–4. In this scenario, either TPR5 itself or a

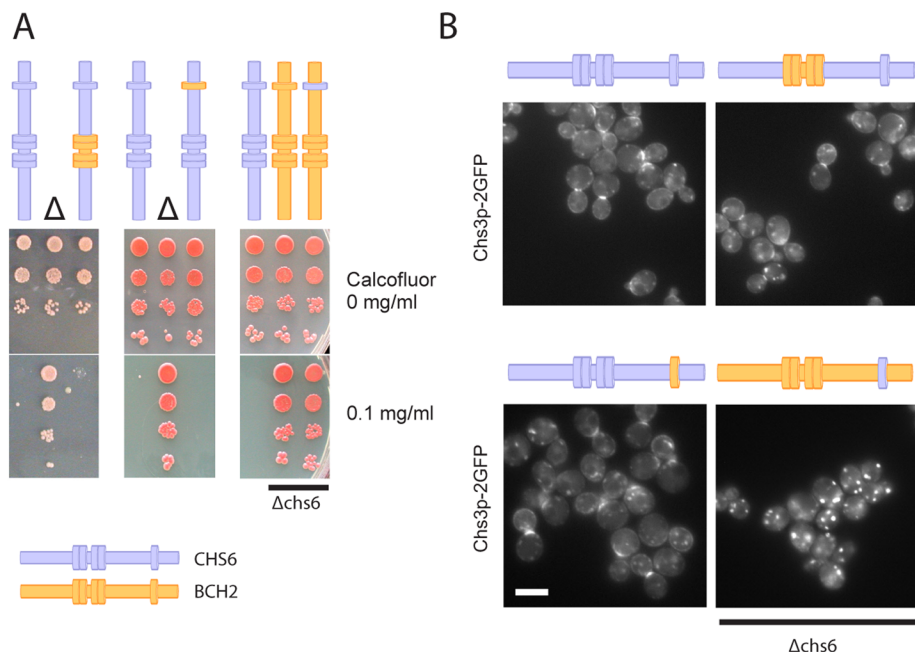


FIGURE 6: The TPRs are interchangeable among ChAPs. (A) Chs6p bearing either TPR1–4 or TPR5 from Bch2p is fully functional. Chimeras in which TPRs from *CHS6* were grafted into *BCH2* (or vice versa) were created by *delitto perfetto*. Drop tests for calcofluor sensitivity were performed as in Figure 2. Transplanting TPR5 from Chs6p to Bch2p did not restore calcofluor sensitivity in a Δ *chs6* background. Blue, Chs6p domains; yellow, Bch2p domains. Δ refers to Δ *chs6*. (B) Live fluorescence imaging of Chs3p-2GFP in the chimeras shown in A confirmed that the TPRs do not contribute to cargo specificity. Scale bar, 5 μ m.

then-exposed sequence would interact with a thus-far-unknown factor at the Golgi to stabilize the TGN localization of ChAPs.

Interestingly, deletions in either TPR1–4 or TPR5 were still able to interact with Chs3p in an *in vitro* cross-linking approach, indicating that in both cases the ability of cargo recognition was maintained and the lack of steady-state localization of these truncations to the TGN was the reason for the defect in exporting Chs3p to the plasma membrane. It is intriguing that Chs6 Δ TPR1–4 was reproducibly more efficiently cross-linked to Chs3p than wild-type Chs6p *in vitro*, even in the absence of Chs5p. Because TPR1–4 are essential for the interaction with Chs5p, it is tempting to speculate that Chs5p, and potentially other ChAPs, may regulate the binding affinity of the Chs6p to the cargo. The affinity of the cargo and its receptor needs to be relatively low to allow readily dissociation of the cargo–receptor complex after either inclusion into the transport carrier or upon release at the target compartment. Although we cannot exclude a regulatory role of the TPRs in cargo binding, they are dispensable for cargo specificity: transplanting TPRs from Bch2p, which has no role in Chs3p trafficking, did not cause mislocalization of Chs3p, hence excluding a function in specific cargo recognition. This was a bit surprising at first because TPRs interact with their ligands through a combination of factors, such as hydrophobic pockets, residue type, charge, and electrostatics (Zeytuni and Zarivach, 2012), and we assumed that these repeats were uniquely suited to recognize a variety of cargoes that do not share sequence homology and are structurally very different, such as Chs3p and Fus1p. Instead, we find that cargo specificity and recognition are located outside the TPRs and are most likely rather complex (Figure 10). Our data indicate that Chs6p-specific sequences from the N-terminus, the central domain, and the C-terminus are involved in the spatial and temporal control of Chs3p localization. In an attempt to narrow down these allegedly large areas, we found that among the N-terminal 246

amino acids there must be many residues that are required for Chs3p export from the TGN and do not form a short linear motif. This analysis made it essentially impossible to go on to define a specific motif that would comprise the Chs3p-binding pocket because our chimera analysis would instead suggest that the folding of the N-terminus would provide a platform or binding pocket for at least part of Chs3p.

Although replacing the entire central domain of Chs6p by Bch2p sequences caused Chs6p to be nonfunctional in terms of Chs3p transport, systematic replacement of parts of the central domain revealed that amino acids 409–563, which are located just downstream of TPR1–4, have a cell cycle–specific role in Chs3p export; they are only required early in the cell cycle. This finding is consistent with the notion that traffic of Chs3p is differentially regulated in the cell cycle (Zanolari *et al.*, 2011). Thus, Chs3p may also contact the central domain of Chs6p for transport. The cell cycle–specific requirements may be due to the posttranslational modifications known to occur in Chs3p (Peng *et al.*, 2003; Valdivia and Schekman, 2003; Lam *et al.*, 2006), some of which could be cell cycle–dependent. Alternatively, accessory proteins might specifically control

the formation of the exomer–Chs3p complex at the TGN in a cell cycle–dependent manner. The reason we favor a second interaction site for Chs3p in the central domain is based on the findings that, first, replacing the entire central domain by Bch2p inhibits Chs3p export from the TGN throughout the cell cycle and, second, the N-terminus of Chs6p is not sufficient to drive export of Chs3p from the TGN. Our data indicate that there is even a third interaction site in the C-terminal region of Chs6p, as we need to transplant sequences from all three regions outside of the TPRs for efficient transport of Chs3p to the bud neck. In principle, our data would be consistent with two models: the first would suggest the presence of three individual binding sites/surfaces for Chs3p, each of which would be necessary but not sufficient. Alternatively, at least two if not all three regions would come together in the folded three-dimensional molecule and present one or two large interaction surfaces. At this point, we cannot distinguish between these two possibilities. However, we can exclude that a simple binding pocket provided by Chs6p that would bind one particular sequence of Chs3p would be sufficient for productive complex formation causing Chs3p plasma membrane localization. We identified a sequence in the C-terminus of Chs3p required for its TGN export, which bound weakly but specifically to Chs6p. Still, this sequence was not sufficient to cause an unrelated protein to become an exomer substrate or to be plasma membrane localized. The idea that the ChAPs do not just require a simple, linear sequence was suggested by Barfield *et al.* (2009), who found that a necessary exomer–interaction sequence was not sufficient to transform a nonexomer cargo into an exomer-dependent cargo. Yet in this case the interpretation was complicated by the simultaneous requirement of two different ChAPs for the transport of Fus1p. Moreover, the Fus1p motif is not contained in Chs3p, and the Chs3p tail is not matched by a homologous sequence in Fus1p. In this study, we were able to extend this notion to a more complex

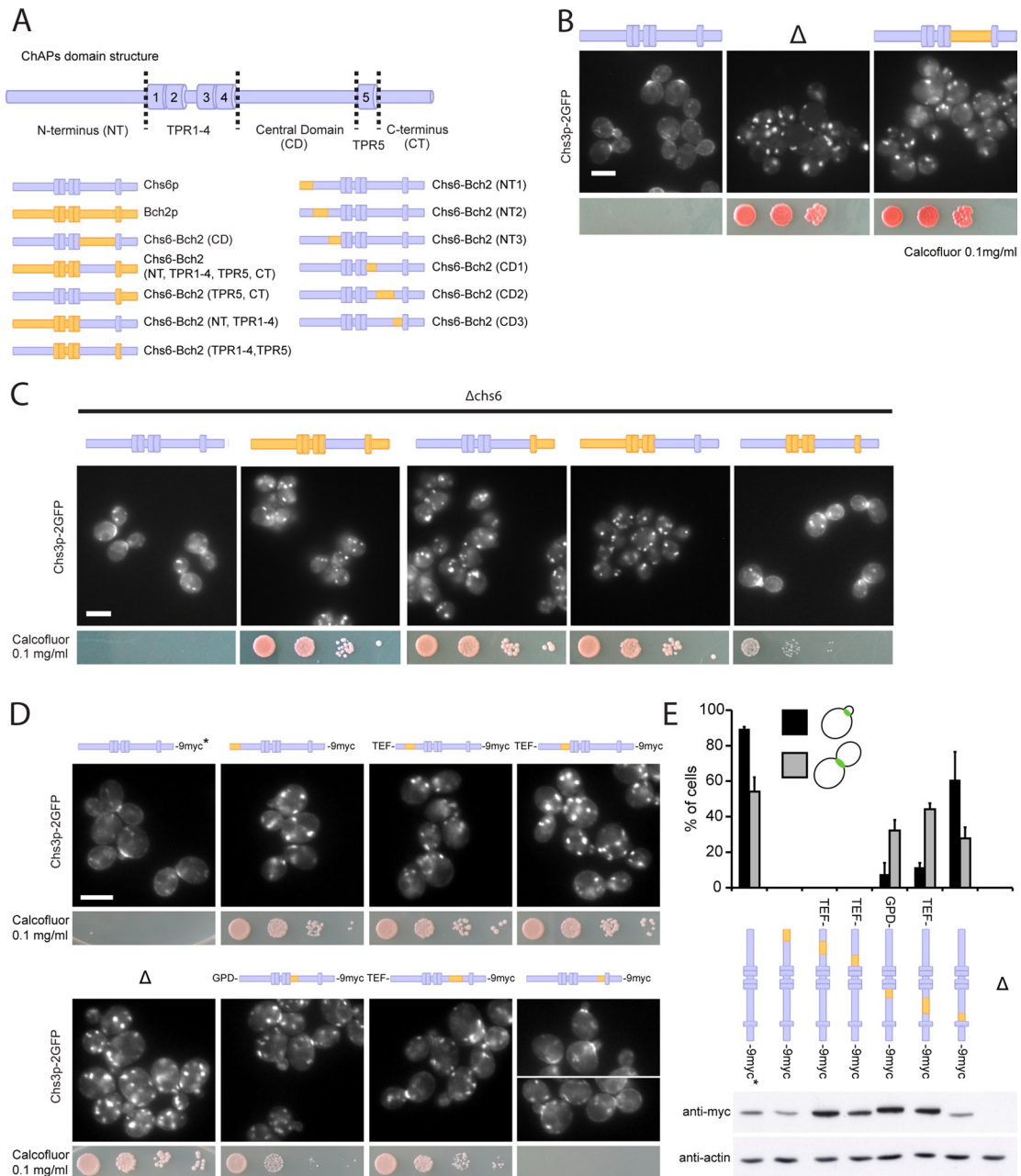


FIGURE 7: The N-terminus, central domain, and C-terminus of the ChAPs are individually necessary and only together sufficient to convey cargo specificity. (A) Schematic representation of ChAPs domain structure and Chs6p-Bch2p chromosomal chimera constructs. (B) The central domain (CD) of the ChAPs is required for cargo specificity. Chimeric Chs6p bearing the CD of Bch2p was unable to export Chs3p-2GFP and rendered cells calcofluor resistant, like a Δ chs6 strain. Chimeras were created by *delitto perfetto*. Blue, Chs6p domains; yellow, Bch2p domains. Δ refers to Δ chs6. Drop assays were performed as in Figure 2. Scale bar, 5 μ m. (C) The N-terminus (NT), CD, and C-terminus (CT) are necessary and together sufficient to determine cargo specificity. In a Δ chs6 background, calcofluor sensitivity was restored by reintroduction of the CHS6 full-length open reading frame into the BCH2 locus but not by transplantation of the following domains from Chs6p to Bch2p: CD, NT + TPR1–4 + CD, or CD + TPR5 + CT. Transplantation of NT, CD, and CT together restored Chs3p export to the bud neck (by ~82% compared with wild-type cells). Scale bar, 5 μ m. (D) Chs3p bud-neck export requires the entire Chs6p N-terminal domain and the majority of the central domain, the latter only early in the cell cycle. Transplantation of short Bch2p NT fragments into Chs6p resulted in exclusive localization of Chs3p-2GFP to internal structures and calcofluor resistance. Transplantation of two short Bch2p CD fragments (aa 409–464 and 465–563), but not the fragment containing aa 564–613, proximal to TPR5 resulted in severely compromised Chs3p cargo export in small-budded cells. Several chimera constructs were expressed chromosomally under the TEF or GPD promoter to achieve protein levels comparable to that of wild-type Chs6p. Drop assays were performed as in Figure 2. Scale bar, 5 μ m. (E) Quantification of results in D and expression levels of particular chimera constructs. Graph shows a total of three experiments. Bud-neck staining was scored in 100 small-budded cells (G1/S phase) and 100 large-budded cells (M phase) in each experiment. Bars, SD. Actin serves as a loading control in immunoblot of yeast lysates. Chs6p in wild-type control used in microscopy studies in D and E is untagged, as indicated by the asterisk.

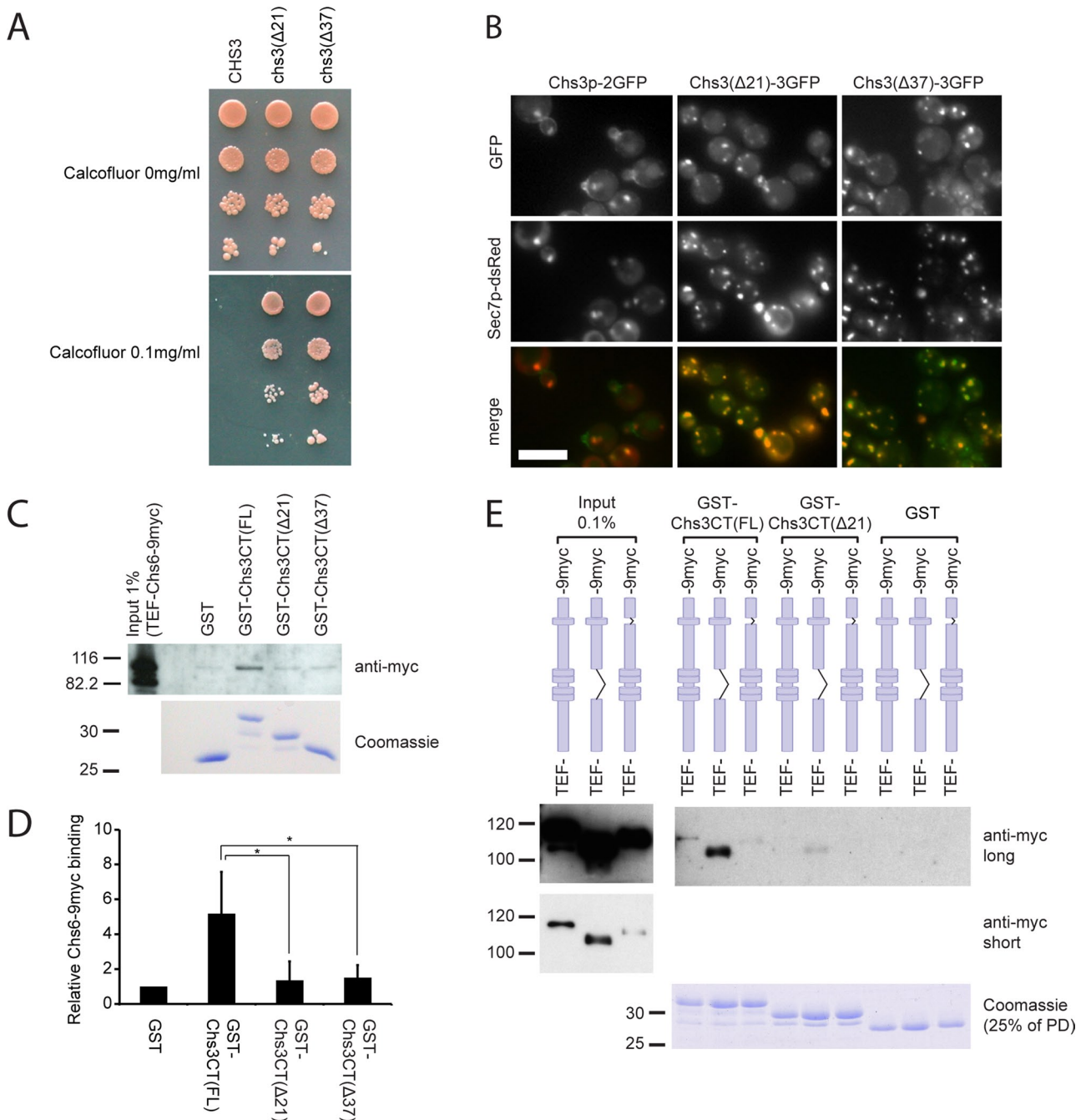


FIGURE 8: The C-terminus of Chs3p contains an exomer-binding site required for Golgi export. (A) The last 21 amino acids of Chs3p are essential for chitin synthesis. Cells expressing Chs3p lacking the C-terminal 21 or 37 amino acids were calcofluor resistant. (B) The C-terminus of Chs3p is required for Golgi export. Chromosomally generated Chs3(Δ 21)-3GFP or Chs3(Δ 37)-3GFP was trapped in internal membranes and colocalized with the TGN marker Sec7p-dsRed. Scale bar, 5 μ m. (C) Chs6p binds to the C-terminus of Chs3p. Lysates from cells expressing Chs6p-9myc were incubated with immobilized GST, GST fused to the C-terminus of Chs3p (FL), or truncated C-terminal constructs (Δ 21 and Δ 37). Chs6p-9myc bound to the full C-terminus, but binding to the truncations was abolished. (D) Quantification of results in C. Graph shows an average of three experiments. The integrated density of Chs6-9myc bands in GST-Chs3CT pull-downs was measured using ImageJ software and normalized to that in the GST pull-down. Bars, SD. * $p < 0.05$. (E) Chs6(Δ TPR1-4)-9myc TPR mutant efficiently binds to the Chs3p C-terminus. GST pull-downs were performed as in C with lysates from cells expressing Chs6(Δ TPR1-4)-9myc or Chs6(Δ TPR5)-9myc.

interaction mode between the ChAPs and their cargo. We showed that large interaction surface(s) and multiple sequences on both the cargo receptor and the cargo are required for cargo export through the exomer-dependent pathway.

Why would the ChAPs have evolved to recognize complex trafficking motifs? One could speculate that similar to the Sec23/24 complex of the COPII coat at the endoplasmic reticulum, a multitude of cargoes have to be transported (Kuehn and Schekman,

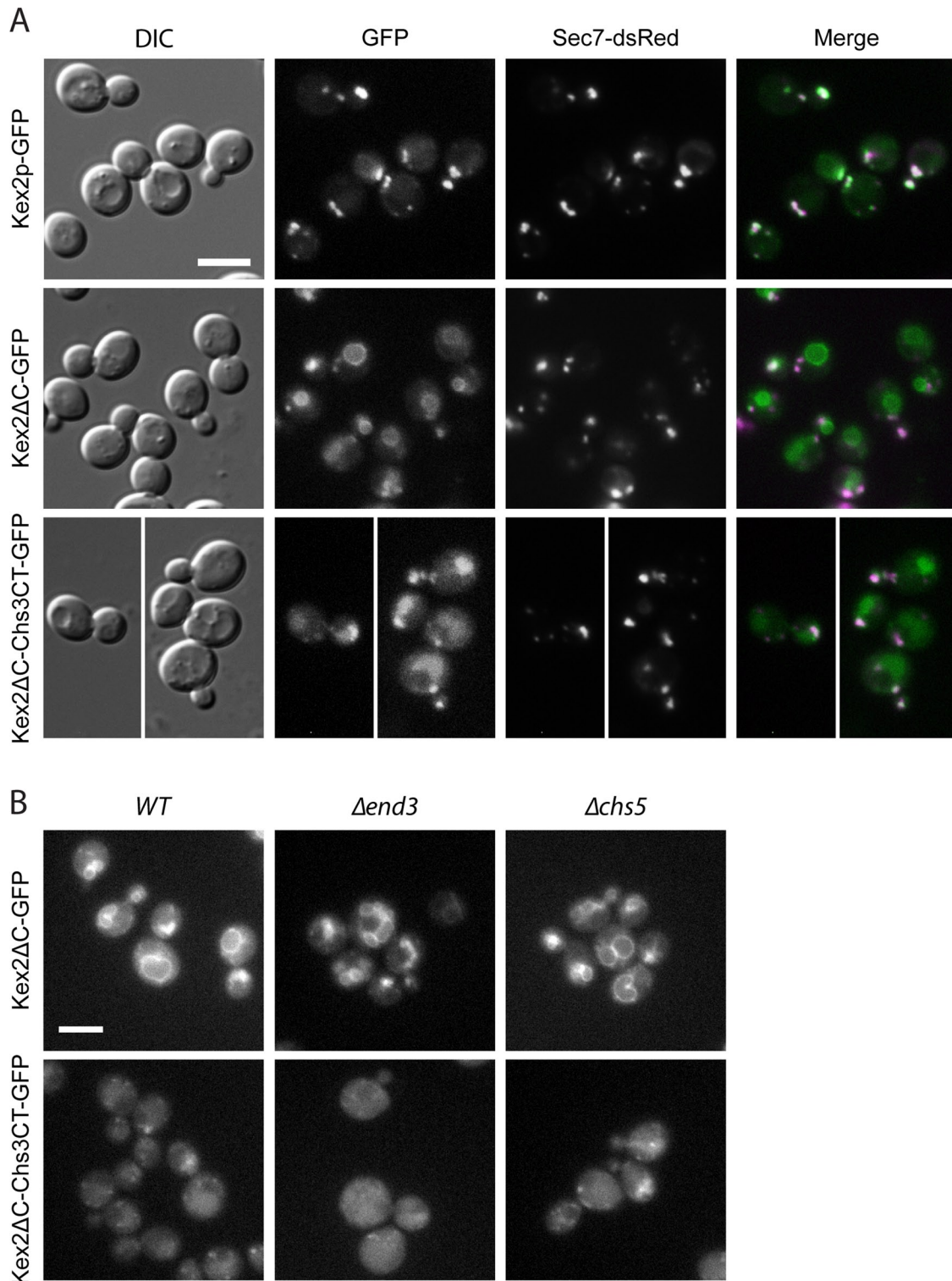


FIGURE 9: (A) The C-terminus of Chs3p is not sufficient for exomer-dependent cargo export. Replacement of the cytosolic domain of Kex2p, a TGN-resident protein, with the Chs3p C-terminus did not direct Kex2ΔC-Chs3CT-GFP to the plasma membrane. Kex2ΔC-Chs3CT-GFP was localized to the vacuolar lumen, whereas Kex2ΔC-GFP localized to the vacuolar rim, indicating an influence of the Chs3p C-terminus on Kex2p sorting. Kex2-GFP, C-terminally truncated Kex2ΔC-GFP, and the Kex2ΔC-Chs3CT-GFP chimera were chromosomally expressed. Sec7-dsRed was used as a TGN marker. Scale bar, 5 μ m. (B) Kex2ΔC-Chs3CT-GFP does not traffic to the plasma membrane, and its localization is exomer independent. To assess potential trafficking through the plasma membrane, the localization of chromosomally expressed Kex2ΔC-GFP and the Kex2ΔC-Chs3CT-GFP was assessed in a $\Delta end3$, endocytosis-deficient strain. Kex2ΔC-GFP and Kex2ΔC-Chs3CT-GFP exomer-dependent localization was assessed in a $\Delta chs5$ strain. Scale bars, 5 μ m.

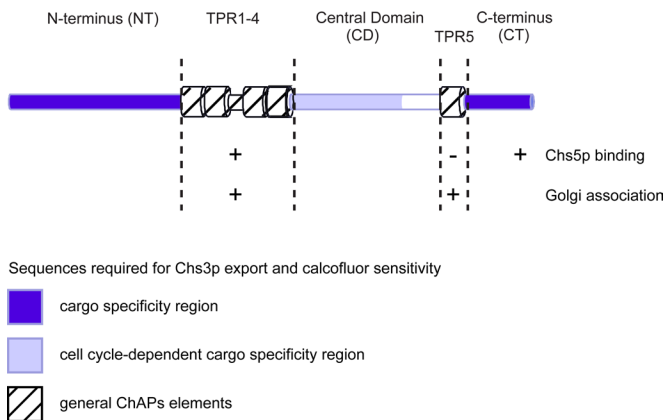


FIGURE 10: Summary scheme of Chs6p domains and their function in regard to cargo-specific interaction, interaction with Chs5p, the core exomer subunit, and TGN recruitment.

1997; Kurihara *et al.*, 2000; Miller *et al.*, 2002, 2003) and therefore large interaction surface or multiple binding sites might be useful. However, the exomer-dependent transport route is not the major export pathway from the TGN. In fact, only two clients for the exomer route have been identified (Sanchatjate and Schekman, 2006; Trautwein *et al.*, 2006; Barfield *et al.*, 2009). Thus the purpose might be different: Chs3p and Fus1p are both proteins that require temporal and spatial regulation of their transport. Therefore, exomer-dependent cargoes may have a very specific role at the plasma membrane that would require a relatively tight control of discharge at the plasma membrane and subsequent endocytosis. At least Chs3p requires endocytic recycling for proper bud-neck localization (Reyes *et al.*, 2007; Sacristan *et al.*, 2012). However, $N = 1$ is obviously too tiny a data set to allow general conclusions. Therefore, the identification and characterization of other exomer-dependent cargoes will shed more light on the function and selectivity of the exomer complex.

MATERIALS AND METHODS

Strains and growth conditions

Yeast strains used in this study are listed in Supplemental Table S1. Standard yeast media were prepared as described (Sherman, 1991). Calcofluor plates were based on minimal medium containing additionally 0.1% yeast extract, 1% 2-(*N*-morpholino)ethanesulfonic acid buffer, pH 6.0, and 0.1 mg/ml Calcofluor White (Sigma-Aldrich, St. Louis, MO).

Yeast genetic methods

Standard genetic techniques were used throughout (Sherman, 1991). Chromosomal tagging and deletions were performed as described (Knop *et al.*, 1999; Gueldener *et al.*, 2002). For C-terminal tagging with 3xGFP, the plasmid pYM-3GFP was used (Zanolari *et al.*, 2011). All PCR-based chromosomal manipulations were confirmed by analytical colony PCR. The Sec7p-dsRed plasmid (pTPQ128) was described previously (Proszynski *et al.*, 2005). Marker-free chromosomal deletions were performed using the *delitto perfetto* method (Storici and Resnick, 2006) and confirmed by sequencing. Genetic chimeras were constructed using a modified version of the same technique: After insertion of the CORE cassette, the desired foreign genetic element was amplified from genomic DNA using chimeric primers, which were homologous to the 45 base pairs upstream and downstream of the *delitto perfetto* site. This PCR product was then directly used for

transformation, thus recombining with the locus and replacing the CORE cassette.

Western blot detection

Epitope tags and proteins were detected using the following antibodies: anti-myc (9E10, 1:1000; Sigma-Aldrich); anti-hemagglutinin (HA; HA11, 1:1000; Eurogentec, Seraing, Belgium); anti-FLAG (M2, 1:1000; Sigma-Aldrich); anti-Chs5p (affinity purified, 1:500); anti-Chs3p (affinity purified, 1:1000); anti-GFP (1:5000, Torrey Pines Biolabs, Secaucus, NJ; or anti-GFP 7.1 and 13.1, 1:500, Roche, Indianapolis, IN); anti-Pgk1 (#A-6457, 1:1000; Invitrogen), anti-Anp1p (1:1000 working solution supplemented with extract from $\Delta anp1$ yeast cells; a gift from S. Munro, MRC Laboratory of Molecular Biology, Cambridge, United Kingdom), and anti-Sec61p serum (1:10,000; a gift from M. Spiess, Biozentrum Basel, Basel, Switzerland). ECL (GE Healthcare, Piscataway, NJ) was used for detection.

For myc epitope detection in cross-linker immunoprecipitation experiments and GST pull-downs, anti-myc 9E10 (1:4000; Sigma-Aldrich) and TrueBlot anti-mouse horseradish peroxidase secondary antibody (1:2500; eBioscience, San Diego, CA) were used, and ECL Advance (GE Healthcare) was used for detection according to the manufacturer's instructions.

Microscopy

Cells were grown to log phase in rich or selective medium supplemented with adenine, then harvested, washed, and mounted. Images were acquired with an AxioCam mounted on a Zeiss Axioplan 2 fluorescence microscope (Carl Zeiss, Jena, Germany), using filters for GFP, dsRed, or 4',6-diamidino-2-phenylindole.

Chitin staining was carried out as described (Lord *et al.*, 2002). Briefly, cells grown for at least 16 h to late log phase were stained after formaldehyde fixation in 1 mg/ml calcofluor, washed three times in water, and imaged directly.

Subcellular fractionation

Ten OD₆₀₀ of mid-log cells were incubated in 1 ml of dithiothreitol (DTT) buffer (10 mM Tris, pH 9.4, 10 mM DTT) for 5 min at 30°C, spun down, and resuspended in 1 ml of SP buffer (75% yeast extract, peptone [YP], 0.7 M sorbitol, 0.5% glucose, 10 mM Tris, pH 7.5). Thirty microliters of zymolyase T20 (10 mg/ml) was added, and the cells were spheroplasted at 30°C for 40 min. Cells were washed once in zymolyase-free SP buffer, resuspended in the same buffer, and incubated at 30°C for 30 min. Regenerated cells were gently spun down and lysed in 1 ml of 50 mM Tris, pH 7.5, 1 mM EDTA, 50 mM NaCl, and protease inhibitors by pipetting up and down. The lysate was cleared at 500 × *g* for 2 min, and the supernatant ("total cell lysate" [TCL]) subjected to centrifugation at 13,000 × *g* (10 min). The supernatant (S13) was carefully taken off with a pipette and subjected to centrifugation at 100,000 × *g* (1 h). Both pellets (P13 and P100) were rinsed with lysis buffer and then resuspended in 1 ml of lysis buffer. All steps were carried out at 4°C. Samples were taken from all final fractions and subjected to immunoblot analysis.

Coimmunoprecipitation

Yeast lysates from 10 OD₆₀₀ of cells were prepared by spheroplasting as described. Spheroplasts were sedimented (2 min, 1000 × *g*), lysed in B150Tw20 buffer (20 mM 4-(2-hydroxyethyl)-1-piperazineethanesulfonic acid [HEPES], pH 6.8, 150 mM K acetate (Ac), 5 mM Mg(Ac)₂, and 1% Tween-20) with protease inhibitors, and cleared by centrifugation (10 min, 16,000 × *g*). Immunoprecipitations were performed with 5 μg of affinity-purified rabbit immunoglobulin

G (Dianova, Hamburg, Germany), 5 µg of affinity-purified anti-Chs5p antibody, 5 µg of anti-HA (HA.11; Eurogentec), 5 µg of anti-myc (9E10; Sigma-Aldrich), or 5 µg of anti-AU5 (Abcam, Cambridge, MA) and 100 µl of 20% protein A–Sepharose per 1 ml of cleared lysate for 1 h at 4°C. The beads were washed and resuspended in sample buffer, and bound proteins were analyzed by immunoblot.

Cross-linker immunoprecipitation

For each sample, 10 OD₆₀₀ of yeast cells were resuspended in 220 µl of B88 buffer (20 mM HEPES, pH 6.8, 150 mM KAc, 5 mM Mg(Ac)₂, 250 mM sorbitol) with protease inhibitors and subjected to FastPrep lysis (MP Biomedicals, Illkirch, France). The lysate was cleared by centrifugation at 13,000 × g for 5 min at 4°C. DSP (2 mM final concentration; Pierce, Rockford, IL) dissolved in dimethyl sulfoxide was added to 140 µl of lysate. The cross-linking reaction took place for 30 min at room temperature and was stopped with 7 µl of 1 M Tris (pH 7.5) for 15 min. Then 8 µl of 20% SDS was added, and the sample was incubated at 65°C for 15 min. A 1.35-ml amount of IP buffer (50 mM Tris/HCl, pH 7.5, 150 mM NaCl, 1% TX-100, 1 µg/µl bovine serum albumin) was added, and the sample was centrifuged for 10 min at 16,000 × g. The supernatant was subjected to immunoprecipitation overnight at 4°C using 5 µg of monoclonal anti-GFP antibody (clones 7.1 and 13.1; Roche) cross-linked to protein A–Sepharose with DMP. Control immunoprecipitations with 5 µg of monoclonal anti-HA antibody (HA.11 clone 16B12; Covance, Berkeley, CA) were performed in parallel. Precipitates were washed once in 50 mM Tris/HCl, pH 7.5, 150 mM NaCl, 1% TX-100, and 0.1% SDS and twice in the same buffer containing 250 mM NaCl. Precipitates were resuspended in 50 mM Tris/HCl, pH 7.5 and 250 mM NaCl and transferred into new tubes. The washed precipitates were incubated at 65°C for 30 min in SDS sample buffer containing 100 mM DTT and analyzed by immunoblot. Alternatively, extracts were prepared by bead lysis, and immunoprecipitations were performed with 5 µg of affinity-purified anti-Chs3p antibody.

BLAST analysis and TPR prediction

The Chs6p primary protein sequence was subjected to fungal BLAST search (available at *Saccharomyces* Genome Database, www.yeastgenome.org) using the default settings of the BLASTP algorithm on all available fungal nuclear genomes, excluding *S. cerevisiae*. TPRs were predicted with the TPRPRED algorithm (Karpenahalli *et al.*, 2007), using the standard settings.

GST pull-downs

The C-terminal full-length tail of Chs3p or C-terminally truncated versions ($\Delta 21$ and $\Delta 37$) were cloned into pGEX-6P-1 using *EcoRI* and *XhoI* restriction sites. The full-length tail comprised the last 55 aa following the last predicted TM domain, whereas truncations of this tail lacked the C-terminal 21 and 37 aa, respectively. Expression in Rosetta *Escherichia coli* cells was induced by the addition of 1 mM isopropyl- β -D-thiogalactoside and growth in Luria Broth (LB) medium at 37°C for 4 h. Cells were lysed in phosphate-buffered saline (PBS)/5% glycerol, and GST fusions were purified with glutathione (GSH) agarose (Sigma-Aldrich), eluted with 40 mM GSH, and dialyzed against PBS/5% glycerol.

GST and GST-tagged Chs3p C-terminus were bound to GSH agarose. For each sample, 10 OD₆₀₀ of yeast cells were resuspended in 250 µl of B88 buffer with protease inhibitors and subjected to bead lysis or resuspended in 220 µl of B88 buffer and subjected to fast prep lysis. Yeast lysates were diluted six times in B150Tw20 to a final protein concentration of approximately 0.5 µg/µl. The lysates were incubated with the coupled resin for 1 h at 4°C. The beads

were washed twice with B150Tw20 buffer and once with B150Tw20 buffer supplemented with 150 mM NaCl and then resuspended in 40 µl of SDS sample buffer, followed by incubation at 95°C for 10 min. Bound proteins were analyzed by immunoblot.

For quantification of Chs6-9myc binding to full-length or truncated C-terminal Chs3p tails. Images of scanned blots were inverted, and intensity values were determined for each band using ImageJ (National Institutes of Health, Bethesda, MD) by drawing a box of fixed size around each band and using the “integrated density” function. Each band was background corrected against the intensity value of the gel lane (below the band). Absolute values were then normalized relative to GST.

ACKNOWLEDGMENTS

We thank B. Zanolari and M. Trautwein for their initial observation of the lithium-sensitivity phenotype and M. Spiess and S. Munro for the anti-Sec61p and anti-Anp1p sera, respectively. We also thank all members of the Spang lab for technical advice and helpful discussion. This work was supported by a graduate student fellowship of the Werner Siemens Foundation to U.R., the University of Basel (A.S.), and the Swiss National Science Foundation (A.S.).

REFERENCES

- Abe Y, Shodai T, Muto T, Mihara K, Torii H, Nishikawa S, Endo T, Kohda D (2000). Structural basis of presequence recognition by the mitochondrial protein import receptor Tom20. *Cell* 100, 551–560.
- Appenzeller C, Andersson H, Kappeler F, Hauri HP (1999). The lectin ERGIC-53 is a cargo transport receptor for glycoproteins. *Nat Cell Biol* 1, 330–334.
- Bard F, Malhotra V (2006). The formation of TGN-to-plasma-membrane transport carriers. *Annu Rev Cell Dev Biol* 22, 439–455.
- Barfield RM, Fromme JC, Schekman R (2009). The exomer coat complex transports Fus1p to the plasma membrane via a novel plasma membrane sorting signal in yeast. *Mol Biol Cell* 20, 4985–4996.
- Biegert A, Mayer C, Remmert M, Soding J, Lupas AN (2006). The MPI Bioinformatics Toolkit for protein sequence analysis. *Nucleic Acids Res* 34, W335–W339.
- Blatch GL, Lassle M (1999). The tetratricopeptide repeat: a structural motif mediating protein-protein interactions. *Bioessays* 21, 932–939.
- Cos T, Ford RA, Trilla JA, Duran A, Cabib E, Roncero C (1998). Molecular analysis of Chs3p participation in chitin synthase III activity. *Eur J Biochem* 256, 419–426.
- D’Andrea LD, Regan L (2003). TPR proteins: the versatile helix. *Trends Biochem Sci* 28, 655–662.
- Gatto GJ Jr, Geisbrecht BV, Gould SJ, Berg JM (2000). Peroxisomal targeting signal-1 recognition by the TPR domains of human PEX5. *Nat Struct Biol* 7, 1091–1095.
- Gueldener U, Heinisch J, Koehler GJ, Voss D, Hegemann JH (2002). A second set of loxP marker cassettes for Cre-mediated multiple gene knockouts in budding yeast. *Nucleic Acids Res* 30, e23.
- Hammond JW, Griffin K, Jih GT, Stuckey J, Verhey KJ (2008). Co-operative versus independent transport of different cargoes by kinesin-1. *Traffic* 9, 725–741.
- Harsay E, Bretscher A (1995). Parallel secretory pathways to the cell surface in yeast. *J Cell Biol* 131, 297–310.
- Harsay E, Schekman R (2002). A subset of yeast vacuolar protein sorting mutants is blocked in one branch of the exocytic pathway. *J Cell Biol* 156, 271–285.
- Hsia KC, Hoelz A (2010). Crystal structure of alpha-COP in complex with epsilon-COP provides insight into the architecture of the COPI vesicular coat. *Proc Natl Acad Sci USA* 107, 11271–11276.
- Kamal A, Stokin GB, Yang Z, Xia CH, Goldstein LS (2000). Axonal transport of amyloid precursor protein is mediated by direct binding to the kinesin light chain subunit of kinesin-I. *Neuron* 28, 449–459.
- Karpenahalli MR, Lupas AN, Soding J (2007). TPRpred: a tool for prediction of TPR-, PPR- and SEL1-like repeats from protein sequences. *BMC Bioinformatics* 8, 2.
- Knop M, Siegers K, Pereira G, Zachariae W, Winsor B, Nasmyth K, Schiebel E (1999). Epitope tagging of yeast genes using a PCR-based strategy: more tags and improved practical routines. *Yeast* 15, 963–972.

- Kuehn MJ, Schekman R (1997). COPII and secretory cargo capture into transport vesicles. *Curr Opin Cell Biol* 9, 477–483.
- Kurihara T, Hamamoto S, Gimeno RE, Kaiser CA, Schekman R, Yoshihisa T (2000). Sec24p and Iss1p function interchangeably in transport vesicle formation from the endoplasmic reticulum in *Saccharomyces cerevisiae*. *Mol Biol Cell* 11, 983–998.
- Lam KK, Davey M, Sun B, Roth AF, Davis NG, Conibear E (2006). Palmitoylation by the DHHC protein Pfa4 regulates the ER exit of Chs3. *J Cell Biol* 174, 19–25.
- Lord M, Chen T, Fujita A, Chant J (2002). Analysis of budding patterns. *Methods Enzymol* 350, 131–141.
- Magliery TJ, Regan L (2004). Beyond consensus: statistical free energies reveal hidden interactions in the design of a TPR motif. *J Mol Biol* 343, 731–745.
- Meissner D, Odman-Naresh J, Vogelpohl I, Merzendorfer H (2010). A novel role of the yeast CaaX protease Ste24 in chitin synthesis. *Mol Biol Cell* 21, 2425–2433.
- Miller E, Antony B, Hamamoto S, Schekman R (2002). Cargo selection into COPII vesicles is driven by the Sec24p subunit. *EMBO J* 21, 6105–6113.
- Miller EA, Beilharz TH, Malkus PN, Lee MC, Hamamoto S, Orci L, Schekman R (2003). Multiple cargo binding sites on the COPII subunit Sec24p ensure capture of diverse membrane proteins into transport vesicles. *Cell* 114, 497–509.
- Muniz M, Nuoffer C, Hauri HP, Riezman H (2000). The Emp24 complex recruits a specific cargo molecule into endoplasmic reticulum-derived vesicles. *J Cell Biol* 148, 925–930.
- Peng J, Schwartz D, Elias JE, Thoreen CC, Cheng D, Marsischky G, Roelofs J, Finley D, Gygi SP (2003). A proteomics approach to understanding protein ubiquitination. *Nat Biotechnol* 21, 921–926.
- Proszynski TJ *et al.* (2005). A genome-wide visual screen reveals a role for sphingolipids and ergosterol in cell surface delivery in yeast. *Proc Natl Acad Sci USA* 102, 17981–17986.
- Reyes A, Sanz M, Duran A, Roncero C (2007). Chitin synthase III requires Chs4p-dependent translocation of Chs3p into the plasma membrane. *J Cell Sci* 120, 1998–2009.
- Sacristan C, Reyes A, Roncero C (2012). Neck compartmentalization as the molecular basis for the different endocytic behaviour of Chs3 during budding or hyperpolarized growth in yeast cells. *Mol Microbiol* 83, 1124–1135.
- Sanchatjate S, Schekman R (2006). Chs5/6 complex: a multiprotein complex that interacts with and conveys chitin synthase III from the *trans*-Golgi network to the cell surface. *Mol Biol Cell* 17, 4157–4166.
- Santos B, Snyder M (1997). Targeting of chitin synthase 3 to polarized growth sites in yeast requires Chs5p and Myo2p. *J Cell Biol* 136, 95–110.
- Santos B, Snyder M (2003). Specific protein targeting during cell differentiation: polarized localization of Fus1p during mating depends on Chs5p in *Saccharomyces cerevisiae*. *Eukaryot Cell* 2, 821–825.
- Sherman F (1991). Getting started with yeast. *Methods Enzymol* 194, 3–21.
- Storici F, Resnick MA (2006). The *delitto perfetto* approach to in vivo site-directed mutagenesis and chromosome rearrangements with synthetic oligonucleotides in yeast. *Methods Enzymol* 409, 329–345.
- Trautwein M, Schindler C, Gauss R, Dengjel J, Hartmann E, Spang A (2006). Arf1p, Chs5p and the ChAPs are required for export of specialized cargo from the Golgi. *EMBO J* 25, 943–954.
- Valdivia RH, Schekman R (2003). The yeasts Rho1p and Pkc1p regulate the transport of chitin synthase III (Chs3p) from internal stores to the plasma membrane. *Proc Natl Acad Sci USA* 100, 10287–10292.
- Wang CW, Hamamoto S, Orci L, Schekman R (2006). Exomer: A coat complex for transport of select membrane proteins from the *trans*-Golgi network to the plasma membrane in yeast. *J Cell Biol* 174, 973–983.
- Zanolari B, Rockenbach U, Trautwein M, Clay L, Barral Y, Spang A (2011). Transport to the plasma membrane is regulated differently early and late in the cell cycle in *Saccharomyces cerevisiae*. *J Cell Sci* 124, 1055–1066.
- Zeytuni N, Zarivach R (2012). Structural and functional discussion of the tetra-trico-peptide repeat, a protein interaction module. *Structure* 20, 397–405.
- Zhang B, Kaufman RJ, Ginsburg D (2005). LMAN1 and MCFD2 form a cargo receptor complex and interact with coagulation factor VIII in the early secretory pathway. *J Biol Chem* 280, 25881–25886.
- Zhang Z, Kulkarni K, Hanrahan SJ, Thompson AJ, Barford D (2010). The APC/C subunit Cdc16/Cut9 is a contiguous tetratricopeptide repeat superhelix with a homo-dimer interface similar to Cdc27. *EMBO J* 29, 3733–3744.
- Ziman M, Chuang JS, Tsung M, Hamamoto S, Schekman R (1998). Chs6p-dependent anterograde transport of Chs3p from the chitosome to the plasma membrane in *Saccharomyces cerevisiae*. *Mol Biol Cell* 9, 1565–1576.

5.1 Supplementary figures

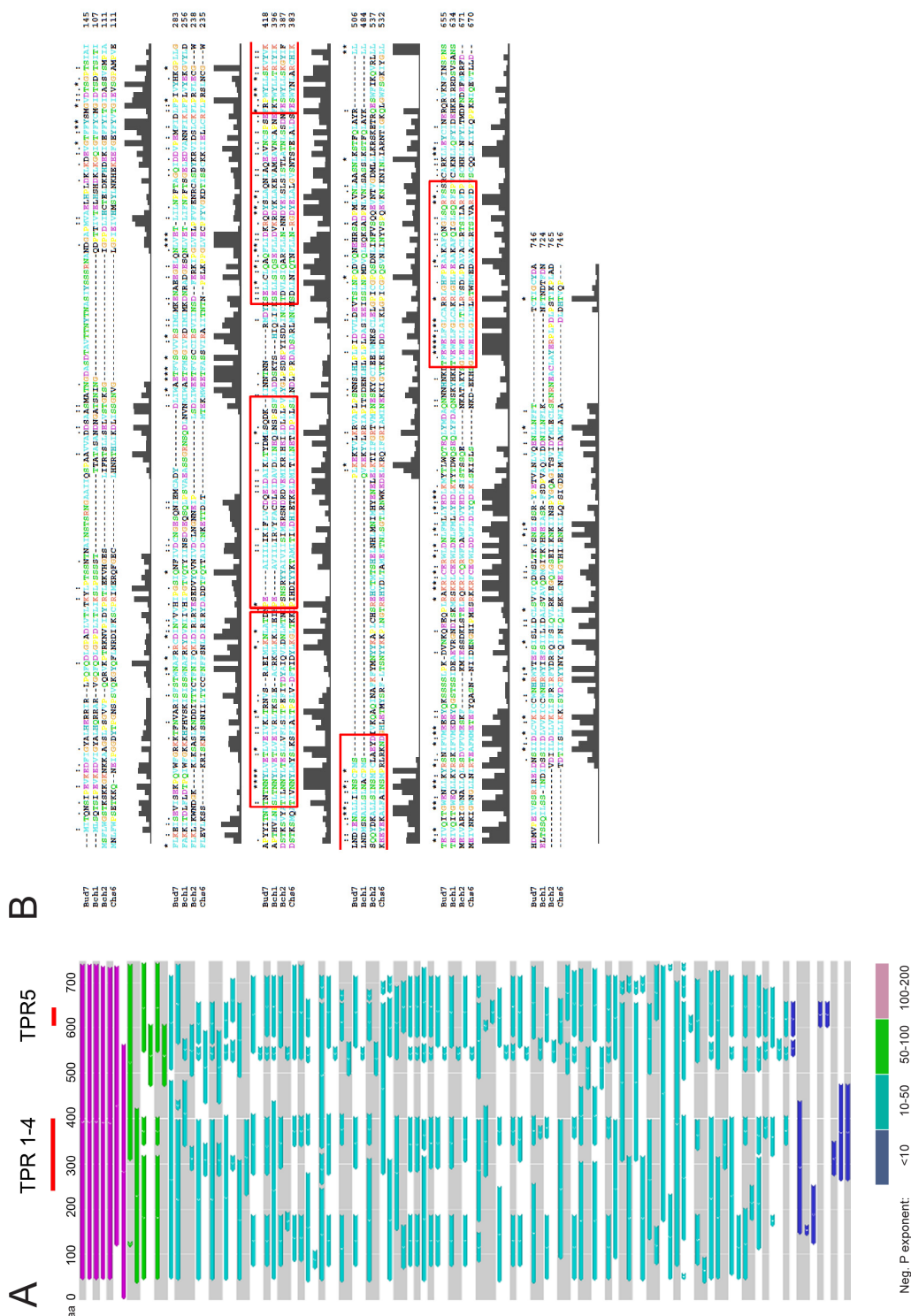


Figure S1. The tetra-tryptophan repeats of the ChAPs family are located in conserved regions (A) BLASTP alignment of *S. cerevisiae* Chs6p against ChAPs proteins in other fungi. Colours display the degree of conservation, as indicated by the scale below. Several regions appeared highly conserved, including TPR3-4 and TPR5 but also other parts such as stretch of about 114 amino acids at the N-terminus whose function is unknown. (B) Sequence alignment of the *S. cerevisiae* ChAPs. Dark grey bars indicate the degree of sequence conservation, red boxes the approximate position of the tetra-tryptophan repeats.

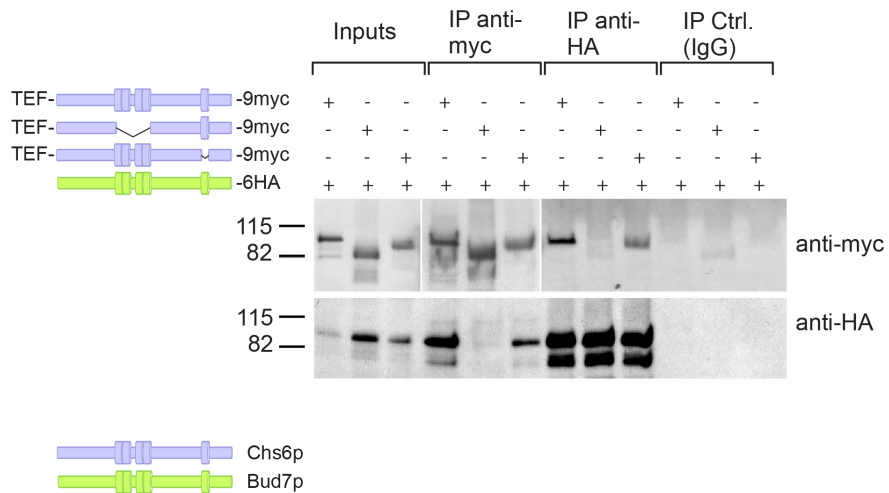


Figure S2. TPR1-4 is required for co-precipitation of Chs6p with Bud7p Co-immunoprecipitation was performed as in Figure 5. Interaction of Chs6(Δ TPR1-4) with Bud7p was entirely abolished, while Chs6(Δ TPR5) only showed a mild reduction in binding, suggesting that TPR1-4 is generally required for co precipitation of the ChAPs family members. Two different exposures were cropped together because of the strong signal of the precipitated myc-tagged constructs.

A

613 GLEWEL^LGLIMLR^LTWHWEDAVACL^LRTSIVARFDP⁶⁴⁶

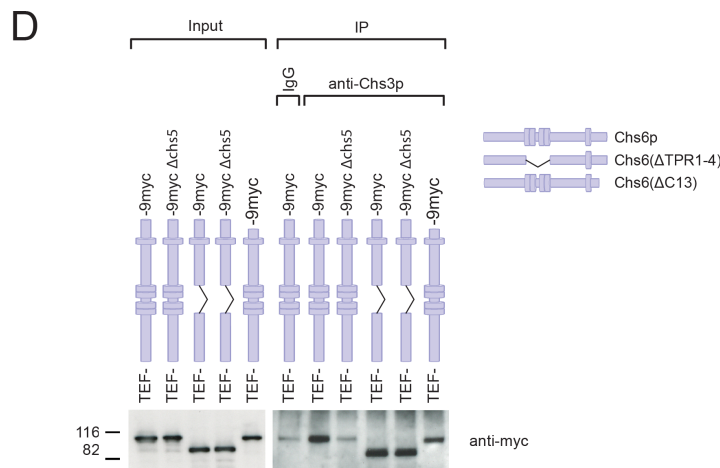
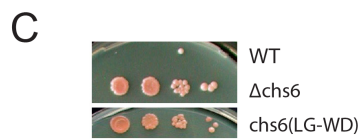
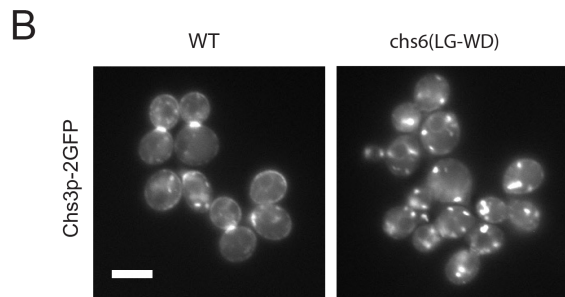


Figure S3
Chs6p requires an intact TPR fold for function

(A) Primary sequence of TPR5 in Chs6p. Residues which were considered part of the conserved TPR backbone are highlighted in red. Chs6p bearing a double point mutation in two neighboring TPR backbone residues (L619G/G620W) was non-functional, as judged by mis-localization of Chs3p (B) and calcofluor resistance (C). Scale bar: 5 μ m (D) Cargo interaction and Chs5p binding by Chs6p can be decoupled. Deletion of TPR1-4 or the last 13 amino acids in Chs6p abolishes Chs5p binding but does not influence the binding of Chs6(Δ TPR1-4) and Chs6(Δ C13) to Chs3p. Cargo interaction was assessed by precipitating Chs3p from DSP-crosslinked lysates with anti-Chs3p antibodies and probing precipitates for different Chs6p constructs

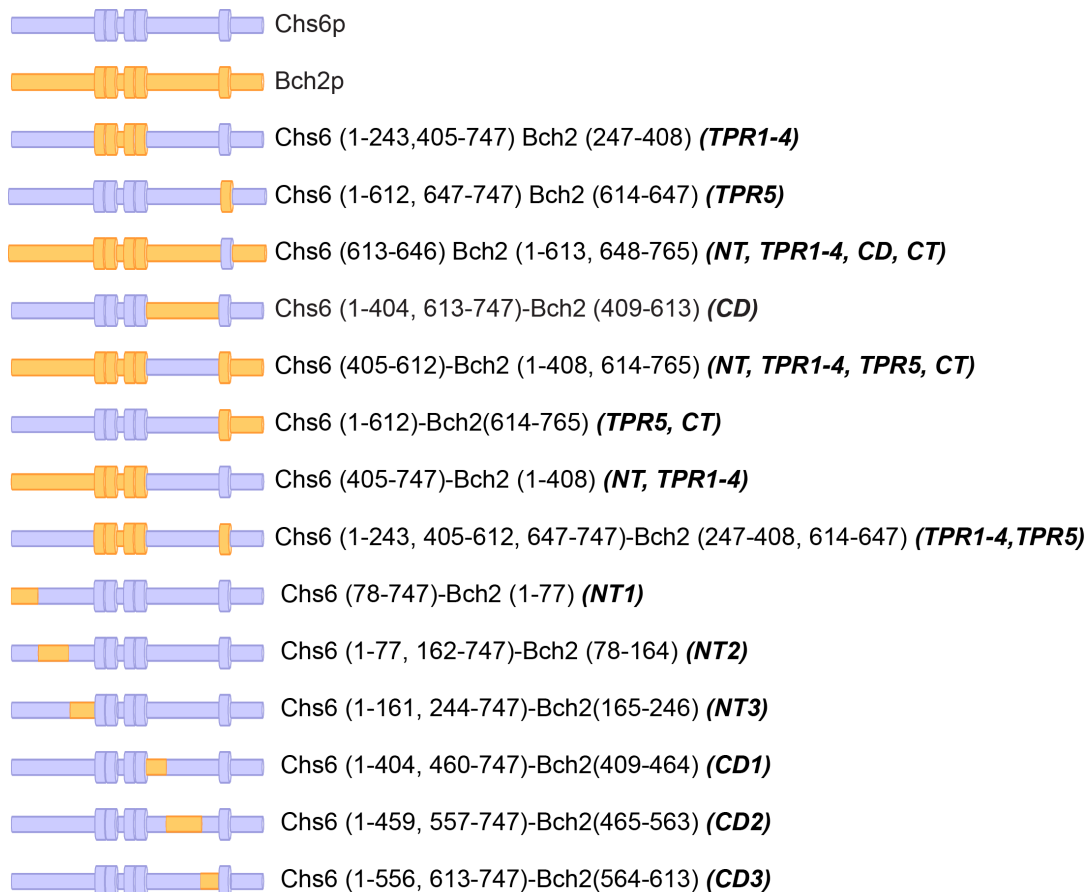


Figure S4. Bch2p-Chs6p chromosomally generated chimera constructs used in the study. Numbers in brackets indicate amino acid sequences of Chs6p and Bch2p domains in each construct. In bold italic: Chs6p domains replaced with corresponding domains of Bch2p.

6. Regulated trafficking of the exomer-dependent cargo, Pin2

6. The prion domain in the exomer-dependent cargo Pin2p serves as a trans-Golgi retention motif

Alicja M. Ritz, Mark Trautwein, Franziska Grassinger, and Anne Spang

Growth & Development, Biozentrum, University of Basel, Klingelbergstrasse 70, CH-4056 Basel, Switzerland

Address of Correspondence:

Anne Spang

Biozentrum

University of Basel

Klingelbergstrasse 70

CH-4056 Basel

Switzerland

Email: anne.spang@unibas.ch

Phone: +41 61 267 2380

The following manuscript was submitted to *Cell Reports* and was under revision at the time of the submission of this thesis. The above authors have contributed to the manuscript as follows:

Alicja M. Ritz performed the experiments in figures 6.1 B-E; 6.2-6.12. She wrote parts of the manuscript and provided critical comments on the rest.

Mark Trautwein performed and analyzed exomer interactors in HBH tagged exomer component pul-downs and identified the cargo Pin2: Figure 6.1 A. He provided critical comments on the manuscript.

Franziska Grassinger performed the experiment in figure 6.2 and initial experiments for figures 6.1 B and 6.3 A.

Anne Spang supervised the study and wrote the manuscript.

6.1 Abstract

Prion and prion-like domains are found in many proteins throughout the animal kingdom. The precise function of prion domains remains elusive, but they are over-represented in RNA binding proteins. We identified a prion-like domain in the novel exomer-dependent cargo Pin2p in *S. cerevisiae*, which is involved in the regulation of protein transport and localization. The domain serves as a retention signal of Pin2p in the trans-Golgi network (TGN). Pin2p is localized in a polarized fashion at the plasma membrane of the bud early in the cell cycle and in the bud neck at cytokinesis. The polarized localization is dependent on both exo- and endocytosis. The prion domain of Pin2p contains part of the exomer binding domain promoting export and the adaptor protein (AP) complex binding motif required for recycling and endocytosis and may therefore control the amount of the protein present at the plasma membrane at any given time. Upon environmental stress, Pin2p is rapidly endocytosed, and the prion domain aggregates and causes sequestration of Pin2p. The aggregation of Pin2p is reversible upon stress removal and Pin2p is rapidly re-exported to the plasma membrane. Together these data uncover a novel role of prion domains as protein localization elements.

6.2 Introduction

Prion proteins can exist in a normally folded state or in an aggregated state. The aggregated state is able to drive normally folded proteins into aggregation. Induction of the yeast Sup35 prion *[PSI⁺]* can occur spontaneously, but is greatly facilitated if the cell has previously achieved a *[PIN⁺]* state (Derkatch *et al.*, 1997). This *[PIN⁺]* state can be reached by the overexpression of number of different factors that contain a prion or prion-like domain (Derkatch *et al.*, 2001). Thus efficient induction of prions may require the presence of other prions.

Genome-wide analyses indicated that ranging from 0.3% (humans) to 24% (*Plasmodium falciparum*, the parasite that causes malaria) of cellular proteins contain a prion or prion-like domain (Michelitsch and Weissman, 2000; Osherovich and Weissman, 2002; Singh *et al.*, 2004). RNA binding proteins were over-represented among the prion domain containing proteins (Michelitsch and Weissman, 2000). In fact, a number of proteins involved in sequestration and decay of RNA contain a prion or prion-like domain (Michelitsch and Weissman, 2000; Decker *et al.*, 2007; Alberti *et al.*, 2009). Obviously not all prion or prion-like domains cause disease, and they might rather act as scaffold or interaction domain. Yet, their precise role remains in most instances elusive.

Transport to the plasma membrane and secretion are essential processes in eukaryotic cells. Cargoes destined for the plasma membrane will be sorted into transport carriers for either direct delivery or through endosomes to reach the plasma membrane. Evidence for the direct route exists in yeast and in mammalian cells. TGN46 containing transport containers have been identified in HeLa cells, which are dependent on protein kinase D and are devoid of VSVG or collagen, indicating a specific sorting mechanism at the TGN (Wakana *et al.*, 2012). In *Saccharomyces cerevisiae*, the chitin synthase Chs3p and Fus1p, a protein involved in mating response, require Chs5p and the ChAPs, which were collectively termed exomer, for their export from the TGN to the plasma membrane (Trautwein *et al.*, 2006; Wang *et al.*, 2006). Chs3p and Fus1p are not permanently localized at the plasma membrane. Both cargoes necessitate a combination of regulated endocytosis and exocytosis to achieve their precise localization at the bud neck for Chs3p and to the bud tip for Fus1p in a cell cycle dependent manner (Valdivia *et al.*, 2002; Barfield *et al.*, 2009).

The ChAP family consists of four homologous proteins, Bch1p, Bch2p, Bud7p, and Chs6p, which can associate with Chs5p to form oligomers of heterotetrameric complexes consisting of two Chs5p molecules and two ChAPs, whereby either two identical or two different ChAPs can be bound to Chs5p (Trautwein *et al.*, 2006; Paczkowski *et al.*, 2012).

The ChAPs may act as adaptor molecules to interact and recruit cargo to specific sites at the TGN from which they reach the plasma membrane. Although in Chs3p and Fus1p motifs have been identified, which were necessary for export from the TGN, none of these motifs was sufficient (Barfield *et al.*, 2009; Rockenbauch *et al.*, 2012; Starr *et al.*, 2012). In addition, the interaction motifs were not conserved between the two cargo proteins. Thus the interaction between the cargoes and exomer appears to be rather complex.

Given the lack of conserved motifs between Chs3p and Fus1p, other interaction sites must be important to control the export of these proteins in a temporally and spatially controlled manner. These interaction sites could potentially adopt an appropriate conformation upon interaction with the ChAPs and then the linear transport signal might be recognized. In support of this notion all ChAPs were able to interact with Chs3p, although only Chs6p is essential for its plasma membrane localization (Trautwein *et al.*, 2006). Examples for such interactions are Src homology domains that recognize phosphorylated tyrosines in proteins (Groffen *et al.*, 1983; Moran *et al.*, 1990), the interaction of the ArfGAP Glo3 with SNAREs and cargo (Rein *et al.*, 2002; Schindler *et al.*, 2009) or prion domain containing proteins that are for example important for processing body and stress granule assembly (Michelitsch and Weissman, 2000; Gilks *et al.*, 2004; Vessey, 2006; Decker *et al.*, 2007; Alberti *et al.*, 2009) or often found in cytoskeletal elements (Michelitsch and Weissman, 2000; Alberti *et al.*, 2009).

Chs3p is a multispinning transmembrane protein and Fus1p becomes only exomer-dependent upon mating. To better understand the exomer-dependent transport pathway, we identified novel cargo proteins, one of which is Pin2p, a single transmembrane protein with a large cytoplasmic domain that contains a prion domain. This prion domain regulates the traffic of Pin2p under normal growth conditions and is essential for Pin2p retention in internal structures upon environmental stress. We have identified a novel transport mechanism in which a prion domain is essential for the temporal and spatial control of intracellular protein localization.

6.3 Results

6.3.1 The prion domain protein Pin2p is a novel exomer-dependent cargo

In order to better understand exomer-dependent transport to the plasma membrane, we aimed to identify novel cargoes. To this end, we appended Chs5p or each of the four members of the ChAPs family with an HBH-tag. The HBH-tag consists of a biotinylation sequence flanked by two His6-tags (Tagwerker *et al.*, 2006). This tag allows the purification of proteins -or after crosslinking- of protein complexes under denaturing conditions. We reasoned that this tag would allow for easy extraction of membrane proteins, which would represent potential cargo proteins, when bound to a component of the exomer complex. Yeast cultures were treated with 1% formaldehyde for 10 min, and cells were lysed in the presence of 8 M urea. The cross-linked complexes were subsequently purified over Ni-NTA and streptavidin beads, and finally subjected to mass-spectrometric analysis (Fig. 6.1A). With this approach, we identified transmembrane containing proteins (potential cargoes) and soluble proteins (potential regulators). We decided to focus on the potential cargoes, and tested them for their ability to be transported to the plasma membrane in a Chs5p-dependent manner. One of the hits that required Chs5p for localization to the bud in small and medium-sized cells and to the bud neck in large-budded cells was the previously uncharacterized prion domain containing protein Pin2p (Fig. 6.1B). In the absence of Chs5p, Pin2p remained in internal structures, similar to what was observed with the other exomer-dependent cargoes, Chs3p and Fus1p (Santos and Snyder, 1997; Trautwein *et al.*, 2006; Barfield *et al.*, 2009). If Pin2p was an exomer-dependent cargo, a deletion of all four ChAPs should phenocopy a $\Delta chs5$ strain. In a $\Delta 4ChAPs$ strain, Pin2p was also found in internal structures (Fig. 6.1B). Therefore, Pin2p represents a novel exomer-dependent cargo.

So far, all exomer-dependent cargoes localize to the bud or bud neck (Chuang and Schekman, 1996; Santos and Snyder, 1997; Barfield *et al.*, 2009), opening the possibility that perhaps all bud-localized proteins were potential exomer clients. However, another candidate from our biochemical screen, Skg6p, which localized to the bud and to the bud neck in a cell cycle-dependent manner similar to Pin2p, reached the plasma membrane through an exomer-independent pathway because deletion of *CHS5* or the four ChAPs had no effect on Skg6p localization (Fig. 6.1B). Thus, the cell-cycle dependent spatial distribution of the proteins alone cannot be used to discriminate between exomer-dependent and -independent cargo.

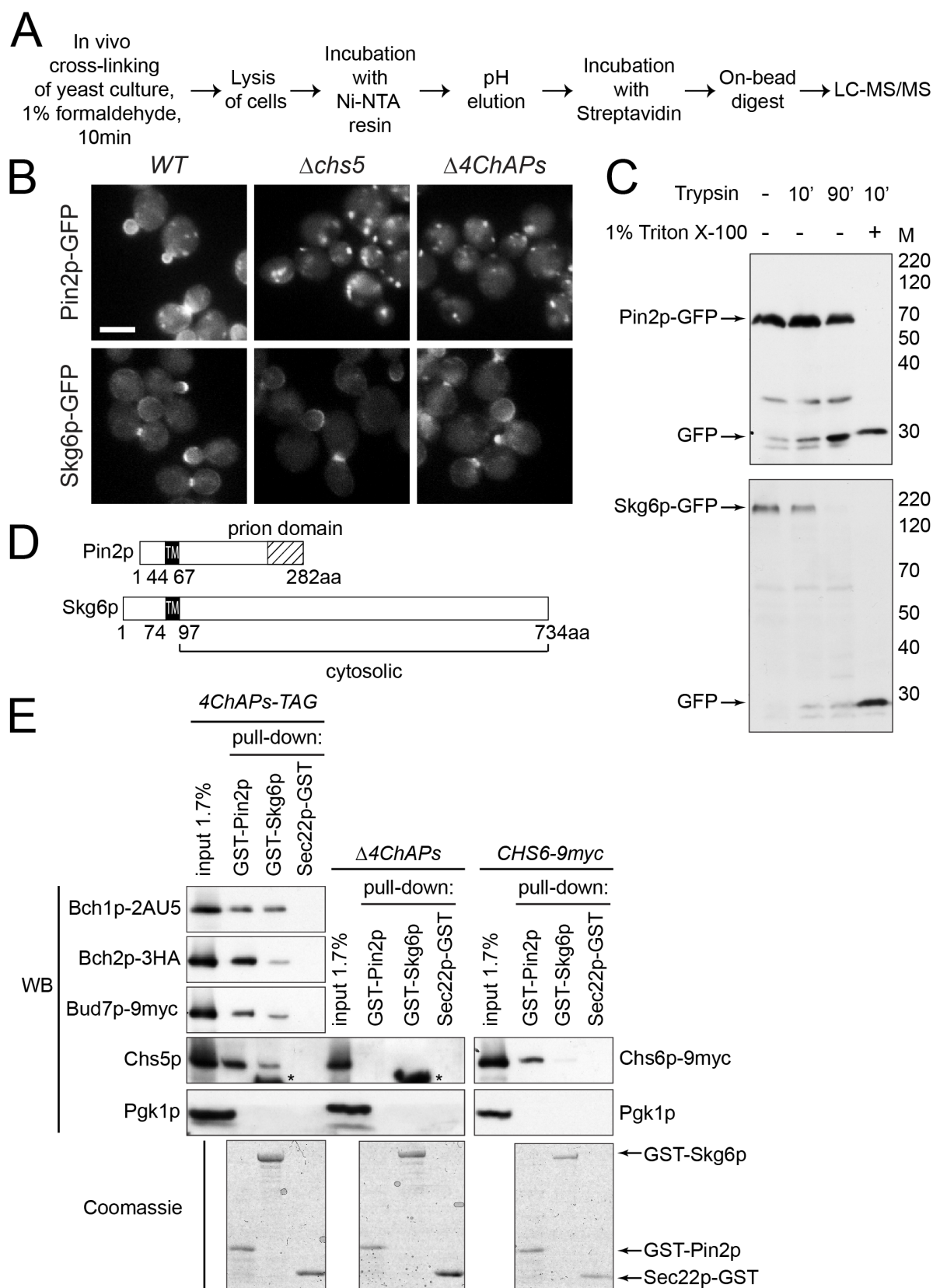


Figure 6.1 Pin2p is an exomer-dependent cargo. (A) Flow-diagram of purification of HBH-tagged exomer subunits followed by mass spectrometry analysis of co-purified interactors. (B) Export of Pin2p, but not Skg6p, to the plasma membrane is dependent on the exomer complex. Fluorescence microscopy images of WT, $\Delta chs5$ or a quadruple ChAP deletion ($\Delta 4ChAPs$) cells expressing chromosomally tagged Pin2p-GFP and Skg6p-GFP. Scale bar: 5 μ m. (Continued on next page).

(Figure 6.1 continued) (C) The C-terminus of Pin2p and Skg6p is cytosolic. Yeast spheroplasts expressing either chromosomally, C-terminally GFP-tagged Pin2p or Skg6p were digested for 10 or 90 minutes with trypsin in the absence or presence of TX-100. Anti-GFP immunoblot of yeast lysates +/- trypsin treatment. (D) Schematic representation of Pin2p and Skg6p topology. (E) Pin2p and Skg6p bind all four ChAPs of exomer and interact with Chs5p through the ChAPs. Pull down of yeast lysates with purified GST-tagged cytosolic domains of Pin2p, Skg6p or Sec22p. GST-Sec22p was used as a negative control. Pull downs were performed with lysates from a strain where all four ChAPs were epitope tagged – *4ChAPs-TAG*, in a quadruple ChAP deletion strain - $\Delta 4ChAPs$, or in a strain where only Chs6p was myc-tagged – *Chs6-9myc*. Samples were immunoblotted for Chs5p, epitope tags present on the ChAPs or Pgk1p – negative control. Asterisks indicate non-specific interaction of GST-Skg6p with the anti-Chs5p antibody. Coomassie staining was used to assess levels of GST-tagged constructs in the pull downs.

6.3.2 Pin2p and Skg6p are membrane proteins with large C-terminal domains facing the cytoplasm.

Pin2p and Skg6p appear to be single-pass transmembrane proteins with unclear topology. To determine the topology of both proteins, we performed trypsin digests of cells expressing chromosomal C-terminal GFP fusions of Pin2p and Skg6p in the presence or absence of 1% TX-100. Pin2p-GFP was resistant to trypsin treatment up to 90 min in the absence of detergent. Solubilizing the plasma membrane rendered Pin2p-GFP protease-sensitive (Fig. 6.1C). Similar results were obtained for Skg6p-GFP. Consistent with these results, high throughput phospho-proteome studies reported phosphorylation sites for both Skg6p and Pin2p in the C-terminal part of the proteins (Bodenmiller *et al.*, 2007; Li *et al.*, 2007; Soulard *et al.*, 2010; Sadowski *et al.*, 2013). Moreover, an N-terminal GFP-Pin2p protein was not functional and was unable to insert into the ER membrane during translation (data not shown). Therefore, the C-terminus of Pin2p and Skg6p face the cytoplasm, and the N-terminus of either protein is exposed to the environment. In both proteins the transmembrane domain is relatively close to the N-terminus, resulting in small extracellular domains (Fig. 6.1D).

6.3.3 Pin2p and Skg6p interact with exomer components in vitro

The determination of the topology allowed us to create GST-fusion proteins of the cytoplasmic exposed tails of Pin2p and Skg6p and to revisit the interaction of both proteins with exomer. We wanted to independently confirm the interaction with exomer, because the initial identification was through a cross-linking approach, which only measures proximity. Therefore, we performed a GST pull-down experiment from yeast lysates in which either three of the four ChAPs (Bch1p, Bch2p, Bud7p) were chromosomally appended with different tags or Chs6p was myc-tagged. The functionality of the tagged proteins had been established previously (Trautwein *et al.*, 2006). Pin2p and Skg6p, but not the ER-Golgi v-

SNARE Sec22p pulled-down exomer components (Fig. 6.1E). This result confirms the interaction of Pin2p with exomer and reinforces the notion that Pin2p is an exomer-dependent cargo. Interestingly, proximity to and even interaction with exomer components appears to be insufficient to describe an exomer-dependent cargo, as Skg6p travels to the plasma membrane in the absence of exomer. It is conceivable, however, that Skg6p can use either pathway to reach the plasma membrane.

To finally prove that Pin2p is an exomer-dependent cargo, we probed the interaction of Pin2p with Chs5p. Chs3p and Fus1p depend on the ChAPs for efficient interaction with Chs5p (Sanchatjate and Schekman, 2006; Rockenbauch *et al.*, 2012). While we could detect a robust interaction between Chs5p and Pin2p in the presence of the ChAPs, this interaction was abolished when the ChAPs were deleted (Fig. 6.1E). Therefore, we conclude that Pin2p is a novel exomer-dependent cargo.

6.3.4 Either Bch1p or Bch2p is sufficient to support Pin2p-GFP plasma membrane localization

Next, we aimed to establish the transport requirements of Pin2p. Exomer-dependent cargoes require one or two members of the ChAPs family for timely exit from the TGN (Ziman *et al.*, 1998; Sanchatjate and Schekman, 2006; Trautwein *et al.*, 2006; Barfield *et al.*, 2009). To establish the trafficking requirements of Pin2p-GFP to the plasma membrane, we tested single and double deletions of the ChAPs for their failure to export Pin2p-GFP from the TGN. None of the single ChAP deletion strains showed an impairment of Pin2p localization (Fig. 6.2). In contrast, the double deletions $\Delta bch1 \Delta bch2$ altered Pin2p-GFP localization (Fig. 6.3 A and B). However, the $\Delta bch1 \Delta bch2$ double deletion did not inhibit Pin2p plasma membrane localization to the same extent as $\Delta chs5$, indicating that also the other ChAPs can contribute to proper Pin2p localization (Fig. 6.3 B).

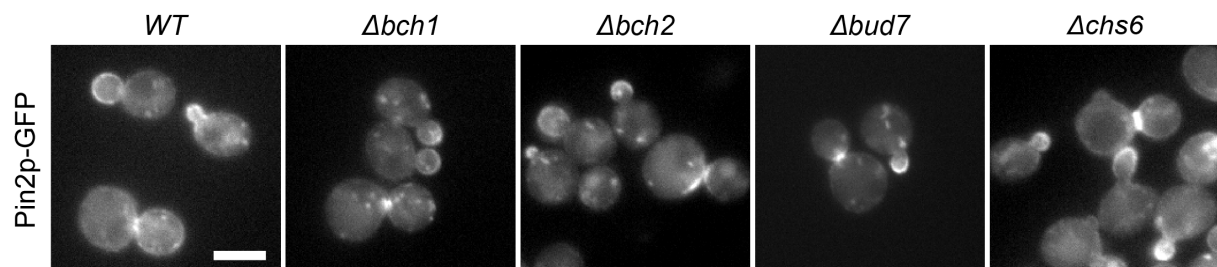


Figure 6.2 Single ChAPs deletions do not inhibit Pin2p export to the plasma membrane. Fluorescence microscopy images of $\Delta bch1$, $\Delta bch2$, $\Delta bud7$ or $\Delta chs6$ strain cells expressing chromosomally tagged Pin2p-GFP. Scale bar: 5 μ m

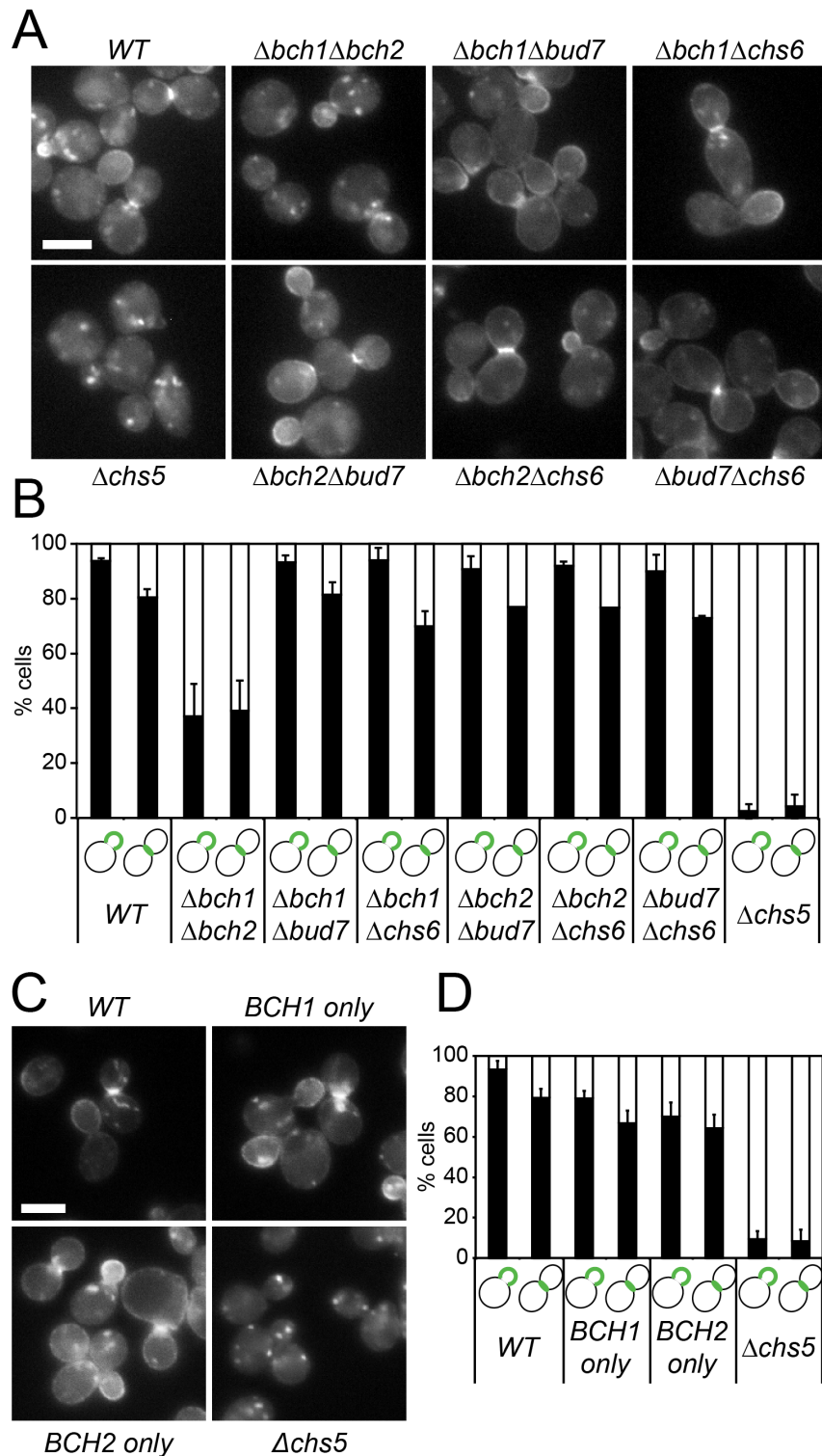


Figure 6.3 Either Bch1p or Bch2p is necessary and sufficient for Pin2p export to the plasma membrane.

(A) $\Delta bch1\Delta bch2$ inhibits Pin2p export to the plasma membrane. Fluorescence microscopy images of WT, $\Delta chs5$ and double ChAP deletion cells, expressing chromosomally tagged Pin2p-GFP. (B) Cells in (A) were scored for Pin2p-GFP expression at the plasma membrane. 100 small and medium budded cells - G1/S and G2 phase and 100 large budded cells - M-phase were quantified in each of 3 independent experiments. Error bars: standard deviation. (C) *BCH1* or *BCH2* are sufficient for Pin2p export to the plasma membrane. Fluorescence microscopy images of WT, $\Delta chs5$ and triple ChAP deletion cells: $\Delta bch2 \Delta bud7 \Delta chs6$ - *BCH1* only, and $\Delta bch1 \Delta bud7 \Delta chs6$ - *BCH2* only, expressing chromosomally tagged Pin2p-GFP. (D) Cells in (C) were analyzed as in (B). Scale bars in (A) and (C): 5 μ m.

Either Bch1p or Bch2p appeared to be necessary for transport to the plasma membrane. Next, we asked whether either ChAP would also be sufficient for Pin2p TGN export. To this end we assessed the localization of Pin2p in strains in which either Bch1p or Bch2p would be the sole ChAP protein present. Under these conditions, Pin2p still was exported to the plasma membrane albeit somewhat less efficiently than in the wild type (Fig.

6.3 C and D). Our data indicate that Bch1p and Bch2p can independently promote export of Pin2p from the TGN to the plasma membrane.

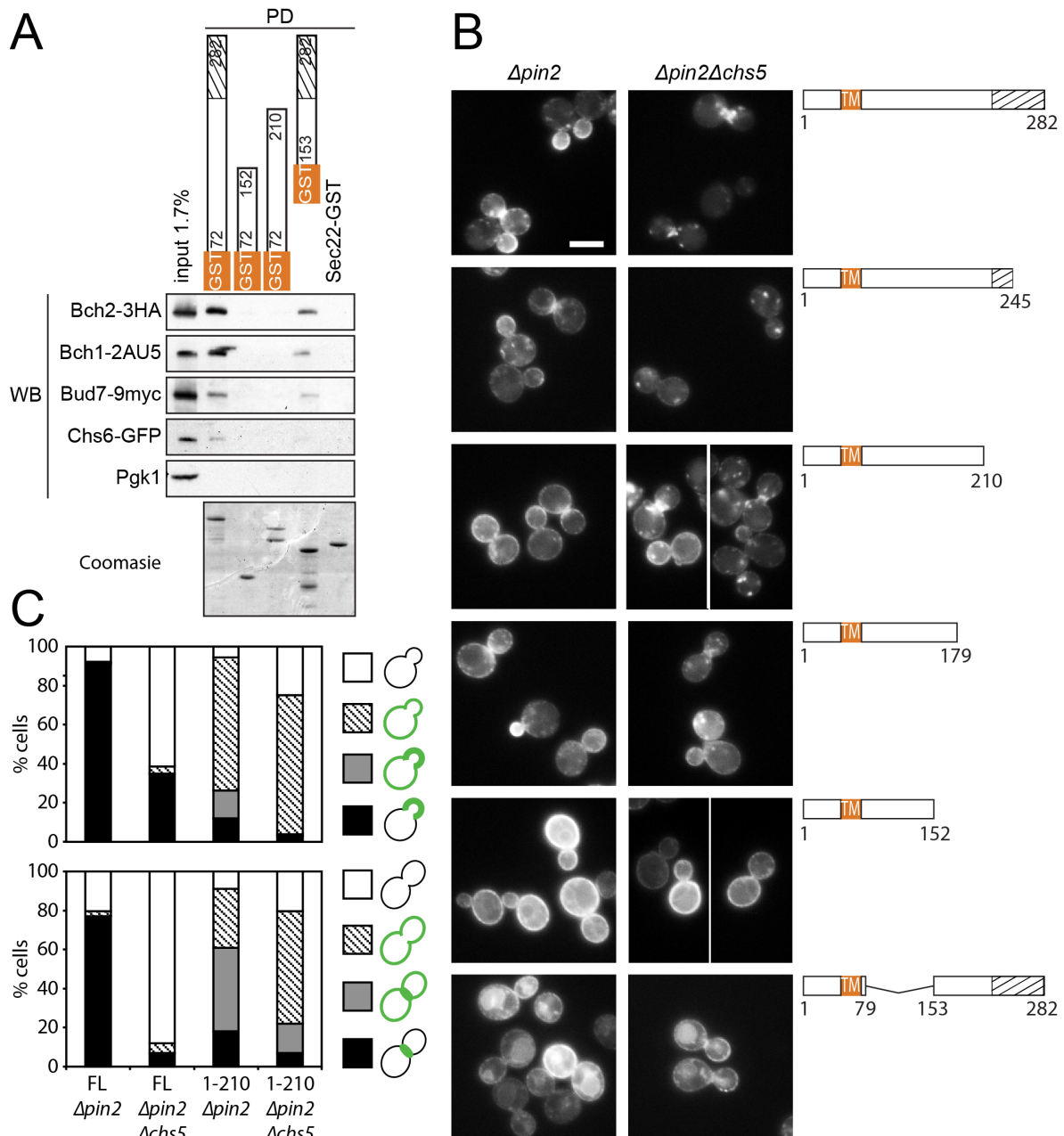


Figure 6.4 The Pin2p cytosolic domain contains motifs for exomer-binding and endocytosis. (A) The C-terminal amino acids 211-282 of Pin2p contain an exomer-binding motif. Pull down of yeast lysates from a strain where all four ChAPs were epitope tagged with purified GST-tagged full-length and truncated Pin2p cytosolic domains. GST-Sec22p was used as a negative control. Pull downs were immunoblotted for epitope tags present on the ChAPs or Pgk1p (negative control). Coomassie staining was used to assess levels of GST-tagged constructs in the pull downs. (B) Δ 211-245 strongly abolishes exomer-dependency while Δ 153-179 completely abrogates polarized localization of Pin2p at the plasma membrane. Fluorescence microscopy images of *Δpin2* and *Δpin2Δchs5* cells expressing GFP tagged Pin2p full length and cytosolic truncations from a centromeric plasmid. Scale bars: 5 μ m. (C) Deletion of *CHS5* only mildly effects Pin2(1-210)p-GFP export. *Δpin2* and *Δpin2Δchs5* cells in were scored for the expression Pin2p-GFP and Pin2(1-210)p-GFP at the plasma membrane and for the extent of the polarity of Pin2p localization. 100 small and medium budded cells and 100 large budded cells were quantified.

6.3.5 Exomer binds to the Pin2p C- terminus *in vitro*

We have shown so far that Pin2p is an exomer-dependent cargo that binds directly to exomer. The interaction of exomer with its cargoes Chs3p and Fus1p is complex and requires more than just a linear sequence motif (Barfield *et al.*, 2009; Rockenbauch *et al.*, 2012). To identify potential interacting regions, we generated three different truncations in the cytoplasmic domain containing GST-Pin2p, in which either parts from the C-terminal region or the central part of Pin2p were removed. As shown above, the cytoplasmic domain of Pin2p interact with all ChAP proteins (Fig. 6.1 E and Fig. 6.4 A). In addition, the construct expressing the C-terminal ~120 amino acids of Pin2p precipitated the ChAPs, albeit more weakly. Since GST-Pin2p(72-210) was unable to interact with exomer, we conclude that the exomer binding site resides in the C-terminal 72 amino acids. Thus, exomer recognizes sequences in Pin2p C-terminus, but other sequences in the molecule might still contribute to the binding efficacy.

Next we wanted to test, whether the C-terminal part of Pin2p would be necessary and sufficient to cause exomer-dependent export (Fig. 6.4 B). First, we generated a construct in which the *in vitro* identified exomer interaction site was eliminated (Pin2p(1-210)-GFP). This construct still reached the plasma membrane in wild-type and to a lesser extent in $\Delta chs5$ cells, however, the polarized localization was lost (Fig. 6.4 B and C). This phenotype is reminiscent of Chs3p localization in a $\Delta chs5 \Delta apm1$, in which recycling from endosomes to the TGN is blocked (Valdivia *et al.*, 2002). A construct that contained only the first 245 of the 282 amino acids of Pin2p still accumulated at the plasma membrane in an exomer-dependent manner. Therefore, the exomer interaction site might reside in residues 210-245 of Pin2p. Trimming the protein further down to 152 residues shifted Pin2p localization entirely to the plasma membrane and the internal pool was depleted, consistent with a defect in endocytosis (Fig. 6.4 B). A similar phenotype has been reported for Chs3p localization in a $\Delta end3$ strain, in which endocytosis was blocked (Chuang and Schekman, 1996; Ziman *et al.*, 1996). Despite a notable plasma membrane localization of Pin2p($\Delta 79-152$)-GFP, most of the protein accumulated in the vacuole in wild-type cells, indicating that also the membrane proximal region of Pin2p may contribute to proper Pin2p localization. Most importantly, the pool that reached the plasma membrane, arrived there in an exomer-independent manner because Pin2p($\Delta 79-152$)-GFP localization in $\Delta chs5$ was indistinguishable from that in wild type cells. Therefore, the C-terminal domain is not sufficient to direct Pin2p into the exomer pathway. The effects we observed were not due to large overexpression of the constructs over the endogenous protein as we used $\Delta pin2$ strains and a centromeric expression vector (Fig. 6.5). Taken together these data indicate that the interaction between Pin2p and exomer

might be rather complex and that it is rather unlikely that a short linear sequence within Pin2p would be necessary and sufficient to promote temporal and spatial controlled plasma membrane localization. These data are in agreement to what has been observed for the other exomer cargoes, Chs3p and Fus1p (Barfield *et al.*, 2009; Rockenbauch *et al.*, 2012)

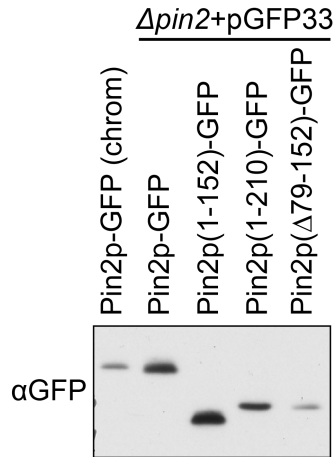
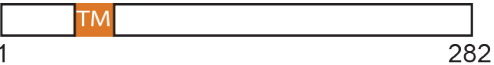
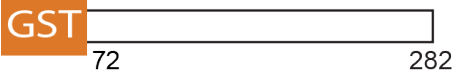
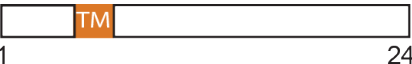
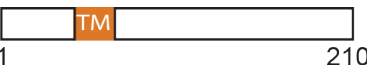
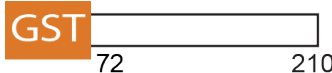
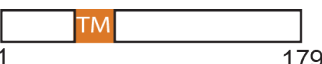


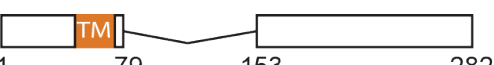
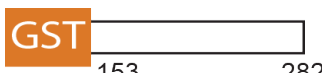


Figure 6.5 Expression of Pin2p truncations. Extracts from cells expressing chromosomally tagged Pin2p-GFP or *Δpin2* cells expressing Pin2p-GFP, Pin2(1-210)p-GFP, Pin2(1-152)p-GFP or Pin2(Δ153-179)p-GFP from a centromeric plasmid were immunoblotted with an anti-GFP antibody.

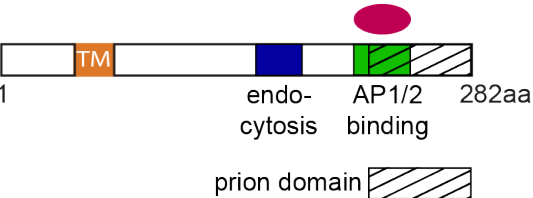
6.3.6 Pin2p recycles between endosomes and TGN

Chs3p and Fus1p have been shown to reach endosomes and to be retrieved from there in an AP-1 dependent pathway (Valdivia *et al.*, 2002; Barfield *et al.*, 2009). In the absence of Chs5p and AP-1, Chs3p and Fus1p reached the plasma membrane through an alternative route. We wished to test whether this recycling is actually a general feature of exomer-dependent cargoes. As shown above Pin2(1-210)p, but not Pin2(1-245)p, was plasma membrane localized, independent of Chs5p, indicating that the region aa 210-245 may contain an AP-1 binding site (Fig. 6.4 B). Similarly to what had been observed for Chs3p Chs5p-independent transport (Valdivia *et al.*, 2002), Pin2p was no longer confined to the bud of the yeast cell, but was equally distributed over the plasma membrane of the mother cell. μ subunits of AP complexes can bind to the Tyr-based sorting motif YXX ϕ (X: any amino acid, ϕ : bulky hydrophobic) (Ohno *et al.*, 1995). We identified in the 210-245 peptide a cryptic Tyr-based motif, YGENYYY (Fig. 6.6 A). Although the spacing for the motif was not perfect, we replaced the Ys and N by As. Transport to the plasma membrane of the Ala mutant was independent of Chs5p (Fig. 6.6 B), indicating that YGENYYY is a functional adaptor complex binding site and mutation of which yielded a phenotype indistinguishable to Pin2(1-210)p. To prove that Pin2p indeed undergoes AP-1 dependent recycling, we deleted the μ subunit of the AP-1 complex, *APM1*. In a *Δchs5 Δapm1* mutant, Pin2p was localized mostly to the plasma membrane, while Skg6p localization was not affected under any of these conditions (Fig. 6.6 D and E).

GFP tagged truncations expressed from centromeric plasmid	PM export	<i>CHS5</i> dependency	Polarized localization	EE/TGN localization	Exomer binding	GST tagged truncations of Pin2 cytosolic domain
	+	+	+	+	+	
	+	+	+	+	-	-
	+	+/-	+/-	+/-	-	
	+	+/-	+/-	+/-	-	-
	+	-	-	-	-	
	+	-	-	-	+	

(vacuole)

exomer binding



1 TM endo-cytosis AP1/2 binding prion domain 282aa

Table 6.1 Summary of phenotypes of Pin2p truncations.

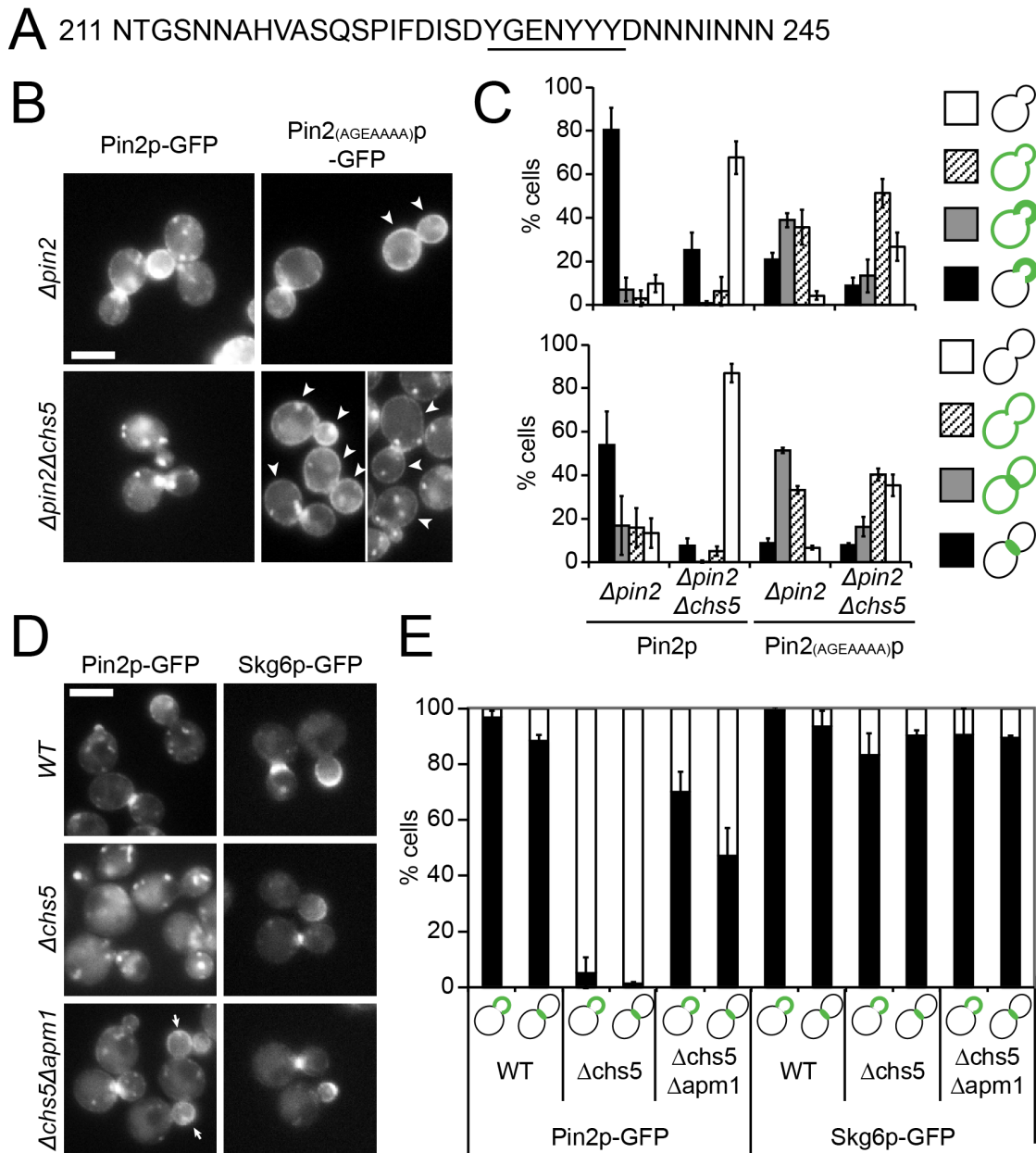


Figure 6.6 Pin2p is retrieved from early endosomes to the trans-Golgi network by AP-1. (A) Amino acids 211-245 of Pin2p, which contain a motif required for exomer-dependency. Underlined is a degenerate tyrosine-based sequence, which could serve as a potential AP-1 binding motif. (B) Mutation of the YGENY Y tyrosine based motif rescues Pin2p export to the plasma membrane in a $\Delta chs5$ strain. Fluorescence microscopy images of $\Delta pin2$ and $\Delta pin2\Delta chs5$ strain cells expressing GFP tagged Pin2p wild type and AGEAAAA mutant from a centromeric plasmid. Arrowheads indicate Pin2(AGEAAAA)p-GFP expressed at the plasma membrane of the daughter and mother cell. (C) $\Delta pin2$ and $\Delta pin2\Delta chs5$ cells were scored for the expression Pin2p-GFP and Pin2(AGEAAAA)p-GFP at the plasma membrane and for the extent of the polarity of Pin2p localization. 100 small and medium budded cells and 100 large budded cells were quantified in each of 3 independent experiments. Error bars: standard deviation. (D) Deletion of the *APM1* subunit of the AP-1 complex rescues Pin2p export to the plasma membrane in a $\Delta chs5$ strain. Fluorescence microscopy images of wild type, $\Delta chs5$ and $\Delta chs5\Delta apm1$ cells expressing chromosomally tagged Pin2p-GFP and Skg6p-GFP (negative control). Arrows indicate Pin2p-GFP localizing exclusively to the plasma membrane of the daughter cell in $\Delta chs5\Delta apm1$ cells. (E) WT, $\Delta chs5$ and $\Delta chs5\Delta apm1$ cells were scored for the expression of Pin2p-GFP and Skg6p-GFP at the plasma membrane. 100 small and medium budded cells and 100 large budded cells were quantified in each of 3 independent experiments. Error bars: standard deviation. Scale bars in (B) and (D): 5 μ m.

Moreover the Pin2(AGEAAAA)p mutant protein did not change its localization in a $\Delta chs5 \Delta apm1$ mutant confirming that indeed we mutated the AP1 site (Fig. 6.7). Therefore, Pin2p cycles between the TGN and endosomes in a similar manner to that of the other exomer-dependent cargoes Chs3p and Fus1p. In addition, the cryptic tyrosine-based signal might also be recognized by the AP-2 complex, which promotes endocytosis at the plasma membrane, because in contrast to $\Delta chs5 \Delta apm1$ cells, in which the mother cell was devoid of Pin2p, Pin2(AGEAAAA)p-GFP localized to the plasma membrane of mother and daughter cells in both wild-type and $\Delta chs5$ (compare Fig 6.6 B and D, arrowheads), indicating that endocytosis may be required for proper Pin2p localization.

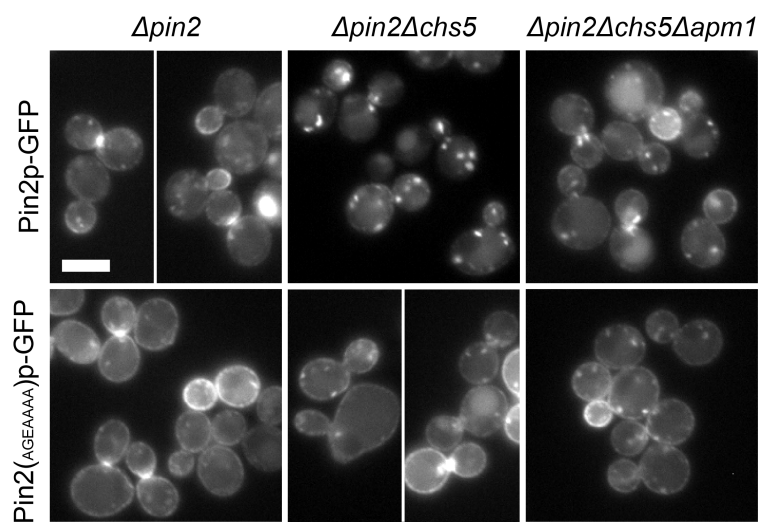


Figure 6.7 Mutation of the Pin2p YGENYYY motif and deletion of APM1 does not have an additive effect on Pin2p localization. Fluorescence microscopy images of $\Delta pin2$, $\Delta pin2 \Delta chs5$ or $\Delta pin2 \Delta chs5 \Delta apm1$ strain cells expressing Pin2p-GFP or Pin2(AGEAAAA)p-GFP mutant from a centromeric plasmid. Scale bar: 5 μ m

6.3.7 Ubiquitin-mediated endocytosis of Pin2p is required for its proper plasma membrane localization

Another feature of Chs3p trafficking is that Chs3p localization at the bud neck is dependent on endocytosis. In the absence of endocytosis, Chs3p was delocalized over the plasma membrane (Ziman *et al.*, 1996; Reyes *et al.*, 2007). Therefore, we tested whether Pin2p localization would depend on endocytosis. Deletion of *END3*, which is essential for endocytosis locked Chs3p and Pin2p at the plasma membrane, while Skg6p was only mildly affected, especially in small to medium budded cells (i.e. before mitosis) (Fig. 6.8 A and B). These results indicate that Pin2p and Chs3p are equally dependent on endocytosis for their proper localization. Moreover, Pin2(AGEAAAA)p-GFP was mislocalized over the entire plasma membrane (Fig. 6.6 B). The Pin2p C-terminal truncation revealed an accumulation of Pin2(1-152)p all over the plasma membrane, while internal stores (endosomes and TGN) were depleted (Fig. 6.4 B). Although Pin2(1-179)p also was mostly present at the plasma membrane, internal structures were still observed (Fig. 6.4 B).

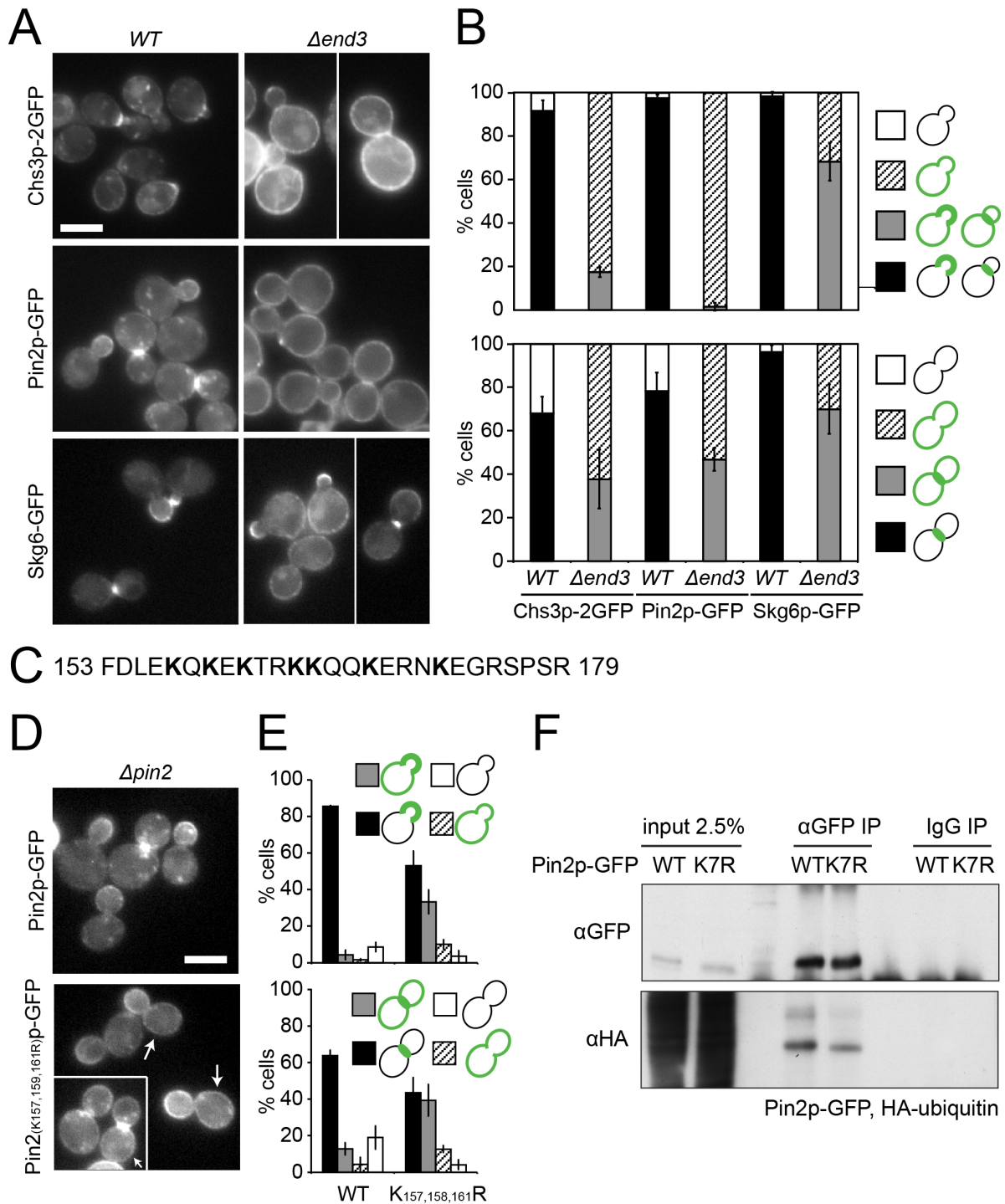


Figure 6.8 Polarized localization of Pin2p is dependent on ubiquitin-mediated endocytosis.

(A) Endocytosis is required to maintain polarized localization of exomer-dependent cargoes at the plasma membrane, particularly in earlier cell cycle stages. Fluorescence microscopy images of *wild type* and $\Delta end3$ cells expressing chromosomally tagged Chs3p-2GFP, Pin2p-GFP and Skg6-GFP. (B) WT and $\Delta end3$ cells were scored for the expression Chs3p-2GFP, Pin2p-GFP or Skg6p-GFP at the plasma membrane and for the extent of the polarity of cargo localization. 100 small and medium budded cells and 100 large budded cells were quantified in each of 3 independent experiments. Error bars: standard deviation. (C) Amino acids 153-179 of Pin2p are required for maintenance of its polarized localization at the plasma membrane. Lysines, are depicted in bold. (D) Mutation of 3 out of 7 lysines within the 153-179 aa region causes a partial loss of Pin2p polarity at the plasma membrane. Fluorescence microscopy images of $\Delta pin2$ yeast expressing Pin2p-GFP WT or Pin2(K157,159,161R)p-GFP mutant from a centromeric plasmid. (Continued on next page)

(Figure 6.8 continued) (E) Cells in (D) were scored for the expression Pin2p-GFP and Pin2(K157,159,161R)p-GFP at the plasma membrane and for the extent of the polarity of Pin2p localization. For quantifications 100 small and medium budded cells and 100 large budded cells were quantified in each of 3 independent experiments. Error bars: standard deviation. (F) Lysines within the 153-179 aa region of Pin2p are ubiquitinated. Denaturing immunoprecipitation of GFP tagged Pin2p or the K7R variant. Pin2p-GFP and Pin2(K7R)p-GFP were expressed from a centromeric plasmid in a HA-ubiquitin overexpressing strain. Co-precipitating HA-ubiquitin was detected by immunoblotting with anti-HA antibodies. Scale bars in (A) and (D): 5µm.

6.3.8 Pin2p contains a prion domain and is a prion-inducing protein

Pin2p has been identified in a screen as a protein that when overexpressed can induce the *[PIN+]* prion phenotype, which is a prerequisite for the prion formation by Sup35, referred to as the *[PSI+]* prion (Derkatch *et al.*, 2001). In addition, Pin2p contains an Asn-rich region, which was referred to as a prion-like domain (Alberti *et al.*, 2009) (Fig. 6.9 A). This domain is located in the C-terminal part of the protein facing the cytoplasm (Fig. 6.9 B). To confirm the ability of Pin2p to induce the *[PIN+]* prion, we over expressed Pin2p in a strain that expresses the N-terminal domain of Sup35 fused to GFP (SUP35NM::GFP) (Derkatch *et al.*, 2001), which also contains a prion domain. In the presence of prion-inducing activity, Sup35NM-GFP will aggregate and green foci and ring-like structures can be observed. When we overexpressed Pin2p in the cured tester strain, Sup35NM-GFP foci were formed, confirming that Pin2p can indeed induce prion formation (Fig. 6.9 C). Sup35 is a translational terminator, and loss of Sup35 causes a read-through in the *ade1-14* nonsense-mutation, allowing strains to grow in the absence of adenine (*ade-*). Aggregation of Sup35 equally allows strains to grow on *ade-* plates; growth on *ade-* plates was induced by overexpression of *PIN2* (Fig. 6.9 C) only in a construct in which the prion domain was present. Moreover, mutating the AP1/2 binding site (Pin2(out)p) (Fig. 6B), strongly reduced the ability of Pin2p to induce prion formation (Fig 6.9 C). In contrast, deleting *CHS5* and hence confining Pin2p to the TGN did not interfere with prion formation.

Next we tested whether Pin2p was itself able to form SDS-resistant aggregates after overexpression, which is considered a hallmark for a prion protein. Pin2p SDS-resistant aggregates were observed in a prion domain-dependent manner (Fig. 6.9 D). The SDS-resistant Pin2p aggregates were abolished when the prion domain was deleted (pin2(1-210), the AP complex motif (pin2out) or Asn and a Gln in the prion domain but away from the AP binding site were mutated to Asp and Glu (Fig. 6.9 A and B; Pin2QNtoEDp). Thus, Pin2p itself is able to form prion-like aggregates *in vivo*.

The prion domain of Pin2p comprises the C-terminal region and the tyrosine-based AP binding motif. Deletion of the prion domain or mutating the retrieval signal caused Pin2p to be delocalized over the plasma membrane. Thus, it was conceivable that the prion domain

could be important for retention of the protein in the cell. To test this possibility we assessed the formation of SDS-resistant Pin2p aggregates in $\Delta chs5$ (all Pin2p in the TGN) and in $\Delta end3$ (all Pin2p at the plasma membrane) mutant strains. However, under both conditions SDS aggregates were formed to a similar extent (Fig. 6.9 D). Thus, the localization of Pin2p per se is not important for prion formation, which may not be unexpected since the prion domain is facing the cytoplasm. Nevertheless, the prion domain of Pin2p may act as a TGN retention signal because Pin2QNtoEDp was exported to the plasma membrane in an exomer-independent and non-polarized fashion (Fig. 6.9 E and F).

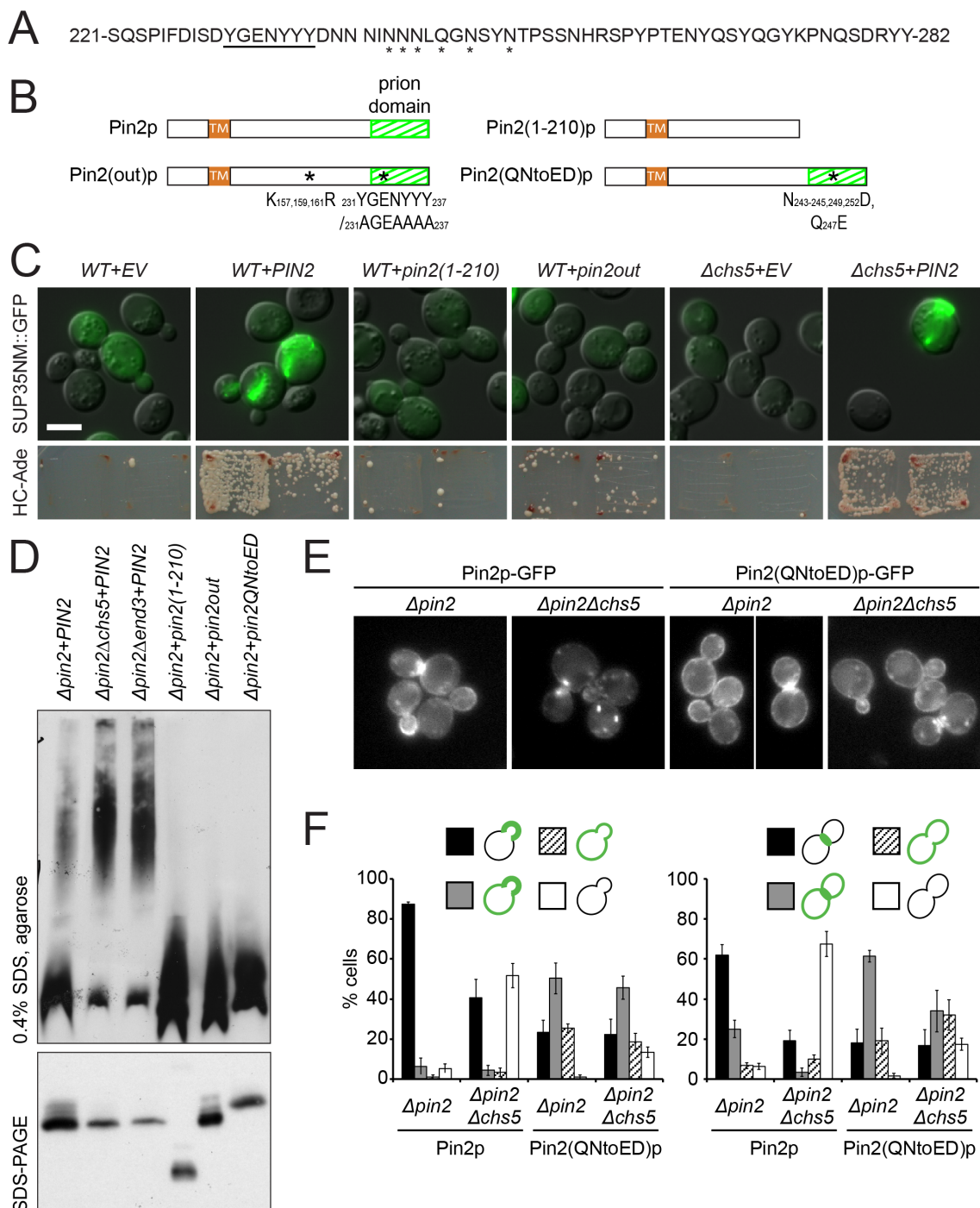


Figure 6.9 (previous page) The prion domain of Pin2p is functional in aggregated formation and acts as a TGN retention signal. (A) Amino acid sequence of the Pin2p prion domain. The potential AP-1-binding motif YGENYYY is underlined. Asterisks indicate residues mutated to disrupt aggregation of the prion domain. (B) Schematic representation of Pin2p with indicated prion domain; Pin2(1-210)p truncation devoid of prion domain; Pin2(out)p mutant in which lysines 157,159,161 and the YGENYYY motif were mutated; and Pin2(QNtoED)p mutant, in which 1 Q and 5 N were mutated to charged residues to disrupt prion domain aggregation. (C) Overexpression of Pin2p, but not mutants with a disrupted prion domain induces *[PSI+]*. *[PSI+]* induction was assessed in a *74-D694* strain overexpressing Pin2p or Pin2p mutants from a high copy number plasmid. *[PSI+]* induction was detected by the appearance of SUP35NM-GFP foci and ring-like structures and growth on medium lacking adenine. Scale bar: 5 μ m. (D) Accumulation of overexpressed Pin2p in SDS-resistant aggregates is prion domain-dependent and is enhanced by Pin2p trafficking block. Agarose gels of SDS-treated extracts from WT, Δ *chs5* or Δ *end3* strains overexpressing Pin2p or Pin2p variants mutated within the prion domain. Anti-Pin2p immunoblot. (E) Disruption of Pin2p aggregation through the prion domain causes loss of exomer-dependency and polarity at the plasma membrane. Fluorescence microscopy images of Δ *pin2* and Δ *pin2\Delta**chs5* strain cells expressing GFP tagged Pin2p or Pin2(QNtoED)p from a centromeric plasmid. Scale bar: 5 μ m. (F) Δ *pin2* and Δ *pin2\Delta**chs5* cells in (E), were scored for the expression Pin2p-GFP and Pin2(QNtoED)p-GFP at the plasma membrane and for the extent of the polarity of Pin2p localization. For quantifications 100 small and medium budded cells and 100 large budded cells were quantified in each of 3 independent experiments. Error bars: standard deviation.

6.3.9 Pin2p forms aggregates upon environmental stress and localizes to internal structures

Using the Δ *chs5* and Δ *end3* strain created a non-physiological all or nothing situation. We aimed to find conditions, in which we could potentially modulate the localization of Pin2p more immediately and less drastically. Others and we observed that under mild heat stress Chs3p is quickly internalized from the bud neck just to reappear delocalized all over the plasma membrane, which is thought to be associated with a stress response (Valdivia and Schekman, 2003; Zanolari *et al.*, 2011). Therefore, we probed the localization of Pin2p after exposure to various stresses (Fig. 6.10). Under a number of stresses, Pin2p was internalized and accumulated in internal structures. In contrast, Skg6p remained largely unaffected by the stressors, indicating that plasma membrane proteins are not randomly endocytosed upon stress encounter.

We chose one stress scenario, lithium treatment, for further analysis. To investigate the kinetics of this internalization, we performed a time course of lithium exposure and analyzed the Pin2p localization. Five minutes after addition of 200 mM LiCl, clusters of Pin2p proteins were present at the plasma membrane, after 15 min most of the Pin2p was internalized (Fig. 6.11 A and B). Pin2p stayed internalized even after treatment over night. The internalization event was signal dependent because interfering with either the osmotic shock signaling pathway (Hog1p MAP kinase) or the cell wall integrity pathway (Sit2p MAP kinase) caused a delay in endocytosis of Pin2p (Fig. 6. 12). Similar clustering of the GFP signal was observed with a mutant in which the ubiquitylation site(s) and the AP complex

binding motif were mutated (Pin2(out)p) and which should be therefore mostly plasma membrane localized. Consistently, the uptake of this construct was largely reduced (Fig. 6.11 A and B). To determine whether this retention for prolonged periods (over night) was dependent on aggregate formation, we used the Pin2p construct (Pin2QNtoEDp) in which critical Asn of the prion domain had been replaced by Asp and Glu (Fig 6.9 B). Similarly to the Pin2(1-210)p and the Pin2(out)p mutant proteins, the steady state localization of Pin2QNtoEDp was predominantly at the plasma membrane independent on the presence of Chs5p (Fig. 6.9 E and F), indicating that under already under normal growth conditions, the prion domain is contributing to the retention of Pin2p in internal structures. The initial uptake kinetics of the prion domain mutant under LiCl were similar to wild-type Pin2p, indicating that we indeed did not interfere with ubiquitin-dependent endocytosis signals. However, the Pin2QNtoEDp was less efficiently retained in internal structures (Fig. 6.11 A and B). Therefore, the prion domain in Pin2p is necessary for its internal retention. To demonstrate that Pin2p aggregates in internal structures, we performed blue native electrophoresis and detected a strong increase in aggregates in the MDa range in a lysate that was treated with LiCl, compared to the untreated control (Fig. 6.11 C). Our results are consistent with the Pin2p prion domain acting as a TGN retention signal under both non-stress and stress conditions. Under stress, the equilibrium of Pin2p would be shifted towards the aggregated state.

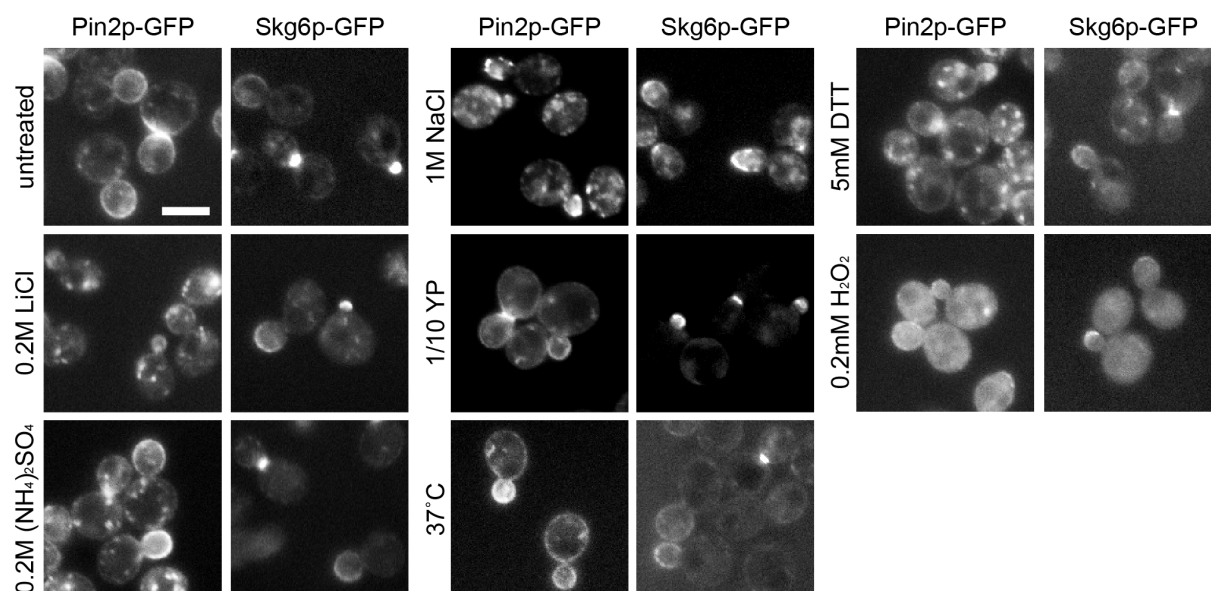


Figure 6. 10 Pin2p localization changes upon environmental stress. Fluorescence microscopy images of cells expressing chromosomally tagged Pin2p-GFP or Skg6p-GFP after 30 min treatment under indicated stress conditions. Scale bar: 5µm.

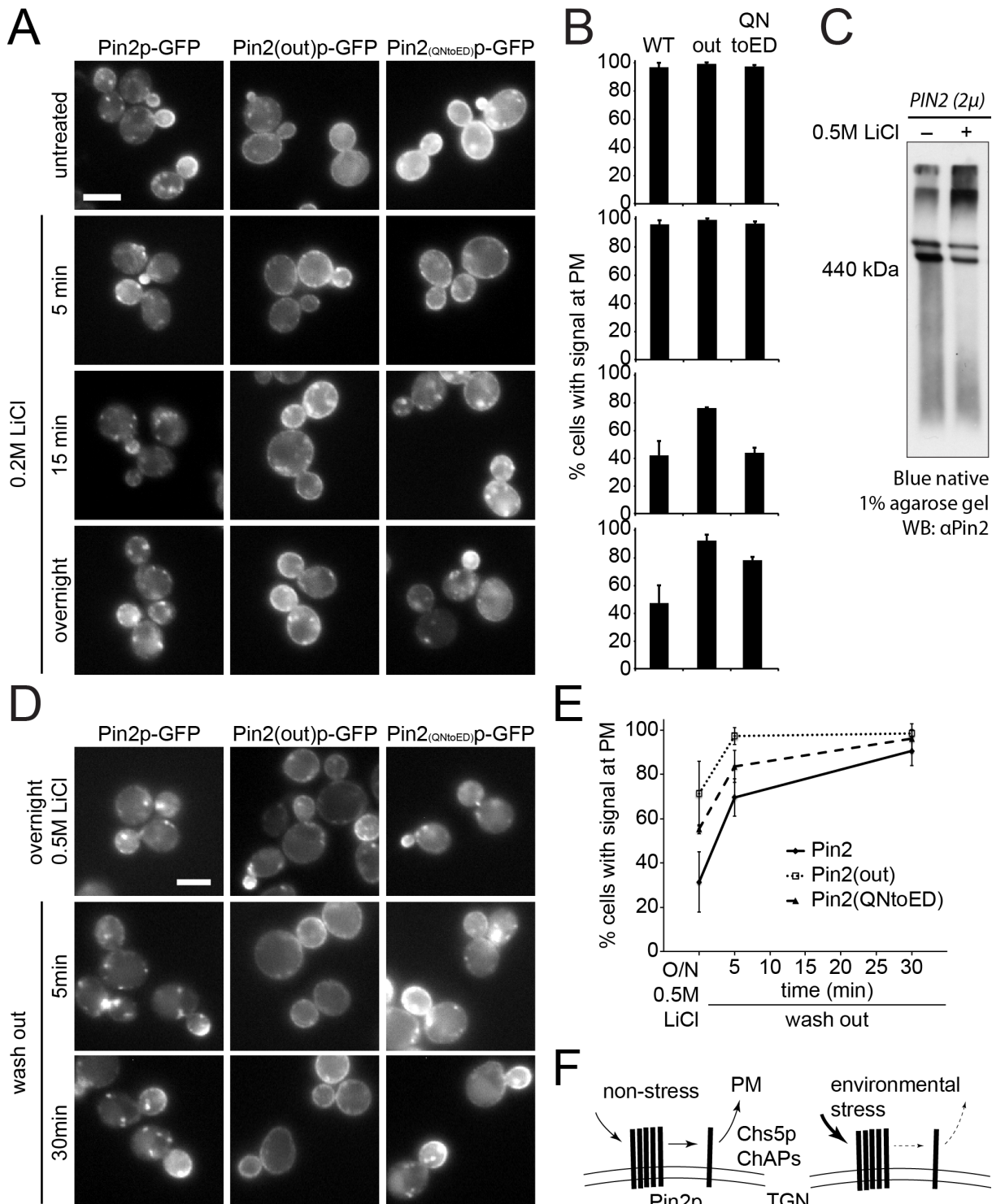


Figure 6.11 The prion domain maintains the dynamic retention of Pin2p in internal compartments upon environmental stress. (A) Pin2p upon exposure to Li⁺ is internalized in an ubiquitin-dependent manner and maintains its internal localization during prolonged exposure in a prion domain-dependent manner. Fluorescence microscopy images of $\Delta pin2$ cells treated for indicated time periods with 0.2 M LiCl, expressing Pin2p-GFP, Pin2(out)p-GFP and Pin2(QNtoED)p-GFP. Scale bar: 5 μ m. (B) Cells in (A) were quantified for the number of cells expressing Pin2p-GFP at the plasma membrane. 30 –100 small and medium budded cells were quantified in each of 3 independent experiments. Error bars: standard deviation. (C) LiCl treatment causes a shift of Pin2p to high molecular weight complexes. Blue native agarose gel electrophoresis of extracts from cells overexpressing Pin2p, untreated or treated for 1 hr with 0.5 M LiCl. Anti-Pin2p immunoblot. (Continued on next page)

(Figure 6.11 continued) (D) Pin2p is rapidly reexported to the plasma membrane upon environmental stress relief. $\Delta pin2$ cells expressing Pin2p-GFP, Pin2(out)p-GFP and Pin2(QNtoED)p-GFP were incubated over-night with 0.5 M LiCl. Cells were harvested by centrifugation, the LiCl containing medium was replaced with fresh HC medium and the cells were imaged at indicated time points after wash out. Scale bar: 5 μ m. (E) Cells in (D) were scored for the presence of Pin2p at the plasma membrane at indicated time points. 30 –100 small and medium budded cells were quantified in each of 3 independent experiments. Error bars: standard deviation. (F) Equilibrium shift model of Pin2p towards aggregate formation and resulting reduction of plasma membrane export upon environmental stress.

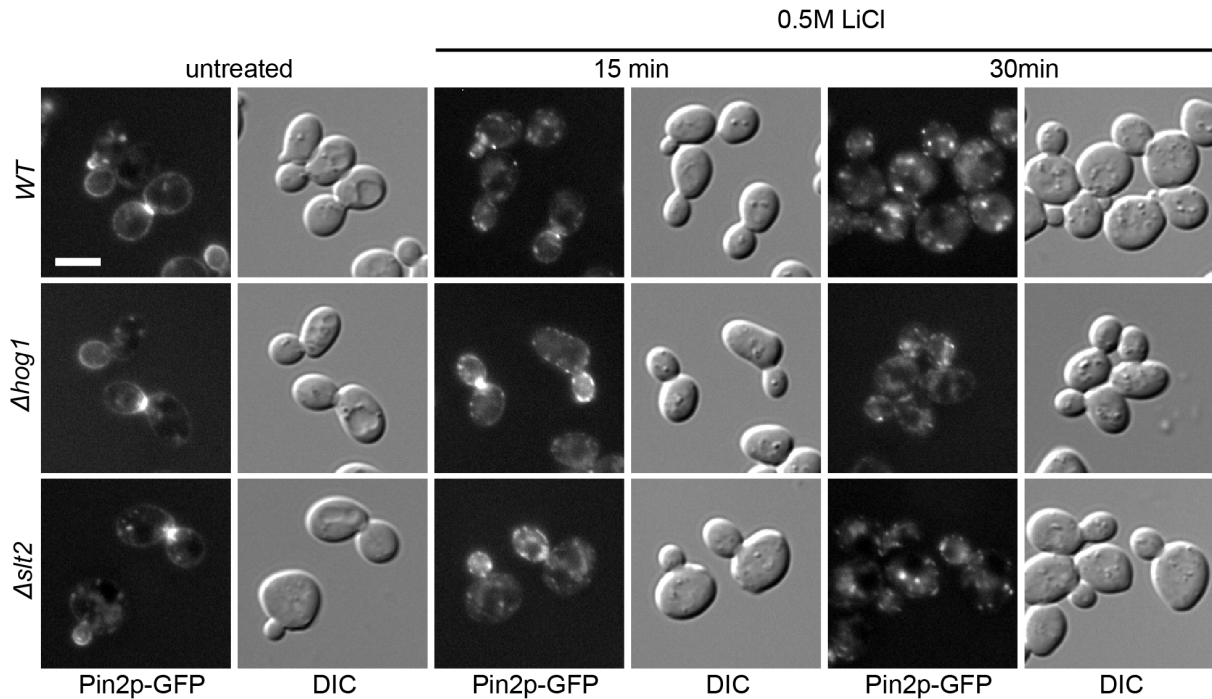


Figure 6.12 Knockout of the HOG1 or SLT2 signaling pathway delays Pin2p internalization upon environmental stress. Fluorescence microscopy images of wild type, $\Delta hog1$ and $\Delta slt2$ scells expressing chromosomally tagged Pin2p-GFP untreated or after 15 min and 30 min 0.5 M LiCl treatment. Scale bar: 5 μ m.

6.3.10 Pin2p aggregation in internal structures is reversible

Normally a cell would try to prevent proteins from aggregation. The prion domain of Pin2p comprises an essential part of the exomer interaction surface as well as the AP complex binding site. Thus aggregate formation would potentially preclude the functionality of these transport motifs, and provide a very efficient sequestering mechanism, and thereby prevent degradation of Pin2p. Therefore, Pin2p would be sequestered in internal structures for the time the stress persists and after stress release, Pin2p should readily appear at the plasma membrane in a polarized fashion. To test this hypothesis, we first treated cells for over night with 500 mM LiCl, to internalize Pin2p (Fig. 6.11 D and E) and then, we washed out the LiCl. Already 5 min after the washout, Pin2p re-appeared at the plasma membrane of the bud, the process being completed within 30 min (Fig. 6.11 D and E). As expected the Pin2(out)p and

Pin2(QNtoED)p were less efficiently retained intracellularly than wild-type Pin2p, but their release from internal stores followed similar kinetics. Thus, the prion domain-mediated aggregation of Pin2p is reversible and may serve as a novel temporary retention mechanism upon encounter of stress and during the cell cycle.

6.4 Discussion

We identified a new exomer-dependent cargo that is localized in a temporally and spatially controlled fashion, like the other well-characterized cargo Chs3p. Moreover, Pin2p shares very similar trafficking requirements to Chs3p, such as that it needs constant endocytosis and recycling through the TGN to maintain its proper localization at the plasma membrane (Table 1). Similar trafficking requirements were also observed for Fus1p, however only after response to mating (Barfield *et al.*, 2009). Thus, from the three exomer-dependent cargoes a common regulatory pathway emerges: all three cargoes require constant endocytosis, recycling from early endosome to the TGN and exocytosis in an exomer-dependent manner for their proper localization at the plasma membrane. However, not all polar localized proteins are bona fide exomer-dependent clients. The protein Skg6p that is localized in a polarized fashion at the bud tip and even can interact with exomer, does not rely on exomer for its localization. Since we detected the interaction by *in vitro* crosslinking and by GST pull-downs, Skg6p may still be able to use the exomer-dependent transport route, but it certainly can also exploit the more classical route via early endosomes.

Although Pin2p, Chs3p and Fus1p are exomer-dependent cargoes, they all use somewhat different recognition signals for their interaction with exomer. Our studies confirm that they are complex and may involve at least two different regions of the protein, as a minimum one may be unstructured and may fold only after interaction with exomer.

However, there seems to be a feature that appears to be distinct between Pin2p and the other two exomer cargoes: Pin2p contains a prion-like domain, and our studies demonstrate that overexpressed Pin2p can form SDS-resistant aggregates *in vivo*. While it is not understood, how Chs3p is kept in internal stores after the bud neck constriction has been finished, we show here for the first time that prion formation can act as a retention signal in internal stores, at least in the case of Pin2p expressed at physiological levels. Prion domains do not always form aggregates that cannot be resolved by the cellular machinery anymore. For example, a number of processing body (P-body) components, which are part of the major mRNA decay machinery in yeast and mammals contain prion-like domains, which are thought to be essential for functional P-body formation (Michelitsch and Weissman, 2000; Decker *et al.*, 2007; Alberti *et al.*, 2009). The prion domain of Pin2p is rich in asparagines,

which is supposed to form benign aggregates, while glutamine-rich domains promote the formation of toxic conformers (Halfmann *et al.*, 2011). These benign aggregates can be resolved again and are non-toxic.

The prion domain is required to regulate Pin2p export to the plasma membrane under normal and stress conditions (Fig. 7F). It is unlikely that Pin2p is the only protein that uses an aggregation mechanism to control its localization. In a census for prion-like domains in *S. cerevisiae*, a number of proteins involved in vesicular traffic have been identified (Michelitsch and Weissman, 2000). However, to our knowledge for none of these cases regulated trafficking depending on the prion domain has been demonstrated. In mammalian cells, Pmel 17 forms benign amyloid fibers in melanosomes to sequester melanin (Berson *et al.*, 2003). Although the aggregate formation in this case is dependent on cleavage by a metalloprotease, the transport of Pmel17 such as export from the ER and endocytosis from the plasma membrane are critical for sorting and its function (Fowler *et al.*, 2006; Theos *et al.*, 2006). An analogous pathway to the exomer route from the TGN to the plasma membrane has also been identified in metazoans (Wakana *et al.*, 2012). Again the number of proteins that take this transport route is rather small to date, and the identifications of more cargoes may also reveal function of prion retention in this pathway. Since between 2-5% of the cellular proteins, depending on the organism, contain a prion-like domain, similar regulation as in the case of Pin2p will also be used by other proteins.

What would be the function of the prion-dependent retention mechanism? During normal growth and under stress, it will regulate the amount of Pin2p present at the plasma membrane. Moreover, this mechanism will prevent the degradation of Pin2p as it remains at least under stress conditions internally for at least 16 hrs. Under those conditions, this retention seems to be important, because Pin2p was released from internal stores already after 5 min after the end of the stress. This release mechanism is much faster than re-synthesis and transport of Pin2p. To our knowledge this is the first prion protein for which such a retention mechanism has been postulated.

The retention of Pin2p by the prion-like domain could be brought about through two non-exclusive mechanisms. Since part of the exomer-interaction domain is located in the prion-like domain, TGN export signals could be masked. Alternatively, the size of the prion-dependent Pin2p aggregate in the TGN is too big to get into transport vesicles. The latter possibility would not only restrict Pin2p from plasma membrane localization but would also protect Pin2p from degradation in the vacuole, because it cannot be transported there.

Similar to Pin2p, Chs3p also reacts to stress. Upon cell-wall stress, Chs3p is rapidly endocytosed and then released at the plasma membrane in a non-polarized fashion

(Valdivia and Schekman, 2003). This release from internal stores, is dependent on the small GTPase Rho1p and the protein kinase Pkc1p (Valdivia and Schekman, 2003). The regulation of the stress response may not be a conserved feature among exomer-dependent cargo, and may be more related to their function as a mutant in PKC1 did not interfere with Pin2p trafficking under Li⁺ stress or the release from it (data not shown).

Why Pin2p would have to be retained in internal stores upon stress, is at the moment unclear. We speculate that it might sense stress and that a fraction might be continuously released to the plasma membrane to check out the environment. Two cyteines in the extracellular N-terminus that are spaced apart by 5 amino acids may be able to sample the environment. Consistent with this hypothesis, Pin2p was found to interact with various components of the cell wall integrity pathway in high throughput analysis (Tarassov *et al.*, 2008; Schlecht *et al.*, 2012) and mutant in MAP kinases of stress sensing pathways, $\Delta slt2$ and $\Delta hog1$, delayed endocytosis of Pin2p upon stress.

6.5 Materials and Methods

6.5.1 Identification of novel exomer-dependent cargo

Cells expressing either a ChAP or Chs5p appended with an HBH-tag (Tagwerker *et al.*, 2006) were grown in YPD to an OD₆₀₀ of 1 at 30°C. one % formaldehyde was added for 10 min. The action of formaldehyde was quenched by 125 mM glycine for 5 min. The cells were harvested, washed, frozen in liquid N₂ and stored at -80°C. Cross-linked cells were lysed in 50 mM NaPi pH 8.0, 8 M urea, 300 mM NaCl, 0.5 % Tween20 20 mM imidazole (buffer 1) + protease inhibitors using a bead beater. Cell debris and heavy membranes were removed by centrifugation (2,500 x g and 20,000 x g for 10 min at RT). The cleared lysate was incubated with Ni-NTA, and the bound proteins were washed in buffer 2 (buffer 1 at pH 6.4, 40 mM imidazole) and eluted in buffer 3 (50 mM NaAc pH 4.3, 8 M urea, 300 mM NaCl, 0.5 % Tween-20). The eluate was readjusted immediately to pH 8.0 and incubated with streptavidin beads O/N. The beads were washed first with buffer 4 (50 mM Tris/HCl pH 8.0, 8 M urea, 300 mM NaCl, 2 % SDS and then with buffer 5 (buffer 4 but with only 0.2 % SDS). The bound proteins were on-bead digested with LysC and trypsin. The resulting peptides were subjected to LC-MS/MS analysis.

6.5.2 Strains, yeast genetic methods and growth conditions

Chromosomal tagging and deletions were performed as described (Knop *et al.*, 1999; Gueldener *et al.*, 2002). PCR-based chromosomal manipulations were confirmed by colony PCR. Standard yeast media were prepared as described (Sherman, 1991). All strains, unless otherwise indicated, were grown at 30°C. HC medium selective for the plasmid was used to grow transformants. For the [PSI⁺] induction assay 74-D694 cells were cured of prions on YPD medium containing 5 mM GuHCl (Tuite *et al.*, 1981) to obtain [*pin*-][*psi*-] cells. HC medium lacking adenine was used to select for [PSI⁺] at 23°C. HC medium selective for the plasmid and 70 μM CuSO₄ or 100 μM CuSO₄ was used to express CUP-1 driven SUP35NM::GFP and HA-ubiquitin constructs, respectively.

6.5.3 Plasmids

For expression of GST tagged full-length cytosolic domains of Pin2p and Skg6p restriction fragments encoding aa 72-282 of Pin2p and aa 98-734 of Skg6p were cloned into pGEX-6P-1 (GE Healthcare) using *Bam*HI and *Eco*RI restriction sites. *Bam*HI and *Xho*I restriction fragments encoding aa: 72-152, 72-210, 153-282 of Pin2p were cloned into pGEX6P-1 to obtain GST-tagged Pin2p cytosolic truncations. For GFP tagged Pin2p constructs *Eco*RI-*Sph*I restriction fragments containing the *PIN2* promoter (600bp upstream of the start codon) and *PIN2* ORF encoding aa: 1-282 (full length), 1-152, 1-179, 1-210 or 1-245 of Pin2p were cloned into pGFP33 (YCPlac33 with inserted GFP-CYC1 terminator *Sph*I-HindIII restriction fragment). To create pGFP33 pin2Δ79-152 a long template PCR approach was applied, in which the entire plasmid containing a *PIN2* promoter – *PIN2* ORF insert was amplified excluding the region encoding aa 79-152 and religated through a *Nhe*I restriction site added on the 5' ends of the primers. For overexpression of *PIN2*, the *PIN2* ORF was cloned into p426GPD plasmid using *Eco*RI/*Bam*HI restriction sites or *Bam*HI/*Eco*RI restriction sites for the pin2(1-210) truncation. To obtain high copy number plasmids an *Eag*I restriction fragment containing the *leu2-d* allele (amplified from pHR81 plasmid) (Nehlin *et al.*, 1989) was cloned into the p426GPD plasmids. All point mutations were introduced using the QuikChange Site-Directed Mutagenesis protocol (Stratagene). The GFP tagged N-terminal domain of Sup35 was overexpressed from pSUP35NM::GFP-HIS3 plasmid (Derkatch *et al.*, 2001). HA tagged ubiquitin was overexpressed from YEpl12 HA-Ub plasmid (Hochstrasser, 1991).

6.5.4 Western Blot detection

Epitope tags and proteins were detected using the following antibodies: anti-myc (Sigma 9E10; 1:1,000); anti-HA (Eurogentec HA11; 1:1,000); anti-AU5 (Abcam, Cambridge, MA; 1:1,000); anti-Chs5p ((Trautwein et al., 2006); affinity-purified; 1:500); anti-Pin2p serum raised against GST-Pin2(72-282)p (1:2,000); anti-GFP (Torrey Pines Biolabs, Secaucus, NJ; 1:5,000 or Roche anti-GFP 7.1 and 13.1; 1:500); anti Pgk1 (Invitrogen #A-6457; 1:1,000). ECL (GE Healthcare) was used for detection.

6.5.5 Microscopy

Cells were grown to OD₆₀₀ 0.2-0.7 in YPD or HC medium selective against plasmid supplemented with adenine, harvested and mounted. Apart from environmental stress assays, cells grown in YPD were washed and resuspended in HC complete medium. Images were acquired with an Axiocam mounted on a Zeiss Axioplan 2 fluorescence microscope, using filters for GFP.

6.5.6 Trypsin protection assay

Five OD of *PIN2-yeGFP::KanMX4* or *SKG6-yeGFP::KanMX4* cells grown to OD₆₀₀ 0.2-0.7 were harvested and spheroplasted as described previously (ref). Spheroplasts were resuspended in 170 µl modified buffer B88 (20 mM HEPES 250 mM sorbitol, 150 mM NaAc pH 5.5, 5 mM Mg(Ac)₂, pH 6.8). The sample was split into 20 µl aliquots and incubated with or without 2.5 µg of trypsin in the presence or absence of 1 % TX-100. Trypsin digestion was stopped after 10 min or 90 min by addition of 1.25 µg of Trypsin inhibitor. Samples were boiled at 68°C in SDS sample buffer.

6.5.7 Protein agarose gel electrophoresis of Pin2p SDS-resistant aggregates

Pin2p SDS-aggregates were visualized in a similar manner as Rnq1 subparticles described previously (Liebman et al., 2006) with some modifications to the protocol. 20 OD₆₀₀ of *pin2Δ::LEU2*, *pin2Δ::LEU2 chs5Δ::HIS5* or *pin2Δ::LEU2 end2Δ::HIS5* cells transformed with p426GPDleu2d plasmids overexpressing PIN2 wild type or mutant variants were harvested per sample. Cells were washed with water and resuspended in 200 µl 20 mM HEPES pH 6.8, 150 mM NaAc, 5 mM Mg(Ac)₂ buffer supplemented with protease inhibitors. Cells were lysed by 10 min vortexing at 4°C with 120 µl of glass beads. Lysates were cleared by gentle centrifugation and Pin2p was extracted from membranes by addition of 1 % Tween 20 and 3 min incubation at RT. Extracts were then centrifuged 5 min 10,000×g. Protein concentrations were adjusted after BCA assay. Lysates were incubated in sample buffer: 25 mM Tris, 200

mM glycine, 0.4 % SDS, 5 % glycerol, bromophenol blue – final concentration, for 5 min at RT. Fifty – 100 µg of protein was loaded onto 1.5 % SeakemGold (Lonza) agarose, 30 % glycerol, 25 mM Tris, 200 mM glycine, 0.1 % SDS gels cast in a vertical system. Casting was performed according to a previously published protocol (Warren et al., 2003). Gels were run in running buffer (25 mM Tris, 200 mM glycine, 0.1 % SDS) at 6 mA constant current. Proteins were transferred at 20 V for 2 hrs at 4°C in running buffer supplemented with 20 % methanol using a semi-dry transfer system. Blocking and antibody incubations were performed in Blotto (5 % milk, 5 % egg albumin, TBST).

6.5.8 Blue native agarose gel electrophoresis

Yeast extracts for BN agarose gel electrophoresis were prepared as lysates for Pin2p SDS-resistant aggregate visualization except that TBXG (50 mM Tricine, 15 mM BisTris, 15 % glycerol, 0.1 % TX-100, pH 7.0) sample buffer was added to the extracts. Fifty – 100 µg of protein was loaded on 1 % SeakemGold (Lonza) agarose, 30 % glycerol, 0.5 M aminocaproic acid, 50 mM BisTris-HCl pH 7.0, 0.005 % TX-100 gels and run in a blue native system (Schägger and Jagow, 1991) at 8 mA constant current.

6.5.9 GST tagged protein purification

GST tagged full length cytosolic domain of Pin2p and cytosolic domain truncations were expressed from pGEX-6P-1 plasmids in E. coli Rosetta cells by induction with 0.2 mM IPTG for 4 hrs at 23°C. Purification was carried out according to standard procedures with GSH agarose (Sigma-Aldrich) in Pin2p buffer: 150 mM KCl, 50 mM Tris-HCl pH 8.0, 0.5 % TX-100, 5 % glycerol. GST-Skg6p lysates from E. coli Rosetta cells were obtained as described for GST-Pin2p except that GST-Skg6p expression was induced for 6 hrs at 23°C and Skg6p buffer was used: 25 mM KCl, 50 mM Tris-HCl pH 8.0, 0.5 % TX-100, 5 % glycerol. Skg6p lysates were snap frozen after centrifugation. Sec22-GST was purified as previously described (Schindler and Spang, 2007).

6.5.10 GST pull downs

For pull-downs 5 µg of GST-Pin2p and Sec22-GST, and 0.5 ml of GST-Skg6p E. coli lysate was prebound to 10 µl of GSH agarose (Sigma Aldrich). 10 OD₆₀₀ per pull down reaction of *BCH1-2AU5::LEU2 BCH2-3HA::HIS3Mx6 BUD7-9myc::TRP1 CHS6-yeGFP::KanMX4, bch1Δ::HIS5 bch2Δ::KanMX4 bud7Δ::LEU2 chs6Δ::URA3 or CHS6-9myc::TRP1* cells were grown to OD₆₀₀ 0.2-0.7 and harvested. Cells were spheroplasted and lysed in 1 ml B150Tw20 (20 mM HEPES pH 6.8, 150 mM KAc, 5 mM Mg(Ac)₂, 1 % Tween-20)

supplemented with protease inhibitors. 900 μ l of yeast extracts were incubated for 1 hr at 4°C with 10 μ l of GSH agarose with prebound GST tagged protein. Pull downs were washed 3 x in B150Tw20 and once in with 20 mM HEPES pH 6.8, 150 mM NaCl. Pull-downs were eluted with 35 μ l of SDS sample buffer and boiled at 68°C.

6.5.11 Denaturing immunoprecipitations

20 OD₆₀₀ of *pin2 Δ ::LEU2* cells transformed with YEp112 HA-ubiquitin plasmid and pGFP33 PIN2 or pGFP33 pin2K7R plasmid were harvested per immunoprecipitation reaction. Cells were spheroplasted and lysed in 200 μ l 20 mM HEPES pH 6.8, 200 mM KCl, 1 mM MgCl₂, 2% TX-100, 1 mM DTT buffer with protease inhibitors (Sogaard et al., 1994). Lysates were cleared by 10 min 10,000 \times g centrifugation. 1 % SDS was added to the supernatants and the lysates were boiled for 3 min at 95°C. Extracts were diluted 10 x in dilution buffer to achieve 20 mM HEPES pH 6.8, 200 mM KCl, 1 mM MgCl₂, 0.5 % TX-100, 0.1 % SDS final buffer concentration and centrifuged for 10 min at 10,000 \times g to remove any precipitate. 1.9 ml of extracts were incubated at 4°C overnight with 5 μ g of anti-GFP antibody (Torrey Pines) or 5 μ g of control affinity purified rabbit IgG antibody (Dianova, Hamburg, Germany) bound to 10 μ l of protein A-Sepharose. Samples were washed 3 x with 20 mM HEPES pH 6.8, 200 mM KCl, 1 mM MgCl₂, 0.5 % TX-100 and once with 20 mM HEPES pH 6.8, 200 mM NaCl buffer. Immunoprecipitates were eluted with 35 μ l SDS sample buffer and heated to 68°C.

6.5.12 [PSI⁺] induction assay

[PSI⁺] induction assay was carried out as described previously (Derkatch *et al.*, 2001). Briefly [pin-][psi-] 74-D694 wild type or *chs5 Δ ::KanMX4* strain was transformed with pSUP35NM::GFP-HIS3 and PIN2 wild type or mutant variant overexpressing p426GPDleu2d plasmids. PIN2 wild type or mutant variant were overexpressed by replica plating transformants for 35 generations on HC –Leu– Ura –his medium, which allowed the p426GPD leu2d plasmids to be amplified to approximately 100 copies per cell. Transformants were then replica plated onto HC –His +Cu²⁺ medium to induce SUP35NM::GFP and allow [PSI⁺] prion formation. Transformants were checked for the presence of SUP35NM::GFP dot and ring-like structure by fluorescence microscopy and 2 random colonies from each strain from HC –His +Cu²⁺ plates were streaked out onto HC – Ade medium to confirm [PSI⁺] induction.

6.6 Acknowledgements

We wish to thank I. Derkatch, S. Liebman and M. Hall for strains and reagents. I.G. Macara is acknowledged for critical reading of the manuscript. We thank P. Jenö and S. Moes of the mass spec facility of the Biozentrum of the University of Basel for the mass spec analysis. This work was supported by the Boehringer Ingelheim Fund (A. R.), the Swiss National Science Foundation (31003AB-126021 and 31003A -141207 to A.S.), and the University of Basel.

7. Chs5, ChAP and Pin2 cytosolic domain interaction

7. Exomer subunits bind in a concerted way to the Pin2p cargo tail.

We observed that either Bch1 or Bch2 were sufficient for Pin2 export. Deletion of both resulted in a strong retention of Pin2 in internal compartments; although to a lesser extent than observed in a *CHS5* deletion strain. To establish which ChAPs would bind directly to Pin2, we performed pull downs of yeast extracts from wild type or triple ChAP deletion strains with the GST-tagged cytosolic domain of Pin2. Each ChAP was able to interact with the Pin2 cargo tail in the absence of all the other ChAPs. This demonstrates that all ChAPs are able to recognize Pin2, and also potentially other cargo, directly. The binding of Bch2

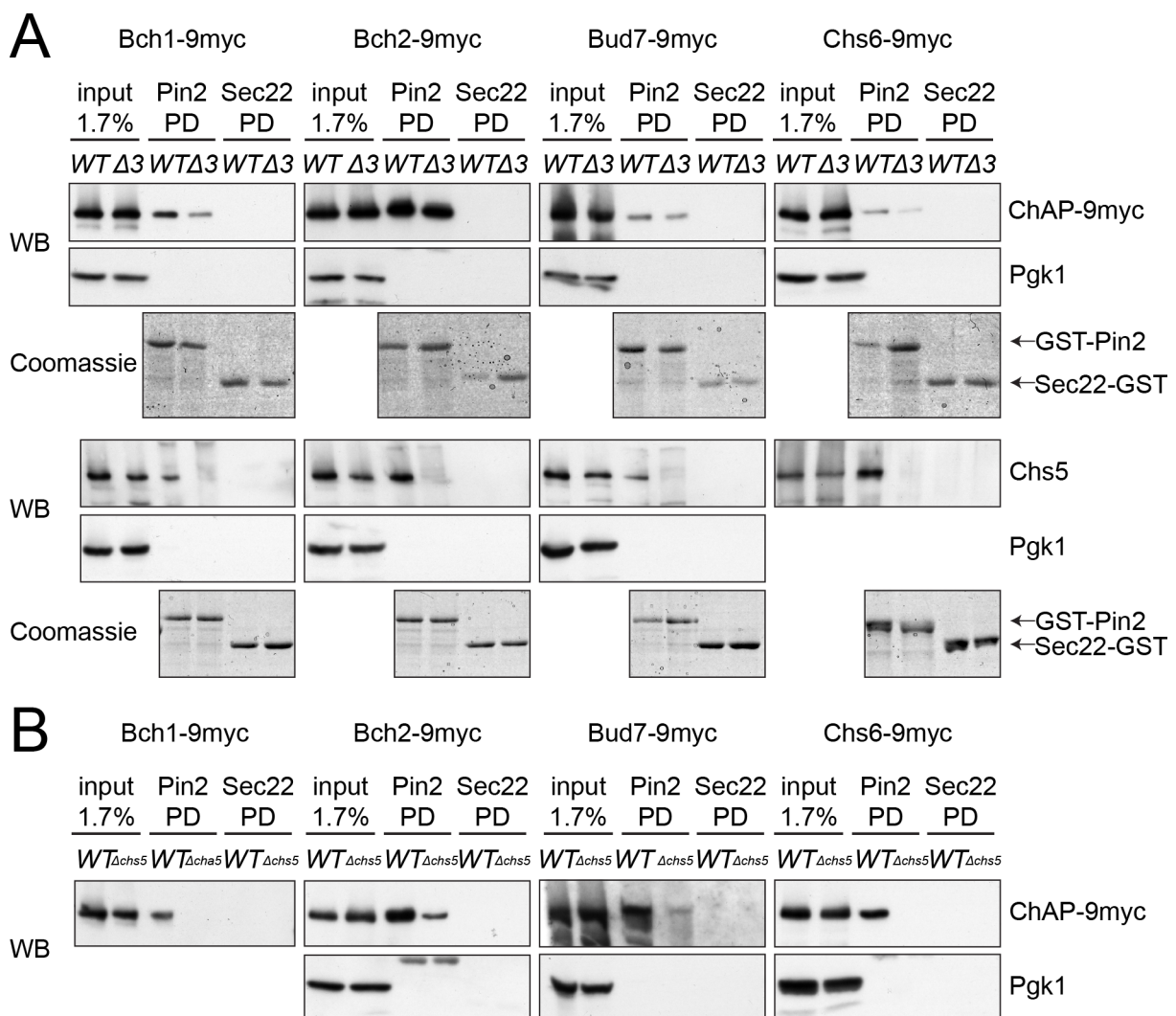


Figure 7.1. Exomer subunits bind in a concerted manner to the Pin2 cytosolic domain. (A) Pull down of yeast lysates with the GST-tagged cytosolic domain of Pin2. Sec22-GST was used as a negative control. Extracts were prepared from wild type and triple ChAP ($\Delta 3$) deletion strains, where the remaining ChAP was chromosomally tagged with 9-myc. Pull downs were immunoblotted for the ChAPs (with 9myc antibody), Chs5 or Pgk1 – negative control. Coomassie staining was used to assess the levels of GST-tagged constructs in the pull-down. (B) Pull down performed as described in (A) except that extracts were prepared from wild type and $\Delta chs5$ cells.

– the strongest Pin2 interactor, was not affected by deletion of the other ChAPs, similarly to what we observe for Bud7. Bch1 and Chs6, however, showed a significantly lower binding affinity to Pin2, when present as the sole ChAP in the cell. We next wanted to test whether single ChAPs would sustain the formation of “functional”, ChAP-Chs5 exomer complexes on the Pin2 cytosolic domain. To this end, we probed the pull downs from $\Delta 3ChAPs$ cell extracts for Chs5. Chs5 interaction with Pin2 was severely decreased, independent of the single ChAP present in the strain (Figure 7.1 A). This data shows that in general ChAPs enhance each other’s binding to Pin2, although Bch2 and Bud7 may act as the initial interactors. In addition, more than one type of ChAP appears to be required for the efficient recruitment of Chs5.

Conversely, we asked whether Chs5 could stabilize the ChAP-Pin2 interaction. To test this possibility we performed a pull down with lysates from $\Delta chs5$ cells. In the absence of Chs5, binding of Bch1 and Chs6 to Pin2 was not detectable. In contrast Bch2 and Bud7, were still able to bind to Pin2 directly, albeit significantly less (Figure 7.1 B). Together these data show that exomer components assemble in a concerted manner on the Pin2 cargo tail and stabilize each other’s binding. Bch2 and Bud7 could most likely mediate the initial contact with Pin2 for complex assembly.

8. Regulation of Pin2 transport by reactive cysteines

8. Cysteines regulate Pin2 trafficking by formation of a luminal pin structure through disulfide linkage and as a signal for palmitoylation.

Alicja M. Ritz and Anne Spang

Growth & Development, Biozentrum, University of Basel, Klingelbergstrasse 70, CH-4056
Basel, Switzerland

This manuscript is in preparation. The above authors made the following contributions:

Alicja M. Ritz performed all experiments and wrote the manuscript.

Anne Spang supervised this study and wrote the manuscript with Alicja Ritz.

8.1 Abstract

Cysteines are rare and highly reactive amino acids that can coordinate metal ions, form disulfide bridges and undergo posttranslational modifications. In this study we investigated the role of cysteines as trafficking signals for the prion-domain containing exomer-dependent cargo, Pin2. Pin2 undergoes regulated, stress-responsive trafficking through cycling between the plasma membrane, trans-Golgi network and early endosomal compartments. Interference with palmitoylation either by mutation of a cluster of four cytosolic cysteines or deletion of five DHHC proteins resulted in a reduction of Pin2 expression at the plasma membrane early in the cell cycle. We also identified a five amino acid, disulfide-linked loop in the luminal domain of Pin2, which is required for efficient export to the plasma membrane. Whether this loop influences Pin2 aggregation through the Pin2 prion domain, the topology of the Pin2 transmembrane domain within the lipid bilayer or has a regulatory role, for example allowing metal ion sensing, remain exciting open questions.

8.2 Introduction

Cysteines appear as special amino acids in protein sequences. Due to the nucleophilicity, redox activity and metal coordination ability of their thiol group, cysteines are highly reactive and thus subject to strong evolutionary pressure. In eukaryotes, cysteines are present in secreted proteins and in the luminal or extracellular domains of transmembrane proteins. They can engage in disulfide bond formation catalyzed in the oxidative environment of the ER (Frandsen *et al.*, 2000; Sevier and Kaiser, 2002). Formation of disulfide links is tightly connected to protein folding and is supposed to stabilize protein structure (Mamathambika and Bardwell, 2008). A disulfide-bonded loop in chromogranin B has been shown to be both required and sufficient for its sorting from the trans-Golgi network into secretory granules (Chanat *et al.*, 1993; Krömer *et al.*, 1998; Glombik *et al.*, 1999).

Cysteines can coordinate metal ions to allow their transport, form specific protein structures such as zinc-fingers or constitute catalytic cores in about 41% of enzymes (Andreini *et al.*, 2008). The Menkes protein (MNK or ATP7A), a copper-transporting CPX-type ATPase involved in intracellular copper homeostasis, possesses six GMXCXXC motifs, which act as putative metal binding sites (MBSs) (Solioz and Vulpe, 1996). MNK localizes to the trans-Golgi network (Petris *et al.*, 1996; Yamaguchi *et al.*, 1996; Dierick *et al.*, 1997) and is redistributed to the plasma membrane upon incubation of cells with high copper medium (Petris *et al.*, 1996; La Fontaine *et al.*, 1998). Interestingly mutation of cysteines in MBSs 5 and 6 abolishes the copper-dependent export of MNK (Strausak, 1999).

Posttranslational modifications such as S-nitrosylation or lipidation by prenylation or S-acylation (palmitoylation) occur on cysteines. Lipidation allows membrane tethering of proteins involved in signalling, membrane trafficking, polarity establishment and synaptic transmission (Iwanaga *et al.*, 2009; Aicart-Ramos *et al.*, 2011). Protein acyltransferase activity has been assigned to the DHHC protein family (Tsutsumi *et al.*, 2008), which has seven identified members in yeast and 23 in humans. DHHC protein acetyl transferases (PATs) are multispanning membrane proteins that localize to the ER, Golgi and plasma membrane (Ohno *et al.*, 2006). There are no known sequence signals required for palmitoylation apart from the presence of membrane-proximal cysteines. Modification of transmembrane domain (TMD)-containing proteins by palmitoylation has been shown to affect their association with lipid rafts for signal transduction (Kabouridis *et al.*, 1997; Zhang *et al.*, 1998), or promote their targeting to the plasma membrane (Alvarez *et al.*, 1990; Blanpain, 2001; Kraft, 2001; Tsutsumi *et al.*, 2008). Interestingly palmitoylation is a reversible modification (Magee *et al.*, 1987), suggesting that it can also undergo dynamic regulation. In

fact the cycling of the small GTPase signaling molecules H-Ras and N-ras between the Golgi and plasma membrane seems to be regulated by recurrent palmitoylation and depalmitoylation (Goodwin *et al.*, 2005; Rocks *et al.*, 2005; 2010).

In this study we focused on the influence of cysteine-based signals on the regulated, environment-responsive trafficking of Pin2. Pin2 shuttles between the plasma membrane, endosomes and the trans-Golgi network (TGN) compartments to allow its regulated expression at the cell surface (Ritz *et al.*, in revision). The export of Pin2 to the plasma membrane occurs directly from the TGN and is mediated by the yeast specific exomer complex (Ritz *et al.*, in revision). Other known exomer cargoes are the yeast chitin synthase III, Chs3 (Santos *et al.*, 1997; Santos and Snyder, 1997; Ziman *et al.*, 1998; Valdivia and Schekman, 2003; Trautwein *et al.*, 2006) involved in cell wall modeling during the cell cycle (Shaw *et al.*, 1991) and under stress conditions (Jung and Levin, 1999) and Fus1 (Santos *et al.*, 1997; Santos and Snyder, 1997), a cell fusion factor during mating (Trueheart *et al.*, 1987). Pin2 is a single-spanning membrane protein that possesses two cysteines at the N-terminus within its short luminal domain and a cluster of four TMD-proximal cysteines, in its cytosolic portion. A seventh cysteine is buried within the TMD sequence. We show that the two luminal and four cytosolic cysteines are required for proper Pin2 trafficking. The cytoplasmic four-cysteine cluster is palmitoylated and necessary for plasma membrane localization of Pin2 early in the cell cycle. The N-terminal cysteines form an intramolecular disulfide bridge, inducing a pin structure in the luminal domain close to the membrane interface. Loss of this pin structure retains Pin2 in internal compartments. Together our results demonstrate the relevance of cysteines as signals for the regulated trafficking of Pin2 and reveal a novel type of structural motif acting on the luminal side of a membrane protein.

8.3 Results

8.3.1 A four-cysteine cluster in Pin2 chelates metal ions in vitro

In a previous study (Ritz *et al.*, submitted), we tested the interaction of the novel exomer cargo, Pin2 with subunits of the cytosolic exomer complex by means of a pull down assay. For this we expressed and purified the GST-tagged cytosolic domain of Pin2 (residues 72-282) in *E. coli*. We observed that GST-Pin2 (aa 72-282) had a distinct ochre color (Figure 8.1 B). This coloration was still present in a GST-Pin2(72-152) C-terminal truncation, but was absent in a GST-Pin2(153-282) construct lacking the first eighty, membrane proximal residues (data not shown). This suggests that Pin2 can chelate metal ions and that the region required for metal coordination must lie within residues 72-152 of the cytosolic

domain. A cluster of four cysteines; cysteine 79, 81, 82 and 84, proximal to the transmembrane domain (TMD) (Figure 8.1 A) would be a likely candidate for a metal coordination site, however this would need to be verified by purification of a GST-Pin2(C79,81,82,84S) mutant. To test whether and which metals would be bound by Pin2 we sent the GST-Pin2(72-282) construct, containing the full length, unmutated Pin2 cytosolic domain for atomic absorption spectroscopy (AAS) analysis. AAS revealed the presence of zinc, iron and copper in a 2:1, 5:1 and 19:1 molar ratio to GST-Pin2(72-282)p, respectively (Table 8.1). These data confirmed that the cytosolic domain of Pin2 could accommodate a metal ion.

Detection method	molecule /element	Concentration in sample [g/kg]	Molecular weight [g/mol]	Moles/kg *10 ⁻⁵	Pin2:element molar ratio
Bradford	GST-Pin2 (72-282)p	4.5	51,000	8.8	-
AAS	Zinc (Zn)	3*10 ⁻³	65	4.6	2:1
	Iron (Fe)	1*10 ⁻³	56	1.8	5:1
	Copper (Cu)	0.3*10 ⁻³	64	0.5	19:1

Table 8.1 The purified GST-tagged Pin2 cytosolic domain can coordinate metal ions. Concentration of zinc, iron and copper ions in a sample of GST-Pin2(72-282)p purified from *E. coli* assessed by atomic absorption spectroscopy. GST-Pin2(72-282)p concentration was assessed by Bradford. Elution buffer was used as reference sample.

Pin2 localizes to plasma membrane of the bud in G1, S and G2 phase and to the bud neck in M phase. It shuttles between the plasma membrane and internal compartments to maintain this polarized localization and is rapidly internalized upon environmental stress, such as lithium treatment (Ritz et al., in revision). We wanted to test whether the presence of metals, which we found to associate with purified GST-Pin2(72-282), would influence Pin2 trafficking. We incubated cells expressing chromosomally GFP tagged Pin2 with low concentrations (10-50 mM) of salts of metals detected in AAS: CuCl₂, ZnCl₂ and a bioavailable form of chelated Fe³⁺ - ammonium ferric citrate, as well as CaCl₂ and MgCl₂. To test for a Pin2-specific response, we monitored the localization of GFP-tagged Skg6. Skg6 is an integral membrane protein with a similar localization pattern, under physiological conditions, as Pin2, but transported through a different trafficking pathway (Ritz et al., in revision). We found that 10 mM CuCl₂ and 50 mM ZnCl₂ caused the internalization of both Pin2-GFP and Skg6-GFP and that 50 mM CaCl₂ effected specifically Skg6-GFP localization (Figure 8.1 C). Interestingly, ammonium ferric citrate caused partial mislocalization of Pin2-GFP at the plasma membrane. This phenotype was only present in cells grown on YPD and not HC medium (Figure 8.1 B and C). Ammonium ferric citrate also did not affect the localization of a Pin2(C79,81,82,84S) mutant (Figure 8.1 D). We would still like to test the

effect of divalent iron ions on Pin2 localization. However, our results so far do not provide strong evidence for the regulation of Pin2 localization by metal coordination.

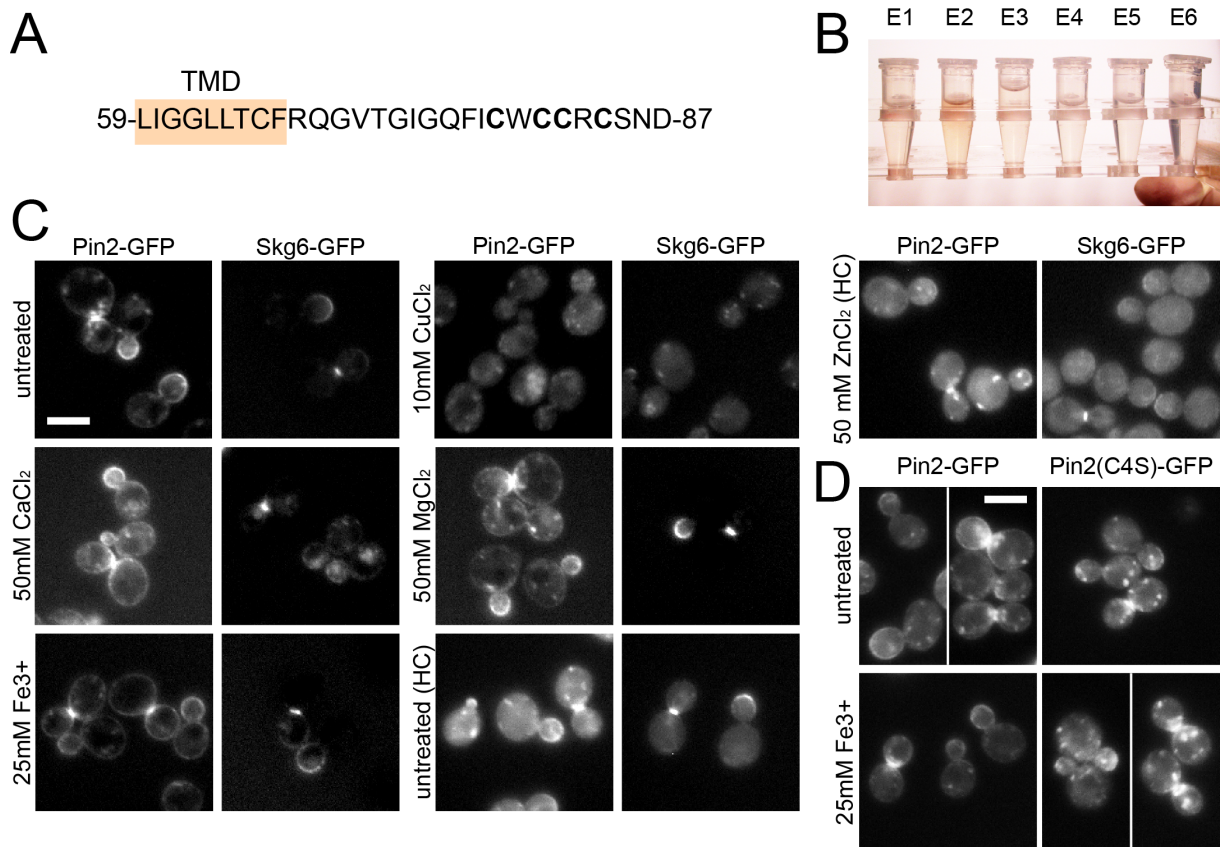


Figure 8.1. The Pin2 cytosolic domain coordinates metal ions *in vitro*. (A) Pin2 sequence containing a part of the transmembrane domain and cytosolic domain with cysteines 79, 81, 82 and 84 indicated in bold. (B) The cytosolic domain of Pin2 chelates metal ions. Elutions of purified, GST-tagged Pin2 cytosolic domain: GST-Pin2(72-282)p, expressed in *E. coli* cells. (C) Microscopy images of chromosomally GFP tagged Pin2 and Skg6 incubated for 20 min with indicated salts. Ammonium ferric citrate was used as a source of Fe³⁺ ions. Images were taken in YPD medium, apart from cells incubated with ZnCl₂, where cells were incubated in HC synthetic medium. Due to high background the brightness and contrast of images of Skg6-GFP cells incubated with ammonium ferric citrate and MgCl₂ was adjusted differently then for the remaining pictures (D) Microscopy images of cells expressing GFP tagged wild type Pin2 and the cytoplasmic four cysteine cluster mutant Pin2(C4S), untreated and incubated for 20 min with ammonium ferric citrate. Scale bars: 5µm.

8.3.2 Palmitoylation of Pin2 is required for its efficient plasma membrane localization

Cysteines 79, 81, 82 and 84 could also be targets of a posttranslational modification, which does not occur in *E. coli*. Indeed, a proteomic study of general yeast protein palmitoylation identified Pin2 as a palmitoylated protein (Roth *et al.*, 2006). Loss of palmitoylation can result in the retention of integral membrane proteins in internal compartments (Blanpain, 2001) or increase the rate of their endocytosis (Alvarez *et al.*, 1990; Kraft, 2001). In accordance with this function, we observed that plasma membrane expression of Pin2(C79,81,82,84S)p-GFP was reduced (Figures 8.1 C, 8.2 A and B).

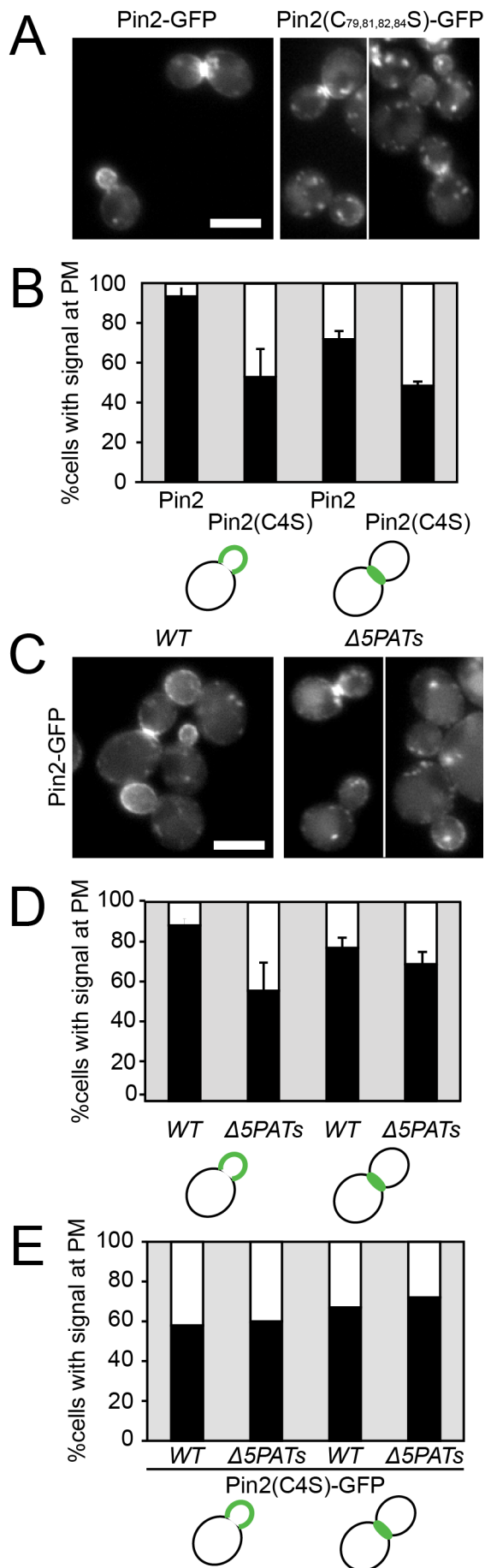


Figure 8.2. Pin2 requires palmitoylation for maintenance at the plasma membrane early in the cell cycle. (A) Cytosolic cysteines 79, 81, 82 and 84 are required for maintenance of Pin2 at the plasma membrane early in the cell cycle. Microscopy images of $\Delta pin2$ cells expressing GFP tagged Pin2 wild type or Pin2(C79,81,82,84S)p mutant from a centromeric plasmid. (B) Quantification of cells in (A). Cells were scored for the Pin2 expression at the plasma membrane. For quantification 100 small and medium budded cells – G1/S and G2 phase, respectively and 100 large budded cells – M phase were quantified in each of 3 experiments. Error bars: standard deviation. (C) Deletion of five acetyl transferases phenocopies the localization defect of the Pin2(C79,81,82,84S)p mutant. Microscopy images of WT and $\Delta akr1 \Delta akr2 \Delta pfa3 \Delta pfa4 \Delta pfa5$ quintuple knock out cells expressing chromosomally tagged Pin2-GFP. (D) Quantification of cells in (C). Cells were scored for the expression of Pin2 at the plasma membrane. For quantification 100 cells small and medium budded cells – G1/S and G2 phase, respectively and 100 large budded cells – M phase were quantified in each of 3 experiments. Error bars: standard deviation. (E) Mutation of Pin2 cytosolic cysteines and the mutation of acetyl transferases do not have a synergistic effect. Wild type and $\Delta akr1 \Delta akr2 \Delta pfa3 \Delta pfa4 \Delta pfa5$ cells expressing Pin2(C79,81,82,84S)p-GFP from a centromeric plasmid were scored for the expression of Pin2 at the plasma membrane. 100 cells small and medium budded cells – G1/S and G2 phase, respectively and 100 large budded cells – M phase were quantified. Scale bars in (C) and (E): 5 μ m.

Deletion of five of the seven known DHHC proteins: *AKR1*, *AKR2*, *PFA3*, *PFA4* and *PFA5*, had a similar effect. To confirm that the less efficient cell surface localization of the Pin2(C79,81,82,84S) mutant was due to loss of palmitoylation rather than a defect in metal binding, we expressed Pin2(C79,81,82,84S)-GFP in the $\Delta akr1 \Delta akr2 \Delta pfa3 \Delta pfa4 \Delta pfa5$ ($\Delta 5PATs$) strain. We saw no enhancement of the previously observed phenotype. This demonstrates that the four-cysteine cluster is palmitoylated to allow efficient targeting of Pin2 to the plasma membrane in earlier stages of the cell cycle.

8.3.3 A luminal pin structure is required for Pin2 export.

Pin2 is exported directly from the TGN to the plasma membrane by the exomer complex. From the cell surface it is recycled back to internal compartments by endocytosis and AP-1 mediated retrieval from early endosomes to the TGN (Ritz et al., in revision). In our previous study, we identified cytosolic motifs that interact with exomer, AP-1 and endocytic machineries to control Pin2 trafficking. Potential palmitoylation that would promote Pin2 plasma membrane expression also occurs on cytosolic cysteines. We therefore tested whether the Pin2 cytosolic domain would be sufficient to transfer Pin2-specific trafficking requirements, including exomer-dependent export to an unrelated protein Mid2, a cell wall integrity pathway sensor. Mid2 is expressed over the entire plasma membrane and is slightly enriched at the mother cell surface. The Mid2(N+TMD)-Pin2(C)-GFP chimera, like Pin2, localizes to the plasma membrane in a polarized fashion. Surprisingly, Mid2-Pin2 export to the plasma membrane was not inhibited in the absence of the core exomer component Chs5 (Figure 8.3). This shows that cytosolic signals are not sufficient for proper Pin2 trafficking. Thus the TMD and/or the luminal part of Pin2 must contribute to exomer-dependent export.

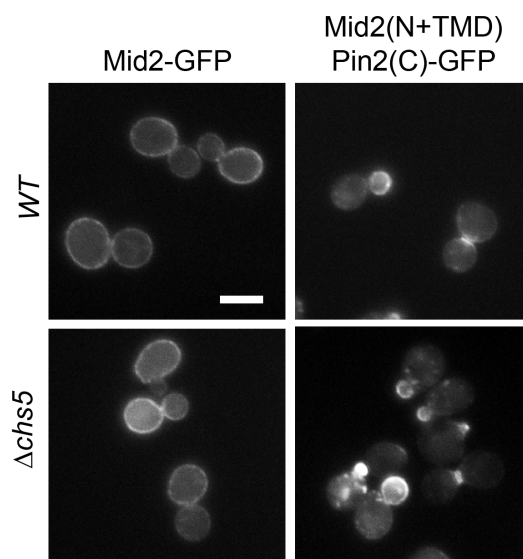


Figure 8.3. The cytosolic domain of Pin2 allows the polarized localization of the Mid2 luminal and transmembrane domains, but is not sufficient for their exomer-dependent transport. Microscopy images of wild type and $\Delta chs5$ cells expressing GFP tagged full length Mid2 or a Mid2(N+TMD)-Pin2(C)-GFP chimera from a centromeric plasmid. Scale bars: 5 μ m.

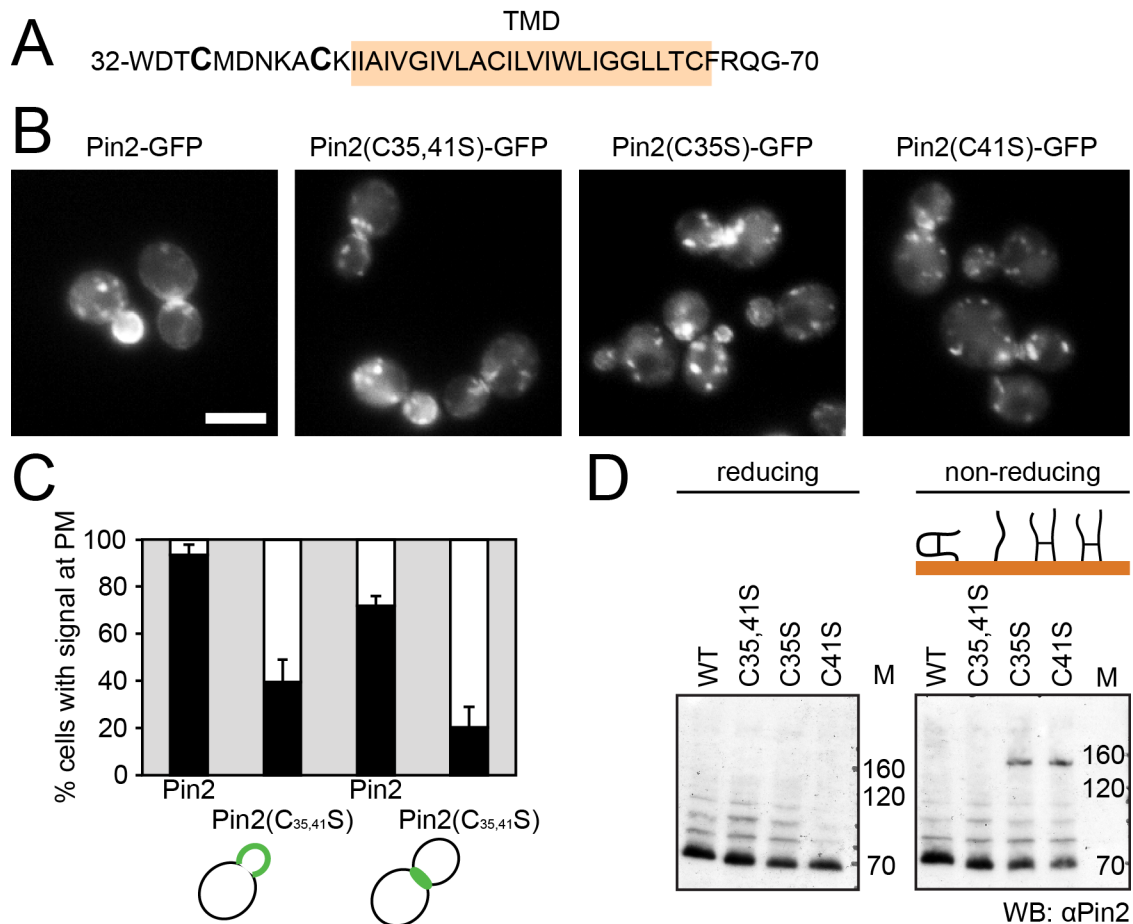


Figure 8.4. A luminal pin structure is required for Pin2 export. (A) Pin2 sequence containing a part of the luminal domain with cysteines 35 and 41 indicated in bold and the transmembrane domain. (B) Single or combined mutation of cysteines 35 and 41, result in export block of Pin2. Microscopy images of $\Delta pin2$ cells expressing GFP tagged Pin2 wild type, Pin2(C35,41S)p, Pin2(C35S)p or Pin2(C41S)p mutant from a centromeric plasmid. Scale bar: 5 μ m. (C) Quantification of cells in (B). Cells were scored for the expression of Pin2-GFP at the plasma membrane. For quantification 100 cells small and medium budded cells – G1/S and G2 phase, respectively and 100 large budded cells – M phase were quantified in each of 3 experiments. Error bars: standard deviation. (D) Cysteines 35 and 41 induce the formation of a pin structure in the Pin2 luminal domain through an intramolecular disulfide bridge. Anti-Pin2 immunoblots of yeast lysates prepared under reducing and non-reducing conditions from $\Delta pin2$ cells expressing Pin2-GFP, Pin2(C35,41S)p, Pin2(C35S)p or Pin2(C41S)p from a centromeric plasmid.

We therefore scrutinized the Pin2 luminal region for presence of any known domains or structural motifs. We found that the Pin2 luminal portion possesses two cysteines: cysteine 35 and 41 (Figure 8.4 A). Given that the lumen of secretory organelles provides an oxidizing environment, the two N-terminal cysteines could potentially either engage in an intra- or intermolecular disulfide link. A double cysteine mutant, Pin2(C35,41S)-GFP was correctly exported from the ER, as Pin2(C35,41S)-GFP showed no ER-like localization, but was predominantly present in internal foci, that resembled the Golgi apparatus during all stages of the cell cycle (Figure 8.4 B and C). This was most likely due to an export defect rather than to an increased endocytosis rate, as Pin2(C35,41S)-GFP, but not Pin2-GFP,

could still be detected in internal structures in an endocytosis deficient, $\Delta end3$, strain (Figure 8.5).

We next wanted to decipher whether the luminal cysteines allow the formation of a Pin2 dimer through an intermolecular disulfide bridge or induce a pin structure in the luminal domain through an internal linkage. We immunoblotted yeast lysates obtained under non-reducing conditions from $\Delta pin2$ cells expressing Pin2-GFP, Pin2(C35,41S)-GFP double cysteine mutant, and Pin2(C35S)-GFP, Pin2(C41S)-GFP single cysteine mutants. Pin2-GFP and Pin2(C35,41S) had a similar migration speed on non-reducing SDS-PAGE. Interestingly, we consistently detected an additional high molecular weight Pin2-positive band, twice the size of the Pin2 monomer in the single cysteine mutant lysates (Figure 8.4 D). These results suggest that cysteines 35 and 41 form an internal disulfide-linked five amino acid loop, protecting Pin2 from unspecific disulfide bridge formation. In case of the Pin2(C35S) and Pin2(C41S) mutants, the single active cysteine is free to engage in disulfide bridge formation with cysteines in other proteins. Given the size and discreteness of the high molecular weight band, they most likely interact with another Pin2 molecule. This also suggests that Pin2 must at least form a dimer through a non-covalent interaction, providing the necessary proximity for linkage formation in the single cysteine mutants. Finally, Pin2(C35S) and Pin2(C41S) display the same export defect as the Pin2(C35,41S) double mutant (Figure 8.4 B). As the single cysteine mutants can still engage in intermolecular disulfide bridge formation, this further supports the idea that an internal luminal pin structure is required for Pin2 export from the TGN to the plasma membrane.

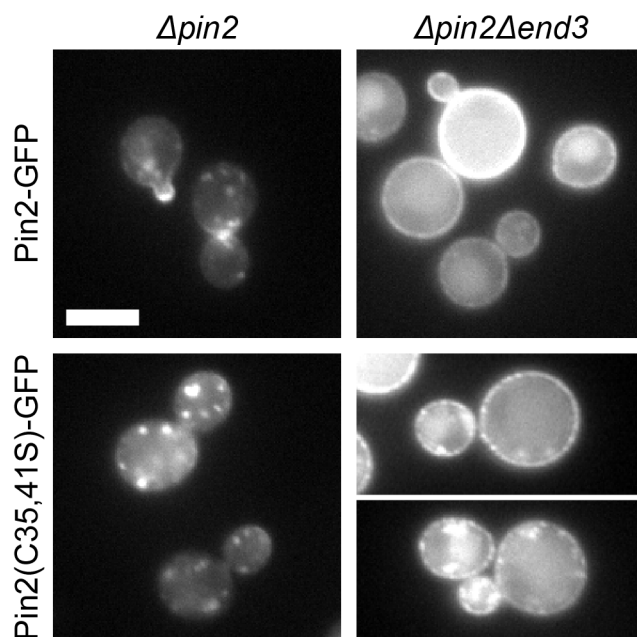


Figure 8.5. Mutation of the luminal pin structure causes a TGN export block. Microscopy images of $\Delta pin2$ and $\Delta pin2\Delta end3$ cells expressing Pin2-GFP and Pin2(C35,41S)-GFP mutant from a centromeric plasmid. Scale bar: 5 μ m

8.4 Discussion and outlook

8.4.1 The cytosolic four-cysteine cluster is most likely palmitoylated *in vivo* and seems to coordinate metal ions *in vitro*.

In this study we demonstrated the role of cysteines present in both the luminal and cytosolic domain for the proper trafficking of Pin2. The cytosolic four-cysteine cluster is palmitoylated for efficient plasma membrane targeting of Pin2 early in the cell cycle. The luminal domain of Pin2 adopts a novel disulfide-linked pin structure, which is required for export to the plasma membrane.

Purified GST-Pin2(72-282) has an ochre color, which we attributed to and confirmed by AAS spectroscopy the presence of metal ions, that are coordinated by the cluster mutant. However, the addition divalent or trivalent metal salts to cells did not alter Pin2 localization specifically nor had a particular effect on the Pin2(C79,81,82,84S), a mutant in a potential metal coordination site. These results rather suggest that the possible coordination of metal ions by Pin2 could be an artifact of purification of GST-Pin2(72-282) from an *E.coli*-based expression systems, where posttranslational modifications such as palmitoylation do not occur.

Deletion of five of the seven DHHC proteins, which display acyltransferase activity, phenocopies the four cluster mutant. Moreover, this quintuple deletion has no additional effect when combined with the mutation of the four-cysteine cluster. In both cases we observed decreased plasma membrane expression of Pin2 in G1, S and G2 phase. Therefore we propose that at least one of cysteines 79, 81, 82 and 84 are palmitoylated. Palmitoylation within a cluster of four cysteines has been shown to modify the localization of the soluble SNARE, SNAP-25 and occur in two isoforms of phosphatidylinositol 4-kinases: PI4KII α and PI4KII β , in mammalian cells (Greaves and Chamberlain, 2011; Barylko et al., 2009). Mutation of increasing amounts of cysteines within SNAP-25 led to a more pronounced TGN and recycling endosome versus plasma membrane localization. (Chamberlain and Greaves, 2011). The presence of a four-cysteine cluster and palmitoylation of a subset of cysteines could therefore fine-tune the localization of a protein. This could have particular significance for Pin2 localization under stress conditions.

The shuttling of peripheral membranes proteins like SNAP-25 or the small signaling GTPases H-Ras and N-Ras between internal compartments and cell surface seems to be accompanied by a cycle of palmitoylation and depalmitoylation (Goodwin *et al.*, 2005; Rocks *et al.*, 2005; 2010; Greaves and Chamberlain, 2011). It would be interesting to test whether the same would operate in the case of Pin2, which also cycles within the late secretory

pathway. To test this, we will immunoprecipitate Pin2 from yeast extracts, in which free thiols are blocked by NEM, palmitoylation thioester links are cleaved by hydroxylamine and subsequently labeled with a biotinylated sulfhydryl specific reagent, Biotin-BMCC (Driscoll and Green, 2004; Roth *et al.*, 2006). The extent of Pin2 palmitoylation could then be assessed by detection of Biotin-BMCC incorporated into Pin2 by Western blotting with streptavidin-HRP. If indeed palmitoylation correlates with Pin2 cycling and promotes Pin2 localization at the plasma membrane, we would expect a stronger biotin signal in a $\Delta end3$ mutant, in which Pin2 is blocked at the cell surface, than in a $\Delta chs5$ mutant, where Pin2 is predominantly present at the TGN.

8.4.2 The luminal cysteines engage in the formation of a disulfide-linked pin structure for Pin2 export

Sorting machineries in vesicular traffic are cytosolic and recognize motifs on cytosolic sides of membrane proteins. Surprisingly, Pin2 requires a specific luminal structure – a TMD-proximal 5 amino acid disulfide-linked loop, for its proper trafficking. Cysteine 35 and 41 double and single mutants still reach the plasma membrane albeit with strongly reduced efficiency and predominantly localize to internal structures that resemble the Golgi apparatus. This however needs to be verified by colocalization experiments with a Golgi, for example marker Sec7. We also do not detect an ER-like signal in any of the GFP-tagged cysteine 35 and 41 mutants. Together our results suggest that mutation of the luminal cysteines does not lead to a major misfolding of Pin2, which would result in ER retention, but gives rise to a Golgi export defect.

A disulfide-linked loop has been previously reported to allow selective aggregation of chromogranin B, driving its TGN sorting into immature secretory granules (Chanat *et al.*, 1993; Krömer *et al.*, 1998; Glombik *et al.*, 1999). Pin2 itself is a prion domain containing protein and has a propensity to aggregate (Derkatch *et al.*, 2001; Ritz *et al.*, in revision). To test whether the luminal cysteines affect Pin2 aggregation, we propose to analyze the migration of cysteine 35 and 41 mutants on a blue native gel. We could also check whether an overexpressed Pin2(C35,41S) mutant forms SDS-resistant aggregates.

Treatment of cells by DTT or expression of a loop-deleted chromogranin B results in its missorting into constitutive sorting vesicles (Chanat *et al.*, 1993; Krömer *et al.*, 1998). Pin2 depends on exomer for its TGN export and it is possible that the luminal disulfide linked structure is required for this specific transport route. Deletion of subunits of the AP-1 complex, involved in retrograde transport from early endosomes to the TGN, allows the alternative export of Pin2 and other exomer cargos to the plasma membrane through

endosomes (Valdivia *et al.*, 2002; Barfield *et al.*, 2009) (Ritz *et al.*, in revision). In a preliminary experiment we were not able to direct the Pin2(C35,41S) mutant to the plasma membrane in cells, in which an *AP-1* subunit was deleted. Although this requires further investigation, this suggests that the trafficking block induced in the absence of the luminal pin structure not only affects the exomer pathway. Accordingly, the exomer cargo Fus1, which has a similar topology to Pin2, has no cysteines in its luminal domain. Therefore, a luminal disulfide-linked pin structure is not a prerequisite for exomer export.

The presence of a luminal pin structure would most likely force the N-terminal domain of Pin2 to closely appose the membrane and the 23-amino acid TMD to slant within the lipid bilayer. Mutation of the luminal cysteines could cause the TMD to “stand upright” and expose additional hydrophobic residues, promoting Pin2 aggregation. A recent study has also shown that the length and residue volume can determine the subcellular localization of membrane proteins (Sharpe *et al.*, 2010). To test whether the luminal pin structure reduces the effective length of the TMD in the lipid bilayer, we could check whether mutation of cysteines 35 and 41 in a variant with a shorter 18-20-residue membrane domain would support efficient plasma membrane localization.

Redox-sensing switches can function through the locking and unlocking of intra and intermolecular disulfide bonds, inducing critical conformational changes in the entire protein (Nagahara, 2010). CxxC motifs have also been shown to accommodate metal ions. An example is the previously mentioned copper-transporting protein MNK (Solioz and Vulpe, 1996). Rad50, involved in DNA damage repair forms a dimer through two CxxC interlocking hooks, which together coordinate one zinc ion (Hopfner *et al.*, 2002). To assess whether the luminal and extracellular disulfide bridge is a structural or a regulatory motif, we would test whether this disulfide linkage is reversible. To achieve this we would label the yeast cell surface and exposing Pin2-luminal domain with an alkylating agent NEM. After lysate preparation, the unlabeled, existing disulfide bridges would be reduced and labeled with maleimided-polyethylene-glycol. This modification would appear as a band shift on polyacrylamide gels and could be compared to total amount of Pin2.

Together our data demonstrate that reactive cysteines within the Pin2 sequence determine Pin2 trafficking through formation of a specific, disulfide-linked structure and reversible posttranslational modifications.

8.5 Materials and methods

8.5.1 Strains, yeast genetic methods, growth conditions and plasmids.

Yeast strains used in this study are listed in Table 2. Standard genetic techniques were used throughout (Sherman, 1991). Chromosomal tagging and deletions were performed as described (Knop *et al.*, 1999; Gueldener *et al.*, 2002). PCR-based chromosomal manipulations were confirmed by colony PCR. Standard yeast media were prepared as described (Knop *et al.*, 1999). All strains were grown at 30°C. HC medium selective for the plasmid was used to grow transformants. For expression of GST tagged full-length cytosolic domain of Pin2 restriction fragments encoding aa 72-282 of Pin2 were cloned into pGEX-6P-1 (GE Healthcare) using *BamHI* and *EcoRI* restriction sites. *BamHI* and *XhoI* restriction fragments encoding aa: 72-152, and 153-282 of Pin2 were cloned into pGEX6P-1 to obtain GST-tagged Pin2 cytosolic truncations. For GFP tagged Pin2 constructs *EcoRI-SphI* restriction fragments containing the *PIN2* promoter (600bp upstream of the start codon) and the full length *PIN2* ORF was cloned into pGFP33 (YCPlac33 with inserted *GFP-CYC1* terminator *SphI-HindIII* restriction fragment). To create the Mid2(N+TMD)-Pin2(C) chimera *SacI* and *PstI* restriction sites were inserted into pGFP33 *PIN2*, before the start codon and between codons 71 and 72 of the *PIN2* ORF, respectively. The created *SacI-PstI* restriction fragment encoding for the Pin2 luminal and TMD domain was excised and replaced by the corresponding domains of Mid2 – ORF encoding aa 1-250. Point mutations were introduced using the QuikChange Site-Directed Mutagenesis protocol (Stratagene).

8.5.2 GST-Pin2(72-282)p purification and atomic absorptions spectroscopy

GST-tagged full length cytosolic domain of Pin2 and cytosolic domain truncations were expressed from pGEX-6P-1 plasmids in *E. coli* Rosetta cells by induction with 0.2 mM IPTG for 4 h at 23°C. Purification was carried out according to standard procedures with GSH agarose (Sigma-Aldirich) in Pin2 buffer: 150 mM KCl, 50 mM Tris-HCl pH 8.0, 0.5 % Triton X-100, 5 % glycerol, 1 mM DTT. Additional two washes with Pin2 buffer supplemented with 1 mM ATP and 5mM MgCl₂ were performed and GST-Pin2 was eluted with 40 mM GSH. GST-Pin2 concentration was assessed by Bradford assay. GST-Pin2 sample analysis for 18 heavy metal elements by inductively coupled plasma atomic emission spectroscopy was performed by Solvias (Kaiseraugst, CH). The elution buffer was used as a reference sample.

8.5.3 Western Blot detection

Pin2 was detected with anti-Pin2 serum raised against GST-Pin2(72-282) (1:2,000). An ECL kit (GE Healthcare) was used for detection.

8.5.4 Microscopy

Cells were grown to OD₆₀₀ 0.2-0.7 in YPD or HC medium selective for the plasmid supplemented with adenine, harvested and mounted. Cells grown in YPD were washed and resuspended in HC complete medium. Images were acquired with an Axiocam mounted on a Zeiss Axioplan 2 fluorescence microscope, using filters for GFP.

8.5.5 Non-reducing SDS-PAGE

Three OD₆₀₀ of cells from a $\Delta pin2$ strain expressing Pin2 wild type or cysteine mutants from a pGFP33 centromeric plasmid were harvested. Cells were resuspended in 150 μ l lysis buffer: 50 mM Tris pH, 1 mM EDTA and protease inhibitors, and lysed by 10 min vortexing at 4°C with 120 μ l glass beads. Lysates were cleared by centrifugation for 10 min at 1,500 \times g and heated 10 min at 68°C in 5x SDS buffer: 62.5 mM Tris pH 6.8, 10 % glycerol, 2 % SDS, bromophenol blue. Lysates for reducing SDS-PAGE were performed as described above, except that 50 mM DTT was included in the lysis buffer and samples were heated in 5x SDS buffer containing 5% β -mercaptoethanol.

9. Further Discussion

9.1 Direct TGN to plasma membrane export of selected cargo mediated by exomer

To establish the role of the exomer complex in cell cycle and stress regulated TGN export in yeast, we identified and characterized a novel exomer cargo, Pin2. Exomer mediates direct transport of a subset of proteins to the plasma through light density vesicles. It mediates the export of the yeast chitin synthase, Chs3 and the Fus1 protein, required for yeast cell fusion during mating (Santos *et al.*, 1997; Santos and Snyder, 1997; Ziman *et al.*, 1998; Santos and Snyder, 2003; Valdivia and Schekman, 2003; Trautwein *et al.*, 2006; Barfield *et al.*, 2009). However, not all cargoes that travel through light secretory vesicles are exomer clients. For example, cell surface expression of Pma1 and Hxt2 is exomer-independent (Zanolari *et al.*, 2011). Distinct phenotypes of ChAP exomer subunit deletions, on the other hand strongly speak for the existence of many other cargoes. Deletion of *BUD7* leads to a random budding phenotype, (Trautwein *et al.*, 2006) and $\Delta bch2 \Delta chs6$ cells are sensitive to lithium (Rockenbauch *et al.*, 2012), suggesting interaction with cargoes involved in bud-site selection or ion homeostasis. In addition, the exomer may recognize cargoes, which could also traffic through other export pathways, such as the integral membrane protein Skg6. Skg6 interacts with exomer in a way reminiscent of a putative cargo – deletion of the cargo recognition subunits (the ChAPs), abolishes the binding of the core component, Chs5 to Skg6. Skg6, however, does not depend on exomer for its export. This shows that either interaction of Skg6 with exomer, does not result in its sorting into exomer-dependent carriers or Skg6 must be able to board another transport route to the plasma membrane and exomer-dependent sorting is not a prerequisite for its plasma membrane targeting.

What is the function of the exomer-dependent trafficking pathway? Pin2 and Chs3 have a polarized localization at the plasma membrane that changes during the vegetative cell cycle. (this study; (Shaw *et al.*, 1991; Chuang and Schekman, 1996; Schmidt, 2003; Valdivia and Schekman, 2003). Fus1, expressed during mating, localizes to the mating projection (Bagnat and Simons, 2002). However, this restricted, cell-cycle dependent surface expression is not abolished by re-direction of Chs3, Pin2 and Fus1 into an alternative export pathway by deletion of AP-1 subunits in the absence of functional exomer (this study; (Valdivia *et al.*, 2002; Barfield *et al.*, 2009). AP-1 is required for early endosome to TGN retrograde transport and thus seems to prevent exomer cargoes from reaching the plasma membrane via early endosomes (Valdivia *et al.*, 2002). Moreover, the exomer-independent cargo, Skg6, also localizes in a polarized fashion at the cell surface, in a manner very similar to Pin2. Taken together these data indicate, that exomer-dependent transport is not the single TGN export pathway that sustains defined localization of proteins. Conversely, the

redistribution of Chs3 to the plasma membrane upon heat stress is dependent on exomer and does not occur in a $\Delta chs6 \Delta AP-1$ strain (Valdivia *et al.*, 2002), implying a specific role for exomer in stress-responsive trafficking. Environmental stress can induce plasma membrane protein internalization. This would allow removal of misfolded proteins under heat stress or remove pumps and transporters to prevent ion leakage under high saline conditions (Szopinska *et al.*, 2011; Zhao *et al.*, 2013). Under these circumstances, activity of specific, regulated secretory pathways, such as the exomer-dependent pathway, could be an advantage. It would be therefore very interesting to test whether the maintenance of Pin2 in internal compartments upon lithium stress would be sustained or more efficiently relieved if Pin2 was redirected to the alternative endosomal export route. Additionally, under heat stress Chs3 undergoes Pkc1-dependent phosphorylation (Valdivia and Schekman, 2003), which could alter ChAP recognition. Similarly, Pin2 might also be phosphorylated under stress conditions.

Exomer acts in the direct pathway from the TGN to the plasma membrane in yeast, and is the only identified sorting machinery in this export branch. Exomer has no known orthologues in higher eukaryotes. In mammalian cells, certain cargoes incorporated into TGN-to-plasma membrane carriers (TPCs) also travel directly to the cell surface and do not display colocalization with early endosomes at any point of transport (Keller *et al.*, 2001). CARTS, which export a subset of proteins such as the desmosome protein, desmoglein or synaptotagmin II, are recently characterized carriers in this pathway (Wakana *et al.*, 2012). The authors of the study, however, were not able to identify a specific sorting machinery or coat associated with CARTS, although this could have been a result of the stringent conditions employed for membrane isolation (Wakana *et al.*, 2012). In *Arabidopsis thaliana* the ECH protein/ECHIDNA was demonstrated to mediate generation of TGN-derived transport vesicles for auxin transporter exocytosis. ECHIDNA also only marginally colocalizes with clathrin at the TGN, suggesting its involvement in a non clathrin-mediated export route (Boutté *et al.*, 2013). It should be noted, though, that the TGN acts as an early endosome in plant cells, therefore all late secretory pathways to the cell surface are in this case direct (Dettmer *et al.*, 2006; Lam *et al.*, 2007; Viotti *et al.*, 2010). Exomer and potentially ECHIDNA could represent unique, highly specialized sorting machineries, which evolved to allow regulated export of a subset of proteins. Evidence exists that sorting, for example of apical GPI-anchored proteins, requires lipid-raft based mechanisms (Surma *et al.*, 2012). It could be therefore plausible that in certain cases, protein-based machineries would be dispensable for cargo sorting into specific post-Golgi transport carriers.

9.2 The concerted binding of Chs5 and ChAPs to cargo

Chs3 is a large protein with six transmembrane domains (Sacristan *et al.*, 2013). Pin2, on the other hand, is a relatively short (282 amino acid long) protein with a single TMD. This topology gave us the opportunity to purify the entire cytosolic domain of Pin2, constituted by the C-terminal portion of the protein, and investigate its interaction with exomer components. We found that Chs5 binding to Pin2 was abolished upon deletion of the four ChAPs, confirming their role as the initial cargo recognition subunits. Reciprocally, we also found that Chs5 is required for the efficient interaction of the ChAPs with the Pin2 cargo tail. This is consistent with a previous result obtained by the Schekman lab, which demonstrated that Chs6 interaction with Chs3 is severely reduced in a $\Delta chs5$ strain (Sanchatjate and Schekman, 2006). The ChAPs' dependence on Chs5 for cargo binding is most likely a regulatory mechanism that could allow dynamic association and dissociation of exomer from the client protein. Deletion of four tetratricopeptide repeats in Chs6 (residues 244-404), required for Chs5 interaction and Chs3 export, does not abolish but rather increases cargo binding. The enhanced binding of Chs6(Δ TPR1-4) to Chs3 can also be observed in a $\Delta chs5$ strain. Regulation of ChAP-cargo interaction by Chs5 could allow dissociation of exomer once sorting or incorporation into a transport carrier is completed, to allow subsequent fusion with the plasma membrane.

Pin2 requires either Bch1 or Bch2 for its export from the TGN. Nonetheless all ChAPs can recognize and bind Pin2 independently. We found that not only Chs5-ChAP interactions allow efficient cargo-exomer association, but also that the ChAPs themselves promote each other's binding to Pin2. This, most likely, does not occur through direct interaction between the ChAPs, as the ChAPs only copurify in the presence of Chs5 (Sanchatjate and Schekman, 2006). Three, not mutually exclusive, scenarios could therefore explain how the ChAPs would enhance each other's binding to the cargo tail. First: efficient binding of Chs5 to the complex requires more than one type of ChAP and in turn would recruit more cargo recognition subunits. Two: specific ChAPs could confer a conformational change in the Chs5-ChAP complex promoting the association of others. Three: the cargo could have more than one binding site for different exomer subunits.

In support of the first possibility, we indeed observe residual Chs5 binding to Pin2 in case of all strains expressing a single ChAP member. On the other hand binding of Bch2 and Bud7, to Pin2 is not affected by the absence of other ChAPs. This points to the second possibility: specific function of distinct ChAPs in the complex. Bch2 is the strongest Pin2 interactor in extracts from wild type, $\Delta 3ChAPs$ and $\Delta chs5$ strains. It also displays the most stable TGN association out of all the ChAPs (Trautwein *et al.*, 2006). Bch2 could therefore, in

principle, form a baseline interaction between cargo and exomer, and promote efficient recruitment of remaining ChAPs. The stable binding of Bud7 to the Pin2 cytosolic domain indicates that it could serve a similar function. This hypothesis could be verified by testing the association of Bch1 and Chs6 from $\Delta bch2$ or $\Delta bch2 \Delta bud7$ strain extracts to the Pin2 C-terminus. It is also possible that the stable interaction of Bch2 with Pin2 is rather a result of it being a Pin2-specific ChAP, than due to its unique function in the exomer complex. This seems to be defied by the fact that Bch1, which binds Pin2 less efficiently in the absence of other ChAPs, is, like Bch2, sufficient for Pin2 export *in vivo*. However, to prove this point we would need to characterize the interaction of Bch2 with another exomer cargo, for example Chs3 or the cytosolic domain of Fus1.

Finally, our studies suggest that exomer-cargo interaction is not mediated by a short, linear motif. This opens the third possibility that Pin2 could possess more than one binding site for different exomer cargoes. Alternatively Pin2 could also form a large interaction surface with a single ChAP. In a pull down assay with Pin2 cytosolic domain truncations, we observed that only the construct containing the last C-terminal 72 residues was able to bind exomer components, albeit to a lesser extent than the full-length construct. Surprisingly, the GFP tagged Pin2(1-210) truncation, devoid of these residues, still showed accumulation in internal structures in a $\Delta ch5$ strain. Therefore Pin2 must contain additional exomer binding sites within its sequence. Although a single IXTPK motif was identified in Fus1 for exomer-binding and export (Barfield *et al.*, 2009), this does not seem to be the case for Chs3. Recently, a DXE motif in the N-terminus of Chs3 was shown to be necessary for its exomer-dependent plasma membrane localization. Mutation of this motif, however, only partially reduced Chs5 interaction (Starr *et al.*, 2012). To complement this finding, our studies show that the Chs3 C-terminus binds exomer and is required for Golgi export. These residues, though, alone are not sufficient to mediate the export of the TGN-endosomal protein, Kex2. A vast portion of Chs6, confers Chs3 cargo specificity. One might therefore expect a proportionally large interaction surface or several exomer-binding sites on Chs3. What is even more compelling is that the central Chs6 residues 409-563, mediate Chs3 export, but only early in the cell cycle. Together our data point, that interaction of cargo with ChAPs must occur through several motifs or larger interaction surfaces. Such a multifaceted interaction could also support the regulation of exomer-dependent export in response to cell cycle (as shown for Chs3) or stress cues.

9.3 Restriction of cargo to the exomer pathway not only requires a cytosolic AP-1 binding motif, but also depends on the luminal domain.

Deletion of exomer components inhibits the TGN export of Pin2, Chs3 and Fus1. In many cases though blocking one TGN-to-plasma membrane transport pathway shifts the cargo into another. One example is invertase, which travels in the heavy-density vesicle fraction (Harsay and Bretscher, 1995). Inhibiting formation of clathrin coated vesicles reroutes invertase into light-density carriers (Harsay and Bretscher, 1995). Exomer cargoes can only undergo alternative export to the plasma membrane through early endosomes in the absence of AP-1 (Valdivia *et al.*, 2002). Therefore AP-1-mediated endosome-to-TGN retrieval probably prevents the escape of exomer cargoes from early endosomes to the cell surface, restricting Chs3, Pin2 and Fus1 to the exomer-dependent export pathway (this study) (Valdivia *et al.*, 2002; Barfield *et al.*, 2009). The tyrosine-based motif, YGENYYY, in the C-terminus of the Pin2 cytosolic domain, is most likely required for AP-1 binding. Yet, the presence of appropriate cytosolic signals is not enough to become an exomer cargo. Although a fusion of the luminal and transmembrane domain of Mid2 with the Pin2 cytosolic portion results in a chimera that localizes to the plasma membrane in a polarized fashion, the Mid2-Pin2 fusion is still exported to the cell surface in $\Delta chs5$ cells. A similar result was obtained for a Kex2-Fus1 chimera (Barfield *et al.*, 2009). This latter case is even more surprising as Kex2 itself does not reach the cell surface, but rather remains in early endosomal-TGN compartments. This clearly points to the function of the transmembrane and/or luminal domains in exomer-dependent cargo trafficking. The luminal domain is essential for trafficking of Pin2, because disruption of a luminal disulfide-linked pin structure leads to accumulation in internal structures. As transmembrane domain length and residue make-up have been shown to correlate with their organelle-specific localization (Sharpe *et al.*, 2010), it would be interesting to test whether switching the Pin2 TMD with that of Mid2 or Kex2 would effect Pin2 exomer-dependent trafficking.

9.4 Cycling within the late secretory pathway as a means to regulate steady state localization of cargos

All three exomer cargoes seem to share the same trafficking requirements to recycle between internal TGN/endosomal compartments and the plasma membrane (Shaw *et al.*, 1991; Chuang and Schekman, 1996; Schmidt, 2003; Barfield *et al.*, 2009). First, they are exported by exomer. Second, they are internalized from the plasma membrane. Finally, exomer cargoes are retrieved from early endosomes to the TGN by AP-1. What would be the

purpose of maintaining cargoes in a constant cycle within the late secretory pathway? One reason would be to support a polarized localization throughout the cell cycle as we observed for Pin2 and as was already described for Chs3 (Chuang and Schekman, 1996; Ziman *et al.*, 1996; Reyes *et al.*, 2007; Zanolari *et al.*, 2011). Another could be to evoke an immediate, reversible response to stress signals, which is what we observed for Pin2. Lithium treatment induces rapid internalization of Pin2. Pin2 can be maintained in internal compartments during prolonged (overnight) lithium exposure, but can regain its physiological localization as early as ten minutes after stress relief. In mammalian cells, EGF receptor cycling between the plasma membrane and endosomes allows modulation of signaling strength. In this pathway endosomes act as a crossroads with the options to recycle back to the plasma membrane for enhanced signaling or lysosomal transport for receptor degradation (Sorkin and Zastrow, 2009). PIN auxin transporters (the name PIN is purely coincidental) in multicellular plants show polarized localization towards specific faces of the plant cell. Shuttling of PINs between endosomal compartments and the plasma membrane, allows their shift into a parallel export pathway towards another cellular face, to redirect intercellular auxin flow in response to gravity cues (Friml *et al.*, 2002; Geldner *et al.*, 2003; Krecek *et al.*, 2009).

Changing the steady state localization of a shuttling cargo could be achieved through a shift in the transport equilibrium, simply by increasing or decreasing internalization and export kinetics. In the case of Pin2, this shift could be induced by reversible posttranslational modifications such as ubiquitination, required for Pin2 endocytosis, or potentially palmitoylation, that promotes its plasma membrane localization. Enhanced ubiquitylation and possible depalmitoylation could aid Pin2 internalization. Both cycles of ubiquitylation-deubiquitylation of EGF as well as Frizzled receptors, and palmitoylation-depalmitoylation of H-Ras and N-Ras signaling regulators have been shown to accompany their recycling in the late secretory pathway (Bowers *et al.*, 2006; Mukai *et al.*, 2010; Pareja *et al.*, 2012; Eisenberg *et al.*, 2013). Another posttranslational modification that could promote a change in steady state localization is phosphorylation. In accordance with this idea, the internalization of Pin2 upon lithium stress is delayed in deletion strains for MAPK components of the HOG1 and cell wall integrity pathway. Although mutations of an identified Pin2 phosphosite did not affect Pin2 localization under physiological or stress conditions, it is conceivable that other phosphorylation sites in Pin2 exist that would regulate Pin2 trafficking. Finally, an equilibrium shift could also be induced by modification of the interaction between Pin2 and the cytosolic sorting machineries – exomer and AP-1. The modification could either stem from a change in Pin2, for example by aggregation of the prion-like domain or in the sorting complex, itself. Identification of potential posttranslational modifications, such as

phosphorylation on exomer subunits and monitoring their change in response to different stress stimuli by mass spectrometry, would be a compelling direction of study.

9.5 Role of the prion domain in Pin2 trafficking

Pin2 is a prion-like domain containing protein. Mutation of several Q/N residues to charged amino acids prevented formation of SDS-resistant Pin2 aggregates. It also affected Pin2 localization. Maintenance in internal compartments upon prolonged lithium exposure was compromised in the Pin2(QNtoED) mutant, suggesting that aggregation through the prion domain could retain Pin2 at the TGN. This could either occur through masking of the identified exomer-binding sites, which reside within the prion domain or sequestering Pin2 away from incorporation into export carriers because of size constraints (Figure 9.1 I).

The potential YGENYYY AP-1/AP-2 retrieval and endocytosis motif is also present within the Pin2 prion domain. Prion domain-mediated Pin2 retention in internal structures could, therefore, be also achieved through another mechanism – enhancement of AP-1 and AP-2 recognition through Pin2 prion domain aggregation (Figure 9.1 II). Protein aggregation upon heat stress has been recently proposed to promote interaction with the Arrestin-Rsp5 adaptor-ubiquitin ligase complex, for plasma membrane protein internalization (Zhao *et al.*, 2013). Under physiological conditions the Pin2 prion-domain mutant phenocopies the mutation of the YGENYYY motif: depolarized localization at the plasma membrane, reduced localization to internal structures; partially exomer-independent export. To decipher between these possibilities and rule out that the QNtoED mutation disrupts the YGENYYY motif, we would like to perform pull down assays with purified prion-domain and AP-1/AP-2 binding site mutants and assay their interaction with exomer and AP-1. Furthermore to confirm the role of aggregation through the prion-like domain in Pin2 trafficking we would like to engineer variants that contain extended Q/N-rich stretches. If indeed Pin2 transport were regulated by a prion-like mechanism, we would expect an enrichment of the Q/N-expansion mutants at the TGN and endosomes.

The retention of Pin2 in internal compartments is fully reversible upon lithium washout and the kinetics of cell surface arrival are similar for both Pin2 wild type and Pin2(QNtoED). Therefore holding of Pin2 in the TGN may arise through transient prion domain interactions. Although prion domains form stable SDS and protease resistant amyloid structures, there are several examples where prion-like aggregates behave in a very dynamic manner. An example is the formation of P-bodies, which sequester mRNAs for their decay and possibly for their storage, a focus of study in our lab. Aggregation of P-body proteins through their Q/N and Q-rich domains under stress conditions allows formation of large structures, detectable

by light microscopy (Decker *et al.*, 2007; Reijns *et al.*, 2008). These aggregates are dynamic as stress relief or cell adaptation results in their dissipation (Bregues *et al.*, 2005; Teixeira and Parker, 2007; Kilchert *et al.*, 2010).

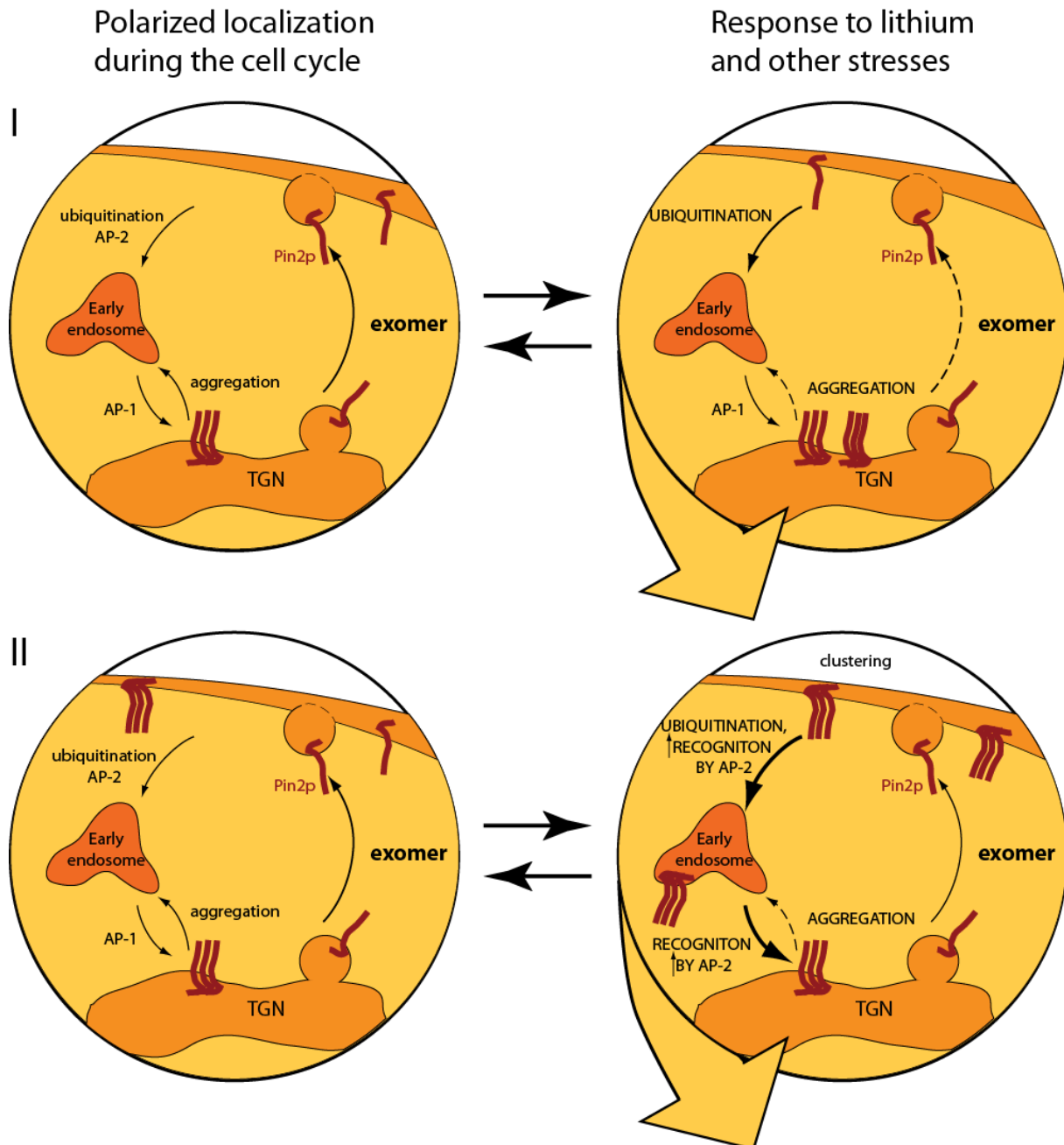


Figure 9.1 Model of Pin2 trafficking and equilibrium shift towards internal compartments upon lithium stress. Internalization of Pin2 is promoted by its ubiquitylation and aggregation of the prion domain. Two possible modes of action for the Pin2 prion domain are illustrated. (I) Aggregation of the Pin2 prion domain sequesters Pin2 at the TGN either through aggregate size or exomer-binding site masking. (II) Aggregation of the prion domain enhances the recognition of the YGENYYYY motif by AP-2 and AP-1, promoting Pin2 localization towards the intracellular pool. Prion domain aggregation, to a lesser extent, would also occur under physiological conditions.

9.6 Pin2 could function as a stress sensor

The localization of Pin2 is regulated in a stress-dependent manner. Pin2 also contains a prion-like domain, which may undergo enhanced aggregation under toxic environmental conditions. These characteristics would point to a stress-sensing function of Pin2. In accordance with this, a global protein complementation assay identified an interaction between Pin2 and cell wall integrity pathway components: Mid2 and Smi1 (Tarassov *et al.*, 2008; Schlecht *et al.*, 2012)(Tarassov *et al.*, 2008, Schlecht *et al.*, 2012). $\Delta mid2$ cells are calcofluor-resistant (Ketela *et al.*, 1999), as calcofluor-induced cell death is a result of signaling than the toxicity of the compound by itself. Deletion of *PIN2*, however, does not phenocopy the calcofluor-resistance of $\Delta mid2$ cells, as would be expected from a CWI sensor (data not shown). Assuming that Pin2 would act in stress signaling, why would it be internalized? One possibility is that Pin2 could function at the TGN and endosomal compartments. GPCR-mediated activation of ERK1, ERK2 and Jun signaling cascades, for example, occurs at endosomes (Sorkin and Zastrow, 2009). In another scenario, presence of Pin2 or signaling associated with Pin2 at the plasma membrane could be detrimental under lithium stress. Pin2 would be endocytosed to protect the cell, as has been suggested for the proton pump Pma1 and several transporters upon treatment with sodium chloride (Szopinska *et al.*, 2011). In any case, mass spectrometry based analysis of Pin2 interactors should shed further light on Pin2 function.

10. Appendix

10.1 Materials

As the methods applied in our lab are standardized, part of the methods in this section were taken from dissertations of former members: Mark Trautwein (Trautwein, 2004), Cornelia Kilchert (Kilchert 2011) and Uli Rockenbauch (Rockenbauch, 2012). Changes have been made when necessary.

10.1.1 Instruments

Instrument	Manufacturer
Axiocam MRm camera	Zeiss
Axioplan 2 epi-fluorescence microscope	Zeiss
Bustulator VIBRAX-VXR	IKA
Cooling centrifuge 5417 R	Eppendorf
Cooling centrifuge 5810 R	Eppendorf
Cooling centrifuge RC5C Plus	Sorvall
Ultracentrifuge Optima	Beckman
Fastprep FP120	Savant
Rotor GS3	Kendro
Rotor SS34	Kendro
Rotor TLA-55	Beckman
Sonifier cell disruptor B15	Branson
Spectrophotometer UltraSpec 3100 pro	Amersham Biosciences

Only non-standard instruments are listed.

10.1.2 Kits

Name	Order no.	Supplier
BCA Protein Assay Kit	23225	Pierce
Biorad protein assay kit	500-0001	Biorad
ECL Advanced Kit	RPN2135	Amersham Bioscience
ECL Kit	RPN2106	Amersham Bioscience
ECL Prime Kit	RPN2232	Amersham Bioscience
Expand High Fidelity PCR System	11681842001	Roche
Nucleospin Gel & PCR Cleanup	740609.5	Machery & Nagel
Pfx Turbo Cx Hotstart	600410-51	Agilent Technologies
rAPid Alkaline Phosphatase	04898133001	Roche
Rapid DNA Ligation Kit	11435722	Roche
Zyppy Plasmid Miniprep Kit	D4019	Zymo Research

10.1.3 Chemicals and consumables

Standard chemicals were obtained from Sigma, Roth and Merck.

Name	Order no.	Supplier
Antipain dihydrochloride	A2129,0025	Applichem
Difco™ Agar granulated	214510	BD
Bacto™ Peptone	211830	BD
Bacto™ Tryptone	211701	BD
Bacto™ Yeast Extract	212730	BD
Difco™ Yeast nitrogen base (YNB) w/o amino acids	291920	BD
Benchmark Protein Ladder	10747-012	Invitrogen
Bromophenol Blue	B-5525	Sigma
Calcofluor white dye	F-3543	Sigma
Complete mini EDTA-free protease inhibitors	1836170	Roche
Coomassie Brilliant Blue G250 (Serva Blue G)	35050	Serva
Coomassie Brilliant Blue R250	35051	Serva
Dextrose	A1349	Applichem
Dimethylpimelimidate (DMP)	21667	Thermo Scientific
Dithiobis(succinimidylpropionate) (DSP)	22586	Thermo Scientific
Glass beads 0.25-0.5 mm	A553.1	Roth
Glutathione (GSH)	737038	Roche
GSH agarose	G4510	Sigma
Leupeptin	L-8511	Sigma
Pepstatin	P-5318	Sigma
Protein A-sepharose CL-4B	17-0780-01	Amersham Bioscience
SeaKem™ Gold Agarose	50152	Lonza
Salmon Sperm DNA	D1626	Sigma
Trypsin	V5111	Promega
Trypsin Inhibitor	T-9128	Sigma
Zymolyase T20 (from <i>Arthrobacter luteus</i>)	120491	Seikagaku Corporation

10.1.4 Media

Standard yeast media were prepared (Sherman, 1991) and autoclaved at 121°C for 20 min. Distilled or double distilled water was used exclusively. “YNB” stands for “yeast nitrogen base”.

LB medium:	10 g tryptone (BD) 5 g yeast extract (BD) 10 g NaCl (Roth) ad 1 l ddH ₂ O and autoclaved 1 ml 1000x ampicillin was added after autoclaving.
LB agar:	5 g tryptone (BD) 2.5 g yeast extract (BD) 5 g NaCl (Roth) 10 g agar (BD) ad 500 ml ddH ₂ O and autoclaved 0.5 ml 1000x ampicillin was added after autoclaving.
SOB-medium:	2.5 g yeast extract (BD) 10 g Bacto-Tryptone (BD) 10 mM NaCl 2.5 mM KCl 10 mM MgSO ₄ 10 mM MgCl ₂ ad 500 ml ddH ₂ O and autoclaved
2xYT medium	16 g Bacto Tryptone (BD) 10 g Bacto Yeast Extract (BD) 5 g NaCl Ad 1l ddH ₂ O
HC medium:	800 ml ddH ₂ O 100 ml 10x HC-XX (without the component to select for) 100 ml 10x YNB w/o amino acids Complemented with 2% (w/v) dextrose after autoclaving.

Calcofluor white plates:	50 ml 10x YNB w/o amino acids 20 ml 50% dextrose 50 ml 10x HC complete 50 ml 10% MES buffer pH 6.0 5 ml 10% yeast extract 350 ml autoclaved agar (60°C), final conc. 2% 1 ml calcofluor white solution (50 mg/ml) was added while stirring. Plates were poured immediately.
HC agar:	hot sterile agar (10 g dissolved in 350 ml H ₂ O) 50 ml 20% dextrose 50 ml 10x YNB w/o amino acids 50 ml 10x HC-XX (without the component to select for)
HC agar + Cu ²⁺	HC agar + 70 µM CuSO ₄
YPD medium:	1% yeast extract (BD) 2% peptone (BD) Complemented with 2% (w/v) dextrose after autoclaving.
YPD agar:	10 g peptone (BD) 5 g yeast extract (BD) 10 g agar (BD) ad 450 ml ddH ₂ O and autoclaved Complemented with 50 ml 20% (w/v) dextrose before plates were poured.

10.1.5 Common solutions and buffers

Double-distilled H₂O was used exclusively for preparation of all solutions and buffers.

1000x ampicillin	100 mg/ml in ddH ₂ O, filter-sterilized
100x G418	20 mg/ml geneticin in ddH ₂ O, filter-sterilized
2000x ClonNAT	200 mg/ml nourseotricin in ddH ₂ O, filter-sterilized
150x IPTG:	150 mM, filter sterilized
50x lysozyme:	50 mg/ml

1000x pepstatin A	1 mg/ml in DMSO
1000x leupeptin	1 mg/ml in DMSO
1000x antipain	1 mg/ml in ddH ₂ O
100x PMSF:	0.1 M in isopropanol
10x HC mixture	0.2 mg/ml adenine hemi-sulfate 0.35 mg/ml uracil 0.8 mg/ml L-tryptophan 0.2 mg/ml L-histidine-HCl 0.8 mg/ml L-leucine 1.2 mg/ml L-lysine-HCl 0.2 mg/ml L-methionine 0.6 mg/ml L-tyrosine 0.8 mg/ml L-isoleucine 0.5 mg/ml L-phenylalanine 1.0 mg/ml L-glutamic acid 2.0 mg/ml L-threonine 1.0 mg/ml L-aspartic acid 1.5 mg/ml L-valine 4.0 mg/ml L-serine 0.2 mg/ml L-arginine-HCl autoclaved for selection media, the components to select for were omitted
Calcofluor white stock:	50 mg/ml NaOH added dropwise to dissolve
6x loading buffer for agarose gel-electrophoresis:	0.25% Bromophenol Blue 0.25% Xylene Cyanol 30% glycerol
B88 buffer:	20 mM HEPES/KOH pH 6.8 250 mM sorbitol 150 mM KAc 5 mM Mg(Ac) ₂ filter sterilized
5x Laemmli buffer:	62.5 mM Tris/HCl pH 6.8 5% b-mercaptoethanol 10% glycerol 2% SDS 0.0025% Bromophenol Blue

Appendix - Materials

50x TAE buffer:	2 M Tris/HAc pH 7.7 5 mM EDTA
20x TBS:	60 g Tris/HCl pH 7.4 160 g NaCl 4 g KCl ad 1 l with H ₂ O
20x PBS	46.6 g Na ₂ HPO ₄ × 12 H ₂ O 4.2 g KH ₂ PO ₄ 175.2 g NaCl 44.8 g KCl ad 1 l with H ₂ O
TBS-T:	TBS with 0.1% Tween-20
Coomassie staining solution:	7.5% acetic acid 50% methanol 0.25% Serva Brilliant Blue R250
Destaining solution:	7.5% acetic acid 50% methanol
Carrier DNA for transformations:	200 mg Salmon Sperm DNA (Sigma D1626) TE buffer ad 100 ml
B150Tw20:	20 mM HEPES/KOH pH 6.8 150 mM KAc 5 mM Mg(Ac) ₂ 1% Tween-20
Transfer buffer:	25 mM Tris 192 mM glycine 0.25% SDS 20% methanol
Ponceau S solution	1 g Ponceau S (Roth) 485 ml ddH ₂ O 15 ml 100% trichloroacetic acid (TCA)
10x YNB:	33.5 g Yeast Nitrogen Base w/o amino acids (BD) ad 500 ml ddH ₂ O wrapped in aluminum foil and autoclaved the same day.

10.2 Plasmids

Plasmid	Description	Expressed protein	Reference
pGEX-6P-1 pin2 72-282	Plasmids for overexpression of N-terminally GST-tagged recombinant proteins from <i>E. coli</i>	GST tagged Pin2p cytosolic domain	This study
pGEX-6P-1 pin2 72-210		GST tagged aa 72-210 of Pin2p - C-terminal truncation of cytosolic domain	This study
pGEX-6P-1 pin2 72-152		GST tagged aa 72-152 of Pin2p - C-terminal truncation of cytosolic domain	This study
pGEX-6P-1 pin2 153-282		GST tagged Pin2p C-terminus aa 153-282	This study
pGEX-6P-1 skg6 98-734		GST tagged Skg6p cytosolic domain	This study
pGFP33 PIN2	Centromeric plasmids for physiological-level, <i>in vivo</i> expression of C-terminally, GFP-tagged Pin2p <i>wild type</i> and mutant variants from <i>PIN2</i> promoter	Pin2p-GFP	This study
pGFP33 pin2(1-245)		Pin2(1-245)p-GFP C-terminal truncation	This study
pGFP33 pin2(1-210)		Pin2(1-210)p-GFP C-terminal truncation	This study
pGFP33 pin2(1-179)		Pin2(1-179)p-GFP C-terminal truncation	This study
pGFP33 pin2(1-152)		Pin2(1-152)p-GFP C-terminal truncation	This study
pGFP33 pin2(Δ 79-152)		Pin2(Δ 79-152)p-GFP internal truncation	This study
pGFP33 pin2(AGEAAAA)		Pin2(Y231,235,236,237A; N234A)p-GFP AP1/2-binding site mutant	This study
pGFP33 pin2(K157,159,161R)		Pin2(K157,159,161R)p-GFP ubiquitylation site mutant	This study
pGFP33 pin2(K7R)		Pin2(K157,159,161,164,165,168,172R)p-GFP ubiquitylation site mutant	This study
pGFP33 pin2(out)		Pin2(K157,159,161R; Y231,235,236,237A; N234A)-GFP AP1/2- and ubiquitylation site mutant	This study
pGFP33 pin2(QNtoED)		Pin2(N243,244,245,249,252D; Q257E)p-GFP prion domain mutant	This study
pGFP33 pin2(C35,41S)		Pin2(C35,41S) luminal double cysteine mutant	This study
pGFP33 pin2(C35S)		Pin2(C35S) luminal single cysteine mutant	This study
pGFP33 pin2(C41S)	Pin2(C41S) luminal single cysteine mutant	This study	
pGFP33 pin2(C79,81,82,84S)	Pin2(C79,81,82,84) cytosolic four cysteine cluster mutant	This study	
p426GPDleu2-d	high copy (100 copies per cell) 2 μ plasmid through insertion of leu2-d allele		This study

p426GPDleu2-d PIN2	2 μ plasmids present at 20 or	Pin2p	This study
p426GPDleu2-d pin2(1-210)	100 copies per cell	Pin2(1-210)p C-terminal, prion domain truncation	This study
p426GPDleu2-d pin2(out)	(depending on selective medium) for overexpression of Pin2p wild type and mutant variants from a strong <i>GPD</i> promoter	Pin2(K157,159,161R; Y231,235,236,237A; N234A)-GFP AP1/2- and ubiquitilation site mutant	This study
p426GPDleu2-d pin2(QNtoED)		Pin2(N243,244,245,249,252D; Q257E)p-GFP prion domain mutant	This study
YEpl12 HA-Ubiquitin	Overexpression of HA-Ubiquitin from inducible <i>CUP-1</i> promoter	HA-Ubiquitin	Hochstrasser et al., 1991
pSUP35NM::GFP-HIS3	Centromeric plasmid for expression of SUP35NM::GFP from inducible <i>CUP-1</i> promoter	N-terminal domain of Sup35 C-terminally fused to GFP	Derkatch et al., 2001
pUG series	Amplification of PCR cassettes for deletion of genes by chromosomal integration		Güldener et al., 2002
pYM series	Amplification of PCR cassettes for C-terminal tagging of genes by chromosomal integration		Janke et al., 2004
pYM-N series	Amplification of PCR cassettes for promoter exchange by chromosomal integration		Janke et al., 2004
pSH series	Expression of Cre recombinase for chromosomal excision of auxotrophy markers flanked by <i>loxP</i> sites		Güldener, et al., 2002
pTPQ128	Expression of Sec7-dsRed		Proszynski et al., 2005

10.3 Strains

Designation	Genotype	Source
YPH499	<i>MAT a ade2 his3 leu2 lys1 trp1 ura3</i>	Sikorski and Hieter, 1989
YPH500	<i>MAT a ade2 his3 leu2 lys1 trp1 ura3</i>	Sikorski and Hieter, 1989
YAS1459	<i>MAT a ade2 his3 leu2 lys1 trp1 ura3 CHS55::CHS5-HBH-kanMX6</i>	This study
YAS1490	<i>MAT a ade2 his3 leu2 lys1 trp1 ura3 CHS6::CHS6-HBH-kanMX6</i>	This study
YAS1491	<i>MAT a ade2 his3 leu2 lys1 trp1 ura3 BCH1::BCH1-HBH-kanMX6</i>	This study
YAS1492	<i>MAT a ade2 his3 leu2 lys1 trp1 ura3 BCH2::BCH2-HBH-kanMX6</i>	This study
YAS1498	<i>MAT a ade2 his3 leu2 lys1 trp1 ura3 BUD7::BUD7-HBH-kanMX6</i>	This study
YAS1905	<i>MAT a ade2 his3 leu2 lys1 trp1 ura3 PIN2::PIN2-yEGFP-KanMX4</i>	This study
YAS1933	<i>MAT a ade2 his3 leu2 lys1 trp1 ura3 PIN2::PIN2-yEGFP-KanMX4 chs5::LEU2</i>	This study
YAS1983	<i>MAT a ade2 his3 leu2 lys1 trp1 ura3 PIN2::PIN2-yEGFP-KanMX4 bch1::HIS5 (S. pombe) bch2::KAN (Tn 903) bud7::LEU2 (K. lactis) chs6::URA3 (K. lactis)</i>	This study
YAS1906	<i>MAT a ade2 his3 leu2 lys1 trp1 ura3 SKG6::SKG6-yEGFP-KanMX4</i>	This study
YAS1934	<i>MAT a ade2 his3 leu2 lys1 trp1 ura3 SKG6::SKG6-yEGFP-KanMX4 chs55::LEU2</i>	This study
YAS1984	<i>MAT a ade2 his3 leu2 lys1 trp1 ura3 SKG6::SKG6-yEGFP-KanMX4 bch1::HIS5 (S. pombe) bch2::KAN (Tn 903) bud7::LEU2 (K. lactis) chs6::URA3 (K. lactis)</i>	This study
YAS792	<i>MAT a ade2 his3 leu2 lys1 trp1 ura3 BCH1::BCH1-2AU5-LEU2 (K. lactis) BCH2::BCH2-3HA-HIS3MX6 BUD7-BUD7-9myc-TRP1 (K. lactis) CHS6::CHS6-yEGFP-kanMX6</i>	Trautwein et al., 2006
YAS563-16A	<i>MAT a ade2 his3 leu2 lys1 trp1 ura3 PIN2::PIN2-yEGFP-KanMX4 bch1::HIS5 (S. pombe) bch2::KAN (Tn 903) bud7::LEU2 (K. lactis) chs6::URA3 (K. lactis)</i>	This study
YAS328	<i>MAT a ade2 his3 leu2 lys1 trp1 ura3 CHS6::CHS6-9myc-TRP1 (K. lactis)</i>	Trautwein et al., 2006
YAS3885	<i>MAT a ade2 his3 leu2 lys1 trp1 ura3 PIN2::PIN2-yEGFP-KanMX4 bch1::HIS5 (S. pombe) bch2::KAN (Tn 903)</i>	This study
YAS3886	<i>MAT a ade2 his3 leu2 lys1 trp1 ura3 PIN2::PIN2-yEGFP-KanMX4 bch1::HIS5 (S. pombe) bud7::KAN (Tn 903)</i>	This study
YAS3888	<i>MAT a ade2 his3 leu2 lys1 trp1 ura3 PIN2::PIN2-yEGFP-KanMX4 bch1::HIS5 (S. pombe) chs6::URA3 (K. lactis)</i>	This study
YAS3887	<i>MAT a ade2 his3 leu2 lys1 trp1 ura3 PIN2::PIN2-yEGFP-KanMX4 bch2::KAN (Tn 903) bud7::LEU2 (K. lactis)</i>	This study
YAS3963	<i>MAT a ade2 his3 leu2 lys1 trp1 ura3 PIN2::PIN2-yEGFP-KanMX4 bch2::KAN (Tn 903) chs6::URA3 (K. lactis)</i>	This study
YAS3962	<i>MAT a ade2 his3 leu2 lys1 trp1 ura3 PIN2::PIN2-yEGFP-KanMX4 BUD7::LEU2 (K. lactis) chs6::URA3 (K. lactis)</i>	This study
YAS3790	<i>MAT a ade2 his3 leu2 lys1 trp1 ura3 PIN2::PIN2-yEGFP-KanMX4 bch2::HIS5 (S. pombe) bud7::LEU2 (K. lactis) chs6::URA3 (K. lactis)</i>	This study
YAS3177	<i>MAT a ade2 his3 leu2 lys1 trp1 ura3 PIN2::PIN2-yEGFP-KanMX4 bch1::loxP bud7::loxP chs6::loxP</i>	This study
YAS2214	<i>MAT a ade2 his3 leu2 lys1 trp1 ura3 pin2::LEU2 (K. lactis)</i>	This study
YAS2573	<i>MAT a ade2 his3 leu2 lys1 trp1 ura3 pin2::LEU2 (K. lactis) chs5::HIS5 (S. pombe)</i>	This study
YAS2530	<i>MAT a ade2 his3 leu2 lys1 trp1 ura3 PIN2::PIN2-yEGFP-KanMX4 chs5::LEU2 apm1::URA3 (K. lactis)</i>	This study

YAS2531	<i>MAT a ade2 his3 leu2 lys1 trp1 ura3 SKG6::SKG6-yEGFP-KanMX4 chs5::LEU2 apm1::URA3 (K. lactis)</i>	This study
YAS946	<i>MAT a ade2 his3 leu2 lys1 trp1 ura3 CHS3-CHS3-2EGFP-TRP1 (K. lactis)</i>	Trautwein et al., 2006
YAS957	<i>MAT a ade2 his3 leu2 lys1 trp1 ura3 CHS3-CHS3-2EGFP-TRP1 (K. lactis) end3::LEU2 (K. lactis)</i>	Zanolari et al., 2010
YAS2545	<i>MAT a ade2 his3 leu2 lys1 trp1 ura3 PIN2::PIN2-yEGFP-KanMX4 end3::LEU2 (K. lactis)</i>	This study
YAS2546	<i>MAT a ade2 his3 leu2 lys1 trp1 ura3 SKG6::SKG6-yEGFP-KanMX4 end3::LEU2 (K. lactis)</i>	This study
L1741	<i>74-D694 1Y1 MATa ade1-14 (UGA) trp1-289 (UAG) ura3 his3 leu2 [PIN+][psi-]</i>	Derkatch et al., 1997
YAS3954	<i>74-D694 1Y1 MATa ade1-14 (UGA) trp1-289 (UAG) ura3 his3 leu2 [pin-][psi-]</i>	This study
YAS3967	<i>74-D694 1Y1 MATa ade1-14 (UGA) trp1-289 (UAG) ura3 his3 leu2 chs5::KAN (Tn 903) [pin-][psi-]</i>	This study
YAS2031	<i>MAT a ade2 his3 leu2 lys1 trp1 ura3 PIN2::PIN2-yEGFP-KanMX4 bch1::HIS5 (S. pombe)</i>	This study
YAS2032	<i>MAT a ade2 his3 leu2 lys1 trp1 ura3 PIN2::PIN2-yEGFP-KanMX4 bch2::KAN (Tn 903)</i>	This study
YAS2034	<i>MAT a ade2 his3 leu2 lys1 trp1 ura3 PIN2::PIN2-yEGFP-KanMX4 bud7::URA3 (K. lactis)</i>	This study
YAS2033	<i>MAT a ade2 his3 leu2 lys1 trp1 ura3 PIN2::PIN2-yEGFP-KanMX4 chs6::URA3 (K. lactis)</i>	This study
YAS4026	<i>MAT a ade2 his3 leu2 lys1 trp1 ura3 PIN2::PIN2-yEGFP-KanMX4 hog1::LEU2 (K. lactis)</i>	This study
YAS4027	<i>MAT a ade2 his3 leu2 lys1 trp1 ura3 PIN2::PIN2-yEGFP-KanMX4 slt2::LEU2 (K. lactis)</i>	This study
YAS328	<i>MAT a ade2 his3 leu2 lys1 trp1 ura3 CHS6::CHS6-9myc-TRP1 (K. lactis)</i>	Trautwein et al., 2006
YAS335	<i>MAT a ade2 his3 leu2 lys1 trp1 ura3 BUD7::BUD7-9myc-TRP1 (K. lactis)</i>	Trautwein et al., 2006
YAS339	<i>MAT a ade2 his3 leu2 lys1 trp1 ura3 BCH1::BCH1-9myc-TRP1 (K. lactis)</i>	Trautwein et al., 2006
YAS589	<i>MAT a ade2 his3 leu2 lys1 trp1 ura3 BCH2::BCH2-9myc-TRP1 (K. lactis)</i>	Trautwein et al., 2006
YAS614	<i>MAT a ade2 his3 leu2 lys1 trp1 ura3 BCH1::BCH1-9myc-TRP1 (K. lactis)bch2::KAN bud7::LEU2 chs6::URA3</i>	Trautwein et al., 2006
YAS615	<i>MAT a ade2 his3 leu2 lys1 trp1 ura3 BUD7::BUD7-9myc-TRP1 (K. lactis) bch1::HIS5 bch2::KAN chs6::URA3</i>	Trautwein et al., 2006
YAS653	<i>MAT a ade2 his3 leu2 lys1 trp1 ura3 CHS6::CHS6-9myc-TRP1 (K. lactis) bch1::HIS5 bch2::KAN bud7::LEU2</i>	Trautwein et al., 2006
YAS654	<i>MAT a ade2 his3 leu2 lys1 trp1 ura3 BCH2::BCH2-9myc-TRP1 (K. lactis) bch1::HIS5 bud7::LEU2 chs6::URA3</i>	Trautwein et al., 2006
YAS579	<i>MAT a ade2 his3 leu2 lys1 trp1 ura3 CHS6::CHS6-9myc-TRP1 (K. lactis) chs5::LEU2</i>	This study
YAS580	<i>MAT a ade2 his3 leu2 lys1 trp1 ura3 BUD7::BUD7-9myc-TRP1 (K. lactis) chs5::LEU2</i>	This study
YAS581	<i>MAT a ade2 his3 leu2 lys1 trp1 ura3 BCH1::BCH1-9myc-TRP1 (K. lactis) chs5::LEU2</i>	This study
YAS582	<i>MAT a ade2 his3 leu2 lys1 trp1 ura3 BCH2::BCH2-9myc-TRP1 (K. lactis) chs5::LEU2</i>	This study
NDY505	<i>MAT a his3 leu2 ura3</i>	Roth et al., 2006
YAS3033	<i>MAT a his3 leu2 ura3 PIN2 ::PIN2-EGFP(HIS3MX6)</i>	This study
NDY1690	<i>MAT a his3 leu2 ura3 akr1Δ akr2Δ pfa3Δ pfa4Δ pfa5Δ ::G418R lys2 ::YCK2(CCIIS)</i>	Roth et al., 2006
YAS3035	<i>MAT a his3 leu2 ura3 akr1Δ akr2Δ pfa3Δ pfa4Δ pfa5Δ ::G418R lys2 ::YCK2(CCIIS) PIN2 ::PIN2-EGFP(HIS3MX6)</i>	This study

10.11 Oligonucleotides

Primer	Designation	Sequence	Purpose
AD2	PIN2_CtermF	CGC GGA TCC ACA GGA ATA GGT CAG TCC ATT TG	amplification of Pin2 from codon 72 (after TM), BamH1 restriction site
AD3	PIN2_CtermR	CCG GAA TTC TTA GTA ATA TCT ATC GCT TTG GTT TG	anneals at the end of the Pin2 gene, EcoI restriction site
AD4	SKG6Cterm_F	CGC GGA TCC AGG AGA AGC AAA AAG GAA GCT G	amplification of Skg6p from codon 98 (after TM), BamH1 restriction site
AD5	SKG6Cterm_R	GAA CAT CTC GAG TCA GTT GAC GGT ATA ATT ATG TGA AG	anneals at the end of the SKG6 gene, EcoRI restriction site
AD16	PIN3'_FL	ATA GCA TGC GTA ATA TCT ATC GCT TTG GTT TGG	Pin2 truncations, anneals at the end of the PIN2 gene, SphI, no stop codon
AD17	PIN23'210	ATA GCA TGC GGC CGC ATT TTG GAT AAA CG	Pin2 truncations, amplifies Pin2 upstream of the 210 codon, SphI, no stop codon
AD18	PIN23'_152	ATA GCA TGC ATC TTC CTC TAA TTC ATA CAC CTC	Pin2 truncations, amplifies Pin2 upstream of the 152 codon, SphI, no stop codon
AD21	PIN23'Flstop	ATA CTC GAG TTA GTA ATA TCT ATC GCT TTG GTT TG	Pin2 truncations, anneals at the end of the PIN2 gene, XhoI, no stop codon
AD23	PIN23'delta	ATA GCT AGC AAT GAA CTG ACC TAT TCC TGT TAC	Pin2 internal truncation, amplifies PIN2 sequence upstream of the 79 codon, NheI, to perform on circularized plasmid
AD24	PIN25'delta	ATA GCT AGC TTC GAT TTG GAA AAA CAA AAA GAG AA	Pin2 internal truncation, amplifies PIN2 sequence downstream of the 153 codon, NheI, PCR to perform on circularized plasmid
AD25	PIN2prom600EcoR1	ATA GAA TTC AGT ACT CGC CAA ATA GAA CCA AC	anneals 600bp upstream of the PIN2 gene, EcoRI
AD26	PIN2-deltestf	CCC GGT CGT GAC TTT TTA GA	anneals 90bp upstream of the PIN2 start codon, for testing of deletion of PIN2 gene
AD28	PIN2-S1	AAA TAC TAG AAA TAT AAT CAA AGA CTC CCA AGC GTA TAC ACA GTA cag ctg aag ctt cgt acg c	Amplification of PIN2 deletion cassette

AD29	PIN2-S2	GTC TGA CTG ATT ATT CAA AAG AAG GGG GAA TAT ATA TTT ACC TCA gca tag gcc act agt gga tct g	Amplification of PIN2 deletion and C-terminal tagging cassette
AD36	Pin2_3'_1-179SphI	ATA CAT GCA TGC CCT ACT AGG GCT GCG TCC TTC	Pin2 truncation, amplifies PIN2 upstream of 179 codon, SphI, no stop
AD37	Pin2_3'_1-245	ATA CAT GCA TGC GTT ATT ATT GAT GTT ATT ATT ATC GTA ATA	Pin2 truncation, amplifies PIN2 upstream of 245 codon, SphI, no stop
AD38	Pin2_palm12p	GCT GGG ACA CCT CCA TGG ACA ATA AAG CAT CTA AAA TTA TTG C	Primer for site-directed mutagenesis for creation of Pin2(C35,41S) mutant, parallel primer
AD39	Pin2_palm12a	GCA ATA ATT TTA GAT GCT TTA TTG TCC ATG GAG GTG TCC CAG C	Primer for site-directed mutagenesis for creation of Pin2(C35,41S) mutant, antiparallel primer
AD42	Pin2_palm4567p	GTC AGT TCA TTT CTT GGT CTT CTC GTT CTT CTA ATG ACA G	Primer for site-directed mutagenesis for creation of Pin2(C79,81,82,84S) mutant, parallel primer
AD43	Pin2_palm4567a	CTG TCA TTA GAA GAA CGA GAA GAC CAA GAA ATG AAC TGA C	Primer for site-directed mutagenesis for creation of Pin2(C79,81,82,84S) mutant, antiparallel primer
AD44	Pin2_5'153-288BamH1	CGC GGA TCC TTC GAT TTG GAA AAA CAA AAA GAG AA	amplifies PIN2 downstream of the 153 codon, BamH1
AD45	PIN2-S3	CAA TCA TAT CAG GGA TAT AAA CCA AAC CAA AGC GAT AGA TAT TAC cgt acg ctg cag gtc gac	Amplification of PIN2 and C-terminal tagging cassette
AD45	PIN2-tagtestf	TAA AGA AGG ACG CAG CCC TA	For testing PIN2 chromosomal C-terminal tagging
AD48	SKG6-tagtestf	CAG AAG TGT AAG CGC AAC CA	For testing SKG6 chromosomal C-terminal tagging
AD51	SKG6-S2	ACA TCA ATT TAT ATA TCG GAT AAT TGT CCG TTC ATT ATC TAC ACT gca tag gcc act agt gga tct g	Amplification of SKG6 deletion and C-terminal tagging cassette
AD52	SKG6-S3	GAT TTA AGA AAA CAA TTA GGC TCT TCA CAT AAT TAT ACC GTC AAC cgt acg ctg cag gtc gac	Amplification of SKG6 and C-terminal tagging cassette
AD53	Pin152REcoR1	CCG GAA TTC ATC TTC CTC TAA TTC ATA CAC CTC	Pin2 truncations, amplifies Pin2 upstream of the 152 codon, EcoRI restriction site, stop codon

AD54	Pin210EcoR1	CCG GAA TTC GGC CGC ATT TTG GAT AAA CG	Pin2 truncations, amplifies Pin2 upstream of the 210 codon, EcoRI restriction site, stop codon
AD58	Pin2palm1a	CTT TAT TGT CCA TGG AGG TGT CCC AGC	Primer for site-directed mutagenesis for creation of Pin2(C35S) mutant, antiparallel primer
AD59	Pin2palm1p	GCT GGG ACA CCT CCA TGG ACA ATA AAG	Primer for site-directed mutagenesis for creation of Pin2(C35S) mutant, parallel primer
AD60	Pin2palm2a	GCA ATA ATT TTA gAT GCT TTA TTG TCC	Primer for site-directed mutagenesis for creation of Pin2(C41S) mutant, antiparallel primer
AD61	Pin2palm2p	GGA CAA TAA AGC ATc TAA AAT TAT TGC	Primer for site-directed mutagenesis for creation of Pin2(C41S) mutant, parallel primer
AD65	Pin2YGENYmut5'	GAC ATC AGC GAT GCT GGC GAG AAC GCT TAT TAC GAT AAT AAT	Primer for site-directed mutagenesis for creation of Pin2(Y231,235,236,237A; N234A) mutant, first parallel primer
AD66	Pin2YGENYmut3'	ATT ATT ATC GTA ATA AGC GTT CTC GCC AGC ATC GCT GAT GTC	Primer for site-directed mutagenesis for creation of Pin2(Y231,235,236,237A; N234A) mutant, first antiparallel primer
AD67	Pin2KERNKmut3'	GCT GCG TCC TTC TCT ATT TCT TTC CCT CTG TTG TTT TTT CC	Primer for site-directed mutagenesis for creation of Pin2(K157,159,161,164,165,168,172R) mutant, antiparallel primer
AD68	Pin2KERNKmut5'	GGA AAA AAC AAC AGA GGG AAA GAA ATA GAG AAG GAC GCA GC	Primer for site-directed mutagenesis for creation of Pin2(K157,159,161,164,165,168,172R) mutant, parallel primer
AD69	Pin2KQKEKmut3'	GTT TTT TCC TTG TTC TCT CTC TTT GTC TTT CCA AAT CGA AAT C	Primer for site-directed mutagenesis for creation of Pin2(K157,159,161R) and Pin2(K157,159,161,164,165,168,172R) mutants, antiparallel primer

AD70	Pin2KQKEKmut5'	GAT TTC GAT TTG GAA AGA CAA AGA GAG AGA ACA AGG AAA AAA C	Primer for site-directed mutagenesis for creation of Pin2(K157,159,161R) and Pin2(K157,159,161,164,165,168,172R) mutants, parallel primer
AD81	Pin2YGENYYYmutp	GAT gcT GGC GAG gcC gcT gcT gcC GAT AAT AAT AAC	Primer for site-directed mutagenesis for creation of Pin2(Y231,235,236,237A; N234A) mutant, second parallel primer
AD82	Pin2YGENYYYmuta	GTT ATT ATT ATC Ggc Agc Agc Ggc CTC GCC Agc ATC	Primer for site-directed mutagenesis for creation of Pin2(Y231,235,236,237A; N234A) mutant, second antiparallel primer
AD83	Pin2tagtest2	GTA GCA ACA ACG CTC ATG TTG CTT C	For testing PIN2 chromosomal C-terminal tagging
AD90	Pin2TMPstlp	CAG GCA AGG GGT Act gca gAC AGG AAT AGG TC	For creation of Mid2-Pin2 chimera, insertion of Pst I restriction site between codons 71 and 72 of PIN2 by site-directed mutagenesis, parallel primer
AD91	Pin2TMPstla	GAC CTA TTC CTG Tct gca gTA CCC CTT GCC TG	For creation of Mid2-Pin2 chimera, insertion of PstI restriction site between codons 71 and 72 of PIN2 by site-directed mutagenesis, antiparallel primer
AD94	Pin2promSaclATGp	CGT ATA CAC AGT Aga gct cAT GAA CGT TTG C	For creation of Mid2-Pin2 chimera, insertion of SacI restriction site before PIN2 start codon by site-directed mutagenesis, parallel primer
AD95	Pin2promSaclATGa	GCA AAC GTT CAT gag ctc TAC TGT GTA TAC G	For creation of Mid2-Pin2 chimera, insertion of SacI restriction site before PIN2 start codon by site-directed mutagenesis, antiparallel primer
AD96	Mid2ATGSacl	Ata gag ctc ATG TTG TCT TTC ACA ACC AAG AAT AG	For creation of Mid2-Pin2 chimera, amplification of Mid2 N terminal and TMD domain

AD97	Mid2upTMPstI	Cta gct gca gGA TAC AAA ACA TGT AAA TTA AAG CCA G	For creation of Mid2-Pin2 chimera, amplification of Mid2 N terminal and TMD domain
AD109	Pin2TRKKQallKp	GAG AGA ACA AGG AgA AgA CAA CAG AGG GAA AG	Primer for site-directed mutagenesis for creation of Pin2(K157,159,161,164,165,168,172R) mutants, parallel primer
AD110	Pin2TRKKQallKp	CTT TCC CTC TGT TGT cTT cTC CTT GTT CTC TC	Primer for site-directed mutagenesis for creation of Pin2(K157,159,161,164,165,168,172R) mutants, antiparallel primer
AD139	LEU2seqprom	TGG AAC GAA CAT CAG AAA TAG C	Sequencing of the <i>leu2-d</i> allele in pHR81 plasmid
AD140	LEU2seq5'	AAT ACC ATT TAG GTG GGT TGG	Sequencing of the <i>leu2-d</i> allele in pHR81 plasmid
AD141	LEU2seq3'	GAG AAA AAC TGT GGA GGA AAC C	Sequencing of the <i>leu2-d</i> allele in pHR81 plasmid
AD142	Leu2dEagI5'	Ata cgg ccg TAT ATA TAT TTC AAG GAT ATA CCA TTG	Amplification of <i>leu2-d</i> allele 5' primer, <i>EagI</i> restriction site
AD143	Leu2dEagI3'	Ata cgg ccg TGT ACA AAT ATC ATA AAA AAA GAG AAT C	Amplification of <i>leu2-d</i> allele 3' primer, <i>EagI</i> restriction site
AD144	GPDpromoterF	Cgg tag gta ttg att gta att ctg	Sequencing primer from GPD promoter
AD157	Pin2NNNc2DDDDp	GAT AAT AAT AAC ATC gAT gAT gAC CTC CAG GGA AAC	Primer for site-directed mutagenesis for creation of Pin2(N243,244,245,249,252D; Q257E) mutant, first parallel primer
AD158	Pin2NNNc2DDDDa	GTT TCC CTG GAG GTc ATc ATc GAT GTT ATT ATT ATC	Primer for site-directed mutagenesis for creation of Pin2(N243,244,245,249,252D; Q257E) mutant, first antiparallel primer
AD165	Pin2EDDonc2p	CgA TgA TgA CCT CgA GGG AgA CAG TTA CgA TAC TCC CTC CTC	Primer for site-directed mutagenesis for creation of Pin2(N243,244,245,249,252D; Q257E) mutant, second parallel primer
AD166	Pin2EDDinc2a	GAG GAG GGA GTA TcG TAA CTG TcT CCC TcG AGG TcA TcA TcG	Primer for site-directed mutagenesis for creation of Pin2(N243,244,245,249,252D; Q257E) mutant, second

			antiparallel primer
CK273	HOG1-delfor	GGA ACA AAG GGA AAA CAG GGA AAA CTA CAA CTA TCG TAT ATA ATA cag ctg aag ctt cgt acg c	S1 primer for amplification of HOG1 deletion cassette
CK278	HOG1-deltestfor2	TTT GTA TAG TGG AAG AGG AAT TTG C	anneals 160bp upstream of the HOG1 start codon, for testing of deletion of HOG1 gene
CK318	HOG1-delrev2	AAA AAG AAG TAA GAA TGA GTG GTT AGG GAC ATT AAA AAA ACA CGT gca tag gcc act agt gga tct g	S2 primer for amplification of HOG1 deletion cassette
CK327	SLT2-pUGdelfor	AAA ATA GTA GAA ATA ATTG AAG GGC GTG TAT AAC AAT TCT GGG AGc agc tga agc ttc gta cg c	S1 primer for amplification of SLT2 deletion cassette
CK328	SLT2-pUGdelrev	TCT ATG GTG ATT CTA TAC TTC CCC GGT TAC TTA TAG TTT TTT GTC gca tag gcc act agt gga tct g	S2 primer for amplification of SLT2 deletion cassette
CK331	slt2-deltestfor	CTA CGT ATG CGG CGA TTT TT	anneals 315bp upstream of the SLT2 start codon, for testing of deletion of SLT2 gene
MT-A9	BUD7-KO-for	TGA GCG CAA AAA AAT AAA GAA CTA AGG AAG AAG AGC TTC CCT CAG cag ctg aag ctt cgt acg c	S1 primer for amplification of BUD7 deletion cassette
MT-A10	BUD7-KO-rev	TCG AAA CTT TGG TCA GAC TCA TAT CTT GAA TAA CCA CAC TTA AAC gca tag gcc act agt gga tct g	S2 primer for amplification of BUD7 deletion cassette
MT-A11	BUD7-deltestfor	AGC GTC ACG TGA ACA CAT TC	testing of deletion of BUD7 gene
MT251	END3-pUGf	GTG GGT ATT GGA AAG GCC GGT AAA GAT AAC AGG GAT CTC TGA AAA cag ctg aag ctt cgt acg c	S1 primer for amplification of END3 deletion cassette
MT252	END3-pUGr	ACA GTA AAT ATT ACA CAT TCA TGT ACA TAA AAT TAA TTA TCG GTG gca tag gcc act agt gga tct g	S2 primer for amplification of END3 deletion cassette
MT257	END3-Delconf	TGG AAA GGC CGG TAA AGA TA	testing of deletion of END3 gene

RG084	KO-Chs5-for	GCG TAG ATG CTA AAT GTT ATC GCG GTT TAG CTT GCA TGT TAC GTT CCA GCT GAA GCT TCG TAC GTG C	S1 primer for amplification of CHS5 deletion cassette
RG085	KO-Chs5-rev	GCT TGG CGG CTA CTG AGT ACC CCT CTC AAG AAA ATG AAG TGA TCG CAT AGG CCA ACT AGT GGA TC	S2 primer for amplification of CHS5 deletion cassette
RG088	KO-cont-Ch5-for	CGG TCG GCC CTT CAA GTT CTC C	testing of deletion of CHS5 gene
RG092	KO-Ykr027-for	GTA TAA GTA GTA AAG TAC AGT TAA CAG ATC AAT TGG CCT CGA GGA ATC CAG CTG AAG CTT CGT ACG TGC	S1 primer for amplification of BCH2 deletion cassette
RG093	KO-Ykr027-rev	GGA TAT TAC CCG CGC TAA AGT ATT AGC ATT ATC GCC GTA AAT TTG CAT AGG CCA ACT AGT GGA TC	S2 primer for amplification of BCH2 deletion cassette
RG096	Contr-Ykr027-for1	GGT TTC CGA GGC ATT GTT ACA CCG	testing of deletion of BCH2 gene
UR0185	Apm1_S1	GAG TAT TTT TGA AAA TTG TAA ATT ACG AAC TTG GAG GGA CAC AGA cag ctg aag ctt cgt acg c	For amplification of APM1 deletion cassette
UR0186	Apm1_S2	GTC CAT GCA CCG TAG AAA TTG CTT TTT TTA TAT ATT TTT CAG ACA gca tag gcc act agt gga tct g	For amplification of APM1 deletion cassette
UR0187	Apm1_del_con_for	GGA AAG TGG GCT GAA CAA AA	testing of deletion of APM1 gene
general	Kan&HIS-Primer	Tgg gcc tcc atg tcg ctg g	Reverse primer for testing of chromosomal gene tagging with KanMx4, cloNAT and HIS3MX6 markers and deletion testing using pUG6 plasmid with kanMX marker
general	TRP-Primer	GCT ATT CAT CCA GCA GGC CTC	Reverse primer for testing of chromosomal gene tagging with kITRP marker
BZ055	pUG73-LEU2-rev	Cta acg tgc ttg cct ctt cc	Reverse primer for testing of gene deletion by integration of LEU2 marker

BZ056	pUG72-URA3-rev	Gga cag aaa att cgc cga ta	Reverse primer for testing of gene deletion by integration of URA3 marker
	pUG27_HIS5_rev	tgt tct ccc ttt tgg ttt gc	Reverse primer for testing of gene deletion by integration of HIS5 marker

10.5 Biochemical Methods

10.5.1 GST-tagged Pin2 protein purification

The GST-tagged full-length cytosolic domain of Pin2 and cytosolic domain truncations were expressed from pGEX-6P-1 plasmids in *E. coli* Rosetta cells. Cells between OD₆₀₀ 0.5 and 0.8 were induced with 0.2 mM IPTG for 4 h at 23°C. Cells were harvested by 10 min centrifugation at 12,000 × g, washed once in cold PBS buffer and snap frozen. Frozen cell pellets from 1.5 l cultures were resuspended in 20 ml Pin2 purification buffer supplemented with 1 mM DTT and Complete Mini, EDTA-free protease inhibitor tablets (Roche). Resuspended cells were incubated with 50 µl DNase I (10 mg/ml) and 500 µl lysozyme (50 mg/ml) for 30 min on ice. Cells were sonicated 3x (7 output control; 50% duty cycle; pulsed setting) for 45 sec with 1 min incubation on ice between sonication rounds. The lysed cells were centrifuged at 18,000 rpm in SS-34 rotor (approx. 39,000 × g) for 20 min at 4°C. The extracts were then incubated for 1 h at 4°C with rotation with 300 µl GSH agarose (Sigma) (600 µl 50% slurry) equilibrated in Pin2 purification buffer. The beads were washed twice with Pin2 purification buffer. To remove heat shock proteins, the beads were incubated twice with Pin2 purification buffer supplemented with 1 mM ATP and 5 mM MgCl₂ for 15 min at 4°C with rotation. The beads were washed again twice with Pin2 purification buffer. During the last wash, beads were transferred into a column. The protein was eluted with 250 µl Pin2 purification buffer supplemented with 40 mM GSH. Samples from elution fractions were analyzed by SDS-PAGE and Coomassie staining. The fractions most abundant for GST-Pin2 were pooled and dialyzed against the Pin2 purification buffer twice – overnight and 3 h at 4°C, to remove GSH.

Pin2 purification buffer

150 mM KCl
50 mM Tris pH 8.0
0.5 % Triton X-100
5 % glycerol

10.5.2 GST-Skg6 lysate preparation

GST-Skg6 lysates from *E. coli* Rosetta cells were obtained as described for GST-Pin2 up to the 18,000 rpm lysate centrifugation step, except that GST-Skg6 expression was induced for 6 h at 23°C and Skg6p buffer was used. Skg6 lysates were snap frozen after centrifugation.

SkG6 purification buffer

25 mM KCl
50 mM Tris pH 8.0
0.5 % Triton X-100
5 % glycerol

10.5.3 Spheroplasting of yeast cells

Ten OD₆₀₀ of cells between OD₆₀₀ 0.2 – 0.7 were harvested and washed once in ddH₂O. Unless otherwise indicated cells were centrifuged at 1,800 × g for 2 min at RT. Cells were resuspended in 1 ml DTT buffer and incubated at RT for 5 min. Cells were centrifuged and resuspended in SP buffer with 30 µl zymolyase T20 (10 mg/ml in water) and incubated for 40 min to 1 h at 30°C with gentle rotation. The cells were harvested by 2 min centrifugation at 1,000 × g. The tubes were turned upside-down on a Kimwipe to remove excess SP buffer.

DTT buffer

100 mM Tris pH 9.4
10 mM DTT

SP buffer

75 % YP
0.7 M sorbitol
0.5 % glucose
10 mM Tris pH 7.5

10.5.4 Yeast extract pull-down with GST-tagged proteins

For pull downs, 5 µg of GST-Pin2 and Sec22-GST, and 0.5 ml of GST-SkG6 *E. coli* lysate was prebound to 10 µl of GSH agarose (Sigma Aldrich) per reaction. 10 OD₆₀₀ of cells were spheroplasted and lysed in 1 ml B150Tw20 supplemented with leupeptin, pepstatin, antipain and 1 mM PMSF. The protein extracts were normalized by BCA assay. 900 µl of yeast extract were incubated for 1 h at 4°C with gentle rotation with 10 µl of GSH agarose with prebound GST-tagged protein. Pull downs were washed 3x in B150Tw20 and 1x in with 20 mM HEPES pH 6.8, 150 mM NaCl and transferred to new tubes. All centrifugation steps with the resin were performed at 1,000 × g for 1 min at 4°C. The remnants of buffer after the final wash were removed with a capillary tip. Pull-downs were eluted with 35 µl of SDS sample buffer and heated at 68°C.

For protein prebinding to GSH agarose: The GSH agarose was pre-equilibrated with Pin2 or SkG6 purification buffer (see chapters 10.6.1 and 10.6.2 for recipes). Purified GST-Pin2 and Sec22-GST were resuspended in 1 ml total volume of Pin2 purification buffer with 1 % BSA. The GST-tagged proteins and GST-SkG6 lysate was incubated with the resin for 1 h at 4°C

with gentle rotation. The resin was washed 2x with Pin2 or Skg6 purification buffer and 3x in B150Tw20.

10.5.5 Denaturing immunoprecipitations

Δpin2 cells transformed with YEp112 HA-ubiquitin plasmid and pGFP33 PIN2 or pGFP33 pin2K7R plasmids were used for denaturing immunoprecipitations. For overexpression of HA-ubiquitin from the *CUP-1* promoter, cells at OD₆₀₀ 0.2 – 0.7 were diluted to OD₆₀₀ 0.1 and induced with 0.1 mM CuSO₄ for 4 h. 20 OD₆₀₀ of cells were harvested per immunoprecipitation reaction. Cells were spheroplasted and lysed in 200 μl lysis buffer with leupeptin, pepstatin, antipain and 1 mM PMSF modified from (Søgaard *et al.*, 1994). Lysates were cleared by 10 min 10,000 × g centrifugation. 10 μl of 20 % SDS was added to 200 μl of supernatants and the lysates were boiled for 3 min at 95°C. Extracts were diluted 10x in dilution buffer to achieve 20 mM HEPES pH 6.8, 200 mM KCl, 1 mM MgCl₂, 0.5 % Triton, 0.1 % SDS final buffer concentration and centrifuged for 10 min at 10,000 × g to remove any precipitate. 1.9 ml of extracts were incubated at 4°C O/N with gentle rotation with 5 μg of anti-GFP antibody (Torrey Pines) or 5 μg of control affinity-purified rabbit IgG antibody (Dianova, Hamburg, Germany) bound to 10 μl of protein A-Sepharose. Samples were washed 3x with wash buffer and once with 20 mM HEPES pH 6.8, 200 mM NaCl buffer and transferred to new tubes. The remnants of buffer after the final wash were removed with a capillary tip. Immunoprecipitates were eluted with 35 μl SDS sample buffer and boiled at 68°C.

For antibody prebinding: antibodies diluted in 500 μl PBS, 1 % BSA were incubated with protein A-Sepharose pre-equilibrated in PBS, 0.2 % Triton for 1 h at 4°C with gentle rotation. The resin was washed twice in PBS, 0.2 % Triton and thrice in lysis buffer prior to incubation with yeast extracts.

Lysis buffer

20 mM HEPES pH 6.8
200 mM KCl
1 mM MgCl₂
2 % Triton
1mM DTT

Dilution buffer

20 mM HEPES pH 6.8
200 mM KCl
1 mM MgCl₂
0.33 % Triton

Wash buffer

20 mM HEPES pH 6.8
200 mM KCl
1 mM MgCl₂
0.5% Triton

10.5.6 Crosslinker immunoprecipitations

Per strain condition, 70 OD₆₀₀ of yeast cells grown to OD₆₀₀ 0.2 - 0.7 were harvested, washed once in water and resuspended in 1.54 ml B88 buffer with leupeptin, pepstatin, antipain and 1 mM PMSF. 1.5 ml of resuspended cells were transferred into 2 ml Sarstedt tubes and beads were added until the buffer reached the top of the tube. The cells were subjected to fast prep lysis: two rounds of 30 sec lysis at speed 6.5. The tubes were incubated on ice between lysis rounds. The lysate was cleared by centrifugation at 13,000 × g for 5 min at 4°C. Protein concentration was measured by Bradford assay and adjusted. For subsequent steps 140 µl lysate was taken per immunoprecipitation reaction. DSP (Pierce) dissolved in DMSO was added to 140 µl lysate (2 mM final concentration). The crosslinking reaction was performed for 30 min at RT and was stopped with 7 µl 1 M Tris pH 7.5 for 15 min. Eight µl 20% SDS was added, the sample was incubated at 65°C for 15 min and 1,350 µl IP buffer supplemented with 1 µg/µl BSA was added. The sample was centrifuged for 10 min at 16,000 × g. The supernatant was subjected to immunoprecipitation O/N at 4°C using 5 µg monoclonal anti-GFP antibody (clones 7.1 and 13.1, Roche) cross-linked to Protein A-sepharose with DMP (Pierce). Control immunoprecipitations with 5 µg monoclonal anti-HA antibody (HA.11 clone 16B12, Covance) were performed in parallel. Precipitates were washed 3x; 1x in IP buffer and 2x in the same buffer containing 250 mM NaCl. Precipitates were resuspended in 50 mM Tris/HCl pH 7.5, 250 mM NaCl and transferred into new tubes. The remnants of buffer after final wash were removed with a capillary tip. Immunoprecipitates were eluted with 35 µl SDS sample buffer containing 100 mM DTT and boiled for 30 min 95°C.

For preparation of Protein A-Sepharose with cross-linked antibodies: The resin was pre-equilibrated in PBS, 0.1 % Triton X-100. Antibodies diluted in 500 µl PBS, 0.1 % Triton X-100, 1% BSA were incubated with 10 µl Protein A-Sepharose per IP reaction for 1 h at 4°C with gentle rotation. The resin was washed 2x in PBS, 0.1 % Triton X-100 and 1x in 0.2 M Triethanolamine (TEA) pH 8.2. 10 µl of beads were resuspended in 50 µl of TEA pH 8.2 with 6.5 mg/ml DMP. The resin was rotated for 1 h at RT. 50 µl of 1 M Tris pH 8.0 was added and incubated with the resin for 1 h at RT under rotation to quench the cross-linking reaction. The beads were washed 3x with IP buffer before incubation with the yeast extracts.

IP buffer

50 mM Tris/HCl pH 7.5

150 mM NaCl

1% Triton X-100

For dilution of yeast lysates the IP buffer was supplemented with 1 µg/µl BSA

10.5.7 Subcellular fractionation

Ten OD₆₀₀ of cells at OD₆₀₀ 0.2 - 0.7 were spheroplasted. Cells were washed once in zymolyase-free SP buffer, resuspended in the same buffer and incubated at 30°C for 30 min. Regenerated cells were harvested by 1,000 × g centrifugation for 2 min and lysed in 1 ml subcellular fractionation buffer with leupeptin, pepstatin, antipain and 1 mM PMSF. The lysate was cleared at 500 × g for 2 min and the supernatant (= "total cell lysate", TCL) subjected to centrifugation at 13,000 × g (10 min). The supernatant (S13) was carefully taken off with a pipette and subjected to centrifugation at 100,000 × g (1 h). Both pellets (P13 and P100) were washed once gently in lysis buffer and resuspended lysis buffer corresponding to the amount of supernatant before the centrifugation step. All steps were carried out at 4°C. Samples were taken from all final fractions. The 100,000 × g pellet was vigorously resuspended in SDS sample buffer, heated for 5 min at 68°C and the sample was vortexed at high speed for 5 min. The sample was again boiled before loading.

Subcellular fractionation buffer

50 mM Tris pH 7.5
1 mM EDTA
50 mM NaCl

10.5.8 Trypsin protection assay

Five OD₆₀₀ of cells were harvested and spheroplasted. Spheroplasts were resuspended in 170 µl modified buffer B88 (20 mM HEPES pH 7.4, 250 mM sorbitol, 150 mM NaAc pH 5.5, 5 mM Mg(Ac)₂, pH 6.8). The sample was split into 20 µl aliquots and incubated with or without 2.5 µg of trypsin in the presence or absence of 1 % Triton X-100. Trypsin digestion was stopped after 10 min or 90 min by addition of 1.25 µg of Trypsin inhibitor. Samples were boiled at 68°C in SDS sample buffer.

10.5.9 Preparation of lysates under non-reducing and reducing conditions

Three OD₆₀₀ of cells from a *Δpin2* strain expressing either wild type Pin2 or the cysteine mutants from a pGFP33 centromeric plasmid were harvested. Cells were resuspended in 150 µl lysis buffer (50 mM Tris pH 7.5, 1 mM EDTA with leupeptin, pepstatin, antipain and 1 mM PMSF) and lysed by 10 min vortexing at 4°C with 120 µl glass beads. Lysates were cleared by centrifugation for 10 min at 1,500 × g and boiled 10 min at 68°C in 5x SDS loading buffer without β-mercaptoethanol. Lysates for reducing SDS-PAGE were performed as

described above, except that 50 mM DTT was included in the lysis buffer and samples were boiled in 5x SDS buffer containing 5% β -mercaptoethanol.

10.5.10 Preparation of samples for blue native agarose gel electrophoresis and agarose gel electrophoresis of Pin2 SDS-resistant aggregates

Twenty OD₆₀₀ of $\Delta pin2$, $\Delta pin2 \Delta chs5$ or $\Delta pin2 \Delta end3$ cells transformed with p426GPDleu2d plasmids overexpressing *PIN2* wild type or mutant variants were harvested per strain. Cells were washed with water and resuspended in 200 μ l extract buffer with pepstatin, leupeptin, antipain and 1 mM PMSF. Cells were lysed by 10 min vortexing at 4°C with 120 μ l of glass beads. Lysates were cleared by gentle centrifugation (500 \times g for 1 min at 4°C) and Pin2 was extracted from membranes by addition of 1 % Tween 20 and 3 min incubation at RT. Extracts were then centrifuged 5 min 10,000 \times g. Protein concentrations were determined by BCA assay and adjusted. Lysates were resuspended in TBXG buffer for Blue Native gel electrophoresis or incubated for 5 min at RT in 0.4% SDS sample buffer for analysis of Pin2 SDS-resistant aggregates. Fifty – 100 μ g of protein was loaded per lane.

<u>Extract buffer</u>	<u>2x 0.4% SDS sample buffer</u>	<u>2x TBXG</u>
20 mM HEPES pH 6.8	50 mM Tris	100 mM Tricine
150 mM NaAc	400 mM glycine	30 mM Bistris
5 mM Mg(Ac) ₂	0.8 % SDS	30 % glycerol
	10 % glycerol	0.2 % Triton X-100
	Bromophenol blue	pH 7.0

10.5.11 Blue native vertical agarose gel electrophoresis

Agarose gels were poured in a vertical system with 16.5 x 13.5 cm plates. Casting was performed according to a previously published protocol (Warren et al., 2003). Briefly, the bottom of the gel was sealed with 1.2 ml of polyacrylamide plug. The plates, pipettes and combs were preheated for at least 30 min at 60°C. Three hundred mg of Seakem Gold agarose (Lonza) (1% total) was melted with 15 ml 50 % glycerol and 5 ml double distilled water. Ten ml 3x SGB buffer was added to the melted agarose under constant mixing. The agarose was poured and the combs were inserted at 1 cm depth maximum. The gels were allowed to set at RT. Before running the wells were thoroughly washed with cathode buffer. Gels were run using a blue native system (Schägger and von Jagow, 1991) with cathode and anode buffer at 8 mA constant current for 6 h.

3x SGB

1.5 M 6-aminocaproic acid
150 mM BisTris-Cl pH 7.0
0.015% Triton X-100

AB-Mix

48 g acrylamide
1.5 mg bisacrylamide
100 ml H₂O

Polyacrylamide plug

400 µl AB-Mix
400 µl 3x SGB
400 µl H₂O
20 µl APS
2 µl TEMED

1000x Blue G

500 mg Brilliant Blue G250

10 ml Tricine/BisTris buffer

Cathode buffer

Tricine/BisTris buffer
0.1 % 1000x Blue G
0.1 % Cysteine-HCl

Anode buffer

50 mM BisTris pH 7.0

20x Tricine/BisTris buffer

1 M Tricine
300 mM BisTris pH 7.0
pH 7.0

10.5.12 Protein agarose vertical gel electrophoresis of Pin2 SDS-resistant aggregates

Agarose gels for gel electrophoresis with SDS were poured as blue native agarose gels. Four hundred fifty mg Seakem Gold agarose (Lonza) (1.5 % final) was melted with 18 ml 50 % glycerol, 9 ml double distilled water and 3 ml 10x Tris/glycine buffer and 150 µl 20 % SDS was added to the constantly stirring agarose. Gels were run in running buffer at 6mA constant current for 4 h.

10x Tris/glycine buffer

250 mM Tris
2 M glycine

Running buffer

Tris/glycine buffer
0.1 % SDS

Polyacrylamide plug

400 µl AB-Mix
120 µl 10x Tris/glycine buffer
680 µl H₂O
20 µl APS
2 µl TEMED

10.5.13 Standard immunoblotting

Proteins were transferred onto nitrocellulose using a semidry transfer system with the following settings: 120 mA per minigel, 45 min transfer standard time and 50 – 55 min transfer for high molecular weight proteins above 100 kDa. The nitrocellulose was briefly stained with Ponceau S, rinsed with water to remove background staining and scanned. The membranes were destained by 5 min incubation with TBST. The blots were blocked for approximately 1 hr with 5 % non-fat milk in TBS, 0.02% NaN₃. The proteins and epitope tags were decorated with primary antibodies for 1-2 h at RT or at 4°C overnight. Primary

antibodies were diluted in 3 % BSA, TBST, 0.02 % NaN₃ solution or 5 % non-fat milk, TBS, 0.02 % NaN₃. Antibodies used in the study are listed in the table below:

Antibody	Type	Dilution for WB	Source
Anti-myc 9E10	Monoclonal	1: 2,500	Sigma
Anti-HA 11 clone 16B2	Monoclonal	1: 1,000	Eurogentec
Anti-Chs5	Rabbit, affinity purified	1: 500	Trautwein et al., 2006
Anti-GST-Pin2(72-282)	Rabbit serum	1: 2,000	This study
Anti-GFP	Rabbit, affinity purified	1: 5,000	Torrey Pines, Biolabs, Secaucus, NJ
Anti-GFP 7.1 & 13.1	Monoclonal	1: 500	Roche
Anti-Pgk1	Monoclonal	1: 1,000	Invitrogen A-6457
Anti-Chs3	Rabbit, affinity purified	1: 1,000	Gift from S. Munro, MRC Laboratory of Molecular Biology, Cambridge
Anti-Anp1	Rabbit serum	1: 1,000	
Anti-Sec61	Rabbit serum	1: 10,000	Gift from M. Spiess, Biozentrum, Basel
Anti-AU5	Rabbit, affinity purified	1: 1,000	Abcam, Cambridge, MA
Goat-anti-mouse HRP	Secondary Ab	1: 15,000	Pierce
Goat-anti-rabbit-HRP	Secondary Ab	1: 15,000	Pierce
Trueblot anti-rabbit-HRP	Secondary Ab	1:2,000	eBioscience
Trueblot anti-mouse-HRP	Secondary Ab	1:2,000	eBioscience

After incubation with primary antibodies, the blots were washed 6 x 5 min in TBST. The nitrocellulose membranes were then incubated with secondary antibodies: goat-anti-mouse-HRP and goat-anti-rabbit-HRP, diluted 1:15,000 in 5 % non-fat milk, TBST for 1-2 h. The blots were washed 6 x 5 min in TBST and developed with ECL (Amersham Bioscience) according to manufacturer's recommendation.

10.5.14 Non-standard immunoblot detection

10.5.14.1 Detection of Anp1

For detection of the Anp1 protein the nitrocellulose membranes were blocked after transfer with 2 % ECL Advanced Block (Amersham Bioscience), TBST, dissolved for at least 40 min with constant stirring. The anti-Anp1 antibody was diluted in 5 % non-fat milk, TBS, 0.02 % NaN₃, 10 % yeast extract from $\Delta anp1$ yeast cells. Blots were developed with ECL Prime (Amersham, Bioscience).

10.5.14.2 Protein detection after crosslinker immunoprecipitation

Membranes for detection of Chs3-2GFP were blotted with anti-GFP (1: 5,000, Torrey Pines) primary antibody and Trueblot anti-rabbit-HRP (1: 2,000, 5 % non-fat milk, TBST) secondary antibody. Membranes for detection of Chs6-9myc were blocked with 2 % ECL Advanced Block, TBST, decorated with anti-myc 9E10 (1:2,500) primary antibody and Trueblot anti-mouse-HRP (5 % non-fat milk, TBST) secondary antibody. Membranes for Chs6-9myc detection were developed with ECL Prime (Amersham, Bioscience).

10.5.14.3 Transfer and immunoblotting of proteins run on agarose gels

Proteins from agarose gels were transferred using a semi-dry transfer system for 2 h at 20 V constant voltage at 4°C. Standard Towbin buffer (25 mM Tris, 200 mM glycine, 0.1 % SDS) was used and the transfer was carried out with six Whatmann papers above and below the nitrocellulose membrane. The membranes were blocked for 2 h at 37°C in Blotto (5% non-fat milk, 5 % egg albumin, TBST, NaN₃). Pin2 was decorated by overnight incubation with anti-Pin2 antibody (1:2,000, Blotto). The membranes were then washed 2x 10 min Blotto, 4x 10 min TBST and incubated for 2 h in goat-anti-rabbit-HRP secondary antibody (1:15 000 in Blotto without NaN₃). The blots were washed 2x 10 min with Blotto (without NaN₃), 2x 10 min TBST and 2x 10 min TBS and developed with standard ECL solutions (Amersham Bioscience).

10.6 Molecular biology techniques

Standard techniques for nucleic acid manipulations were used throughout in this study (Sambrook et al., 1989).

10.6.1 Plasmids

For expression of GST tagged full-length cytosolic domains of Pin2 and Skg6 restriction fragments encoding aa 72-282 of Pin2 and aa 98-734 of Skg6 were cloned into pGEX-6P-1 (GE Healthcare) using *Bam*HI and *Eco*RI restriction sites. *Bam*HI and *Xho*I restriction fragments encoding aa: 72-152, 72-210, 153-282 of Pin2 were cloned into pGEX6P-1 to obtain GST-tagged Pin2 cytosolic truncations. For GFP-tagged Pin2 constructs *Eco*RI-*Sph*I restriction fragments containing the *PIN2 promoter* (600bp upstream of the start codon) and *PIN2 ORF* encoding aa: 1-282 (full length), 1-152, 1-179, 1-210 or 1-245 of Pin2 were cloned

into pGFP33 (YCPlac33 with inserted *GFP-CYC1* terminator *SphI-HindIII* restriction fragment). To create pGFP33 pin2Δ79-152 a long template PCR approach was applied, in which the entire plasmid containing a *PIN2 promoter – PIN2 ORF* insert was amplified excluding the region encoding aa 79-152 and religated through a *NheI* restriction site added on the 5' ends of the primers. For overexpression of *PIN2*, the *PIN2 ORF* was cloned into p426GPD plasmid using *EcoRI/BamHI* restriction sites or *BamHI/EcoRI* restriction sites for the *pin2(1-210)* truncation. To obtain high copy number plasmids an *EagI* restriction fragment containing the *leu2-d* allele (amplified from pHR81 plasmid, Nehlin et al., 1989) was cloned into the p426GPD plasmids. To create the Mid2(N+TMD)-Pin2(C) chimera *SacI* and *PstI* restriction sites were inserted into pGFP33 *PIN2*, before the start codon and between codons 71 and 72 of the *PIN2 ORF*, respectively. The created *SacI-PstI* restriction fragment encoding the Pin2 luminal and TMD domain was excised and replaced by the corresponding domains of Mid2 – *ORF* encoding aa 1-250.

10.6.2 Site-directed Mutagenesis

The Stratagene Site Directed Mutagenesis Kit protocol was used with modifications for the Pfu Turbo Cx enzyme. Briefly, two complementary primers were designed containing 11-15 bases upstream and downstream of the mutation site and ending optimally with two (or at least one) G/Cs at the 3' end. The following PCR and cycling was used:

<u>PCR Mix</u>	<u>Cycles</u>	
1 µl template (0.1× diluted miniprep)	2 min 95°C	
125 ng parallel primer	30 sec 95°C	12× for single nucleotide change 16× for single aa change 18× for several aa change
125 ng antiparallel primer	1 min 55°C	
2.5 µl 2mM dNTPs	X min 72°C*	
5 µl Pfu Cx buffer	10 min 72°C	
1 µl Pfu Cx		
Fill up to 50 µl with ddH ₂ O		
* X = 2min/1kb		

To calculate the volume of 10 µM primers the following formula was used:

$$\mu\text{l primer} = (125\text{ng oligo}) / (330 \times \text{no. of bases in oligo}) \times 100$$

50 µl of PCR product was digested for 1hr at 37°C with 1 µl DpnI. 1 µl of digested product was transformed into 100 µl of XL-1 Blue chemically competent cells. If no colonies appeared after transformation the PCR reaction was repeated with a lower annealing temperature – 51-52°C.

10.6.3 Chromosomal manipulation of yeast DNA

To delete or manipulate genes in yeast cells, established methods were followed (Güldener *et al.*, 1996; Knop *et al.*, 1999; De Antoni and Gallwitz, 2000; Gueldener *et al.*, 2002). Briefly, PCR was performed on template plasmids with primers having 45 bp 5'-overhangs homologous to the desired target site in the yeast genome. The PCR-product was transformed directly into yeast cells without further purification. Cells were selected for with the corresponding auxotrophy/resistance markers. Correct integrations were confirmed by analytical colony PCR. Wherever possible, the expression was checked by immunoblotting of total yeast lysates.

10.6.4 Yeast transformation

Yeast cells were transformed by a high-efficiency lithium acetate transformation method (Gietz *et al.*, 1995). Cells were grown in 50 ml liquid culture to an OD₆₀₀ 0.1 - 0.15. The cells were harvested and incubated for 5-15 min at 30°C in 100 mM LiAc. Subsequently, they were resuspended in 360 µl transformation mix and mixed thoroughly for 1 min. One yeast culture described above was generally divided into 4-6 aliquots for different transformations. A heat-shock was employed for 40 min at 42°C, after which the cells were pelleted for 30 sec at 3,000 × g. The cell pellet was resuspended in sterile water and spread on appropriate selection plates. In case a G418 or ClonNAT resistance cassette was transformed, cells were first incubated in YPD for 3 h at 30°C before plating on YPD-G418 or YPD-CloNat plates. Colonies usually appeared after 2 – 3 days and were singled out and tested by analytical PCR.

Transformation mix

240 µl 50% (w/v) PEG

36 µl 1 M LiAc

50 µl 2 mg/ml single-stranded salmon sperm DNA

(obtained by heating for 5 min at 95°C and fast cooling on ice)

10 µl of PCR product, 2 µl plasmid DNA (0.1× diluted miniprep), for double plasmid transformations: 5 µl of each plasmid DNA (0.1× diluted miniprep)

ddH₂O ad 360 µl

10.6.5 Analytical PCR of yeast colonies

Analytical PCR of yeast colonies was performed to confirm chromosomal manipulations of yeast cells. The primers were chosen in a way that the resulting PCR product indicated a successful manipulation either through its presence or size. Single colonies were picked with a pipette tip and incubated in 3 μ l 20 mM NaOH at 100°C for 10 min, then the PCR reaction mix was added. A typical reaction contained 16.4 μ l ddH₂O, 2.5 μ l 10x reaction buffer, 2.5 μ l 2 mM dNTPs, 2.5 μ l MgCl₂, 2x 0.5 μ l 10 μ M oligonucleotide primer, 0.1 μ l FirePol DNA-polymerase (Solis BioDyne). The annealing temperature was adjusted to 1-2°C below the melting temperature of the primers, the elongation time was 1 min per kb of expected product, and 40 cycles were used for amplification. Routinely, 15 μ l of the reaction were analyzed by agarose gel electrophoresis.

10.6.6 Drop assays

Strains were grown overnight, diluted and grown to logarithmic phase (OD₆₀₀ 0.2 - 0.5). After adjusting to equal cell concentrations (OD₆₀₀ between 0.1 and 0.2), four serial dilutions (1:10) were dropped onto different plates using a “frogger” stamp (custom-built). The plates were incubated for 2 – 9 days at 30°C unless indicated otherwise, and photographed for documentation.

10.6.7 Live fluorescence microscopy

Cells were grown overnight in YPD medium or HC selective medium for plasmid selection. The cultures were diluted in the morning and grown for an additional three generations to OD₆₀₀ between 0.2 - 0.7. Cultures contained 50 mg/l adenine to suppress cellular autofluorescence. An aliquot of cells was harvested by spinning at RT for 30 sec. Cells were briefly washed in HC complete medium, resuspended in a small volume of 20-50 μ l and visualized directly under a Zeiss Axioplan 2 epifluorescence microscope using filters for GFP and dsRed. Pictures were taken using an Axiocam MRm CCD camera and Axiovision software. Image processing was performed using ImageJ and Adobe Photoshop. All pictures from the same experiment were treated equally. Per strain, a minimum of one hundred cells from at least three independent experiments was counted when quantification was required.

10.6.8 [*PSI+*] induction assay

[*PSI+*] induction assay was carried out as described previously (Derkatch et al., 2001). Briefly, the [*PIN+*][*psi-*] 74-D694 strains was cured by patching cells on YPD medium supplemented with 5 mM GuHCl and incubating them for 2 days at 30°C. This was repeated two additional times. [*pin-*][*psi-*] 74-D694 wild type or *chs5Δ::KanMX4* strain was transformed with pSUP35NM::GFP-HIS3 and *PIN2* wild type or mutant variant overexpressing p426GPDleu2d plasmids. *PIN2* was overexpressed by replica plating transformants for 35 generations on HC –leu– ura –his medium, which allowed the p426GPD leu2d plasmids to be amplified to approximately 100 copies per cell. The number of generations was determined by counting number of cells from a colony patch directly after replica plating and after three days growth. The patches were excised with agar and vortexed for 3 min in 100 μl to 1 ml ddH₂O. Five μl of water with resuspended cells was transferred into Neubauer chamber for counting. After overexpression of the *PIN2* constructs, transformants were then replica plated onto HC –his +Cu²⁺ medium to induce SUP35NM::GFP and allow [*PSI+*] formation. Transformants were checked for the presence of SUP35NM::GFP dot and ring-like structure by fluorescence microscopy. Two random colonies from each strain from HC –his +Cu²⁺ plates were streaked out onto HC –ade medium and grown at 23°C for 9 to 12 days to confirm [*PSI+*] induction.

10.7 Formulas and web resources

10.7.1 Determination of protein secondary structure and transmembrane domains

For creation of truncations protein secondary structure was determined using the Jpred3 server (<http://www.compbio.dundee.ac.uk/www-jpred/>) (Cole *et al.*, 2008). The HMMTOP server (<http://www.enzim.hu/hmmtop/index.php>) was used for prediction of transmembrane helices.

10.7.2 Retrieval of annotated data on genes and proteins

Information on protein function, abundance, localization and topology was usually obtained from the Saccharomyces Genome Database (www.yeastgenome.org) or from Biobase Biological Databases

(https://portal.biobase-international.com/cgi-bin/build_ghpywl/idb/1.0/searchengine/start.cgi).

10.7.3 Determination of yeast generation times

The following formula was used to determine the generation time of a yeast strain under defined conditions:

$$t_g = T \times \log_2 / \log \left[\left(\frac{OD_2}{OD_1} \right) \right]$$

tg: generation time

T: time of logarithmic growth

OD1: OD₆₀₀ value at the beginning of the growth phase

OD2: OD₆₀₀ value at the end of the growth phase

(Note that the formula can only be used for logarithmically growing cells.)

10.8 Abbreviations

aa	amino acid
Ac	acetate
AP	adaptor protein
ARF1	ADP ribosylation factor 1
ATP	adenosine-5'-triphosphate
bp	base pair
BSA	bovine serum albumin
CARTS	CARriers of the TGN to the cell Surface
CCV	clathrin-coated vesicle
ChAPS	Chs5p-Arf1p-binding proteins
CFW	calcofluor white
CME	clathrin-mediated endocytosis
COPI	coat protein complex I
COPII	coat protein complex II
CWI	cell wall integrity
DAG	diacylglycerol
ddH ₂ O	water bidest.
DMP	dimenthylpimelimidate
DMSO	dimethylsulfoxide
DNA	desoxyribonucleic acid
DNase	DNA-hydrolyzing enzyme
dNTPs	desoxynucleotide triphosphates
dsRed	drFP583 red fluorescent protein (from <i>Discosoma</i> species)
DTT	dithiothreitol
DSP	Dithiobis(succinimidylpropionate)
<i>E. coli</i>	<i>Escherichia coli</i>
ECL	enhanced chemoluminescence
EDTA	ethylenediaminetetraacetic acid
EGFP	enhanced GFP
eqFP611	<i>Entacmaea quadricolor</i> fluorescent protein, emission maximum at 611 nm
ER	endoplasmic reticulum
EtOH	ethanol
g	gravitational acceleration constant (also: gram)
G418R	resistance to G418 (geneticin)
GAP	GTPase-activating protein

Appendix – Abbreviations

GDP	guanosin-5'-diphosphate
GEF	guanine nucleotide exchange factor
GFP	green fluorescent protein
GGA	Golgi-localized, γ -ear containing, ARF-binding
GPI	glycosylphosphatidylinositol
GST	glutathion-S-transferase
GTP	guanosine-5'-triphosphate
GTPase	GTP hydrolyzing enzyme
h	hours
HEPES	N-(2-hydroxyethyl)piperazine-N'-(2-ethanesulfonic acid)
HRP	horseradish peroxidase
IP	immunoprecipitation
K. lactis	Kluyveromyces lactis
kb	kilobase
LB	lysogeny broth
min	minutes
mRNA	messenger RNA
MVB	multivesicular body
MW	molecular weight
n.d.	not determined
O/N	over night
OD ₆₀₀	optical density at 600 nm
PAGE	polyacrylamide gel electrophoresis
PAUF	pancreatic adenocarcinoma upregulated factor
PBS	phosphate-buffered saline
PCR	polymerase chain reaction
[PIN+]	Psi-INducibility
PEG	polyethylene glycol
PM	plasma membrane
PMSF	sphenylmethylsulfonylfluoride
PVC	prevacuolar compartment
RNA	ribonucleic acid
rpm	revolutions per minute
RT	room temperature
S. cerevisiae	Saccharomyces cerevisiae
SDS	sodium dodecyl sulfate
sec	seconds
SNARE	SNAP (Soluble NSF Attachment Protein) REceptor
TBS	Tris-buffered saline

TEA	triethanolamine
TGN	trans-Golgi network
TMD	transmembrane domain
TPR	tetratricopeptide repeat
Tris	tris(hydroxymethylaminomethane)
ts	temperature-sensitive
w/o	without
w/v	weight per volume
w/w	weight per weight
WT	wild-type
yeGFP	yeast codon-optimized GFP
YNB	yeast nitrogen base

10.9 References

Acconcia, F., Sigismund, S., and Polo, S. (2009). Ubiquitin in trafficking: the network at work. *Exp. Cell Res.* *315*, 1610–1618.

Adams, A. E., and Pringle, J. R. (1984). Relationship of actin and tubulin distribution to bud growth in wild-type and morphogenetic-mutant *Saccharomyces cerevisiae*. *The Journal of Cell Biology* *98*, 934–945.

Adda, C. G. *et al.* (2009). Plasmodium falciparum merozoite surface protein 2 is unstructured and forms amyloid-like fibrils. *Mol. Biochem. Parasitol.* *166*, 159–171.

Ahn, S. H., Tobe, B. T., Fitz Gerald, J. N., Anderson, S. L., Acurio, A., and Kron, S. J. (2001). Enhanced cell polarity in mutants of the budding yeast cyclin-dependent kinase Cdc28p. *Molecular Biology of the Cell* *12*, 3589–3600.

Aicart-Ramos, C., Valero, R. A., and Rodriguez-Crespo, I. (2011). Protein palmitoylation and subcellular trafficking. *BBA - Biomembranes* *1808*, 2981–2994.

Alberti, S., Halfmann, R., King, O., Kapila, A., and Lindquist, S. (2009). A Systematic Survey Identifies Prions and Illuminates Sequence Features of Prionogenic Proteins. *Cell* *137*, 146–158.

Alvarez, E., Gironès, N., and Davis, R. J. (1990). Inhibition of the receptor-mediated endocytosis of diferric transferrin is associated with the covalent modification of the transferrin receptor with palmitic acid. *J. Biol. Chem.* *265*, 16644–16655.

Amor, J. C., Harrison, D. H., Kahn, R. A., and Ringe, D. (1994). Structure of the human ADP-ribosylation factor 1 complexed with GDP. *Nature* *372*, 704–708.

Andag, U., Neumann, T., and Schmitt, H. D. (2001). The coatamer-interacting protein Dsl1p is required for Golgi-to-endoplasmic reticulum retrieval in yeast. *J. Biol. Chem.* *276*, 39150–39160.

Andreini, C., Bertini, I., Cavallaro, G., Holliday, G. L., and Thornton, J. M. (2008). Metal ions in biological catalysis: from enzyme databases to general principles. *J. Biol. Inorg. Chem.* *13*, 1205–1218.

Ang, S. F., and Fölsch, H. (2012). The role of secretory and endocytic pathways in the maintenance of cell polarity. *Essays Biochem.* *53*, 29–39.

Anitei, M., and Hoflack, B. (2011). Exit from the trans-Golgi network: from molecules to mechanisms. *Current Opinion in Cell Biology* *23*, 443–451.

Appenzeller-Herzog, C. (2006). The ER-Golgi intermediate compartment (ERGIC): in search of its identity and function. *Journal of Cell Science* *119*, 2173–2183.

Bagnat, M., and Simons, K. (2002). Cell surface polarization during yeast mating. *Proc. Natl. Acad. Sci. U.S.A.* *99*, 14183–14188.

Bard, F. *et al.* (2006). Functional genomics reveals genes involved in protein secretion and Golgi organization. *Nature* *439*, 604–607.

- Bard, F., and Malhotra, V. (2006). The Formation of TGN-to-Plasma-Membrane Transport Carriers. *Annu. Rev. Cell Dev. Biol.* *22*, 439–455.
- Barfield, R. M., Fromme, J. C., and Schekman, R. (2009). The exomer coat complex transports Fus1p to the plasma membrane via a novel plasma membrane sorting signal in yeast. *Molecular Biology of the Cell* *20*, 4985–4996.
- Barlowe, C. (1997). Coupled ER to Golgi transport reconstituted with purified cytosolic proteins. *The Journal of Cell Biology* *139*, 1097–1108.
- Barlowe, C., Orci, L., Yeung, T., Hosobuchi, M., Hamamoto, S., Salama, N., Rexach, M. F., Ravazzola, M., Amherdt, M., and Schekman, R. (1994). COPII: a membrane coat formed by Sec proteins that drive vesicle budding from the endoplasmic reticulum. *Cell* *77*, 895–907.
- Barral, Y., Mermall, V., Mooseker, M. S., and Snyder, M. (2000). Compartmentalization of the cell cortex by septins is required for maintenance of cell polarity in yeast. *Mol. Cell* *5*, 841–851.
- Behnia, R., and Munro, S. (2005). Organelle identity and the signposts for membrane traffic. *Nature Publishing Group* *438*, 597–604.
- Berson, J. F., Theos, A. C., Harper, D. C., Tenza, D., Raposo, G., and Marks, M. S. (2003). Proprotein convertase cleavage liberates a fibrillogenic fragment of a resident glycoprotein to initiate melanosome biogenesis. *The Journal of Cell Biology* *161*, 521–533.
- Bethani, I., Lang, T., Geumann, U., Sieber, J. J., Jahn, R., and Rizzoli, S. O. (2007). The specificity of SNARE pairing in biological membranes is mediated by both proof-reading and spatial segregation. *The EMBO Journal* *26*, 3981–3992.
- Bi, E., and Park, H. O. (2012). Cell Polarization and Cytokinesis in Budding Yeast. *Genetics* *191*, 347–387.
- Bilodeau, P. S., Winistorfer, S. C., Allaman, M. M., Surendhran, K., Kearney, W. R., Robertson, A. D., and Piper, R. C. (2004). The GAT domains of clathrin-associated GGA proteins have two ubiquitin binding motifs. *J. Biol. Chem.* *279*, 54808–54816.
- Blanpain, C. (2001). Palmitoylation of CCR5 Is Critical for Receptor Trafficking and Efficient Activation of Intracellular Signaling Pathways. *Journal of Biological Chemistry* *276*, 23795–23804.
- Bock, J. B., Matern, H. T., Peden, A. A., and Scheller, R. H. (2001). A genomic perspective on membrane compartment organization. *Nature* *409*, 839–841.
- Bodenmiller, B. *et al.* (2007). PhosphoPep--a phosphoproteome resource for systems biology research in *Drosophila* Kc167 cells. *Mol. Syst. Biol.* *3*, 139.
- Boehm, M., and Bonifacino, J. S. (2001). Adaptins: the final recount. *Molecular Biology of the Cell* *12*, 2907–2920.
- Boevink, P., Oparka, K., Santa Cruz, S., Martin, B., Betteridge, A., and Hawes, C. (1998). Stacks on tracks: the plant Golgi apparatus traffics on an actin/ER network. *Plant J.* *15*, 441–447.

- Bonifacino, J. S., and Glick, B. S. (2004). The mechanisms of vesicle budding and fusion. *Cell* *116*, 153–166.
- Bonifacino, J. S., and Rojas, R. (2006). Retrograde transport from endosomes to the trans-Golgi network. *Nat Rev Mol Cell Biol* *7*, 568–579.
- Boutté, Y., Jonsson, K., McFarlane, H. E., Johnson, E., Gendre, D., Swarup, R., Friml, J., Samuels, L., Robert, S., and Bhalerao, R. P. (2013). ECHIDNA-mediated post-Golgi trafficking of auxin carriers for differential cell elongation. *Proc. Natl. Acad. Sci. U.S.A.* *110*, 16259–16264.
- Bowers, K., Piper, S. C., Edeling, M. A., Gray, S. R., Owen, D. J., Lehner, P. J., and Luzio, J. P. (2006). Degradation of endocytosed epidermal growth factor and virally ubiquitinated major histocompatibility complex class I is independent of mammalian ESCRTII. *J. Biol. Chem.* *281*, 5094–5105.
- Boyd, C. (2004). Vesicles carry most exocyst subunits to exocytic sites marked by the remaining two subunits, Sec3p and Exo70p. *The Journal of Cell Biology* *167*, 889–901.
- Braakman, I., and Bulleid, N. J. (2011). Protein Folding and Modification in the Mammalian Endoplasmic Reticulum. *Annu. Rev. Biochem.* *80*, 71–99.
- Bremser, M., Nickel, W., Schweikert, M., Ravazzola, M., Amherdt, M., Hughes, C. A., Söllner, T. H., Rothman, J. E., and Wieland, F. T. (1999). Coupling of coat assembly and vesicle budding to packaging of putative cargo receptors. *Cell* *96*, 495–506.
- Bregues, M., Teixeira, D., and Parker, R. (2005). Movement of eukaryotic mRNAs between polysomes and cytoplasmic processing bodies. *Science* *310*, 486–489.
- Brown, F. C., and Pfeffer, S. R. (2010). An update on transport vesicle tethering. *Mol Membr Biol* *27*, 457–461.
- Brown, H. A., Gutowski, S., Moomaw, C. R., Slaughter, C., and Sternweis, P. C. (1993). ADP-ribosylation factor, a small GTP-dependent regulatory protein, stimulates phospholipase D activity. *Cell* *75*, 1137–1144.
- Buttery, S. M., Kono, K., Stokasimov, E., and Pellman, D. (2012). Regulation of the formin Bnr1 by septins and a MARK/Par1-family septin-associated kinase. *Molecular Biology of the Cell* *23*, 4041–4053.
- Cai, H., Yu, S., Menon, S., Cai, Y., Lazarova, D., Fu, C., Reinisch, K., Hay, J. C., and Ferro-Novick, S. (2007). TRAPPI tethers COPII vesicles by binding the coat subunit Sec23. *Nature* *445*, 941–944.
- Chanat, E., Weiss, U., Huttner, W. B., and Tooze, S. A. (1993). Reduction of the disulfide bond of chromogranin B (secretogranin I) in the trans-Golgi network causes its missorting to the constitutive secretory pathways. *The EMBO Journal* *12*, 2159–2168.
- Chavrier, P., Parton, R. G., Hauri, H. P., Simons, K., and Zerial, M. (1990). Localization of low molecular weight GTP binding proteins to exocytic and endocytic compartments. *Cell* *62*, 317–329.
- Chen, Y. A., and Scheller, R. H. (2001). SNARE-mediated membrane fusion. *Nat Rev Mol Cell Biol* *2*, 98–106.

- Chowdhury, S., Smith, K. W., and Gustin, M. C. (1992). Osmotic stress and the yeast cytoskeleton: phenotype-specific suppression of an actin mutation. *The Journal of Cell Biology* *118*, 561–571.
- Chuang, J. S., and Schekman, R. W. (1996). Differential trafficking and timed localization of two chitin synthase proteins, Chs2p and Chs3p. *The Journal of Cell Biology* *135*, 597–610.
- Clague, M. J., Liu, H., and Urbé, S. (2012). Governance of Endocytic Trafficking and Signaling by Reversible Ubiquitylation. *Developmental Cell* *23*, 457–467.
- Cole, C., Barber, J. D., and Barton, G. J. (2008). The Jpred 3 secondary structure prediction server. *Nucleic Acids Res.* *36*, W197–W201.
- Costanzo, M., and Zurzolo, C. (2013). The cell biology of prion-like spread of protein aggregates: mechanisms and implication in neurodegeneration. *Biochem. J.* *452*, 1–17.
- De Antoni, A., and Gallwitz, D. (2000). A novel multi-purpose cassette for repeated integrative epitope tagging of genes in *Saccharomyces cerevisiae*. *Gene* *246*, 179–185.
- De Matteis, M. A., and Luini, A. (2008). Exiting the Golgi complex. *Nat Rev Mol Cell Biol* *9*, 273–284.
- de Nobel, H., Ruiz, C., Martin, H., Morris, W., Brul, S., Molina, M., and Klis, F. M. (2000). Cell wall perturbation in yeast results in dual phosphorylation of the Slt2/Mpk1 MAP kinase and in an Slt2-mediated increase in FKS2-lacZ expression, glucanase resistance and thermotolerance. *Microbiology (Reading, Engl.)* *146 (Pt 9)*, 2121–2132.
- Decker, C. J., Teixeira, D., and Parker, R. (2007). Edc3p and a glutamine/asparagine-rich domain of Lsm4p function in processing body assembly in *Saccharomyces cerevisiae*. *The Journal of Cell Biology* *179*, 437–449.
- Delley, P. A., and Hall, M. N. (1999). Cell wall stress depolarizes cell growth via hyperactivation of RHO1. *The Journal of Cell Biology* *147*, 163–174.
- DeMarini, D. J., Adams, A. E., Fares, H., De Virgilio, C., Valle, G., Chuang, J. S., and Pringle, J. R. (1997). A septin-based hierarchy of proteins required for localized deposition of chitin in the *Saccharomyces cerevisiae* cell wall. *The Journal of Cell Biology* *139*, 75–93.
- Derkatch, I. L., Bradley, M. E., Hong, J. Y., and Liebman, S. W. (2001). Prions affect the appearance of other prions: the story of [PIN(+)]. *Cell* *106*, 171–182.
- Derkatch, I. L., Bradley, M. E., Zhou, P., Chernoff, Y. O., and Liebman, S. W. (1997). Genetic and environmental factors affecting the de novo appearance of the [PSI⁺] prion in *Saccharomyces cerevisiae*. *Genetics* *147*, 507–519.
- Derkatch, I. L., Chernoff, Y. O., Kushnirov, V. V., Inge-Vechtormov, S. G., and Liebman, S. W. (1996). Genesis and variability of [PSI] prion factors in *Saccharomyces cerevisiae*. *Genetics* *144*, 1375–1386.
- Dettmer, J., Hong-Hermesdorf, A., Stierhof, Y.-D., and Schumacher, K. (2006). Vacuolar H⁺-ATPase activity is required for endocytic and secretory trafficking in *Arabidopsis*. *Plant Cell* *18*, 715–730.

- Di Paolo, G., and De Camilli, P. (2006). Phosphoinositides in cell regulation and membrane dynamics. *Nature* *443*, 651–657.
- Diekmann, Y., Seixas, E., Gouw, M., Tavares-Cadete, F., Seabra, M. C., and Pereira-Leal, J. B. (2011). Thousands of rab GTPases for the cell biologist. *PLoS Comput. Biol.* *7*, e1002217.
- Dierick, H. A., Adam, A. N., Escara-Wilke, J. F., and Glover, T. W. (1997). Immunocytochemical localization of the Menkes copper transport protein (ATP7A) to the trans-Golgi network. *Hum. Mol. Genet.* *6*, 409–416.
- Doyle, T., and Botstein, D. (1996). Movement of yeast cortical actin cytoskeleton visualized in vivo. *Proc. Natl. Acad. Sci. U.S.A.* *93*, 3886–3891.
- Drgonová, J., Drgon, T., Tanaka, K., Kollár, R., Chen, G. C., Ford, R. A., Chan, C. S., Takai, Y., and Cabib, E. (1996). Rho1p, a yeast protein at the interface between cell polarization and morphogenesis. *Science* *272*, 277–279.
- Drisdell, R. C., and Green, W. N. (2004). Labeling and quantifying sites of protein palmitoylation. *BioTechniques* *36*, 276–285.
- Egea, G., Lázaro-Diéguéz, F., and Vilella, M. (2006). Actin dynamics at the Golgi complex in mammalian cells. *Current Opinion in Cell Biology* *18*, 168–178.
- Eisenberg, S., Laude, A. J., Beckett, A. J., Mageean, C. J., Aran, V., Hernandez Valladares, M., Henis, Y. I., and Prior, I. A. (2013). The role of palmitoylation in regulating Ras localization and function. *Biochem. Soc. Trans.* *41*, 79–83.
- Elias, M., Brighouse, A., Gabernet-Castello, C., Field, M. C., and Dacks, J. B. (2012). Sculpting the endomembrane system in deep time: high resolution phylogenetics of Rab GTPases. *Journal of Cell Science* *125*, 2500–2508.
- Ellgaard, L., and Helenius, A. (2003). Quality control in the endoplasmic reticulum. *Nat Rev Mol Cell Biol* *4*, 181–191.
- Engqvist-Goldstein, Å. E. Y., and Drubin, D. G. (2003). A CTINA SSEMBLY ANDE NDOCYTOSIS: From Yeast to Mammals. *Annu. Rev. Cell Dev. Biol.* *19*, 287–332.
- Faini, M., Beck, R., Wieland, F. T., and Briggs, J. A. G. (2013). Vesicle coats: structure, function, and general principles of assembly. *Trends in Cell Biology* *23*, 279–288.
- Farkas, V., Kovarík, J., Kosinová, A., and Bauer, S. (1974). Autoradiographic study of mannan incorporation into the growing cell walls of *Saccharomyces cerevisiae*. *J. Bacteriol.* *117*, 265–269.
- Farquhar, M. G., and Palade, G. E. (1981). The Golgi apparatus (complex)-(1954-1981)-from artifact to center stage. *The Journal of Cell Biology* *91*, 77s–103s.
- Fasshauer, D., Bruns, D., Shen, B., Jahn, R., and Brunger, A. T. (1997). A structural change occurs upon binding of syntaxin to SNAP-25. *J. Biol. Chem.* *272*, 4582–4590.
- Ferrigno, P., Posas, F., Koepp, D., Saito, H., and Silver, P. A. (1998). Regulated nucleo/cytoplasmic exchange of HOG1 MAPK requires the importin beta homologs NMD5 and XPO1. *The EMBO Journal* *17*, 5606–5614.

- Finger, F. P., Hughes, T. E., and Novick, P. (1998). Sec3p is a spatial landmark for polarized secretion in budding yeast. *Cell* *92*, 559–571.
- Fowler, D. M., Koulov, A. V., Alory-Jost, C., Marks, M. S., Balch, W. E., and Kelly, J. W. (2006). Functional amyloid formation within mammalian tissue. *PLoS Biol.* *4*, e6.
- Frand, A. R., Cuzzo, J. W., and Kaiser, C. A. (2000). Pathways for protein disulphide bond formation. *Trends in Cell Biology* *10*, 203–210.
- Friml, J., Wiśniewska, J., Benková, E., Mendgen, K., and Palme, K. (2002). Lateral relocation of auxin efflux regulator PIN3 mediates tropism in Arabidopsis. *Nature* *415*, 806–809.
- Galan, J. M., Moreau, V., André, B., Volland, C., and Haguener-Tsapis, R. (1996). Ubiquitination mediated by the Npi1p/Rsp5p ubiquitin-protein ligase is required for endocytosis of the yeast uracil permease. *J. Biol. Chem.* *271*, 10946–10952.
- Gall, W. E., Geething, N. C., Hua, Z., Ingram, M. F., Liu, K., Chen, S. I., and Graham, T. R. (2002). Drs2p-dependent formation of exocytic clathrin-coated vesicles in vivo. *Curr Biol* *12*, 1623–1627.
- Gallusser, A., and Kirchhausen, T. (1993). The beta 1 and beta 2 subunits of the AP complexes are the clathrin coat assembly components. *The EMBO Journal* *12*, 5237–5244.
- García-Rodríguez, L. J., Trilla, J. A., Castro, C., Valdivieso, M. H., Durán, A., and Roncero, C. (2000). Characterization of the chitin biosynthesis process as a compensatory mechanism in the fks1 mutant of *Saccharomyces cerevisiae*. *FEBS Letters* *478*, 84–88.
- Geldner, N., Anders, N., Wolters, H., Keicher, J., Kornberger, W., Müller, P., Delbarre, A., Ueda, T., Nakano, A., and Jürgens, G. (2003). The Arabidopsis GNOM ARF-GEF mediates endosomal recycling, auxin transport, and auxin-dependent plant growth. *Cell* *112*, 219–230.
- Gietz, R. D., Schiestl, R. H., Willems, A. R., and Woods, R. A. (1995). Studies on the transformation of intact yeast cells by the LiAc/SS-DNA/PEG procedure. *Yeast* *11*, 355–360.
- Gilks, N., Kedersha, N., Ayodele, M., Shen, L., Stoecklin, G., Dember, L. M., and Anderson, P. (2004). Stress granule assembly is mediated by prion-like aggregation of TIA-1. *Molecular Biology of the Cell* *15*, 5383–5398.
- Gillingham, A. K. (2004). The GTPase Arf1p and the ER to Golgi cargo receptor Erv14p cooperate to recruit the golgin Rud3p to the cis-Golgi. *The Journal of Cell Biology* *167*, 281–292.
- Glombik, M. M., Krömer, A., Salm, T., Huttner, W. B., and Gerdes, H. H. (1999). The disulfide-bonded loop of chromogranin B mediates membrane binding and directs sorting from the trans-Golgi network to secretory granules. *The EMBO Journal* *18*, 1059–1070.
- Goldberg, J. (1998). Structural basis for activation of ARF GTPase: mechanisms of guanine nucleotide exchange and GTP-myristoyl switching. *Cell* *95*, 237–248.
- Goodwin, J. S., Drake, K. R., Rogers, C., Wright, L., Lippincott-Schwartz, J., Philips, M. R., and Kenworthy, A. K. (2005). Depalmitoylated Ras traffics to and from the Golgi complex via a nonvesicular pathway. *The Journal of Cell Biology* *170*, 261–272.

- Grant, B. D., and Donaldson, J. G. (2009). Pathways and mechanisms of endocytic recycling. *Nat Rev Mol Cell Biol* 10, 597–608.
- Gravotta, D., Carvajal-Gonzalez, J. M., Mattera, R., Deborde, S., Banfelder, J. R., Bonifacino, J. S., and Rodriguez-Boulan, E. (2012). The Clathrin Adaptor AP-1A Mediates Basolateral Polarity. *Developmental Cell* 22, 811–823.
- Greaves, J., and Chamberlain, L. H. (2011). Differential palmitoylation regulates intracellular patterning of SNAP25. *Journal of Cell Science* 124, 1351–1360.
- Griffiths, G., and Simons, K. (1986). The trans Golgi network: sorting at the exit site of the Golgi complex. *Science* 234, 438–443.
- Groffen, J., Heisterkamp, N., Reynolds, F. H., and Stephenson, J. R. (1983). Homology between phosphotyrosine acceptor site of human c-abl and viral oncogene products. *Nature* 304, 167–169.
- Gueldener, U., Heinisch, J., Koehler, G. J., Voss, D., and Hegemann, J. H. (2002). A second set of loxP marker cassettes for Cre-mediated multiple gene knockouts in budding yeast. *Nucleic Acids Res.* 30, e23.
- Guo, W., Tamanoi, F., and Novick, P. (2001). Spatial regulation of the exocyst complex by Rho1 GTPase. *Nat Cell Biol* 3, 353–360.
- Güldener, U., Heck, S., Fielder, T., Beinhauer, J., and Hegemann, J. H. (1996). A new efficient gene disruption cassette for repeated use in budding yeast. *Nucleic Acids Res.* 24, 2519–2524.
- Haglund, K., and Dikic, I. (2012). The role of ubiquitylation in receptor endocytosis and endosomal sorting. *Journal of Cell Science* 125, 265–275.
- Halfmann, R., Alberti, S., Krishnan, R., Lyle, N., O'Donnell, C. W., King, O. D., Berger, B., Pappu, R. V., and Lindquist, S. (2011). Opposing effects of glutamine and asparagine govern prion formation by intrinsically disordered proteins. *Mol. Cell* 43, 72–84.
- Hanson, P. I., Roth, R., Morisaki, H., Jahn, R., and Heuser, J. E. (1997). Structure and conformational changes in NSF and its membrane receptor complexes visualized by quick-freeze/deep-etch electron microscopy. *Cell* 90, 523–535.
- Harrison, P. M., and Gerstein, M. (2003). A method to assess compositional bias in biological sequences and its application to prion-like glutamine/asparagine-rich domains in eukaryotic proteomes. *Genome Biol.* 4, R40.
- Harsay, E. (2002). A subset of yeast vacuolar protein sorting mutants is blocked in one branch of the exocytic pathway. *The Journal of Cell Biology* 156, 271–286.
- Harsay, E., and Bretscher, A. (1995). Parallel secretory pathways to the cell surface in yeast. *The Journal of Cell Biology* 131, 297–310.
- He, B., Xi, F., Zhang, J., TerBush, D., Zhang, X., and Guo, W. (2007). Exo70p mediates the secretion of specific exocytic vesicles at early stages of the cell cycle for polarized cell growth. *The Journal of Cell Biology* 176, 771–777.

- Hehnly, H., and Stamnes, M. (2007). Regulating cytoskeleton-based vesicle motility. *FEBS Letters* *581*, 2112–2118.
- Hein, C., Springael, J. Y., Volland, C., Haguenaer-Tsapis, R., and André, B. (1995). NPI1, an essential yeast gene involved in induced degradation of Gap1 and Fur4 permeases, encodes the Rsp5 ubiquitin-protein ligase. *Mol. Microbiol.* *18*, 77–87.
- Heldwein, E. E., Macia, E., Wang, J., Yin, H. L., Kirchhausen, T., and Harrison, S. C. (2004). Crystal structure of the clathrin adaptor protein 1 core. *Proc. Natl. Acad. Sci. U.S.A.* *101*, 14108–14113.
- Hille-Rehfeld, A. (1995). Mannose 6-phosphate receptors in sorting and transport of lysosomal enzymes. *Biochim. Biophys. Acta* *1241*, 177–194.
- Hinners, I. (2003). Changing directions: clathrin-mediated transport between the Golgi and endosomes. *Journal of Cell Science* *116*, 763–771.
- Hirschberg, K., Miller, C. M., Ellenberg, J., Presley, J. F., Siggia, E. D., Phair, R. D., and Lippincott-Schwartz, J. (1998). Kinetic analysis of secretory protein traffic and characterization of golgi to plasma membrane transport intermediates in living cells. *The Journal of Cell Biology* *143*, 1485–1503.
- Hirst, J., Barlow, L. D., Francisco, G. C., Sahlender, D. A., Seaman, M. N. J., Dacks, J. B., and Robinson, M. S. (2011). The fifth adaptor protein complex. *PLoS Biol.* *9*, e1001170.
- Hirst, J., Borner, G. H. H., Antrobus, R., Peden, A. A., Hodson, N. A., Sahlender, D. A., and Robinson, M. S. (2012). Distinct and Overlapping Roles for AP-1 and GGAs Revealed by the “Knocksideways” System. *Curbio* *22*, 1711–1716.
- Hochstrasser, M. (1991). Functions of intracellular protein degradation in yeast. *Genet. Eng. (N.Y.)* *13*, 307–329.
- Holthuis, J. C., Nichols, B. J., Dhruvakumar, S., and Pelham, H. R. (1998). Two syntaxin homologues in the TGN/endosomal system of yeast. *The EMBO Journal* *17*, 113–126.
- Hopfner, K.-P. *et al.* (2002). The Rad50 zinc-hook is a structure joining Mre11 complexes in DNA recombination and repair. *Nature* *418*, 562–566.
- Hou, F., Sun, L., Zheng, H., Skaug, B., Jiang, Q.-X., and Chen, Z. J. (2011). MAVS forms functional prion-like aggregates to activate and propagate antiviral innate immune response. *Cell* *146*, 448–461.
- Höning, S., Griffith, J., Geuze, H. J., and Hunziker, W. (1996). The tyrosine-based lysosomal targeting signal in lamp-1 mediates sorting into Golgi-derived clathrin-coated vesicles. *The EMBO Journal* *15*, 5230–5239.
- Huotari, J., and Helenius, A. (2011). Endosome maturation. *The EMBO Journal* *30*, 3481–3500.
- Hutagalung, A. H., and Novick, P. J. (2011). Role of Rab GTPases in Membrane Traffic and Cell Physiology. *Physiological Reviews* *91*, 119–149.
- Huttner, W. B. (1988). Existence of distinct tyrosylprotein sulfotransferase genes: molecular characterization of tyrosylprotein sulfotransferase-2. *Annu. Rev. Physiol.* *50*, 363–376.

- Itzen, A., and Goody, R. S. (2011). GTPases involved in vesicular trafficking: Structures and mechanisms. *Seminars in Cell and Developmental Biology* 22, 48–56.
- Iwanaga, T., Tsutsumi, R., Noritake, J., Fukata, Y., and Fukata, M. (2009). Dynamic protein palmitoylation in cellular signaling. *Progress in Lipid Research* 48, 117–127.
- Jamieson, J. D., and Palade, G. E. (1967). Intracellular transport of secretory proteins in the pancreatic exocrine cell. I. Role of the peripheral elements of the Golgi complex. *The Journal of Cell Biology* 34, 577–596.
- Jose, M., Tollis, S., Nair, D., Sibarita, J. B., and McCusker, D. (2013). Robust polarity establishment occurs via an endocytosis-based cortical corralling mechanism. *The Journal of Cell Biology* 200, 407–418.
- Jung, U. S., and Levin, D. E. (1999). Genome-wide analysis of gene expression regulated by the yeast cell wall integrity signalling pathway. *Mol. Microbiol.* 34, 1049–1057.
- Kabouridis, P. S., Magee, A. I., and Ley, S. C. (1997). S-acylation of LCK protein tyrosine kinase is essential for its signalling function in T lymphocytes. *The EMBO Journal* 16, 4983–4998.
- Kaksonen, M., Toret, C. P., and Drubin, D. G. (2005). A Modular Design for the Clathrin- and Actin-Mediated Endocytosis Machinery. *Cell* 123, 305–320.
- Kamada, Y., Jung, U. S., Piotrowski, J., and Levin, D. E. (1995). The protein kinase C-activated MAP kinase pathway of *Saccharomyces cerevisiae* mediates a novel aspect of the heat shock response. *Genes & Development* 9, 1559–1571.
- Kamena, F., and Spang, A. (2004). Tip20p prohibits back-fusion of COPII vesicles with the endoplasmic reticulum. *Science* 304, 286–289.
- Kato, M. *et al.* (2012). Cell-free Formation of RNA Granules: Low Complexity Sequence Domains Form Dynamic Fibers within Hydrogels. *Cell* 149, 753–767.
- Keller, P., Toomre, D., Díaz, E., White, J., and Simons, K. (2001). Multicolour imaging of post-Golgi sorting and trafficking in live cells. *Nat Cell Biol* 3, 140–149.
- Ketela, T., Green, R., and Bussey, H. (1999). *Saccharomyces cerevisiae* mid2p is a potential cell wall stress sensor and upstream activator of the PKC1-MPK1 cell integrity pathway. *J. Bacteriol.* 181, 3330–3340.
- Kilchert C. (2011). mRNA localization and turnover in mutants of the small GTPase Arf1p in *S.cerevisiae*, Universität Basel, Basel
- Kilchert, C., Weidner, J., Prescianotto-Baschong, C., and Spang, A. (2010). Defects in the secretory pathway and high Ca²⁺ induce multiple P-bodies. *Molecular Biology of the Cell* 21, 2624–2638.
- Knop, M. (2011). Yeast cell morphology and sexual reproduction--a short overview and some considerations. *C. R. Biol.* 334, 599–606.
- Knop, M., Siegers, K., Pereira, G., Zachariae, W., Winsor, B., Nasmyth, K., and Schiebel, E. (1999). Epitope tagging of yeast genes using a PCR-based strategy: more tags and improved practical routines. *Yeast* 15, 963–972.

- Kota, J. (2004). Specialized membrane-localized chaperones prevent aggregation of polytopic proteins in the ER. *The Journal of Cell Biology* 168, 79–88.
- Kozubowski, L., Panek, H., Rosenthal, A., Bloecher, A., DeMarini, D. J., and Tatchell, K. (2003). A Bni4-Glc7 phosphatase complex that recruits chitin synthase to the site of bud emergence. *Molecular Biology of the Cell* 14, 26–39.
- Kraft, K. (2001). Characterization of Sequence Determinants within the Carboxyl-terminal Domain of Chemokine Receptor CCR5 That Regulate Signaling and Receptor Internalization. *Journal of Biological Chemistry* 276, 34408–34418.
- Krauss, M., Kinuta, M., Wenk, M. R., De Camilli, P., Takei, K., and Haucke, V. (2003). ARF6 stimulates clathrin/AP-2 recruitment to synaptic membranes by activating phosphatidylinositol phosphate kinase type Igamma. *The Journal of Cell Biology* 162, 113–124.
- Krecek, P., Skupa, P., Libus, J., Naramoto, S., Tejos, R., Friml, J., and Zazimalová, E. (2009). The PIN-FORMED (PIN) protein family of auxin transporters. *Genome Biol.* 10, 249.
- Krömer, A., Glombik, M. M., Huttner, W. B., and Gerdes, H. H. (1998). Essential role of the disulfide-bonded loop of chromogranin B for sorting to secretory granules is revealed by expression of a deletion mutant in the absence of endogenous granin synthesis. *The Journal of Cell Biology* 140, 1331–1346.
- Kruckeberg, A. L., Ye, L., Berden, J. A., and van Dam, K. (1999). Functional expression, quantification and cellular localization of the Hxt2 hexose transporter of *Saccharomyces cerevisiae* tagged with the green fluorescent protein. *Biochem. J.* 339 (Pt 2), 299–307.
- La Fontaine, S., Firth, S. D., Lockhart, P. J., Brooks, H., Parton, R. G., Camakaris, J., and Mercer, J. F. (1998). Functional analysis and intracellular localization of the human menkes protein (MNK) stably expressed from a cDNA construct in Chinese hamster ovary cells (CHO-K1). *Hum. Mol. Genet.* 7, 1293–1300.
- Lam, K. K. Y., Davey, M., Sun, B., Roth, A. F., Davis, N. G., and Conibear, E. (2006). Palmitoylation by the DHHC protein Pfa4 regulates the ER exit of Chs3. *The Journal of Cell Biology* 174, 19–25.
- Lam, S. K., Tse, Y. C., Robinson, D. G., and Jiang, L. (2007). Tracking down the elusive early endosome. *Trends Plant Sci.* 12, 497–505.
- Lasiecka, Z. M., and Winckler, B. (2011). Mechanisms of polarized membrane trafficking in neurons — Focusing in on endosomes. *Molecular and Cellular Neuroscience* 48, 278–287.
- Lee, C., Zhang, H., Baker, A. E., Occhipinti, P., Borsuk, M. E., and Gladfelter, A. S. (2013). Protein aggregation behavior regulates cyclin transcript localization and cell-cycle control. *Developmental Cell* 25, 572–584.
- Lee, M. C. S., Miller, E. A., Goldberg, J., Orci, L., and Schekman, R. (2004). BI-DIRECTIONAL PROTEIN TRANSPORT BETWEEN THE ER AND GOLGI. *Annu. Rev. Cell Dev. Biol.* 20, 87–123.
- Levin, D. E. (2011). Regulation of Cell Wall Biogenesis in *Saccharomyces cerevisiae*: The Cell Wall Integrity Signaling Pathway. *Genetics* 189, 1145–1175.

- Lew, D. J., and Reed, S. I. (1993). Morphogenesis in the yeast cell cycle: regulation by Cdc28 and cyclins. *The Journal of Cell Biology* *120*, 1305–1320.
- Li, J. *et al.* (2012). The RIP1/RIP3 necrosome forms a functional amyloid signaling complex required for programmed necrosis. *Cell* *150*, 339–350.
- Li, S. C., and Kane, P. M. (2009). The yeast lysosome-like vacuole: Endpoint and crossroads. *BBA - Molecular Cell Research* *1793*, 650–663.
- Li, X., Gerber, S. A., Rudner, A. D., Beausoleil, S. A., Haas, W., Villén, J., Elias, J. E., and Gygi, S. P. (2007). Large-scale phosphorylation analysis of alpha-factor-arrested *Saccharomyces cerevisiae*. *J. Proteome Res.* *6*, 1190–1197.
- Lillie, S. H., and Brown, S. S. (1994). Immunofluorescence localization of the unconventional myosin, Myo2p, and the putative kinesin-related protein, Smy1p, to the same regions of polarized growth in *Saccharomyces cerevisiae*. *The Journal of Cell Biology* *125*, 825–842.
- Lin, C. H., MacGurn, J. A., Chu, T., Stefan, C. J., and Emr, S. D. (2008). Arrestin-Related Ubiquitin-Ligase Adaptors Regulate Endocytosis and Protein Turnover at the Cell Surface. *Cell* *135*, 714–725.
- Lord, C., Bhandari, D., Menon, S., Ghassemian, M., Nycz, D., Hay, J., Ghosh, P., and Ferro-Novick, S. (2011). Lord2011_tethercoatinteraction. *Nature* *473*, 181–186.
- Magee, A. I., Gutierrez, L., McKay, I. A., Marshall, C. J., and Hall, A. (1987). Dynamic fatty acylation of p21N-ras. *The EMBO Journal* *6*, 3353–3357.
- Majumdar, A. *et al.* (2012). Critical role of amyloid-like oligomers of *Drosophila* Orb2 in the persistence of memory. *Cell* *148*, 515–529.
- Mamathambika, B. S., and Bardwell, J. C. (2008). Disulfide-Linked Protein Folding Pathways. *Annu. Rev. Cell Dev. Biol.* *24*, 211–235.
- Martin, H. (2000). Regulatory Mechanisms for Modulation of Signaling through the Cell Integrity Slt2-mediated Pathway in *Saccharomyces cerevisiae*. *Journal of Biological Chemistry* *275*, 1511–1519.
- Masison, D. C., and Wickner, R. B. (1995). Prion-inducing domain of yeast Ure2p and protease resistance of Ure2p in prion-containing cells. *Science* *270*, 93–95.
- Matile, P., and Wiemken, A. (1967). The vacuole as the lysosome of the yeast cell. *Arch Mikrobiol* *56*, 148–155.
- Maxfield, F. R., and McGraw, T. E. (2004). Endocytic recycling. *Nat Rev Mol Cell Biol* *5*, 121–132.
- Mayor, S., and Pagano, R. E. (2007). Pathways of clathrin-independent endocytosis. *Nat Rev Mol Cell Biol* *8*, 603–612.
- Meyer, C., Zizioli, D., Lausmann, S., Eskelinen, E. L., Hamann, J., Saftig, P., Figura, von, K., and Schu, P. (2000). mu1A-adaptin-deficient mice: lethality, loss of AP-1 binding and rerouting of mannose 6-phosphate receptors. *The EMBO Journal* *19*, 2193–2203.

- Michelitsch, M. D., and Weissman, J. S. (2000). A census of glutamine/asparagine-rich regions: implications for their conserved function and the prediction of novel prions. *Proc. Natl. Acad. Sci. U.S.a.* *97*, 11910–11915.
- Milstein, C., Brownlee, G. G., Harrison, T. M., and Mathews, M. B. (1972). A possible precursor of immunoglobulin light chains. *Nature New Biol.* *239*, 117–120.
- Misra, S., Puertollano, R., Kato, Y., Bonifacino, J. S., and Hurley, J. H. (2002). Structural basis for acidic-cluster-dileucine sorting-signal recognition by VHS domains. *Nature* *415*, 933–937.
- Moran, M. F., Koch, C. A., Anderson, D., Ellis, C., England, L., Martin, G. S., and Pawson, T. (1990). Src homology region 2 domains direct protein-protein interactions in signal transduction. *Proc. Natl. Acad. Sci. U.S.a.* *87*, 8622–8626.
- Moreau, V., Galan, J. M., Devilliers, G., Haguenauer-Tsapis, R., and Winsor, B. (1997). The yeast actin-related protein Arp2p is required for the internalization step of endocytosis. *Molecular Biology of the Cell* *8*, 1361–1375.
- Morgan, J. R., Prasad, K., Hao, W., Augustine, G. J., and Lafer, E. M. (2000). A conserved clathrin assembly motif essential for synaptic vesicle endocytosis. *Journal of Neuroscience* *20*, 8667–8676.
- Moseley, J. B., and Goode, B. L. (2006). The Yeast Actin Cytoskeleton: from Cellular Function to Biochemical Mechanism. *Microbiol. Mol. Biol. Rev.* *70*, 605–645.
- Mukai, A., Yamamoto-Hino, M., Awano, W., Watanabe, W., Komada, M., and Goto, S. (2010). Balanced ubiquitylation and deubiquitylation of Frizzled regulate cellular responsiveness to Wg/Wnt. *The EMBO Journal* *29*, 2114–2125.
- Mulholland, J., Wesp, A., Riezman, H., and Botstein, D. (1997). Yeast actin cytoskeleton mutants accumulate a new class of Golgi-derived secretory vesicle. *Molecular Biology of the Cell* *8*, 1481–1499.
- Nagahara, N. (2010). Intermolecular disulfide bond to modulate protein function as a redox-sensing switch. *Amino Acids* *41*, 59–72.
- Nakayama, K., and Wakatsuki, S. (2003). The structure and function of GGAs, the traffic controllers at the TGN sorting crossroads. *Cell Struct. Funct.* *28*, 431–442.
- Nebenführ, A., Gallagher, L. A., Dunahay, T. G., Frohlick, J. A., Mazurkiewicz, A. M., Meehl, J. B., and Staehelin, L. A. (1999). Stop-and-go movements of plant Golgi stacks are mediated by the acto-myosin system. *Plant Physiol.* *121*, 1127–1142.
- Nehlin, J. O., Carlberg, M., and Ronne, H. (1989). Yeast galactose permease is related to yeast and mammalian glucose transporters. *Gene* *85*, 313–319.
- Newby, G. A., and Lindquist, S. (2013). Blessings in disguise: biological benefits of prion-like mechanisms. *Trends in Cell Biology* *23*, 251–259.
- Newpher, T. M., Smith, R. P., Lemmon, V., and Lemmon, S. K. (2005). In Vivo Dynamics of Clathrin and Its Adaptor-Dependent Recruitment to the Actin-Based Endocytic Machinery in Yeast. *Developmental Cell* *9*, 87–98.

- Nikko, E., and Pelham, H. R. B. (2009). Arrestin-Mediated Endocytosis of Yeast Plasma Membrane Transporters. *Traffic* *10*, 1856–1867.
- Nikko, E., Sullivan, J. A., and Pelham, H. R. B. (2008). Arrestin-like proteins mediate ubiquitination and endocytosis of the yeast metal transporter Smf1. *EMBO Rep* *9*, 1216–1221.
- Novick, P., Field, C., and Schekman, R. (1980). Identification of 23 complementation groups required for post-translational events in the yeast secretory pathway. *Cell* *21*, 205–215.
- Oh, Y., and Bi, E. (2011). Septin structure and function in yeast and beyond. *Trends in Cell Biology* *21*, 141–148.
- Ohno, H., Stewart, J., Fournier, M. C., Bosshart, H., Rhee, I., Miyatake, S., Saito, T., Gallusser, A., Kirchhausen, T., and Bonifacino, J. S. (1995). Interaction of tyrosine-based sorting signals with clathrin-associated proteins. *Science* *269*, 1872–1875.
- Ohno, Y., Kihara, A., Sano, T., and Igarashi, Y. (2006). Intracellular localization and tissue-specific distribution of human and yeast DHHC cysteine-rich domain-containing proteins. *Biochim. Biophys. Acta* *1761*, 474–483.
- Okamoto, M., Kurokawa, K., Matsuura-Tokita, K., Saito, C., Hirata, R., and Nakano, A. (2012). High-curvature domains of the ER are important for the organization of ER exit sites in *Saccharomyces cerevisiae*. *Journal of Cell Science* *125*, 3412–3420.
- Orci, L., Glick, B. S., and Rothman, J. E. (1986). A new type of coated vesicular carrier that appears not to contain clathrin: its possible role in protein transport within the Golgi stack. *Cell* *46*, 171–184.
- Oshervich, L. Z., and Weissman, J. S. (2002). The utility of prions. *Developmental Cell* *2*, 143–151.
- Owen, D. J., Collins, B. M., and Evans, P. R. (2004). Adaptors for clathrin coats: structure and function. *Annu. Rev. Cell Dev. Biol.* *20*, 153–191.
- Owen, D. J., Vallis, Y., Pearse, B. M., McMahon, H. T., and Evans, P. R. (2000). The structure and function of the beta 2-adaptin appendage domain. *The EMBO Journal* *19*, 4216–4227.
- Paczkowski, J. E., Richardson, B. C., Strassner, A. M., and Fromme, J. C. (2012). The exomer cargo adaptor structure reveals a novel GTPase-binding domain. *The EMBO Journal* *31*, 4191–4203.
- Paleotti, O., Macia, E., Luton, F., Klein, S., Partisani, M., Chardin, P., Kirchhausen, T., and Franco, M. (2005). The small G-protein Arf6GTP recruits the AP-2 adaptor complex to membranes. *J. Biol. Chem.* *280*, 21661–21666.
- Panaretou, C., and Tooze, S. A. (2002). Regulation and recruitment of phosphatidylinositol 4-kinase on immature secretory granules is independent of ADP-ribosylation factor 1. *Biochem. J.* *363*, 289–295.
- Pareja, F. *et al.* (2012). Deubiquitination of EGFR by Cezanne-1 contributes to cancer progression. *Oncogene* *31*, 4599–4608.

- Park, H.-O., and Bi, E. (2007). Central roles of small GTPases in the development of cell polarity in yeast and beyond. *Microbiol. Mol. Biol. Rev.* *71*, 48–96.
- Parlati, F., Varlamov, O., Paz, K., McNew, J. A., Hurtado, D., Söllner, T. H., and Rothman, J. E. (2002). Distinct SNARE complexes mediating membrane fusion in Golgi transport based on combinatorial specificity. *Proc. Natl. Acad. Sci. U.S.a.* *99*, 5424–5429.
- Pasqualato, S., Renault, L., and Cherfils, J. (2002). Arf, Arl, Arp and Sar proteins: a family of GTP-binding proteins with a structural device for “front-back” communication. *EMBO Rep* *3*, 1035–1041.
- Pearse, B. M. (1975). Coated vesicles from pig brain: purification and biochemical characterization. *Journal of Molecular Biology* *97*, 93–98.
- Peng, J., Schwartz, D., Elias, J. E., Thoreen, C. C., Cheng, D., Marsischky, G., Roelofs, J., Finley, D., and Gygi, S. P. (2003). A proteomics approach to understanding protein ubiquitination. *Nat. Biotechnol.* *21*, 921–926.
- Petris, M. J., Mercer, J. F., Culvenor, J. G., Lockhart, P., Gleeson, P. A., and Camakaris, J. (1996). Ligand-regulated transport of the Menkes copper P-type ATPase efflux pump from the Golgi apparatus to the plasma membrane: a novel mechanism of regulated trafficking. *The EMBO Journal* *15*, 6084–6095.
- Pfeffer, S. R. (2013). Rab GTPase regulation of membrane identity. *Current Opinion in Cell Biology* *25*, 414–419.
- Polishchuk, E. V., Di Pentima, A., Luini, A., and Polishchuk, R. S. (2003). Mechanism of constitutive export from the golgi: bulk flow via the formation, protrusion, and en bloc cleavage of large trans-golgi network tubular domains. *Molecular Biology of the Cell* *14*, 4470–4485.
- Polishchuk, R. S., San Pietro, E., Di Pentima, A., Teté, S., and Bonifacino, J. S. (2006). Ultrastructure of long-range transport carriers moving from the trans Golgi network to peripheral endosomes. *Traffic* *7*, 1092–1103.
- Popolo, L., Gilardelli, D., Bonfante, P., and Vai, M. (1997). Increase in chitin as an essential response to defects in assembly of cell wall polymers in the *ggp1delta* mutant of *Saccharomyces cerevisiae*. *J. Bacteriol.* *179*, 463–469.
- Posas, F., Chambers, J. R., Heyman, J. A., Hoeffler, J. P., de Nadal, E., and Arino, J. (2000). The transcriptional response of yeast to saline stress. *J. Biol. Chem.* *275*, 17249–17255.
- Prusiner, S. B., McKinley, M. P., Bowman, K. A., Bolton, D. C., Bendheim, P. E., Groth, D. F., and Glenner, G. G. (1983). Scrapie prions aggregate to form amyloid-like birefringent rods. *Cell* *35*, 349–358.
- Pruyne, D. W., Schott, D. H., and Bretscher, A. (1998). Tropomyosin-containing actin cables direct the Myo2p-dependent polarized delivery of secretory vesicles in budding yeast. *The Journal of Cell Biology* *143*, 1931–1945.
- Pruyne, D., and Bretscher, A. (2000). Polarization of cell growth in yeast. *Journal of Cell Science* *113* (Pt 4), 571–585.

- Pruyne, D., Gao, L., Bi, E., and Bretscher, A. (2004). Stable and dynamic axes of polarity use distinct formin isoforms in budding yeast. *Molecular Biology of the Cell* *15*, 4971–4989.
- Puertollano, R., van der Wel, N. N., Greene, L. E., Eisenberg, E., Peters, P. J., and Bonifacino, J. S. (2003). Morphology and dynamics of clathrin/GGA1-coated carriers budding from the trans-Golgi network. *Molecular Biology of the Cell* *14*, 1545–1557.
- Qadota, H., Python, C. P., Inoue, S. B., Arisawa, M., Anraku, Y., Zheng, Y., Watanabe, T., Levin, D. E., and Ohya, Y. (1996). Identification of yeast Rho1p GTPase as a regulatory subunit of 1,3-beta-glucan synthase. *Science* *272*, 279–281.
- Rapoport, T. A. (2007). Protein translocation across the eukaryotic endoplasmic reticulum and bacterial plasma membranes. *Nature* *450*, 663–669.
- Reijns, M. A. M., Alexander, R. D., Spiller, M. P., and Beggs, J. D. (2008). A role for Q/N-rich aggregation-prone regions in P-body localization. *Journal of Cell Science* *121*, 2463–2472.
- Rein, U., Andag, U., Duden, R., Schmitt, H. D., and Spang, A. (2002). ARF-GAP-mediated interaction between the ER-Golgi v-SNAREs and the COPI coat. *The Journal of Cell Biology* *157*, 395–404.
- Ren, X., Fariás, G. G., Canagarajah, B. J., Bonifacino, J. S., and Hurley, J. H. (2013). Structural Basis for Recruitment and Activation of the AP-1 Clathrin Adaptor Complex by Arf1. *Cell* *152*, 755–767.
- Rep, M., Krantz, M., Thevelein, J. M., and Hohmann, S. (2000). The transcriptional response of *Saccharomyces cerevisiae* to osmotic shock. Hot1p and Msn2p/Msn4p are required for the induction of subsets of high osmolarity glycerol pathway-dependent genes. *J. Biol. Chem.* *275*, 8290–8300.
- Reyes, A., Sanz, M., Duran, A., and Roncero, C. (2007). Chitin synthase III requires Chs4p-dependent translocation of Chs3p into the plasma membrane. *Journal of Cell Science* *120*, 1998–2009.
- Richardson, H., Lew, D. J., Henze, M., Sugimoto, K., and Reed, S. I. (1992). Cyclin-B homologs in *Saccharomyces cerevisiae* function in S phase and in G2. *Genes & Development* *6*, 2021–2034.
- Robinson, M. S., and Bonifacino, J. S. (2001). Adaptor-related proteins. *Current Opinion in Cell Biology* *13*, 444–453.
- Rockenbauch U. (2012) A specialized exit route: Specific recognition and cell cycle-dependent cargoes in *Saccharomyces cerevisiae*, Universität Basel, Basel
- Rockenbauch, U., Ritz, A. M., Sacristan, C., Roncero, C., and Spang, A. (2012). The complex interactions of Chs5p, the ChAPs, and the cargo Chs3p. *Molecular Biology of the Cell* *23*, 4402–4415.
- Rocks, O. *et al.* (2010). The palmitoylation machinery is a spatially organizing system for peripheral membrane proteins. *Cell* *141*, 458–471.
- Rocks, O., Peyker, A., Kahms, M., Verveer, P. J., Koerner, C., Lumbierres, M., Kuhlmann, J., Waldmann, H., Wittinghofer, A., and Bastiaens, P. I. H. (2005). An acylation cycle regulates localization and activity of palmitoylated Ras isoforms. *Science* *307*, 1746–1752.

- Rodal, A. A., Kozubowski, L., Goode, B. L., Drubin, D. G., and Hartwig, J. H. (2005). Actin and septin ultrastructures at the budding yeast cell cortex. *Molecular Biology of the Cell* *16*, 372–384.
- Rossanese, O. W., Soderholm, J., Bevis, B. J., Sears, I. B., O'Connor, J., Williamson, E. K., and Glick, B. S. (1999). Golgi structure correlates with transitional endoplasmic reticulum organization in *Pichia pastoris* and *Saccharomyces cerevisiae*. *The Journal of Cell Biology* *145*, 69–81.
- Roth, A. F., Wan, J., Bailey, A. O., Sun, B., Kuchar, J. A., Green, W. N., Phinney, B. S., Yates, J. R., III, and Davis, N. G. (2006). Global Analysis of Protein Palmitoylation in Yeast. *Cell* *125*, 1003–1013.
- Sabatini, D. D., Blobel, G., Nonomura, Y., and Adelman, M. R. (1971). Ribosome-membrane interaction: Structural aspects and functional implications. *Adv Cytopharmacol* *1*, 119–129.
- Sacristan, C., Manzano-Lopez, J., Reyes, A., Spang, A., Muñiz, M., and Roncero, C. (2013). Oligomerization of the chitin synthase Chs3 is monitored at the Golgi and affects its endocytic recycling. *Mol. Microbiol.*, n/a–n/a.
- Sadowski, I. *et al.* (2013). The PhosphoGRID *Saccharomyces cerevisiae* protein phosphorylation site database: version 2.0 update. *Database (Oxford)* *2013*, bat026.
- Salnikova, A. B. (2004). Nonsense Suppression in Yeast Cells Overproducing Sup35 (eRF3) Is Caused by Its Non-heritable Amyloids. *Journal of Biological Chemistry* *280*, 8808–8812.
- Sambrook, J., Fritsch, E.F., and Maniatis, T. (1989). *Molecular cloning: A Laboratory Manual*. Second Edition. Cold Spring Harbor Laboratory Press
- Sanchatjate, S., and Schekman, R. (2006). Chs5/6 complex: a multiprotein complex that interacts with and conveys chitin synthase III from the trans-Golgi network to the cell surface. *Molecular Biology of the Cell* *17*, 4157–4166.
- Sandvig, K., and van Deurs, B. (2002). Transport of protein toxins into cells: pathways used by ricin, cholera toxin and Shiga toxin. *FEBS Letters* *529*, 49–53.
- Santos, B., and Snyder, M. (1997). Targeting of chitin synthase 3 to polarized growth sites in yeast requires Chs5p and Myo2p. *The Journal of Cell Biology* *136*, 95–110.
- Santos, B., and Snyder, M. (2003). Specific protein targeting during cell differentiation: polarized localization of Fus1p during mating depends on Chs5p in *Saccharomyces cerevisiae*. *Eukaryotic Cell* *2*, 821–825.
- Santos, B., Durán, A., and Valdivieso, M. H. (1997). CHS5, a gene involved in chitin synthesis and mating in *Saccharomyces cerevisiae*. *Molecular and Cellular Biology* *17*, 2485–2496.
- Schägger, H., and Jagow, von, G. (1991). Blue native electrophoresis for isolation of membrane protein complexes in enzymatically active form. *Anal. Biochem.* *199*, 223–231.
- Schindler, C., and Spang, A. (2007). Interaction of SNAREs with ArfGAPs precedes recruitment of Sec18p/NSF. *Molecular Biology of the Cell* *18*, 2852–2863.

- Schindler, C., Rodriguez, F., Poon, P. P., Singer, R. A., Johnston, G. C., and Spang, A. (2009). The GAP domain and the SNARE, coatamer and cargo interaction region of the ArfGAP2/3 Glo3 are sufficient for Glo3 function. *Traffic* *10*, 1362–1375.
- Schlecht, U., Miranda, M., Suresh, S., Davis, R. W., and St Onge, R. P. (2012). Multiplex assay for condition-dependent changes in protein-protein interactions. *Proc. Natl. Acad. Sci. U.S.a.* *109*, 9213–9218.
- Schmidt, M. (2003). Septins, under Cla4p Regulation, and the Chitin Ring Are Required for Neck Integrity in Budding Yeast. *Molecular Biology of the Cell* *14*, 2128–2141.
- Schott, D. H., Collins, R. N., and Bretscher, A. (2002). Secretory vesicle transport velocity in living cells depends on the myosin-V lever arm length. *The Journal of Cell Biology* *156*, 35–39.
- Scott, P. M., Bilodeau, P. S., Zhdankina, O., Winistorfer, S. C., Hauglund, M. J., Allaman, M. M., Kearney, W. R., Robertson, A. D., Boman, A. L., and Piper, R. C. (2004). GGA proteins bind ubiquitin to facilitate sorting at the trans-Golgi network. *Nature Publishing Group* *6*, 8–259.
- Segev, N. (2011). Coordination of intracellular transport steps by GTPases. *Seminars in Cell and Developmental Biology* *22*, 33–38.
- Sevier, C. S., and Kaiser, C. A. (2002). Formation and transfer of disulphide bonds in living cells. *Nat Rev Mol Cell Biol* *3*, 836–847.
- Sharpe, H. J., Stevens, T. J., and Munro, S. (2010). A comprehensive comparison of transmembrane domains reveals organelle-specific properties. *Cell* *142*, 158–169.
- Shaw, J. A., Mol, P. C., Bowers, B., Silverman, S. J., Valdivieso, M. H., Durán, A., and Cabib, E. (1991). The function of chitin synthases 2 and 3 in the *Saccharomyces cerevisiae* cell cycle. *The Journal of Cell Biology* *114*, 111–123.
- Sherman, F. (1991). Getting started with yeast. *Meth. Enzymol.* *194*, 3–21.
- Singer, B., and Riezman, H. (1990). Detection of an intermediate compartment involved in transport of alpha-factor from the plasma membrane to the vacuole in yeast. *The Journal of Cell Biology* *110*, 1911–1922.
- Singer-Krüger, B., Frank, R., Crausaz, F., and Riezman, H. (1993). Partial purification and characterization of early and late endosomes from yeast. Identification of four novel proteins. *J. Biol. Chem.* *268*, 14376–14386.
- Singh, G. P., Chandra, B. R., Bhattacharya, A., Akhouri, R. R., Singh, S. K., and Sharma, A. (2004). Hyper-expansion of asparagines correlates with an abundance of proteins with prion-like domains in *Plasmodium falciparum*. *Mol. Biochem. Parasitol.* *137*, 307–319.
- Solioz, M., and Vulpe, C. (1996). CPx-type ATPases: a class of P-type ATPases that pump heavy metals. *Trends in Biochemical Sciences* *21*, 237–241.
- Sorkin, A., and Zastrow, von, M. (2009). SorkinandZastrow2009_endosignalling. 1–14.
- Sossin, W. S., Fisher, J. M., and Scheller, R. H. (1990). Sorting within the regulated secretory pathway occurs in the trans-Golgi network. *The Journal of Cell Biology* *110*, 1–12.

- Soulard, A., Cremonesi, A., Moes, S., Schütz, F., Jenö, P., and Hall, M. N. (2010). The rapamycin-sensitive phosphoproteome reveals that TOR controls protein kinase A toward some but not all substrates. *Molecular Biology of the Cell* *21*, 3475–3486.
- Spang, A. (2008). Membrane traffic in the secretory pathway. *Cell. Mol. Life Sci.* *65*, 2781–2789.
- Spang, A. (2009). On the fate of early endosomes. *Biological Chemistry* *390*, 753–759.
- Spang, A., and Schekman, R. (1998). Reconstitution of retrograde transport from the Golgi to the ER in vitro. *The Journal of Cell Biology* *143*, 589–599.
- Spang, A., Shiba, Y., and Randazzo, P. A. (2010). Arf GAPs: Gatekeepers of vesicle generation. *FEBS Letters* *584*, 2646–2651.
- Stanley, P. (2011). Golgi Glycosylation. *Cold Spring Harbor Perspectives in Biology* *3*, a005199–a005199.
- Starr, T. L., Pagant, S., Wang, C.-W., and Schekman, R. (2012). Sorting signals that mediate traffic of chitin synthase III between the TGN/endosomes and to the plasma membrane in yeast. *PLoS ONE* *7*, e46386.
- Stimpson, H. E. M., Toret, C. P., Cheng, A. T., Pauly, B. S., and Drubin, D. G. (2009). Early-arriving Syp1p and Ede1p function in endocytic site placement and formation in budding yeast. *Molecular Biology of the Cell* *20*, 4640–4651.
- Strausak, D. (1999). The Role of GMXCXXC Metal Binding Sites in the Copper-induced Redistribution of the Menkes Protein. *Journal of Biological Chemistry* *274*, 11170–11177.
- Surma, M. A., Klose, C., and Simons, K. (2012). Lipid-dependent protein sorting at the trans-Golgi network. *BBA - Molecular and Cell Biology of Lipids* *1821*, 1059–1067.
- Sutton, R. B., Fasshauer, D., Jahn, R., and Brunger, A. T. (1998). Crystal structure of a SNARE complex involved in synaptic exocytosis at 2.4 Å resolution. *Nature* *395*, 347–353.
- Szopinska, A., Degand, H., Hochstenbach, J. F., Nader, J., and Morsomme, P. (2011). Rapid Response of the Yeast Plasma Membrane Proteome to Salt Stress. *Molecular & Cellular Proteomics* *10*, M111.009589–M111.009589.
- Søgaard, M., Tani, K., Ye, R. R., Geromanos, S., Tempst, P., Kirchhausen, T., Rothman, J. E., and Söllner, T. (1994). A rab protein is required for the assembly of SNARE complexes in the docking of transport vesicles. *Cell* *78*, 937–948.
- Tagwerker, C., Zhang, H., Wang, X., Larsen, L. S. Z., Lathrop, R. H., Hatfield, G. W., Auer, B., Huang, L., and Kaiser, P. (2006). HB tag modules for PCR-based gene tagging and tandem affinity purification in *Saccharomyces cerevisiae*. *Yeast* *23*, 623–632.
- Tang, H. Y., Munn, A., and Cai, M. (1997). EH domain proteins Pan1p and End3p are components of a complex that plays a dual role in organization of the cortical actin cytoskeleton and endocytosis in *Saccharomyces cerevisiae*. *Molecular and Cellular Biology* *17*, 4294–4304.

- Tang, H. Y., Xu, J., and Cai, M. (2000). Pan1p, End3p, and S1a1p, three yeast proteins required for normal cortical actin cytoskeleton organization, associate with each other and play essential roles in cell wall morphogenesis. *Molecular and Cellular Biology* *20*, 12–25.
- Tarassov, K., Messier, V., Landry, C. R., Radinovic, S., Serna Molina, M. M., Shames, I., Malitskaya, Y., Vogel, J., Bussey, H., and Michnick, S. W. (2008). An in vivo map of the yeast protein interactome. *Science* *320*, 1465–1470.
- Taylor, K. L. (1999). Prion Domain Initiation of Amyloid Formation in Vitro from Native Ure2p. *Science* *283*, 1339–1343.
- Teixeira, D., and Parker, R. (2007). Analysis of P-body assembly in *Saccharomyces cerevisiae*. *Molecular Biology of the Cell* *18*, 2274–2287.
- Ter-Avanesyan, M. D., Dagkesamanskaya, A. R., Kushnirov, V. V., and Smirnov, V. N. (1994). The SUP35 omnipotent suppressor gene is involved in the maintenance of the non-Mendelian determinant [psi+] in the yeast *Saccharomyces cerevisiae*. *Genetics* *137*, 671–676.
- TerBush, D. R., Maurice, T., Roth, D., and Novick, P. (1996). The Exocyst is a multiprotein complex required for exocytosis in *Saccharomyces cerevisiae*. *The EMBO Journal* *15*, 6483–6494.
- Theos, A. C. *et al.* (2006). Dual loss of ER export and endocytic signals with altered melanosome morphology in the silver mutation of Pmel17. *Molecular Biology of the Cell* *17*, 3598–3612.
- Toombs, J. A., Petri, M., Paul, K. R., Kan, G. Y., Ben-Hur, A., and Ross, E. D. (2012). De novo design of synthetic prion domains. *Proc. Natl. Acad. Sci. U.S.A.* *109*, 6519–6524.
- Tooze, S. A. (1998). Biogenesis of secretory granules in the trans-Golgi network of neuroendocrine and endocrine cells. *Biochim. Biophys. Acta* *1404*, 231–244.
- Toshima, J. Y., Toshima, J., Kaksonen, M., Martin, A. C., King, D. S., and Drubin, D. G. (2006). Spatial dynamics of receptor-mediated endocytic trafficking in budding yeast revealed by using fluorescent alpha-factor derivatives. *Proc. Natl. Acad. Sci. U.S.A.* *103*, 5793–5798.
- Touz, M. C., Kulakova, L., and Nash, T. E. (2004). Adaptor protein complex 1 mediates the transport of lysosomal proteins from a Golgi-like organelle to peripheral vacuoles in the primitive eukaryote *Giardia lamblia*. *Molecular Biology of the Cell* *15*, 3053–3060.
- Traub, L. M. (2003). Sorting it out: AP-2 and alternate clathrin adaptors in endocytic cargo selection. *The Journal of Cell Biology* *163*, 203–208.
- Traub, L. M. (2005). Common principles in clathrin-mediated sorting at the Golgi and the plasma membrane. *Biochimica Et Biophysica Acta (BBA) - Molecular Cell Research* *1744*, 415–437.
- Traub, L. M., and Kornfeld, S. (1997). The trans-Golgi network: a late secretory sorting station. *Current Opinion in Cell Biology* *9*, 527–533.
- Traub, L. M., and Lukacs, G. L. (2007). Decoding ubiquitin sorting signals for clathrin-dependent endocytosis by CLASPs. *Journal of Cell Science* *120*, 543–553.

- Trautwein, M. (2004). Die kleine GTPase Arf1p aus *Saccharomyces cerevisiae* geht neue Wege: Neue Funktionen im mRNA Transport und bei der Bildung von spezialisierten Golgi-Vesikeln, Eberhard-Karls Universität Tübingen
- Trautwein, M., Schindler, C., Gauss, R., Dengjel, J., Hartmann, E., and Spang, A. (2006). Arf1p, Chs5p and the ChAPs are required for export of specialized cargo from the Golgi. *The EMBO Journal* *25*, 943–954.
- Trilla, J. A., Durán, A., and Roncero, C. (1999). Chs7p, a new protein involved in the control of protein export from the endoplasmic reticulum that is specifically engaged in the regulation of chitin synthesis in *Saccharomyces cerevisiae*. *The Journal of Cell Biology* *145*, 1153–1163.
- Trueheart, J., Boeke, J. D., and Fink, G. R. (1987). Two genes required for cell fusion during yeast conjugation: evidence for a pheromone-induced surface protein. *Molecular and Cellular Biology* *7*, 2316–2328.
- Tsutsumi, R., Fukata, Y., Noritake, J., Iwanaga, T., Perez, F., and Fukata, M. (2008). Identification of G Protein Subunit-Palmitoylating Enzyme. *Molecular and Cellular Biology* *29*, 435–447.
- Tuite, M. F., Mundy, C. R., and Cox, B. S. (1981). Agents that cause a high frequency of genetic change from [psi+] to [psi-] in *Saccharomyces cerevisiae*. *Genetics* *98*, 691–711.
- Valdivia, R. H., and Schekman, R. (2003). The yeasts Rho1p and Pkc1p regulate the transport of chitin synthase III (Chs3p) from internal stores to the plasma membrane. *Proc. Natl. Acad. Sci. U.S.A.* *100*, 10287–10292.
- Valdivia, R. H., Baggott, D., Chuang, J. S., and Schekman, R. W. (2002). The yeast clathrin adaptor protein complex 1 is required for the efficient retention of a subset of late Golgi membrane proteins. *Developmental Cell* *2*, 283–294.
- Valdivieso, M. H., Ferrario, L., Vai, M., Durán, A., and Popolo, L. (2000). Chitin synthesis in a gas1 mutant of *Saccharomyces cerevisiae*. *J. Bacteriol.* *182*, 4752–4757.
- Vanrheenen, S. M., Reilly, B. A., Chamberlain, S. J., and Waters, M. G. (2001). Dsl1p, an essential protein required for membrane traffic at the endoplasmic reticulum/Golgi interface in yeast. *Traffic* *2*, 212–231.
- Vessey, J. P. (2006). Dendritic Localization of the Translational Repressor Pumilio 2 and Its Contribution to Dendritic Stress Granules. *Journal of Neuroscience* *26*, 6496–6508.
- Viotti, C. *et al.* (2010). Endocytic and secretory traffic in Arabidopsis merge in the trans-Golgi network/early endosome, an independent and highly dynamic organelle. *Plant Cell* *22*, 1344–1357.
- Waddle, J. A., Karpova, T. S., Waterston, R. H., and Cooper, J. A. (1996). Movement of cortical actin patches in yeast. *The Journal of Cell Biology* *132*, 861–870.
- Wakana, Y., van Galen, J., Meissner, F., Scarpa, M., Polishchuk, R. S., Mann, M., and Malhotra, V. (2012). Wakana2012_CARRS. *The EMBO Journal* *31*, 3976–3990.

- Wang, C.-W., Hamamoto, S., Orci, L., and Schekman, R. (2006). Exomer: A coat complex for transport of select membrane proteins from the trans-Golgi network to the plasma membrane in yeast. *The Journal of Cell Biology* *174*, 973–983.
- Ward, T. H., and Brandizzi, F. (2004). Dynamics of proteins in Golgi membranes: comparisons between mammalian and plant cells highlighted by photobleaching techniques. *Cell. Mol. Life Sci.* *61*, 172–185.
- Weber, T., Zemelman, B. V., McNew, J. A., Westermann, B., Gmachl, M., Parlati, F., Söllner, T. H., and Rothman, J. E. (1998). SNAREpins: minimal machinery for membrane fusion. *Cell* *92*, 759–772.
- Wickner, R. B., Edskes, H. K., Bateman, D. A., Kelly, A. C., Gorkovskiy, A., Dayani, Y., and Zhou, A. (2013). Amyloids and Yeast Prion Biology. *Biochemistry* *52*, 1514–1527.
- Witte, K., Schuh, A. L., Hegermann, J., Sarkeshik, A., Mayers, J. R., Schwarze, K., Yates, J. R., Eimer, S., and Audhya, A. (2011). TFG-1 function in protein secretion and oncogenesis. *Nature Publishing Group* *13*, 550–558.
- Yamaguchi, Y., Heiny, M. E., Suzuki, M., and Gitlin, J. D. (1996). Biochemical characterization and intracellular localization of the Menkes disease protein. *Proc. Natl. Acad. Sci. U.S.A.* *93*, 14030–14035.
- Yamochi, W., Tanaka, K., Nonaka, H., Maeda, A., Musha, T., and Takai, Y. (1994). Growth site localization of Rho1 small GTP-binding protein and its involvement in bud formation in *Saccharomyces cerevisiae*. *The Journal of Cell Biology* *125*, 1077–1093.
- Young, M. E. (2004). Yeast actin patches are networks of branched actin filaments. *The Journal of Cell Biology* *166*, 629–635.
- Zanolari, B., Rockenbauch, U., Trautwein, M., Clay, L., Barral, Y., and Spang, A. (2011). Transport to the plasma membrane is regulated differently early and late in the cell cycle in *Saccharomyces cerevisiae*. *Journal of Cell Science* *124*, 1055–1066.
- Zhang, W., Triple, R. P., and Samelson, L. E. (1998). LAT palmitoylation: its essential role in membrane microdomain targeting and tyrosine phosphorylation during T cell activation. *Immunity* *9*, 239–246.
- Zhao, Y., MacGurn, J. A., Liu, M., and Emr, S. (2013). The ART-Rsp5 ubiquitin ligase network comprises a plasma membrane quality control system that protects yeast cells from proteotoxic stress. *Elife* *2*, e00459.
- Zhu, Y., Traub, L. M., and Kornfeld, S. (1998). ADP-ribosylation factor 1 transiently activates high-affinity adaptor protein complex AP-1 binding sites on Golgi membranes. *Molecular Biology of the Cell* *9*, 1323–1337.
- Ziman, M., Chuang, J. S., and Schekman, R. W. (1996). Chs1p and Chs3p, two proteins involved in chitin synthesis, populate a compartment of the *Saccharomyces cerevisiae* endocytic pathway. *Molecular Biology of the Cell* *7*, 1909–1919.
- Ziman, M., Chuang, J. S., Tsung, M., Hamamoto, S., and Schekman, R. (1998). Chs6p-dependent anterograde transport of Chs3p from the chitosome to the plasma membrane in *Saccharomyces cerevisiae*. *Molecular Biology of the Cell* *9*, 1565–1576.

10.10 Curriculum Vitae

Name: Alicja Maria Ritz

Place and date of birth: Gdansk, 31.01.1984

Address: Alemannenweg 7, 3900 Brig-Glis

Contact telephone number: +41 267 21 57

Email: alicja.drozdowska@unibas.ch

Nationality: Polish

EDUCATION AND RESEARCH EXPERIENCE:

Jan. 2010 to date	Doctoral Student in the laboratory of Prof. Dr. Anne Spang, Biozentrum, University of Basel “Investigation of regulated exocytosis and endocytosis in <i>Saccharomyces cerevisiae</i> ”
Sep. 2007 – Dec. 2009	Doctoral student in the laboratory of Prof. Dr. Hemmo Meyer, Institute of Biochemistry, ETH Zürich “Defining a ubiquitin-dependent pathway that regulates chromatin-associated Aurora B during mitosis”
Feb. 2006 – Jun. 2007	Master thesis in the laboratory of Prof. Dr. Jaroslaw Marszalek, Institute of Biotechnology, University of Gdansk “Intramitochondrial localization of Mdj1p and its role in mitochondrial DNA maintenance in <i>Saccharomyces cerevisiae</i> ”
Oct. 2005 – Jul. 2007	Master’s Degree Studies in the Field of Biotechnology, University and Medical University of Gdansk
Sep. 2005 – Jan. 2006	Apprenticeship in the laboratory of Dr. Nia J. Bryant
Oct. 2002 – Jun. 2005	Bachelor’s Degree in the Field of Biotechnology, University and Medical University of Gdansk
1998 – 2002	High school education: Gdanskie Liceum Autonomiczne
1996 – 1998	Elementary school education: Szkoła Podstawowa nr 86, Gdansk
1991 – 1996	William B. Ogden Elementary School, Chicago, IL

SELECTED FURTHER ACADEMIC ACTIVITIES:

Mar. 2012	ESF-EMBO Conference, “Cell polarity and membrane traffic”, Pultusk, Poland
Jun. 2011	Lecture course “Biomembrane dynamics: from molecules to cells”, Cargese, France
Sep. 2009	EMBO Conference, “Ubiquitin and ubiquitin-like modifiers in health and disease”, Rive del Garda, Italy
Sep. 2003	Practical course “Introduction into chromatography”, Bremen, Germany

SCHOLARSHIPS AND PRIZES:

Apr. 2012	Poster prize, ESF-EMBO Symposium: Cell Polarity and Membrane Traffic, Pultusk, Poland
Nov. 2008 – Nov. 2010	PhD Fellowship, Boehringer Ingelheim Fonds
Feb. 2006 – Jun. 2007 Feb. 2002 – Jun. 2005	scholarship awarded by University of Gdansk for curricular achievements
Sep. 2005 – Jan. 2006	Socrates/Erasmus scholarship

ACADEMIC MEMBERSHIPS

Jun. 2011 to date	Member of Swiss Society for Biochemistry
-------------------	--

TEACHING EXPERIENCE

2010 – 2012	Biochemistry Block Course, Biozentrum Basel
2008 – 2009	Grundlagen Praktikum, ETH Zürich

MEMBERSHIP IN STUDENT ORGANIZATIONS

Sep. 2003 – Aug. 2007	Student Touristic Guide Club (Studencki Klub Przewodnikow Turystycznych), Gdansk head of club (2006 – 2007)
-----------------------	--

PUBLICATIONS:

Ritz AM, Trautwein M, Grassinger F, Spang A. The prion domain in the exomer-dependent cargo Pin2p serves as a trans-Golgi retention motif. Submitted

Rockenbauch U, Ritz AM, Sacristan C, Roncero C, Spang A. The complex interactions of Chs5p, the ChAPs, and the cargo Chs3p. *Mol Biol Cell*. 2012 Nov; 23(22): 4402-15

Meyer H, Drozdowska A, Dobrynin G. A role for Cdc48/p97 and Aurora B in controlling chromatin condensation during exit from mitosis. *Biochem Cell Biol*. 2010 Feb; 88(1): 23-8.

Struthers MS, Shanks SG, MacDonald C, Carpp LN, Drozdowska AM, Kioumourtzoglou D, Furgason ML, Munson M, Bryant NJ Functional homology of mammalian syntaxin 16 and yeast Tlg2p reveals a conserved regulatory mechanism. *J Cell Sci*. 2009 Jul 1; 122(Pt 13): 2292-9.

10.11 Acknowledgements

I would like to express my sincerest thanks to the following people:

Anne Spang for taking me in and providing me with a wonderfully diverse and compelling project. For your constant support and always being there to help, explain and give advice. I really appreciated our collaboration – getting that push in the right direction, when I needed it, getting new ideas and being able to pursue my own. Thank you for putting the excitement in science!

My thesis committee members, **Martin Spiess** and **Yves Barral**, for your time, helpful comments and giving me a broader perspective of my work.

Franziska Grassinger and **Mark Trautwein** who started the Pin2 project and provided me with a very strong basis for this study.

Melanie Diefenbacher, **Cornelia Kilchert**, **Julie Weidner** and **Uli Rockenbauch** for introducing me to working with yeast in our lab.

Julia Stevens and **Jachen Solinger**. Thank you for jumping at every request, keeping the lab running and the loud lab loud. It is great fun working with you.

Sabine Probst, **Lukas Thiel**, **Alejandra Fernandez-Belmonte**, **Adela**, **Isabel** and **Sangmo** for preparing many solutions and cleaning up after me. I feel very pampered to work with such wonderful support staff.

All the members of the Spang lab past and present: **Benjamin Abitbol**, **Karin Ackema**, **Florian Baier**, **Ivana Bratic Hench**, **Melanie Diefenbacher**, **Alejandra Fernandez-Belmonte**, **Alejandro Fernandez-Estrada**, **Stefan Hümmer**, **Martina Huranova**, **Cornelia Kilchert**, **Heidi Mergentaler**, **Sabine Probst**, **Uli Rockenbauch**, **Alicia Siliezar**, **Jachen Solinger**, **Julia Stevens**, **Akshay Subramanian**, **Lukas Thiel**, **Congwei Wang** and **Bettina Zanolari**. Thank you for being great colleagues, friends and making my Mondays cheerful.

Stefanie Hiptmair for help on the Pin2 cysteine mutants.

Irina Derkatch and **Susan W. Liebman** for extensive experimental advice, strains and plasmids for our prion studies.

Boehringer Ingelheim Fonds for funding and numerous opportunities to meet and discuss with other PhD students – a most interesting and pleasant way to learn about other research.

Hemmo Meyer and the **past members of the Meyer lab** for showing me how to do biochemistry and be a real experimental worker.

Brigitte Olufsen for going out of your way to help me with any official business and organizing our floor outings.

The Appenzeller, Hall, Pieters and **Spiess labs** for your friendliness and sharing your knowledge, reagents and equipment.

My parents and **sister** for your constant long-distance support, friendship and the great times we spend together.

My new family in Switzerland for adopting me.

Danilo, for your care and making me a happy wife.

